JULIANA RODRIGUES DO CARMO

DRIED MANGO ENRICHED WITH ISOMALTULOSE BY USING ULTRASOUND AND PULSED VACUUM IN OSMOTIC DEHYDRATION WITH SUBSEQUENT DRYING

LAVRAS-MG

2022

JULIANA RODRIGUES DO CARMO

DRIED MANGO ENRICHED WITH ISOMALTULOSE BY USING ULTRASOUND AND PULSED VACUUM IN OSMOTIC DEHYDRATION WITH SUBSEQUENT DRYING

Tese apresentada à Universidade Federal de Lavras, como parte das exigências do Programa de Pós-graduação em Ciência dos Alimentos, área Ciência dos Alimentos, para a obtenção do título de Doutora.

Prof. Dr. Jefferson Luiz Gomes Corrêa

Orientador

Prof. Dr. Javier Telis Romero

Co-orientador

LAVRAS-MG

2022

Ficha catalográfica elaborada pelo Sistema de Geração de Ficha Catalográfica da Biblioteca Universitária da UFLA, com dados informados pelo(a) próprio(a) autor(a).

Carmo, Juliana Rodrigues do.

Dried mango enriched with isomaltulose by using ultrasound and pulsed vacuum in osmotic dehydration with subsequent drying / Juliana Rodrigues do Carmo. - 2022.

242 p. : il.

Orientador(a): Jefferson Luiz Gomes Corrêa.

Coorientador(a): Javier Telis Romero.

Tese (doutorado) - Universidade Federal de Lavras, 2022.

Bibliografia.

1. Isomaltulose. 2. Osmotic dehydration. 3. Hot air convective drying. I. Corrêa, Jefferson Luiz Gomes. II. Telis Romero, Javier. III. Título.

JULIANA RODRIGUES DO CARMO

DRIED MANGO ENRICHED WITH ISOMALTULOSE BY USING ULTRASOUND AND PULSED VACUUM IN OSMOTIC DEHYDRATION WITH SUBSEQUENT DRYING

MANGA SECA ENRIQUECIDA COM ISOMATULOSE ATRAVÉS DO USO DE ULTRASSOM E PULSO DE VÁCUO EM DESIDRATAÇÃO OSMÓTICA COM SECAGEM SUBSEQUENTE

Tese apresentada à Universidade Federal de Lavras, como parte das exigências do Programa de Pós-graduação em Ciência dos Alimentos, área Ciência dos Alimentos, para a obtenção do título de Doutora.

APROVADA em 08 de agosto de 2022.

Dra. Bruna de Souza Nascimento (UFLA)

Dr. Rosinelson da Silva Pena (UFPA)

Dr. Tiago Carregari Polachini (UNESP)

Prof. Dr. Jefferson Luiz Gomes Corrêa

Orientador

Prof. Dr. Javier Telis Romero

Co-orientador

LAVRAS-MG

2022

Aos meus pequenos, Mateus, Miguel e Marina, que tornaram os meus dias longe de casa mais felizes, dedico.

AGRADECIMENTOS

Ao fim de mais este ciclo, agradeço ao papai, mamãe, irmã, cunhado e agora, ao nosso baby Carmo. Juntos estamos vivendo um dos momentos mais sublimes das nossas vidas. Nunca imaginei viver tantos momentos bons e ruins longe deles, mas sabemos que na nossa frente há coisas muito melhores do que as que temos aberto mão hoje. Tem valido a pena e pela Fé, valerá muito mais;

à minha família que sempre me alcançou em orações e torcidas;

aos meus amigos de infância que sempre acompanharam estes processos e nunca hesitaram em me dar sua atenção e afeto. Em especial, aos estrangeiros, que me ensinaram o que é ser resiliente;

aos amigos lavrenses, que marcaram a minha trajetória e me deram tudo que um estudante de outra localidade necessita e por várias vezes minimizaram a saudade de casa. Em especial, aos da igreja, onde passei boa parte do meu tempo e pude desenvolver a minha vocação e o meu chamado, que de longe se equiparam a todo o conhecimento que venho adquirindo na academia;

aos colegas de laboratório por todo companheirismo e todo o conhecimento compartilhado. De fato, todo dia é um aprendizado pessoal e científico ao lado deles. Em especial, a todos que, sendo de outros laboratórios e departamentos, me ajudaram. São tantas as lembranças de empenho deles a mim, que por conta disso, todas as análises que propus nessa tese foram realizadas. Nenhuma ficou pendente;

aos meus professores, que ao longo da vida partilharam com generosidade tanto conhecimento. Em especial, ao prof. Clóvis, que uma vez me disse que para onde eu fosse, eu daria certo. E eu com muita segurança, me apossei daquelas palavras;

à banca, composta pelos professores: Jefferson, que me orientou neste doutorado com todo o seu conhecimento, muita solicitude e disposição, palavras que mais lhe definem; Javier, que valorizou cada teste que eu compartilhava, transformando em ideias que resultaram em trabalhos que muito me motivaram nos meus dias de cansaço e dúvidas; Bruna, que esteve presente em várias etapas nessa caminhada e por ser a figura de uma profissional e mãe dedicada, mostrando que isso é possível; Tiago, que é um jovem professor e pesquisador, muito competente e cheio de humildade, que inspira a nossa geração; Rosinelson, que há anos me acompamha e que mesmo em quatro anos distantes, nunca largou minha mão, me ajudando durante as férias com análises e sempre me ensinando através das suas correções, na verdade, muito mais com seu compromisso em tudo a que se dispõe e por isso, é muito admirado;

aos coautores dos artigos, que de muito longe me ajudaram, deixando seu tempo para construir algo comigo. A maioria deles sequer vi pessoalmente e nem sei se verei, mas foram colocados no meu caminho a fim de me mostrar que eu não faria nada sozinha.

ao CNPq, CAPES e FAPEMIG pelo suporte financeiro a este projeto; ao Departamento de Ciência dos Alimentos; e à UFLA.

Por fim, agradeço a Deus, presente em tudo e em todos, que pôs sobre mim um jugo suave e um fardo leve. Incrivelmente eu sabia que mais uma vez Ele não me deixaria.

Bendito seja o Senhor Deus de nossos pais que (...) estendeu para mim a sua benignidade perante o rei e os seus conselheiros e todos os príncipes poderosos do rei. Assim me animei, segundo a mão do Senhor meu Deus sobre mim (Esdras 7.27,28)

RESUMO GERAL

A manga (*Mangifera indica* L. cv. Tommy Atkins) é um dos frutos tropicais mais populares. Ele é um fruto climatérico e perecível, que necessita de cuidados específicos para sua conservação. A desidratação osmótica (DO) e a secagem estão entre as técnicas que podem melhorar a estabilidade do fruto. Os carboidratos, como a sacarose, são comumente aplicados na DO. No entanto, é necessário substituir este açúcar por outros mais saudáveis. O carboidrato isomaltulose, conhecido comercialmente como Palatinose®, é um dissacarídeo redutor que possui propriedades físico-químicas e sensoriais muito semelhantes as da sacarose, com as seguintes vantagens: não-cariogênico, baixos índices glicêmico e insulinêmico. O objetivo deste estudo foi enriquecer frutos de manga com isomaltulose por meio de processos de DO – somados à utilização de tecnologias como o ultrassom e o pulso de vácuo, a fim de avaliar a influência desses processos e da secagem subsequente nas características físicas, químicas, nutricionais e higroscópicas do produto final. Além disso, estudos sobre as propriedades da isomaltulose em soluções aquosas, processos osmóticos em diferentes tipos de solutos, temperaturas e concentrações de solutos; e higroscopicidade e propriedades termodinâmicas de sorção também foram realizados. Os principais resultados destacam que: a isomaltulose pode ser promissora na substituição da sacarose em processos osmóticos; a cinética de DO foi representada com boa precisão pelo modelo linearizado de Azuara; as melhores condições para incorporação de isomaltulose em mangas, segundo os modelos multiníveis foram 45°C e 35% de concentração de soluto; ensaios a vácuo mostraram que o uso de 10 min e 48 kPa de pressão absoluta promoveram maior enriquecimento dos frutos, e melhores características físico-químicas em relação aos maiores níveis de vácuo e tempo; a incorporação de isomaltulose por ultrassom e vácuo pulsado antes da secagem resultou em um produto mais estável, do ponto de vista higroscópico, além de melhorar as propriedades de qualidade; e a abordagem termodinâmica mostrou que os comportamentos da entalpia e da entropia indicaram interação entre a água e os componentes do produto, que foi semelhante às propriedades físicas da água pura, a partir de 0,35 g de água/g de matéria seca. O valor de energia livre de Gibbs indicou que a sorção do fruto fresco foi um processo não-espontâneo, enquanto que os produtos pré-tratados com sacarose e isomaltulose foram processos espontâneos. A teoria da compensação entalpia-entropia indicou que os processos de sorção de todos os produtos foram controlados pela entalpia.

Palavras-chave: Tommy Atkins. Carboidrato saudável. Processos osmóticos. Secagem convectiva por ar quente.

GENERAL ABSTRACT

Mango (*Mangifera indica* L. cv. Tommy Atkins) is one of the most popular tropical fruits. It is a climacteric and perishable fruit, which need specific care for its conservation. Osmotic dehydration (OD) and drying are among the techniques that can improve the stability of the fruit. The carbohydrates, such as sucrose, are commonly applied in OD. However, replacing this sugar by healthier ones is required. Isomaltulose, commercially known as Palatinose®, is a reducing disaccharide that has physicochemical and sensory properties very similar to those of sucrose, with the following advantages: non-cariogenic, low glycemic and insulinemic indexes. The aim of this study was enriching mangos with isomaltulose through OD processes – in addition to the use of technologies such as ultrasound and pulsed vacuum, in order to evaluate the influence of these processes and subsequent drying on the physical, chemical nutritional and hygroscopic characteristics of the product. Moreover, studies about the isomaltulose properties in aqueous solutions, osmotic processes at different solutes type, temperatures and solute concentrations; and hygroscopicity and thermodynamic sorption properties were also carried out in this research. The main results highlighting that: isomaltulose can be promising in the replacement of sucrose in osmotic processes. the OD kinetics were represented with good accuracy by linearized Azuara model; the best conditions for incorporation of isomaltulose in mangos, according to multilevel models, were 45 °C and 35% solute concentration; vacumm assays showed that the use of 10 min and 48 kPa of absolute pressure promoted greater fruit enrichment, and best physicochemical characteristics in relation to higher vacuum and time levels; the incorporation of isomaltulose by ultrasound and pulsed vacuum before drying resulted in more stable product, from a hygroscopic point of view, besides the best quality properties; and the thermodynamic approach showed that the enthalpy and entropy behaviors showed interaction between water and the product components, which was similar to physical properties of pure water from 0.35 g water/g dry matter. Gibbs free energy value indicated that sorption of fresh mango was a non-spontaneous process, while for pretreated with sucrose and isomaltulose were spontaneous processes. The enthalpy-entropy compensation theory indicated the sorption processes of all products were enthalpy-controlled.

Keywords: Tommy Atkins. Healthy carbohydrate. Osmotic processes. Hot air convective drying.

FIGURE LIST

TABLE LIST

SUMMARY

FIRST SECTION

1 GENERAL INTRODUCTION

Fruits are functional foods that provide nutrients for the proper functioning of the body and whose nutritional value is associated with substances with protective properties. In most cases, functionality is associated with its antioxidant activity (KOZŁOWSKA; SZOSTAK-WEGIEREK, 2014; SCHIASSI et al., 2018). Although consumed fresh, the fruits can be processed such as sauces, jams, juices, ice creams, jellies and other desserts, as alternatives for preservation since they have high perishability, due to their high moisture content (KUMAR; SAGAR, 2014).

Mango (*Mangifera indica* L.) is one of the most popular tropical fruits. It is native to Southeast Asia, where most of its production is concentrated. It is a source of fiber, phenolic compounds and vitamins, such as C and pro-vitamin A (beta-carotene) (MALDONADO-CELIS et al., 2019). It is a climacteric and perishable fruit, which needs specific care for its preservation (ZHAO et al., 2014). In addition, it has been marketed almost exclusively in its whole form or such as concentrated juice, nectar and frozen pulp (LEBAKA et al., 2021).

Drying is one of the oldest and most common methods of food preservation (MAISNAM et al., 2017). Among the drying methods, hot air is the most used. However, the low efficiency and the long process time are the main disadvantages. These problems can be minimized with the use of pre-treatments such as osmotic dehydration (OD) (MACEDO et al., 2021).

OD consists of immersing the food in a hypertonic solution, with consequent water loss (WL) and solid gain (SG) in simultaneous isothermal flows without any phase change. In OD, three types of counter-current mass transfer occur: (i) water flows from the product to the solution, (ii) a solute transfer from solution to the product and (iii) a leaching out of the native solutes (sugars, organic acids, minerals, vitamins, etc.) (JUNQUEIRA et al., 2017). The OD process offers the possibility of modifying food properties, especially in relation to taste and structural characteristics (UDOMKUN et al., 2015). In addition, it can be used as a pre-treatment for conventional drying procedures in order to provide a previous dehydration, which reduces energy consumption and possibilities of improving the quality of the dry product (ABRAHÃO; CORRÊA, 2021).

Despite the advantages mentioned above, Corrêa et al. (2017) reported that the combined process of DO and drying is still relatively late. The use of ultrasound assisted

osmotic dehydration (UAOD) and pulsed vacuum (PVOD) have been employed to further increase the mass transfer rate during the process and, consequently, decrease the osmotic pre-treatment and drying time (JUNQUEIRA et al., 2021; VIANA; CORRÊA; JUSTUS, 2014).

Sucrose is commonly used in osmotic solution composition. However, it is cariogenic and high glycemic index carbohydrate, which is associated with diseases such as diabetes and obesity. Alternatively, recent OD works has tested the use of other sweeteners such as polyols (ASSIS; MORAIS; MORAIS, 2016; MENDONÇA et al., 2016), isomaltulose, oligofructose and aqueous stevia extract (CARMO et al., 2022a; MACEDO et al., 2021) in osmotic solutions preparation.

Isomaltulose, commercially known as Palatinose®, is a reducing disaccharide, isomer of sucrose, obtained by microbial enzymatic conversion from sucrose. This carbohydrate has a mild sweet taste and physicochemical and sensory properties very similar to those of sucrose (CARMO et al., 2022a). Additionally, this carbohydrate has healthy aspects due to low glycemic and insulinemic indexes (SHYAM; RAMADAS; CHANG, 2018).

The general aim of this work was to enrich mangos with isomaltulose through of OD processes – with the use of technologies such as ultrasound and pulsed vacuum during OD – in order to evaluate the influence of these processes and subsequent drying on physical, chemical and nutritional qualities, and higroscopicity of the product. Studies about the isomaltulose properties in aqueous solutions. osmotic processes at different solutes type, temperatures and solute concentrations; and hygroscopicity and thermodynamic sorption properties were also carried out in this research.

2 THEORETICAL REFERENCE

2.1 MANGO (*Mangifera indica* L.) cv. TOMMY ATKINS

Mango (*Mangifera indica* L.) is one of the most appreciated fruits for consumption, due to its texture and flavor. Commercial mango production is concentrated in countries such as China, Thailand, Indonesia, Mexico and Brazil (LEBAKA et al., 2021). Mango fruit has a yellow or orange pulp with a fibril structure and contains about 14% of the total sugar, with sucrose as the main constituent, followed by vitamin C (37 mg/100 g), minerals such as calcium, phosphorus and iron and a considerable amount of carotenes (MALDONADO-CELIS et al., 2019).

Tommy Atkins cultivar is the most consumed in the world, being considered the main commercial cultivar (FERREIRA et al., 2020). The greater mechanical and thermal resistance of this fruit during transport, the prolonged storage time and the good tolerance of the variety to anthracnose and to technological processes, such as floral induction and water stress, led this cultivar to be preferred by farmers (BURTON-FREEMAN; SANDHU; EDIRISINGHE, 2017).

Despite their considerable nutritional value, mangoes are extremely perishable. Damage to fruits can be caused by microorganisms, enzymatic activity or oxidation; and although these fruits can be preserved by freezing, energy costs and the lack of freezing facilities in some rural areas limit the use of this strategy (AMIT et al., 2017). Thus, other strategies are necessary to preserve the fruit. Dehydration techniques can provide products with physicochemical and sensory qualities similar to those of fresh fruit (ABRAHÃO; CORRÊA, 2021).

2.2 FOOD DRYING

Drying is defined as the process of vaporizing and removing water or other liquids from a solution, suspension or other solid-liquid mixture to give a dry solid (BERK, 2013). Foods such as fruits and vegetables have a moisture content greater than 80 g H_2O/100 g (wet basis), which makes them highly susceptible to spoilage bacteria. Dehydration preserves food to stable and safe conditions by reducing water activity (a_w), extending the shelf life much longer than that of fresh products, and in addition, it reduces the weight and volume of food, makes it easier to store, pack and transport, and also provides different flavors and aromas to food (RODRIGUEZ-GONZALEZ et al., 2015).

Drying occurs in two simultaneous transport processes: heat transfer, to vaporize the liquid, and mass transfer, in the form of liquid and/or vapor from the interior of the material to

the surface (STRUMILLO; KUDRA, 1986). This technique can be classified into three main groups: convective, conductive and radiative. Convective drying is the most popular method to obtain more than 90% of dried foods. It is used to remove water from food substances through the application of convection heat in equipment intended for drying, while the removal of vapors is achieved using forced air (SAGAR; KUMAR, 2010).

The low thermal conductivity of the food material during the convective drying process causes limited heat transfer to the inner section of the material. The high temperature and long drying time in conventional hot air drying can alter the taste, color and rehydration capacity of dry products (KROEHNKE et al., 2021). In all cases, drying efficiency and energy demand are associated with drying time, which is highly related to the volume of water in a material to be removed or the rate at which drying can be performed. Furthermore, lowering the process temperature grants great potential to improve the quality of dry products (KHUBBER et al., 2020). However, under such conditions, the operating time and associated cost becomes unacceptable. To reduce operating cost, different pretreatments and new low temperature and low energy drying methods have been developed. In this context, OD has been used as pretreatment for the drying of different types of fruits (CORRÊA et al., 2017; MENDONÇA et al., 2017; FERNANDES et al., 2019; YAO et al., 2020).

2.3 OSMOTIC DEHYDRATION

2.3.1 Mass transfer mechanism during osmotic dehydration

OD consists of immersion of food in hypertonic solutions with consequent removal of water and solid gain (JUNQUEIRA; CORRÊA; ERNESTO, 2017; NOWACKA et al., 2014). The raw material is placed in soluble solids concentrated solutions with higher osmotic pressure and reduced a_w. This results in three types of mass transfer phenomena in the OD process (ABRAHÃO; CORRÊA, 2021): (1) Water diffuses from the product to the solution at an initially faster rate, which after a period of time proceeds slowly; (2) a transfer of solute from the solution to the product, which makes it possible to introduce the desired amount of an active ingredient, a preservative, or any solute of nutritional interest, or even improve the product sensory quality; (3) leaching of solutes (sugar, organic acids, minerals, vitamins, etc.) from the product own, which are quantitatively negligible when compared to the first two types of transfer, but essential with regard to the composition of the final product (CORRÊA et al., 2015).

OD process can be characterized by dynamic and static (equilibrium) periods. In the dynamic period, mass transfer rates increase or decrease until equilibrium is reached. Equilibrium is the end of the osmotic process, that is, the momentum when the mass transfer rate is zero. The study of the steady state is necessary for the modeling of the osmotic process as a unit of operation and also important for a good understanding of the mass transfer mechanisms involved in this system. In addition, knowledge of the endpoint criteria can lead to the development of theoretical models, which can be used to calculate the process parameters (LENART; FLINK, 1984).

2.3.2 Advantages and disadvantages of osmotic dehydration

DO can improve the quality characteristics of the product, in addition it is associated with an increase in the energy savings of the process, since the water from the product is removed without a phase change, which does not occur in conventional drying, for example. Furthermore, this process is advantageous as it only depends on the osmotic solution as the drying force. (PRINZIVALLI et al., 2006). However, despite this, it is not recommended to use the DO technique for more than 50% weight reduction due to decreased osmosis rate over time (RAMYAN; JAIN, 2017), besides is a late process. Another disadvantage is that such a long exposure of the material in the osmotic solution inevitably leads to the breakdown of cell tissue (PRINZIVALLI et al., 2006). In this sense, to improve OD efficiency and minimize product quality loss, pretreatments are required, as mentioned below.

2.3.3 Ultrasound assisted osmotic dehydration (UAOD)

In solid materials, alternative compressions and expansions generated by the ultrasonic waves produce an effect similar to that seen when a sponge is repeatedly squeezed and released (LAGNIKA et al., 2018). This "sponge effect" produces the release of liquid from the inside of the particle to the solid surface and the entry of fluid from the outside. The forces involved in this mechanism can be greater than surface tension, which keeps water molecules inside the material's capillaries, creating microscopic channels and facilitating matter transfers (MURALIDHARA; ENSMINGER; PUTNAM, 1985). For these reasons, ultrasound has been widely used to enhance transport phenomena in solid-liquid systems, such as OD processes (AMAMI et al., 2017; CORRÊA et al., 2017; DELGADO et al., 2017; FERNANDES et al., 2016; SOQUETTA et al., 2018).

The use of ultrasound assisted osmotic dehydration (UAOD) improves the changes caused by ultrasound pretreatment. This makes this technology suitable for application in more porous fruits (PRITHANI; DASHA, 2020), as it increases tissue structure deformation due to ultrasonic waves and pressure-generating osmotic channels. These channels decrease the diffusion boundary layer and improve convective mass transfer in the sample (La FUENTE; TADINI, 2017; NOWACKA et al., 2014).

The application of ultrasound technology is still a challenge in dense and less porous fruits and vegetables, such as mango. In a recent study, Fernandes et al. (2019) observed that mangos pre-treated with UAOD reduced the apparent water diffusivity during hot air drying, due to the saturation of the surface of the mango samples with sucrose, which increased the mass transfer resistance between the fruit and the solution. Despite the lower water diffusivity, the reduction in the initial moisture content after the osmotic process culminated in a shorter drying time and shorter process time under the conditions studied.

2.3.4 Pulsed vacuum osmotic dehydration (PVOD)

Traditionally, OD is performed at atmospheric pressure. However, it can be carried out at reduced pressure (vacuum) in the first minutes of the process. Pulsed vacuum osmotic dehydration (PVOD) consists of applying a vacuum in the solid-solution system, for a short period at the beginning of the process, to remove part of the air present inside the pores of the food, allowing the entry of the osmotic solution through a hydrodynamic mechanism (HDM) (OLIVEIRA et al., 2021). When the pressure of the system is recovered, the liquid that is in contact with the food penetrates inside the pores, due to the macroscopic pressure gradients and capillarity (MACEDO et al., 2022).

The PVOD process involves a rapid change in the composition of the food through the exit of gases from the interior of the pores and their filling with the osmotic solution, thus altering the physical and transport properties of the food tissue (CORRÊA et al., 2014). The works related to the PVOD technique indicate an improvement in the mass transfer process, when compared to the use of atmospheric pressure or continuous vacuum pressure, in addition to providing shorter times for the impregnation of solutes (JUNQUEIRA et al., 2021).

Despite these advantages, changes in the density and structure of the product can alter the physicochemical properties of the food and also cause mechanical damage to the cell structure, such as cell separation, associated with the deformation of the sample, which occurs

when the vacuum pulse is applied (LIN; LUO; CHEN, 2016). Because of this, the time and vacuum pressure for each food during the PVOD process must be evaluated.

Studies about pretreatments with ultrasound (FONG-IN et al., 2021; KROEHNKE et al., 2021; MEHTA et al., 2021; TASOVA; POLATCI; GOKDOGAN, 2022) and pulsed vacuum (ARAÚJO; PENA, 2022; GHELLAM et al., 2021; HU et al., 2021) on OD for several foods and with the use of sucrose are very common in scientific literature. However, studies with these pretreatments for mangos are still scarce (ITO et al., 2007; LIN, LUO, CHEN; 2016; MEDEIROS et al., 2019; ZOU et al., 2013). Moreover, the studies with use of isomaltulose on OD processes are now showing the first findings (CARMO et al., 2022b; KIM et al., 2018; MACEDO et al., 2021).

2.4 ISOMALTULOSE: AN EMERGING OSMOTIC AGENT

Hypertonic sucrose solutions are widely used in the OD process of several fruits (BERA; ROY, 2015; CHAUDHARI; DHAKE; BARI, 2015; LIN; LUO; CHEN, 2016; MENDONÇA et al., 2017; RAMYA; JAIN, 2017). However, sucrose is considered a highly cariogenic carbohydrate, digested quickly, inducing a high glycemic and insulinemic response. One way to circumvent these disadvantages is the substitution of sucrose for other carbohydrates in the OD of fruits. Recent studies have used other carbohydrates such as xylitol, sorbitol, glycerol, maltodextrin and polydextrose (BROCHIER; MARCZAK; NOREÑA 2015; MENDONÇA et al., 2016) during the OD in view of the healthiness of the dehydrated products obtained. Besides, the use of isomaltulose appears as a promising substitute of sucrose in the OD of fruits, which has been recently studied (CARMO et al., 2022b; KIM et al., 2018; MACEDO et al., 2021).

Isomaltulose (D-glucopyranosyl-1, 6-fructose) is present in honey and sugarcane juice. It has a flavor and physical properties similar to sucrose, and a sweetening power of 42% compared to sucrose (PERICHE et al., 2014). Isomatulose can be considered a healthy carbohydrate, since it is non-cariogenic and has low glycemic and insulinemic indices (FLEDDERMANN et al., 2016).

Studies have shown that oral administration of isomaltulose resulted in significant improvements in diet-induced metabolic abnormalities, which would help prevent obesity and its complications (SHYAM; RAMADAS; CHANG, 2018; YOUNG; BENTON, 2015). This is because isomaltulose improves glucose homeostasis and prevents fatty liver, in contrast to the effects of sucrose, which has fructose-glucose-like α-1-2 bonds (SAWALE et al., 2017).

Furthermore, consumption of isomaltulose instead of sucrose has been shown to reduce postprandial glucose-dependent insulinotropic peptide and insulin release in mice (KEYHANI-NEJAD et al., 2015). In studies with mice, it was observed that the difference in the physiological effects of sucrose and isomaltulose is caused by the slower cleavage of α-1-6 bond in isomaltulose by intestinal glycosidases compared to that of α-1-2 bond in sucrose. In this way, absorption and release of monosaccharides by isomaltulose in the small intestine after ingestion proceeds slowly. Blood glucose and insulin levels are raised more slowly and the blood glucose level is also reached gradually (SHYAM; RAMADAS; CHANG, 2018).

2.5 HYGROSCOPICITY AND SORPTION THERMODYNAMIC PROPERTIES

The hygroscopicity of foods is linked to its physical, chemical, and microbiological stability, which behavior can be assessed from moisture sorption isotherms (CAVALCANTE et al., 2018). The different solutes used in OD can affect the characteristics of the food, modifying its moisture sorption isotherms.

Sorption isotherms describe the relationship between equilibrium moisture content and a_w of a product at constant temperature (CARMO; PENA, 2019). Several mathematical empirical, semi-empirical, or theoretical models have been proposed to describe the behavior of moisture sorption in foods (KAR; SUTAR, 2022).

Sorption thermodynamic properties of foods such as sorption net isosteric heat (q_{st}) or differential enthalpy (ΔH), differential entropy (ΔS), isokinetic temperature (T_B), Gibbs free energy (ΔG) and enthalpy-entropy compensation theory can be estimated from moisture sorption isotherms obtained at different temperatures (IGLESIAS; CHIRIFE, 1976). In general, these properties are used to estimate the amount of energy involved in the moisture sorption process, besides providing information about the state of water in a food product.

REFERENCES

ABRAHÃO, F. R.; CORRÊA, J. L. G. Osmotic dehydration: More than water loss and solid gain. **Critical Reviews in Food Science and Nutrition**, v. 1, p. 1-20, 2021.

AMAMI, E. et al. Effect of ultrasound assisted osmotic dehydration pretreatment on the convective drying of strawberry. **Ultrasonics – Sonochemistry**, v. 36, n. 1, p. 286-300, 2017.

AMIT, S. K., et al. A review on mechanisms and commercial aspects of food preservation and processing. **Agriculture & Food Security**, v. 6, n. 51, p. 1-22, 2017.

ARAUJO, A. L; PENA, R. D. Influence of process conditions on the mass transfer of osmotically dehydrated jambolan fruits. **Food Science and Technology**, v. 42, n. e37520, p. 1-10, 2022.

ASSIS, F. R.; MORAIS , R. M. S. C.; MORAIS, A. M. M. B. Mathematical modelling of osmotic dehydration kinetics of apple cubes. **Journal of Food Processing and Preservation**, v. 41, n. 3, p. 1-16, 2016.

BERA, D.; ROY, L. Osmotic dehydration of litchi using sucrose solution: effect of mass transfer. **Journal of Food Processing and Technology**, v. 6, n. 7, p. 1-7, 2015.

BERK, Z. **Food Process Engineering and Technology** (2nd Ed.). Massachusetts: Academic Press, 2013. 690 p.

BROCHIER, B.; MARCZAK, L. D. F.; NOREÑA, C. P. Z. Use of different kinds of solutes alternative to sucrose in osmotic dehydration of yacon. **Brazilian Archives of Biology and Technology**, v. 58, n. 1, p. 34-40, 2015.

BURTON-FREEMAN, B. M.; SANDHU, A. K.; EDIRISINGHE, I. Mangos and their bioactive components: Adding variety to the fruit plate for health. **Food and Function**, v. 8, n. 9, p. 3010-3032, 2017.

CARMO, J. R. et al. Properties of Isomaltulose (Palatinose®) – an emerging healthy carbohydrate: effect of temperature and solute concentration. **Journal of Molecular Liquids**, v. 347, n. 118304, p. 1-11, 2022a.

CARMO, J. R. et al. Mango enriched with sucrose and isomaltulose (Palatinose®) by osmotic dehydration: effect of temperature and solute concentration through the application of a multilevel statistical models. **Journal of Processing and Preservation**, *In press*, 2022.

CARMO, J. R.; PENA, R. S. Influence of the temperature and granulometry on the hygroscopic behavior of tapioca flour. **CyTA – Journal of Food**, v. 17, n. 1, p. 900-906, 2019.

CAVALCANTE, C. E. B. et al. Hygroscopic behaviour of spray dried soursop pulp powder. **Brazilian Jounal of Food Techology**, v. 21, e2017121, p. 1-8, 2018.

CHAUDHARI, A. P.; DHAKE, K. P.; BARI, M. R. Osmotic dehydration of pineapple. **International Journal of Engineering Science**, v. 3, n. 4, p. 11-20, 2015.

CORRÊA, J. L. et al. Optimisation of vacuum pulse osmotic dehydration of blanched pumpkin. **International Journal of Food Science and Technology**, v. 49, 2008-2014, 2014.

CORRÊA, J. L. G. et al. Osmotic dehydration of tomato assisted by ultrasound, evaluation of the liquid media on mass transfer and product quality. **International Journal of Food Engineering**, v. 11, n. 4, p. 2008-2014, 2015.

CORRÊA, J. L. G. et al. Influence of ultrasound application on both the osmotic pretreatment and subsequent convective drying of pineapple (*Ananas comosus*). **Innovative Food Science & Emerging Technologies**, v. 41, p. 284-291, 2017.

DELGADO, T. et al. Osmotic dehydration effects on major and minor components of chestnut (*Castanea sativa* Mill.) slices. **Journal of Food Science and Technology**, v. 54, n. 9, p. 2694-2703, 2017.

FERNANDES, F. A. N. et al. Use of ultrasound for dehydration of mangoes (*Mangifera indica* L.): kinetic modeling of ultrasound-assisted osmotic dehydration and convective air-drying. **Journal of Food Science and Technology**, v. 56, n. 4, p. 1793-1800, 2019.

FERNANDES, F. A. N. et al. Effects of ultrasound-assisted air-drying on vitamins and carotenoids of cherry tomatoes. **Drying Technology**, v. 34, n. 8, p. 986-996, 2016.

FERREIRA, K. M. et al. Physiological and biochemical aspects of 'Tommy Atkins' mango subjected to doses and methods of application of paclobutrazol. **Scientia Plena**, v. 16, n. 10, p. 1-9, 2020.

FLEDDERMANN, M. et al. Effects of a follow-on formula containing isomaltulose (Palatinose™) on metabolic response, acceptance, tolerance and safety in infants: a randomized-controlled trial. **PLoS One**, v. 11, n. 3, p. 1-14, 2016.

FONG-IN, S. et al. Ultrasound-assisted osmotic dehydration of litchi: effect of pretreatment on mass transfer and quality attributes during frozen storage. **Journal of Food Measurement and Characterization**, v. 15, n. 4, p. 3590-3597, 2021.

GHELLAM, M. et al. Vacuum-assisted osmotic dehydration of autumn olive berries: modeling of mass transfer kinetics and quality assessment. **Foods**, v. 10, n. 10, p. 2286, 2021.

HU, X. et al. Changes in water state, distribution, and physico-chemical properties of preserved kumquats during different processing methods. **Journal of Food Process Engineering,** v. 44, n. 7, p. e13716, 2021.

IGLESIAS, H. A.; CHIRIFE, J. Prediction of the effect of temperature on water sorption isotherms of food material. **Journal of Food Technology**, v. 11, p. 109-116. 1976.

ITO, A. P. et al. Influence of process conditions on the mass transfer kinetics of pulsed vacuum osmotically dehydrated mango slices. **Drying Technology**, v. 25, n. 10, p. 1769-1777, 2007.

JUNQUEIRA, J. R. J.; CORRÊA, J. L. G.; ERNESTO, D. B. Microwave, convective, and intermittent microwave-convective drying of pulsed vacuum osmodehydrated pumpkin slices. **Journal of Food Processing and Preservation**, v. 41, n. 6, p. 1-8, 2017.

JUNQUEIRA, J. R. et al. Modeling mass transfer during osmotic dehydration of different vegetable structures under vacuum conditions. **Food Science and Technology**, v. 41, n. 2, p. 439-448, 2021.

KAR, S.; SUTAR, P. P. Shelf life prediction of dried garlic powder under accelerated storage conditions. **Journal of Food Science and Technology (Mysore)**, *In press*. 2022.

KEYHANI-NEJAD, F. et al. Nutritional strategy to prevent fatty liver and insulin resistance independent of obesity by reducing glucose-dependent insulinotropic polypeptide responses in mice. **Diabetologia**, v. 58, n. 2, p. 374-383, 2015.

KIM, H. et al. Effect of isomaltulose used for osmotic extraction of *Prunus mume* fruit juice substituting sucrose. **Food Science and Biotechnology**, v. 27, n. 6, p. 1599-1605, 2018.

KOZŁOWSKA, A.; SZOSTAK-WEGIEREK, D. Flavonoids – food source and health benefits. **Roczniki Panstwowego Zakladu Higieny**, v. 65, n. 2, p. 79-85, 2014.

KHUBBER, S. et al. Non-conventional osmotic solutes (honey and glycerol) improve mass transfer and extend shelf life of hot-air dried red carrots: kinetics, quality, bioactivity, microstructure, and storage stability, **LWT - Food Science and Technology**, v. 131, n. 109764, p. 1-10, 2020.

KROEHNKE, J. et al. Osmotic dehydration and convective drying of kiwifruit (*Actinidia deliciosa*) – The influence of ultrasound on process kinetics and product quality. **Ultrasonics – Sonochemistry**, v. 71, n. 105377, p.1-11, 2021.

KUMAR, P. S.; SAGAR, V. R. Drying kinetics and physico-chemical characteristics of Osmo-dehydrated mango, guava and *Aonla* under different drying conditions. **Journal of Food Science and Technology**, 51, n. 8, p. 1540-1546, 2014.

LA FUENTE, C. I. A.; TADINI, C. C. Unripe banana flour produced by air-drying assisted with ultrasound – description of the mechanisms involved to enhance the mass transfer in two approaches. **International Journal of Food Engineering**, v. 13, n. 11, p. 1-13, 2017.

LAGNIKA, C. et al. Ultrasound-assisted osmotic process on quality of microwave vacuum drying sweet potato, **Drying Technology**, v. 36, n. 11, p. 1367-1379, 2018.

LEBAKA, V. R. et al. Nutritional composition and bioactive compounds in three different parts of mango fruit. **International Journal of Environmental Research and Public Health**, v. 18, n. 2, p. 741, 2021.

LENART, A.; FLINK, J. M. Osmotic concentration of potato: I. Criteria for the end-point of the osmosis process. **Journal of Food Technology**, v. 19, n. 1, p. 45-63, 1984.

LIN, X.; LUO, C.; CHEN, Y. Effects of vacuum impregnation with sucrose solution on mango tissue. **Journal of Food Science**, v. 81, n. 6, p. 1412-1418, 2016

MACEDO, L. L. et al. Convective drying with ethanol pre-treatment of strawberry enriched with isomaltulose. **Food and Bioprocess Technology**, v. 14, p. 2046-2061, 2021.

MACEDO, L. L. et al. Effect of osmotic agent and vacuum application on mass exchange and qualitative parameters of osmotically dehydrated strawberry. **Journal of Food Processing and Preservation**, n. e14057, p. 1-13, 2022

MAISNAM, D. et al. Recent advances in conventional drying of foods. **Journal of Food Technology and Preservation**, v. 1, n. 1, p. 25-34, 2017.

MALDONADO-CELIS, M. E. et al. Chemical composition of mango (*Mangifera indica* L.) fruit: nutritional and phytochemical compounds. **Frontiers in Plant Science**, v. 10, n. 1073, p. 1-21, 2019.

MEHTA, A. et al. Ultrasonic induced effect on mass transfer characteristics during osmotic dehydration of aonla (*Phyllanthus emblica* L.) slices: A mathematical modeling approach. **Journal of Food Process Engineering**, v. 44, n. 12, p. e13887, 2021.

MENDONÇA, K. S. et al. Influences of convective and vacuum drying on the quality atributes of osmo-dried pequi (*Caryocar brasiliense* Camb.) slices. **Food Chemistry**, v. 224, n. 1, p. 212-218, 2017.

MENDONÇA, K. S. et al. Optimization of osmotic dehydration of yacon slices. **Drying Technology**, v. 34, n. 4, p. 386-394, 2016.

MEDEIROS, R. A. B. et al. Effect of different grape residues polyphenols impregnation techniques in mango. **Journal of Food Engineering**, v. 262, p. 1-8, 2019

MURALIDHARA, H.S.; ENSMINGER, D.; PUTNAM, A. Acoustic dewatering and drying (low and high frequency): state of the art review. **Drying Technology**, v. 3, n. 4, p. 529-566, 1985.

NOWACKA, M. et al. Effect of ultrasound treatment on the water state in kiwifruit during osmotic dehydration. **Food Chemistry**, v.144, p.18-25, 2014.

OLIVEIRA, L. F. et al. Drying of 'yacon' pretreated by pulsed vacuum osmotic dehydration. **Revista Brasileira de Engenharia Agrícola e Ambiental**, v. 25, n.8, p. 560-565, 2021.

PERICHE, A. et al. Optical, mechanical and sensory properties of based-isomaltulose gummy confections. **Food Bioscience**, v. 7, p. 37-44, 2014.

PRINZIVALLI, C. et al. Effect of osmosis time on structure, texture and pectic composition of strawberry tissue. **European Food Research and Technology**, v. 224, n. 1, p. 119-27, 2006.

PRITHANI, R.; DASHA, K. K. Mass transfer modelling in ultrasound assisted osmotic dehydration of kiwi fruit. **Innovative Food Science & Emerging Technologies**, v. 64, n. 102407, p. 1-11, 2020.

RAMYA, V.; JAIN, K. A review on osmotic dehydration of fruits and vegetables: an integrated approach. **Journal of Food Process Engineering**, v. 40, n. 3, p. 1-22, 2017.

RODRIGUEZ-GONZALEZ, O. et al. Energy requirements for alternative food processing Technologies – principles, assumptions, and evaluation of efficiency. **Comprehensive Reviews in Food Science and Food Safety**, v. 14, n. 5, p. 536-554, 2015.

SAGAR, V. R.; KUMAR, P. S. Recent advances in drying and dehydration of fruits and vegetables: a review. **Journal of Food Science and Technology**, v. 47, n. 1, p. 15-26, 2010.

SAWALE P. et al. Isomaltulose (Palatinose) – an emerging carbohydrate. **Food Bioscience**, v. 18, p. 46-52, 2017.

SCHIASSI, M. C. E. et al. Fruits from the Brazilian cerrado region: physico-chemical characterization, bioactive compounds, antioxidant activities, and sensory evaluation. **Food Chemistry**, v. 245, n. 15 p. 305-311, 2018.

SHYAM, S.; RAMADAS, A.; CHANG, S. K. Isomaltulose: recent evidence for health benefits. **Journal of Functional Foods**, v. 48, p. 173-178, 2018.

SOQUETTA, M. B. et al. Effects of pretreatment ultrasound bath and ultrasonic probe, in osmotic dehydration, in the kinetics of oven drying and the physicochemical properties of beet snacks. **Journal of Food Processing and Preservation**, v. 42, n. 4, e13393, 2018.

STRUMILLO, C.; KUDRA, T. **Drying: Principles, applications and design**. New York: Gordeon and Breach Science Publishers, 1986. 448 p.

TASOVA, M.; POLATCI, H.; GOKDOGAN, O. Effect of osmotic dehydration pre-treatments on physicochemical and energy parameters of Kosia (Nashi) pear slices dried in a convective oven. **Journal of Food Processing and Preservation**. *In press*, 2022.

UDOMKUN, P. et al. Single layer drying kinetics of papaya amidst vertical and horizontal airflow. **LWT - Food Science and Technology**, v. 64, n. 1, p. 67-73, 2015.

VIANA, A. D.; CORRÊA, J. L. G.; JUSTUS, A. Optimisation of the pulsed vacuum osmotic dehydration of cladodes of fodder palm. **International Journal of Food Science and Technology**, v. 49, n. 3, p. 726-732, 2014.

YAO, L.; FAN, L.; DUAN, Z. Effect of different pretreatments followed by hot-air and far-infrared drying on the bioactive compounds, physicochemical property and microstructure of mango slices. **Food Chemistry**, v. 305, n. 125477, p. 1-9, 2020.

YOUNG, H.; BENTON, D. The effect of using isomaltulose (Palatinose™) to modulate the glycaemic properties of breakfast on the cognitive performance of children. **European Journal of Nutrition**, v. 54, n. 6, p. 1013-1020, 2015.

ZHAO, J.-H. et al. Osmotic dehydration pretreatment for improving the quality attributes of frozen mango: effects of different osmotic solutes and concentrations on the samples. **International Journal of Food Science and Technology**, v. 49, n. 4, p. 960-968, 2014.

ZOU, K. et al. Effect of osmotic pretreatment on quality of mango chips by explosion puffing drying. **LWT – Food Science and Technology**, v. 51, n. 1, p. 253-259, 2013.

SECOND SECTION

ARTICLE 1 – **Properties of Isomaltulose (Palatinose®) – an emerging healthy carbohydrate: effect of temperature and solute concentration**

Juliana Rodrigues do CARMO [a*], Jefferson Luiz Gomes CORRÊA [a], Tiago Carregari POLACHINI [b], Javier TELIS-ROMERO [b]

[a] Department of Food Science (DCA), Federal University of Lavras, Lavras 37200-900, Brazil.
[b] Department of Food Engineering and Technology, São Paulo State University, São José do Rio Preto 15054-000, Brazil.

[*]Corresponding author:
E-mail address: juliana_docarmo@yahoo.com.br

(Accepted in the Journal of molecular Liquids)

***Abstract*:** Isomaltulose (Palatinose®) is an emerging low glycemic and low insulinemic carbohydrate with several health benefits. Therefore, data about the properties (solubility (*IS*), density (ρ), specific heat capacity (c_p), thermal conductivity (λ), and dynamic viscosity (μ)) of isomaltulose solutions in a wide range of temperature and concentrations are scarce. The influence of the temperature and solute concentration was evaluated by fitting empirical equations commonly applied for carbohydrate solutions to the experimental data. The generic polynomial model concerning the significant variables predicted the experimental values with good accuracy (R^2>0.99; p<3.91%). The μ showed an Arrhenius exponential-type behavior (R^2>0.97; p<8.02%). *IS* increase with temperature (*T*). The ρ and μ increased with isomaltulose concentrations (*IC*) and decreased with *T*. The c_p and λ increased with *T* and decreased with *IC*. The availability of these properties covers a lack of data for the effective design of food processing equipment and unit operations such as osmotic dehydration, pumping, and pasteurization.

Keywords: solubility; thermophysical properties; viscosity; sucrose; modeling.

(doi: 10.1016/j.molliq.2021.118304)

1 Introduction

Isomaltulose (6-*O*-D-glucopyranosyl-D-fructose; CAS. Nº 13718-94-0), commercially known as Palatinose®, is a naturally-occurring disaccharide in honey, sugarcane, and molasses. It can also be obtained from sucrose using microbial enzymatic conversion [1]. Although isomaltulose has half of the sweet taste and similar caloric value of sucrose (~4 kcal·g^{-1}), it is more slowly digested by α-glucosidase in the small intestine than sucrose [2]. Clinical studies provided convincing evidence to support its applications for controlling postprandial glucose profile in humans, besides being a non-cariogenic carbohydrate [3,4].

Isomaltulose is commonly used in diets based on low glycemic and insulinemic indexes. Due to it, this disaccharide is becoming more and more used by athletes and diabetic, obese, and heart disease people [5]. One can find industrial products with isomaltulose in bakery products, candies, canned fruits, chewing gum, chocolate-based products, confectionery, and ready-to-drink products such as sports drinks, instant drinks, and milk-based drinks [6,7].

In the intent of enriching and obtaining a healthy product, isomaltulose could be added to fruits and vegetables by osmotic dehydration (OD) [8,9].

Heat transfer properties are essential for designing evaporation and heat exchange processes like pasteurization, sterilization, and temperature control of the own OD process [10]. Momentum transfer properties play an essential role in pumping and mixing processes [11]. Determining how these properties behave when temperature and concentration change provides useful information about the intermolecular interactions and the physicochemical phenomena involved in such carbohydrate solutions [12]. Moreover, their experimental determination in a wide range of solute concentrations and temperature serves as a database for scientific and industrial application, as the osmotic dehydration processes.

Mathematical models that comprise the effect of temperature and solute concentration for predicting properties have been used to represent aqueous carbohydrates solutions or carbohydrates-based foods [13,10,14]. They are responsible for providing ready-to-use data with high accuracy and allowing a better comprehension of the effects of the variables on each property. These facts highlight their essential role in representing experimental data for a given product.

Recently, Martins et al. [14] investigated the thermophysical properties of saturated sucrose and maltitol solutions. The study aimed to evaluate the behavior of these properties with temperature. Studies are scarce over a wide range of temperatures and concentrations in the

concerns of the thermophysical properties of isomaltulose solutions. To the best of our knowledge, the existing data are restricted to industries [15], or some are reported in narrower ranges of temperature (283.15–323.15 K) [16]. Thus, the study was focused on determining and evaluating the thermophysical properties (density, specific heat, thermal conductivity, and dynamic viscosity) of isomaltulose in the widest range of solute concentration (from 0.05 kg isomaltulose·kg solution^{-1} up to threshold isomaltulose solubility) at different working temperatures (273.15–353.15 K).

2 Material and Methods

2.1 Raw material and solution preparation

Isomaltulose (Palatinose®) (Beneo, Mannheim, German), with a molecular weight of 360.32 g·mol^{-1} (>99.0% purity), was dissolved in previously degassed distilled water at concentrations ranging from 0.05 kg isomaltulose·kg solution^{-1} to the threshold solubility at each working temperature. The conductivity of water used to prepare the solutions was 0.626 ± 0.004 W·m^{-1}·K^{-1} and measured specific resistance was 1.82 MΩ·cm. The isomaltulose was weighed in an analytical balance model AUX220 with an accuracy of 0.1 mg (Shimadzu, Kyoto, Japan). The isomaltulose solutions were maintained under stirring to ensure complete solubilization. Then, it was placed in sealed glass vials for the experimental procedures. All sample preparations were carried in triplicate at the working temperature at which each experimental condition was performed.

2.2 Experimental measurements

2.2.1 Isomaltulose Solubility (IS)

The *IS* solutions was determined according to Peres and Macedo [17] with adaptations. The solid-liquid equilibrium study was conducted under atmospheric pressure in jacketed glass cells with 100–150 mL capacity, coupled to a thermostatic bath to maintain the system in the isothermal conditions of 273.15–363.15 K. The cells were filled with water and, subsequently, an amount of isomaltulose was added in excess. Then, the cells were subjected to magnetic stirring for 12 h to maximize the solute transfer to the solvent. After this period, the agitation stopped, and the system was kept isothermal under rest for 24 h. After that, aliquots of 20 mL were removed from the side opening of the cells by using a plastic syringe. The aliquots were placed in a 25 mL flat-bottomed flask previously weighed through an analytical balance and

then sealed with a glass lid. After reaching room temperature in the desiccators, samples were weighed. The flasks were subjected to a vacuum oven-drying at 353.15 K. When the samples reached the constant weight and total water removal, the mass of isomaltulose soluble in water was determined.

The *IS* in mass fraction (kg isomaltulose·kg solution^{-1}) was calculated by the relation between the mass of isomaltulose after drying and the solution before drying.

2.2.2 Density (ρ)

The ρ (kg·m^{-3}) of the isomaltulose solutions was determined in a density meter (Anton Paar, DMA 4500M, Austria), which two integrated Pt 100 platinum thermometers provide the highest accuracy (0.01 K) of temperature control, previously calibrated with air and deionized water. The volume of sample used for the measurements was approximately 2 mL. Measurements with 0.1 kg·m^{-3} of uncertainty were carried out after establishing temperatures. The equipment was programmed to perform readings at temperatures between 273.15 K and 353.15 K, with intervals of 5 K. For the saturated conditions, a new sample was inserted, and measurements were taken at the temperature corresponding to the saturation point. The results, in triplicate, were transferred to the computer using a data acquisition system.

2.2.3 Specific heat capacity (c_p)

The c_p (kJ·kg^{-1}·K^{-1}) of the isomaltulose solutions was measured, in triplicate, using a differential scanning calorimeter (model DSC 8000, Perkin Elmer, Shelton, CT, USA). The temperature of the apparatus was previously calibrated with indium (melting point of 429.75 K, enthalpy of fusion ΔH_f = 28.45 kJ·kg^{-1}) at a heating rate of 10 K·min^{-1}. Nitrogen (99.5% purity) was used as the purge gas at a constant flow of ~20 mL·min^{-1}. Aluminum pans 24.01 ± 0.04 mg (ref. number 0219-0062, Perkin Elmer) were used as a baseline and also as a holder for samples and reference material (3 mm sapphire standard disks; ref. number 0219-1268, Perkin Elmer) [18]. Samples were sealed and weighed before and after experimental procedures to ensure the weight variations were not higher than 3%. Baseline, reference material, and samples were subjected to the following temperature program: isothermal at 273.15 K for 4 min, a heating rate of 10 K·min^{-1} until reaching 353.15 K, and kept isothermal for 4 min at this temperature. The procedures followed the ASTM-E1269 method (ASTM, 2005). The PYRIS 11.0 (Perkin Elmer) software was used to analyze and plot the thermal data. The c_p results of

the isomaltulose solution samples with 0.001 kJ·kg^{-1}·K^{-1} of uncertainty were calculated using Eq. (1)

$$c_p = D_S / W_s \theta \quad (1)$$

where c_p is the specific heat capacity (kJ·kg^{-1}·K^{-1}); D_s is the vertical displacement between the thermal curves of the sample and the reference material at a given temperature (mW); W_s is the sample mass (mg); and θ is the heating rate (K·s^{-1}).

2.2.4 Thermal conductivity (λ)

The same apparatus described by Martins et al. [10] was used for measuring, in triplicate, λ (W·m^{-1}·K^{-1}) of isomaltulose solutions. It consisted of a coaxial dual-cylinder device containing an inner resistance (220 mm-long and 10 mm-inner diameter), which provides a uniform heat flow. The samples were added into the annular space between the inner and outer cylinders (20 mm-inner, 24 mm-outer diameters, both with 220 mm-length). Both ends were sealed with nylon stoppers to prevent axial heat transfer [11]. Subsequently, the apparatus was immersed into the thermostatic bath (MA-184 model, Marconi, São Paulo, Brazil). The input power by resistance was controlled by a laboratory DC power supply MPS-3006D (Minipa, São Paulo, Brazil), which can adjust the current with a stability of 0.05%.

The temperature profile was monitored using a NI 9213 data logger (National Instruments, Austin, TX) and LabVIEW (National Instruments, Austin, TX) acquisition system. The temperatures were measured using four copper-constantan thermocouples fixed on the surfaces of the inner and outer cylinders. After reaching the steady-state heat conduction, the one-dimensional heat flow inside the cell was described by the Fourier equation in cylindrical coordinates, considering boundary conditions of constant temperature at the two concentric cylindrical surfaces. Thus, λ of the samples with 0.001 W·m^{-1}·K^{-1} of uncertainty could be calculated by Eq. (2) [19].

$$\lambda = q \frac{log\left(\frac{r_2}{r_1}\right)}{2\pi l\left(T_1 - T_2\right)} \quad (2)$$

where λ is the thermal conductivity (W·m^{-1}·K^{-1}); q is the heat flow in the thermal resistance (W); r_1 and r_2 are the external and internal radius of the cylinder (m), respectively; l is the cell

length (m); T_1 is the temperature of the inner cylinder (K); and T_2 is the temperature of the outer cylinder (K).

2.2.5 Dynamic viscosity (μ)

The μ (mPa·s) of the isomaltulose solutions was determined in triplicate at temperatures between 273.15 and 353.15 K, with a 5 K interval, using a stress-controlled rotational rheometer (AR-G2, TA Instruments, USA). The equipment was coupled with a concentric cylinder geometry (5920 μm gap). Aliquots (19.6 mL) of the different solutions were pipetted into the concentric cylinder cup, and an increasing shear rate ramp was established from 2.5 up to 315 s^{-1} at fixed temperature using the Rheology Advantage software version 5.7.1 (TA Instruments, USA) [20]. The corresponding shear stress (mPa) was acquired by the Universal Analysis 2000 data acquisition system (v. 4.7, TA Instruments, USA). The μ values could be measured with 0.001 mPa·s of uncertainty by the slope of the resulting flow curves for each temperature and concentration studied.

2.3 Mathematical modeling

Mathematical models, represented by Eq. (3)–(6), were fitted to the experimental properties of the aqueous isomaltulose solutions at range of solute concentration from 0.05 kg isomaltulose·kg solution^{-1} up to threshold isomaltulose solubility and temperature range from 273.15 to 353.15 K. These equations concern the effect of both temperature (T, K) and isomaltulose concentration (IC, kg·kg solution^{-1}) and were recently used by Martins et al. [10] to predict thermophysical properties of different carbohydrates solutions.

$$\beta = a + (bIC) + (cIC^2) + (dT) + (eT^2) + f(ICT) \quad (3)$$

$$\beta = a\,exp(b/RT)exp(cIC) \quad (4)$$

$$\beta = a\,exp(b/RT)IC^c \quad (5)$$

$$\beta = a(bIC)T^c \quad (6)$$

where β is the corresponding property; a, b, c, d, e, and f are the parameters of models; R is the gas constant (8.314 J·mol^{-1}·K^{-1}); T is the temperature (K); and IC is the isomaltulose concentration (kg of solute·kg of solution^{-1}). In Eq. (4) and (5), the parameter b corresponds to the activation energy (J·mol^{-1}). For equation (3), the means were subjected to the analysis of variance (ANOVA) to evaluate the significant effect (p_{value}<0.05) of isomaltulose concentration

and temperature on the analyzed property (ρ, c_p, λ, and μ) of the aqueous solutions. A resulting model was obtained for each property according to the significant effects.

The fitting procedure was performed using Statistica 10.0 software (StatSoft Inc., Tulsa, USA) and the Levenberg-Marquardt algorithm with a convergence criterion of 10^{-6}.

The accuracy of fit was assessed using the determination coefficient (R^2) and mean relative error (p). They are represented by the following Eq. (7) and Eq. (8), respectively:

$$R^2 = 1 - \left(SS_{res} / SS_{tot}\right) \tag{7}$$

$$p = \frac{100}{N} \sum_{i=1}^{N} \frac{\left|\beta_p - \beta_e\right|}{\beta_e} \tag{8}$$

where R^2 is determination coefficient; SS_{res} is the residual sum of squares; SS_{tot} is the total sum of squares (proportional to the variance of the data); p is the mean relative error; β_p is the predicted property; β_e is the experimental property, and N is the number of experimental determinations. The models that resulted in R^2 values close to 1 and p<10% were considered effective for practical purposes [21,22].

3. Results and discussion

3.1 Isomatulose Solubility (IS)

The experimental values of *IS* are shown in Table 1. The *IS* in aqueous solutions ranged from 0.2328 to 0.7278 kg of solute·kg of solution^{-1} in the range of temperature assessed (273.15–363.15 K).

Solubility plays an important role in the product preparation to avoid the exceeding use of solute and its consequent precipitation. Moreover, understanding how solubility is affected by temperature is particularly interesting in several processes as osmotic dehydration. It is attributed to the fact that controlling heating and cooling processes may favor or prevent a particular component from precipitating when working at the threshold concentration [23]. In which concerns the isomaltulose industrial processing, this carbohydrate goes through several separation processes to be purified. In these processes, isomaltulose crystallization cycles are the main vital steps. For this reason, it is necessary to determine the solubility of isomaltulose in potential solvents [16] – being water the most used universal solvent in food processes.

Table 1. Isomaltulose solubility (*IS*) and sucrose solubility (*SS*).

Temperature (K)	*IS* (kg isomaltulose·kg solution^{-1})	*IS* (kg isomaltulose·kg solution^{-1})[a]	*IS* (kg isomaltulose·kg solution^{-1})[b]	*SS* (kg sucrose·kg solution^{-1})[c]
273.15	0.2328±0.002	-	-	0.6440
278.15	0.2319±0.006	-	-	0.6481
283.15	0.2393±0.004	0.2684	0.2336	0.6532
288.15	0.2545±0.003	-	-	0.6592
293.15	0.2766±0.003	0.3258	0.2930	0.6660
298.15	0.3044±0.002	-	-	0.6735
303.15	0.3367±0.003	0.3824	0.3482	0.6818
308.15	0.3720±0.002	-	-	0.6907
313.15	0.4092±0.001	0.4629	0.4048	0.7001
318.15	0.4470±0.004	-	-	0.7100
323.15	0.4846±0.008	0.5532	0.4735	0.7204
328.15	0.5213±0.006	-	-	0.7310
333.15	0.5567±0.004	-	-	0.7420
338.15	0.5902±0.004	-	-	0.7532
343.15	0.6218±0.002	-	-	0.7645
348.15	0.6514±0.003	-	-	0.7759
353.15	0.6788±0.002	-	-	0.7874
358.15	0.7042±0.004	-	-	0.7987
363.15	0.7278±0.002	-	-	0.8100

[a]Song et al. (2019); [b]Schiweck (1980); [c]Mullin (1993) and Norrish (1967); Mean values ± standard deviation of the triplicate.

The experimental *IS* values were shown to be positively related to temperature (p_{value}<0.05). Figure 1 represents the trend of isomaltulose solubility values with temperature in an endothermic process. According to Song et al. [16], isomaltulose solubility in water was relatively higher than in other solvents, e.g., methanol, ethanol, isopropanol, and acetone, probably due to the higher polarity of water – characterized by higher dielectric constant – in comparison with these solvents. It occurs due to the presence of large dipole moments in isomaltulose, which offers stronger non-specific dipole−dipole interactions with the water to form hydrogen bonds. Thus, besides being considered the most suitable solvent in the purification and separation process of isomaltulose, water is a food-grade ingredient that can be used as a transporting medium by osmotic dehydration processes. It could be seen that isomaltulose could reach a higher concentration in water, which makes it possible to work under higher driving forces for mass transfer to promote water removal and solids incorporation.

Table 1 also compares the isomaltulose solubility with data previously reported in the literature for isomaltulose itself and sucrose as a commonly used carbohydrate for food applications. Compared to the present study, the slight differences in the isomaltulose solubility reported by Song et al. [16] and Schiweck [24] can be attributed to the measuring method. The low relative difference observed (<18% in Song et al. [16] and <6% in Schiweck [24]) makes the experimental data of the present work reliable and applicable in the wider range of temperatures. It can also be observed that the isomaltulose solubility of ~11–64% is lower than sucrose, being this difference reduced with temperature. This behavior could be due to the difference in the heat of the solution of the carbohydrates. Being the heat of solution, the enthalpy associated with dissolution, a dissolution process could be explained by an energetic point of view by establishing new interactions between solute and solvent [25]. As seen as the heat solution of isomaltulose crystal (23.46 kJ·mol^{-1}) is higher compared to sucrose crystal (6.22 kJ·mol^{-1}), so the former demands more energy to be dissolved and, consequently, the dissolution process is facilitated under higher temperature [15]. Maugeri et al. [26] suggested that carbohydrates can present different physicochemical properties despite having very similar molecular structures. It agrees with the findings, which reported different solubilities even though sucrose and isomaltulose are isomers

.

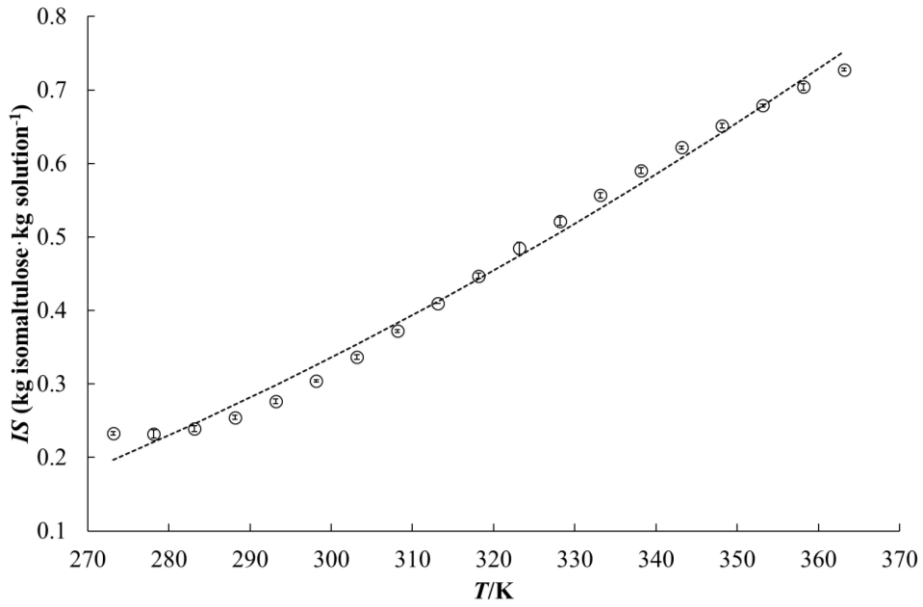

Fig. 1. Variation of isomaltulose solubility (*IS*) with temperature (*T*). The dashed line represents the fitted Eq. (3).

Table 3 presents the fitting parameters of the generic polynomial model (Eq. (3)) to the experimental solubility data of the isomaltulose solutions. According to Crestani et al. [27], the solubility of carbohydrates in aqueous solutions can be represented by polynomial equations, as recommended by the International Commission for Uniform Methods of Sugar Analysis (ICUMSA). After the analysis of variance (ANOVA), the linear and quadratic terms accompanying the temperature were significant at 95% of confidence. So, the fitted Eq. (3) could be represented in Figure 1 with good predictability of the experimental data (R^2>0.99 and p<3.91%) at the temperature range from 273.15 to 363.15 K.

3.2 Density (ρ)

Means and standard deviation for ρ values ranged from 978.3 up to 1198.8 kg·m^{-3} in the temperature interval studied (Table 2). According to the data shown in Figure 2A, ρ increased non-linearly with isomaltulose concentration (p_{value}<0.05). Martins et al. [10] stated that it is a consequence of the partial replacement of water molecules by the corresponding carbohydrate in solution. As the isomaltulose concentration is close to the threshold solubility, ρ was closer to the sucrose solutions [10,28,29,30]. However, slightly higher density values are still observed for sucrose solutions [31]. It means that, for the same solute concentration, sucrose solutions demand more energy to be mixed and pumped when compared to isomaltulose solutions – highlighting the advantage of using the latter in terms of energy expenses.

The linear decrease in density values as the temperature increase may be related to the agitation level of the molecules (Figure 2B). Polachini et al. [20] stated that molecules in solution tend to move away from each other at higher temperatures, and this behavior leads to a volume expansion and ρ to decrease.

The ρ is associated with several unit operations as pumping and evaporation what makes the evaluation of ρ required [10].

As observed by the analysis of variance, a generic polynomial model could be obtained concerning the significant parameters that influence density behavior (Eq. 3). Table 3 presents the fitting parameters of the Eq. (3) and the fitting parameters of the Eqs. (4)–(6) to comprise the simultaneous influence of the temperature and solute concentrations in the density values.

Although all of them were able to predict with good accuracy (R^2 ≥0.844 and p≤1.49%), from 0.05 kg isomaltulose·kg solution^{-1} up to threshold isomaltulose solubility and temperature range

from 273.15 to 353.15 K, the experimental density of the isomaltulose solutions according to the solute concentration and temperature, the fitted Eq. (3) showed the best determination coefficient (R^2) and lower mean relative error (p).

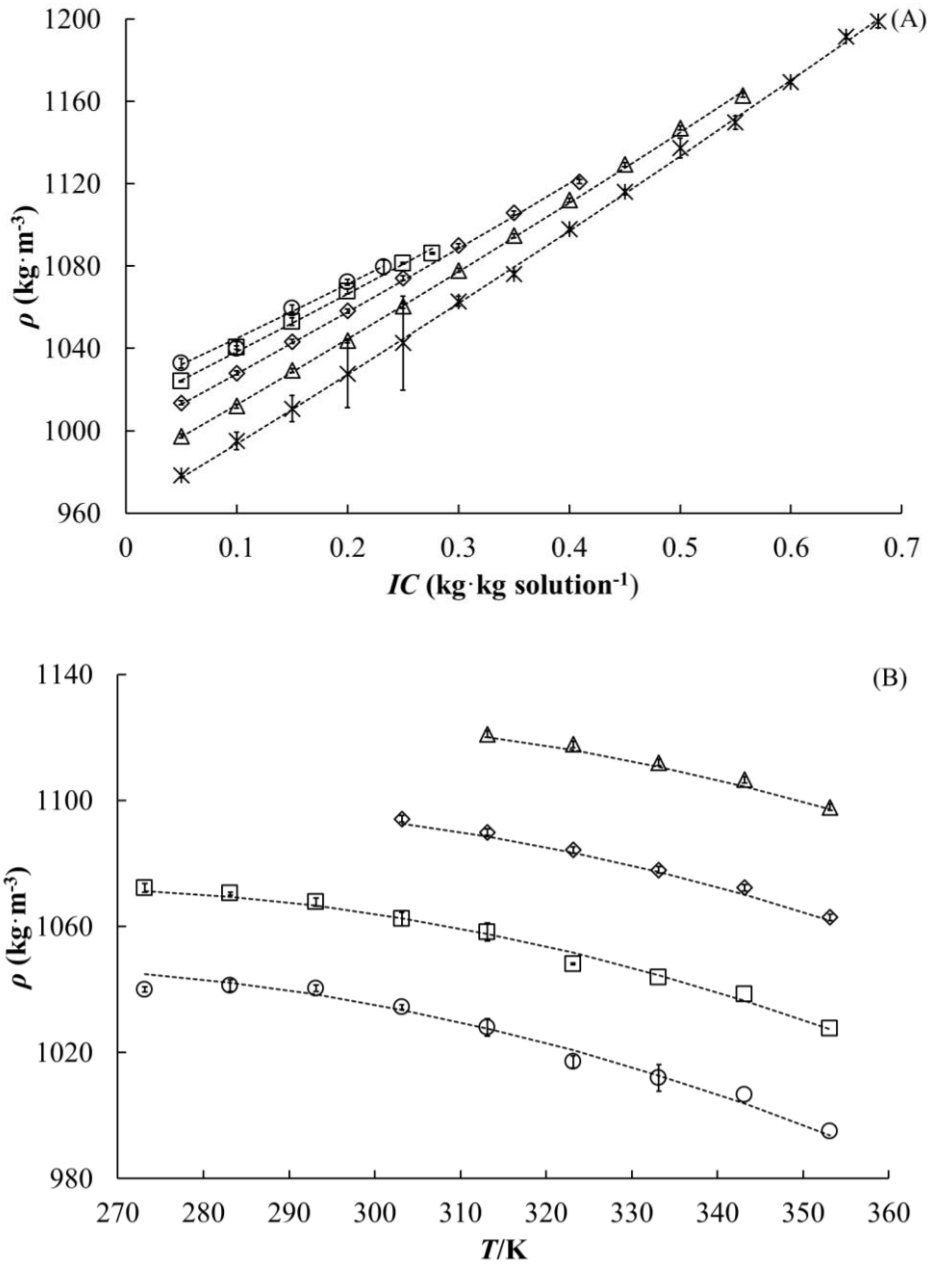

Fig. 2. (A) Mean experimental density (ρ) for isomaltulose solutions as function of isomaltulose concentration (*IC*) ((○) 273.15 K; (□) 293.15 K; (◇) 313.15 K; (△) 333.15 K ; (∗) 353.15 K). (B) Mean experimental ρ for isomaltulose solutions as function of temperature (*T*) ((○) 0.1 kg·kg solution^{-1}; (□) 0.2 kg·kg solution^{-1}; (◇) 0.3 kg·kg solution^{-1}; (△) 0.4 kg·kg solution^{-1}) with standard deviations bars. Dashed lines represent the fitted Eq. (3).

3.3 Specific heat capacity (c_p)

The values of c_p for isomaltulose solution and standard deviation are presented in Table 2. It ranged from 2.977 to 4.052 kJ·kg^{-1}·K^{-1}. The c_p increased with temperature and decreased with isomaltulose concentration. Although the c_p was similar to the ones reported in the literature for other carbohydrate solutions, slightly higher c_p values were found for sucrose solutions at similar conditions of temperature and solute concentration [10,32,33] in comparison with isomaltulose solutions. In this sense, isomaltulose solutions require slightly less energy than sucrose solutions for altering temperature in industrial processes. Thus, besides the health-promoting benefits of isomaltulose, its use in sucrose replacement might reduce the energy costs in processes that deal with temperature control [4].

The heat transfer process is essential in several food applications, from ingredient production to the product's final quality. It is reported to be crucial for processing the carbohydrate itself, syrups, juices, and beverages and in related areas such as osmotic dehydration [34]. Accurate, specific heat values are a must for designing heat loads, holding times, and equipment as they are strongly influenced by the heat capacity of a given product [32].

The experimental c_p values in Figure 3A showed that diluted solutions tend to demand more energy to increase the temperature than the same mass of the more concentrated one. This required energy rises slightly as the solution temperature increases during a given process [34]. At low solute concentrations (0.05 kg isomaltulose·kg solution^{-1}), c_p tends to increase until reaching similar values to pure water. At constant temperature, the c_p decreased quadratically (p_{value}<0.05) with increasing the isomaltulose concentration, being this trend more pronounced above 313.15 K. It is associated with the decrease in the vapor pressure of the solution and reduction in solution water content under high solute concentrations [32].

The increase of the c_p occurred linearly as the temperature increased (p_{value}<0.05) (Figure 3B). Similar behavior was found in other studies, which reported linear variations in the specific

heat of different food products above the freezing point [35,36,37]. In general, c_p is less affected by temperature when compared to solute concentration [32]. According to these results, the generic Eq. (3) was successfully obtained with the significant parameters while the Eqs. (4) and (6) could also be used as alternatives to represent the experimental c_p values (all of them with $R^2 \geq 0.998$ and $p \leq 0.238\%$) from 0.05 kg isomaltulose·kg solution^{-1} up to threshold isomaltulose solubility and temperature range from 273.15 to 353.15 K.

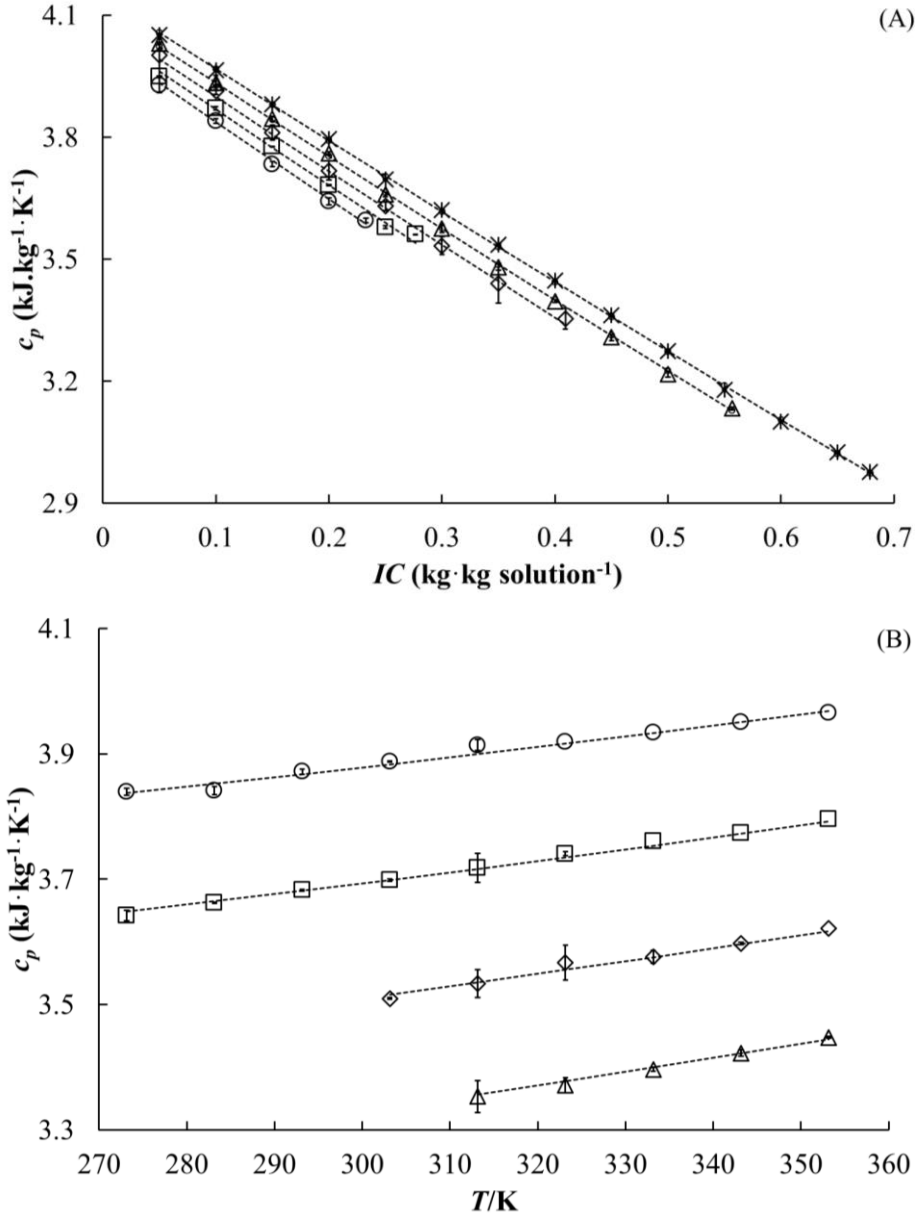

Fig. 3. (A) Mean experimental specific heat capacity (c_p) for isomaltulose solutions as function of isomaltulose concentration (*IC*) ((○) 273.15 K; (□) 293.15 K; (◇) 313.15 K; (△) 333.15 K ; (∗) 353.15 K). (B) Mean experimental c_p for isomaltulose solutions as function of temperature (*T*) ((○) 0.1 kg·kg solution^{-1}; (□) 0.2 kg·kg solution^{-1}; (◇) 0.3 kg·kg solution^{-1}; (△) 0.4 kg·kg solution^{-1}) with standard deviations bars**.** Dashed lines represent the fitted Eq. (3).

3.4 Thermal conductivity (λ)

The mean experimental values of λ ranged from 0.403 up to 0.610 $W \cdot m^{-1} \cdot K^{-1}$. (Table 2). These values were decreasing with isomaltulose concentration. The carbohydrate acted as a barrier against the thermal conduction what explains the decrease of λ with isomaltulose concentration (Figure 4A) [38]. This behavior was quadratic and similar to other carbohydrates solutions (glucose and sucrose) and fruits juices [38,31]. The slight increase in λ with temperature is associated with the higher degree of molecular agitation, and consequently, the higher energy required for promoting heat conduction through the solution (Figure 4B). This slight linear increase caused the values to increase up to 2% at the same solute concentration (Table 2).

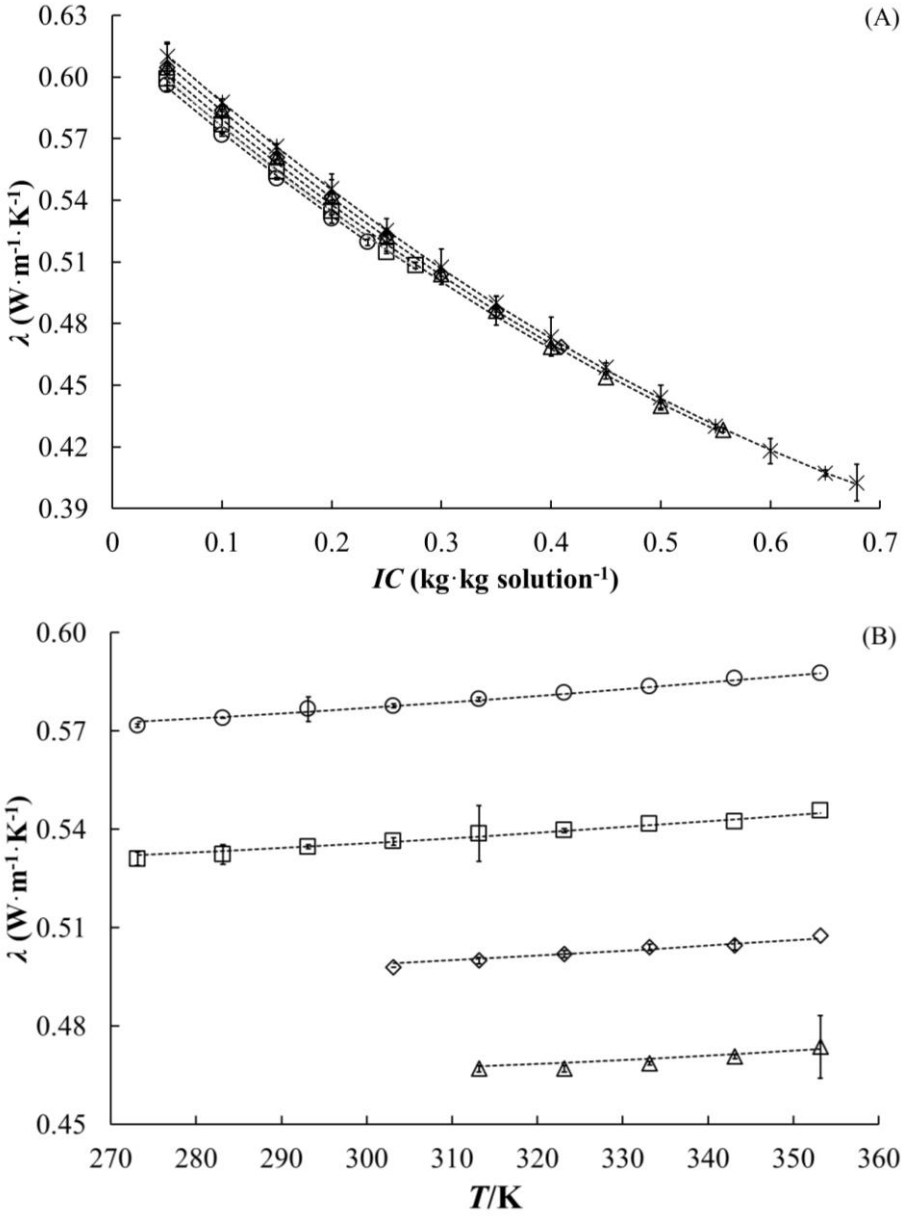

Fig. 4. (A) Mean experimental thermal conductivity (λ) for isomaltulose solutions as function of isomaltulose concentration (*IC*) ((○) 273.15 K; (□) 293.15 K; (◇) 313.15 K; (△) 333.15 K; (∗) 353.15 K). (B) Mean experimental λ for isomaltulose solutions as function of temperature (*T*) ((○) 0.1 kg·kg solution^{-1}; (□) 0.2 kg·kg solution^{-1}; (◇) 0.3 kg·kg solution^{-1}; (△) 0.4 kg·kg solution^{-1}) with standard deviations bars. Dashed lines represent the fitted Eq. (3).

Knowledge about the thermal conductivity of food is important for the process and equipment design and for predicting and controlling various thermal changes occurring in food during thermal processing such as pasteurization, concentration, drying, cooling, transportation, storage, and cooking.

Slightly higher values were observed in the present study for isomaltulose when compared to the ones reported for sucrose solutions and other carbohydrate-based food products, including fruit juices, under similar conditions [10,33,38,39,40]. These results showed that isomaltulose solutions conduct thermal energy better than sucrose solutions.

The generic Eq. (3) fitting parameters could be obtained with good accuracy based on the significant parameters from 0.05 kg isomaltulose·kg solution^{-1} up to threshold isomaltulose solubility and temperature range from 273.15 to 353.15 K. Similarly, Eqs. (4)–(6) were also able to represent the experimental thermal conductivity values of isomaltulose solution according to temperature and solute concentration ($R^2 \geq 0.902$ and $p \leq 2.973\%$).

3.5 Dynamic viscosity (μ)

Data of shear stress and the shear rate was plotted for each isomaltulose solution at the corresponding temperature. It was showed a linear dependence of the shear stress by the shear rate ($R^2 > 0.999$), which means that the isomaltulose solutions presented Newtonian behavior for the studied range of solute concentration and temperature. Thus, the μ could be obtained by the slope of the corresponding rheograms. The mean experimental values ranged from 0.169 up to 7.218 mPa·s (Table 2). The μ increased with isomaltulose concentration (Figure 5A) and decreased with temperature (Figure 5B) in a non-linear manner ($p_{value} < 0.05$). In general, experimental values of μ were in close agreement with reports for other sugar solutions [41,15]. In which concerns the increase of solute concentration, many studies reported the increased viscosity as the food products are more concentrated in carbohydrates. It is the case of fruit

juices, syrups, and many others [42,43,44,45]. The increase in the carbohydrate concentration creates more hydrogen bonds in the solution, making the intermolecular interactions higher. The enhanced chemical interaction increases the cohesive forces among the molecules and so the friction forces that maintained the fluid layer together during the flow. The higher the solute concentration, the more difficult it is to overcome the frictional resistance and chemical interaction that holds molecules together.

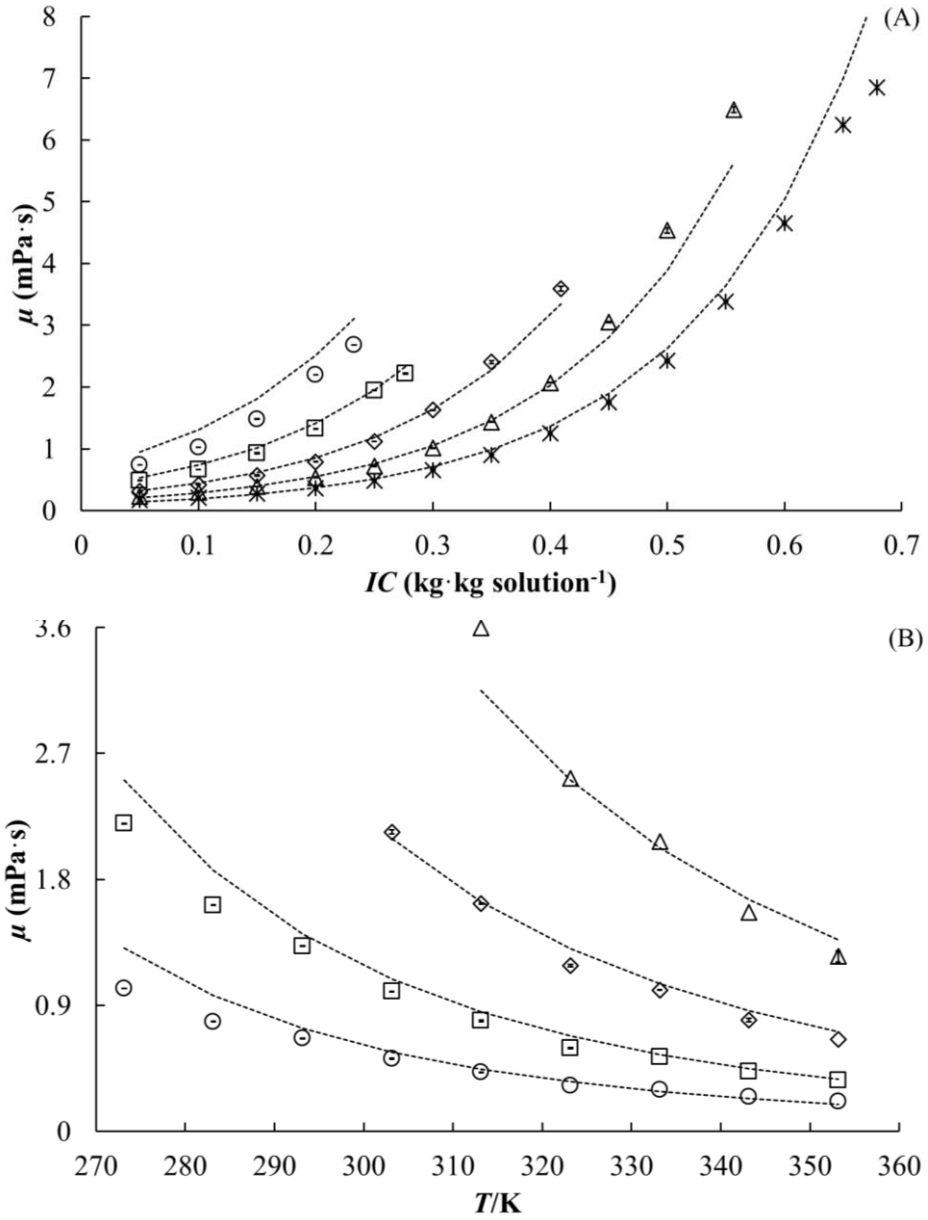

Fig. 5. (A) Mean experimental dynamic viscosity (μ) for isomaltulose solutions as function of isomaltulose concentration (*IC*) ((○) 273.15 K; (□) 293.15 K; (◇) 313.15 K; (△) 333.15 K; (∗) 353.15 K). (B) Mean experimental μ for isomaltulose solutions as function of temperature (*T*) ((○) 0.1 kg·kg solution^{-1}; (□) 0.2 kg·kg solution^{-1}; (◇) 0.3 kg·kg solution^{-1}; (△) 0.4 kg·kg solution^{-1}) with standard deviations bars. Dashed lines represent the fitted Eq. (4).

When the temperature increases, the agitation degree of the molecules also becomes higher [20]. It means that the intermolecular forces among them and, consequently, the fluid resistance against the flow are decreased in these conditions. In addition to an enhanced diffusion coefficient, working under temperatures makes the fluid transport easier – demanding less energy for pumping/mixing while the external resistance for mass transfer is reduced.

In general, the μ of isomaltulose solutions are slightly lower than for sucrose solutions [45]. However, above 45 °C and 0.4 kg of isomaltulose·kg of the solution^{-1}, the flow resistance of isomaltulose in an aqueous solution tends to be slightly higher than for sucrose. After reaching this solute concentration, the effect of the molecular interactions becomes more noticeable. The isomerase reaction that converts sucrose into isomaltulose rearranges the fructose and glucose monomers so that the hydroxyl groups in isomaltulose are more available for creating hydrogen bonds. The reduced steric hindrance for occurring hydrogen bonds allows the isomaltulose molecules to better interact among themselves and with the water molecules, leading to a slightly increased viscosity at similar conditions [46]. Thus, for isomaltulose in concentrations below 40% and up to 45 °C is possible to use the same equipment and industrial working conditions as conventional sucrose solutions.

The models represented by Eqs. (4) and (6) had good fitting accuracy ($R^2 \geq 0.976$ and $p \leq 8.017$) from 0.05 kg isomaltulose·kg solution^{-1} up to threshold isomaltulose solubility and temperature range from 273.15 to 353.15 K. It is consolidated that an Arrhenius exponential-type equation commonly represents dynamic viscosity. This type of equation provides essential information about the activation energy, which allows evaluating the viscosity dependence on temperature for each solution. Further approaches tended to represent the activation energy by an equation that relates viscosity with both temperature and solids concentration [47]. By comparing Eq. (4) and (5), the first could better represent experimental viscosity with adequate accuracy. The corresponding *b* values, representing the activation energy (J·mol^{-1}), are following the ones reported for other carbohydrate solutions as sucrose, glucose, and fructose [45] and fruits juices

as sour cherry [48], merlot grape [49], pomegranate [50]; although these studies evaluated the activation energy by independent equations as functions of temperature exclusively.

Table 2. Density (ρ), specific heat capacity (c_p), thermal conductivity (λ), and dynamic viscosity (μ) of the isomaltulose solutions at different temperatures (T) and isomaltulose concentration (IC).

T (K)	IC (kg·kg solution^{-1})	ρ (kg·m^{-3})	c_p (kJ·kg^{-1}·K^{-1})	λ (W·m^{-1}·K^{-1})	μ (mPa·s)
273.15	0.0500	1032.8±2.4	3.928±0.018	0.596±0.003	0.739±0.001
	0.1000	1040.0±3.4	3.840±0.006	0.572±0.001	1.022±0.001
	0.1500	1059.5±1.7	3.734±0.006	0.551±0.001	1.483±0.002
	0.2000	1072.2±1.4	3.642±0.009	0.531±0.002	2.199±0.002
	0.2328	1079.4±3.6	3.596±0.006	0.520±0.002	2.683±0.002
278.15	0.0500	1030.3±2.6	3.951±0.006	0.596±0.005	0.675±0.001
	0.1000	1042.6±1.3	3.848±0.001	0.572±0.001	0.926±0.003
	0.1500	1057.8±1.8	3.750±0.002	0.553±0.003	1.332±0.003
	0.2000	1069.9±1.7	3.645±0.005	0.531±0.001	1.956±0.006
	0.2319	1076.9±0.7	3.607±0.005	0.521±0.001	2.359±0.008
283.15	0.0500	1030.8±0.2	3.959±0.003	0.595±0.004	0.577±0.001
	0.1000	1041.3±0.6	3.841±0.007	0.574±0.001	0.784±0.001
	0.1500	1057.5±0.2	3.759±0.006	0.553±0.001	1.112±0.001
	0.2000	1070.4±0.5	3.662±0.001	0.532±0.003	1.615±0.002
	0.2393	1078.8±1.2	3.589±0.009	0.520±0.004	2.053±0.001
288.15	0.0500	1027.7±1.4	3.949±0.001	0.598±0.001	0.543±0.002
	0.1000	1041.5±3.6	3.863±0.001	0.575±0.002	0.743±0.001
	0.1500	1054.6±1.2	3.759±0.002	0.554±0.002	1.044±0.004
	0.2000	1069.3±2.6	3.670±0.002	0.534±0.004	1.504±0.012
	0.2545	1082.3±3.5	3.584±0.008	0.516±0.002	2.141±0.007
293.15	0.0500	1024.0±0.2	3.949±0.001	0.599±0.003	0.488±0.001
	0.1000	1040.4±0.8	3.872±0.004	0.577±0.004	0.664±0.002
	0.1500	1060.0±1.9	3.777±0.001	0.554±0.001	0.926±0.010
	0.2000	1067.7±1.3	3.682±0.001	0.535±0.001	1.323±0.002
	0.2500	1081.3±0.5	3.579±0.004	0.515±0.001	1.944±0.004
	0.2766	1086.1±0.5	3.561±0.001	0.508±0.002	2.219±0.012
298.15	0.0500	1021.6±2.2	3.954±0.026	0.599±0.013	0.438±0.001
	0.1000	1038.1±2.2	3.882±0.011	0.576±0.002	0.591±0.001
	0.1500	1050.9±4.2	3.777±0.006	0.555±0.003	0.818±0.003
	0.2000	1065.8±7.9	3.680±0.014	0.535±0.003	1.159±0.003
	0.2500	1079.6±11.8	3.594±0.017	0.516±0.008	1.687±0.003
	0.3044	1092.8±2.4	3.503±0.003	0.499±0.003	2.394±0.002
303.15	0.0500	1019.9±0.3	3.982±0.010	0.602±0.002	0.386±0.001
	0.1000	1034.4±1.8	3.888±0.001	0.578±0.001	0.519±0.004
	0.1500	1048.7±1.5	3.793±0.007	0.557±0.001	0.709±0.005

	0.2000	1062.4±2.1	3.699±0.002	0.536±0.001	0.999±0.002
	0.2500	1079.2±0.7	3.599±0.002	0.516±0.001	1.441±0.003
	0.3000	1094.2±0.3	3.510±0.002	0.498±0.001	2.139±0.016
	0.3367	1102.0±0.1	3.459±0.006	0.490±0.003	2.636±0.022
308.15	0.0500	1016.3±3.5	3.994±0.057	0.600±0.004	0.355±0.002
	0.1000	1029.8±3.0	3.895±0.012	0.579±0.003	0.474±0.009
	0.1500	1046.1±2.6	3.802±0.021	0.558±0.003	0.642±0.001
	0.2000	1059.6±1.2	3.702±0.024	0.537±0.001	0.902±0.003
	0.2500	1075.4±0.8	3.615±0.015	0.517±0.003	1.289±0.006
	0.3000	1091.8±0.4	3.526±0.041	0.500±0.004	1.887±0.036
	0.3500	1107.6±0.9	3.428±0.050	0.482±0.001	2.814±0.047
	0.3720	1111.0±0.9	3.400±0.035	0.478±0.005	3.085±0.007
313.15	0.0500	1013.6±1.0	4.002±0.052	0.604±0.012	0.318±0.001
	0.1000	1028.0±1.0	3.914±0.009	0.580±0.001	0.422±0.001
	0.1500	1043.3±2.1	3.811±0.019	0.559±0.002	0.569±0.006
	0.2000	1058.2±2.9	3.718±0.023	0.539±0.009	0.790±0.007
	0.2500	1074.1±0.5	3.631±0.012	0.518±0.009	1.119±0.003
	0.3000	1089.9±0.8	3.533±0.022	0.500±0.001	1.628±0.004
	0.3500	1105.8±0.5	3.440±0.048	0.483±0.007	2.405±0.024
	0.4092	1121.0±1.7	3.353±0.026	0.467±0.001	3.595±0.038
318.15	0.0500	1010.2±0.3	4.003±0.009	0.604±0.002	0.295±0.001
	0.1000	1025.1±1.9	3.910±0.003	0.580±0.001	0.388±0.008
	0.1500	1039.9±0.3	3.819±0.002	0.560±0.001	0.522±0.007
	0.2000	1055.3±0.1	3.727±0.006	0.539±0.001	0.719±0.007
	0.2500	1071.0±0.2	3.635±0.005	0.519±0.002	1.010±0.005
	0.3000	1087.1±1.3	3.543±0.007	0.500±0.001	1.448±0.029
	0.3500	1103.7±0.3	3.444±0.004	0.484±0.002	2.127±0.033
	0.4000	1119.8±0.1	3.359±0.002	0.467±0.001	3.187±0.010
	0.4470	1131.3±2.2	3.296±0.019	0.456±0.001	4.267±0.058
323.15	0.0500	1005.2±0.6	3.983±0.007	0.603±0.001	0.248±0.001
	0.1000	1017.1±0.7	3.919±0.021	0.582±0.001	0.327±0.002
	0.1500	1037.5±2.4	3.829±0.017	0.559±0.001	0.431±0.001
	0.2000	1048.1±0.2	3.741±0.003	0.540±0.001	0.593±0.004
	0.2500	1065.6±0.2	3.638±0.022	0.520±0.003	0.827±0.003
	0.3000	1084.3±1.2	3.567±0.028	0.502±0.001	1.185±0.008
	0.3500	1100.7±0.8	3.475±0.016	0.484±0.002	1.695±0.002
	0.4000	1117.8±1.2	3.372±0.012	0.467±0.001	2.522±0.009
	0.4500	1134.5±0.2	3.286±0.015	0.452±0.001	3.826±0.052
	0.4846	1142.0±0.4	3.241±0.005	0.446±0.001	4.605±0.015
328.15	0.0500	1003.9±10.6	4.010±0.003	0.606±0.003	0.245±0.001
	0.1000	1016.3±6.0	3.920±0.008	0.583±0.001	0.321±0.010
	0.1500	1033.7±7.8	3.836±0.006	0.561±0.001	0.421±0.012
	0.2000	1043.7±2.0	3.746±0.007	0.540±0.003	0.576±0.003
	0.2500	1064.9±2.4	3.655±0.002	0.521±0.003	0.796±0.004
	0.3000	1084.0±3.2	3.562±0.001	0.504±0.001	1.129±0.037
	0.3500	1089.3±11.4	3.468±0.003	0.485±0.002	1.601±0.047

	0.4000	1121.7±8.5	3.384±0.006	0.468±0.001	2.358±0.018
	0.4500	1132.9±10.7	3.293±0.004	0.454±0.001	3.512±0.019
	0.5000	1150.4±12.1	3.204±0.004	0.438±0.001	5.316±0.022
	0.5213	1135.9±18.2	3.185±0.015	0.437±0.002	5.712±0.032
333.15	0.0500	997.4±2.1	4.031±0.003	0.605±0.001	0.228±0.004
	0.1000	1012.0±2.8	3.934±0.018	0.584±0.003	0.296±0.001
	0.1500	1029.2±1.6	3.845±0.006	0.561±0.001	0.391±0.002
	0.2000	1043.8±1.4	3.760±0.004	0.542±0.002	0.530±0.001
	0.2500	1060.5±2.6	3.659±0.006	0.523±0.001	0.722±0.014
	0.3000	1077.9±0.7	3.576±0.010	0.504±0.001	1.010±0.003
	0.3500	1094.8±2.5	3.481±0.008	0.486±0.001	1.436±0.009
	0.4000	1112.0±0.7	3.397±0.004	0.469±0.001	2.069±0.005
	0.4500	1129.3±2.3	3.308±0.007	0.454±0.001	3.050±0.012
	0.5000	1147.0±2.3	3.217±0.007	0.440±0.001	4.538±0.043
	0.5567	1163.0±2.6	3.133±0.004	0.428±0.001	6.495±0.047
338.15	0.0500	993.3±1.8	4.031±0.010	0.606±0.001	0.206±0.001
	0.1000	1006.7±1.9	3.933±0.001	0.585±0.001	0.266±0.001
	0.1500	1021.7±1.4	3.853±0.002	0.563±0.001	0.350±0.002
	0.2000	1032.5±1.1	3.766±0.003	0.543±0.001	0.467±0.001
	0.2500	1045.9±0.7	3.677±0.008	0.523±0.001	0.636±0.001
	0.3000	1075.2±0.2	3.585±0.002	0.505±0.002	0.883±0.001
	0.3500	1091.6±0.4	3.500±0.004	0.488±0.001	1.247±0.008
	0.4000	1108.9±0.5	3.411±0.024	0.471±0.001	1.776±0.001
	0.4500	1126.4±0.1	3.326±0.008	0.456±0.001	2.561±0.018
	0.5000	1141.8±1.9	3.235±0.002	0.441±0.001	3.726±0.007
	0.5500	1164.0±2.1	3.143±0.001	0.427±0.001	5.559±0.018
	0.5902	1172.8±0.7	3.095±0.004	0.420±0.001	6.930±0.021
343.15	0.0500	986.2±0.2	4.038±0.009	0.605±0.004	0.191±0.001
	0.1000	1004.2±2.3	3.951±0.014	0.586±0.004	0.246±0.004
	0.1500	1018.7±0.5	3.862±0.004	0.563±0.001	0.320±0.004
	0.2000	1038.5±1.2	3.774±0.003	0.542±0.001	0.428±0.006
	0.2500	1053.7±0.6	3.681±0.011	0.524±0.001	0.574±0.003
	0.3000	1072.3±1.0	3.597±0.002	0.505±0.002	0.795±0.013
	0.3500	1085.2±0.2	3.507±0.007	0.486±0.004	1.105±0.013
	0.4000	1106.6±0.1	3.423±0.005	0.471±0.001	1.565±0.002
	0.4500	1120.7±1.9	3.334±0.007	0.456±0.001	2.248±0.027
	0.5000	1141.3±0.2	3.246±0.002	0.441±0.001	3.213±0.020
	0.5500	1160.2±0.2	3.163±0.021	0.428±0.001	4.659±0.040
	0.6000	1176.3±0.2	3.062±0.021	0.416±0.001	6.694±0.021
	0.6218	1183.4±0.7	3.053±0.005	0.414±0.001	7.218±0.042
348.15	0.0500	983.6±0.2	4.046±0.004	0.610±0.002	0.179±0.001
	0.1000	999.7±1.1	3.959±0.004	0.587±0.003	0.227±0.001
	0.1500	1015.9±1.9	3.871±0.008	0.565±0.004	0.295±0.003
	0.2000	1031.6±1.8	3.783±0.008	0.544±0.002	0.390±0.001
	0.2500	1049.2±1.5	3.697±0.012	0.525±0.009	0.525±0.001
	0.3000	1066.6±0.4	3.613±0.021	0.507±0.005	0.715±0.002

	0.3500	1084.1±0.3	3.523±0.007	0.489±0.003	0.988±0.011
	0.4000	1100.8±0.1	3.435±0.004	0.472±0.003	1.385±0.001
	0.4500	1119.9±1.9	3.359±0.020	0.458±0.002	1.967±0.008
	0.5000	1137.0±0.2	3.261±0.003	0.442±0.001	2.762±0.025
	0.5500	1154.2±0.4	3.173±0.008	0.429±0.008	3.932±0.027
	0.6000	1175.5±0.4	3.087±0.021	0.418±0.011	5.518±0.038
	0.6514	1190.7±0.7	3.019±0.003	0.408±0.002	7.201±0.068
353.15	0.0500	978.3±1.0	4.052±0.001	0.610±0.007	0.169±0.001
	0.1000	995.0±4.2	3.966±0.005	0.588±0.002	0.214±0.001
	0.1500	1010.8±6.4	3.882±0.001	0.566±0.001	0.277±0.001
	0.2000	1027.6±16.3	3.796±0.002	0.546±0.007	0.364±0.004
	0.2500	1042.6±22.8	3.696±0.001	0.525±0.001	0.487±0.002
	0.3000	1062.9±2.3	3.622±0.001	0.508±0.009	0.657±0.005
	0.3500	1076.2±1.2	3.536±0.002	0.490±0.003	0.900±0.001
	0.4000	1097.8±0.9	3.448±0.002	0.474±0.010	1.249±0.004
	0.45000	1116.0±1.2	3.363±0.003	0.459±0.002	1.752±0.014
	0.5000	1137.4±4.8	3.274±0.002	0.444±0.006	2.423±0.008
	0.5500	1149.7±3.3	3.180±0.001	0.430±0.001	3.388±0.003
	0.6000	1169.3±0.9	3.101±0.001	0.418±0.006	4.649±0.014
	0.6500	1191.4±1.1	3.025±0.002	0.407±0.002	6.246±0.016
	0.6788	1198.8±3.1	2.977±0.001	0.403±0.009	6.851±0.031

Mean values ± standard deviation of the triplicate.

Table 3. Fitting parameters of the mathematical models for isomaltulose solubility (*IS*), density (ρ), specific heat capacity (c_p), and thermal conductivity (λ) of isomaltulose solutions.

Property	Parameter	Equation			
		Eq. (3)			
***IS* (kg·kg solution^{-1})**	***a***	0.079			
	b	-			
	c	-			
	d	-0.004			
	e	1.6×10^{-5}			
	f	-			
	R²	0.991			
	***p* (%)**	3.908			
		Eq. (3)	**Eq. (4)**	**Eq. (5)**	**Eq. (6)**
ρ (kg·m^{-3})	***a***	718.486	836.051	1081.748	2664.537
	b	NS	444.383	234.761	0.307
	c	40.059	0.307	0.062	-0.172
	d	2.521	-	-	-
	e	-0.005	-	-	-
	f	0.920	-	-	-
	R²	0.997	0.992	0.844	0.992
	***p* (%)**	0.1510	0.335	1.490	0.315
c_p (kJ·kg^{-1}·K^{-1})	***a***	3.836	4.744	3.128	1.772
	b	-2.361	-377.923	NS	-0.494
	c	0.100	-0.493	-0.092	0.146
	d	1.2×10^{-4}	-	-	-
	e	2.2×10^{-6}	-	-	-
	f	1.6×10^{-3}	-	-	-
	R²	0.999	0.998	0.863	0.998
	***p* (%)**	0.151	0.238	2.331	0.228
λ (W·m^{-1}·K^{-1})	***a***	0.609	0.688	0.420	0.343
	b	-0.404	-266.092	NS	-0.699
	c	0.219	-0.699	-0.134	0.103
	d	1.0×10^{-4}	-	-	-
	e	5.0×10^{-7}	-	-	-
	f	-2.5×10^{-4}	-	-	-
	R²	0.999	0.997	0.903	0.997
	***p* (%)**	0.167	0.438	2.973	0.432
μ (mPa·s)	***a***	14.095	1.5×10^{-4}	1.0×10^{-3}	2.1×10^{18}
	b	51.307	1.92×10^{4}	2.25×10^{-4}	6.658
	c	32.270	6.522	2.936	-7.601
	d	-0.096	-	-	-
	e	1.7×10^{-4}	-	-	-
	f	-0.182	-	-	-
	R²	0.980	0.976	0.962	0.982
	***p* (%)**	23.306	8.017	36.911	7.157

a, *b*, *c*, *d*, *e*, and *f* – parameters of the model; R^2 – determination coefficient; *p* – mean relative error; NS – not significant at 95% of confidence.

4 Conclusions

Properties of isomaltulose solutions were experimentally determined in a wide range of temperature and solute concentrations. Solubility of isomaltulose in water increased with increasing temperature, characterizing the dissolution as an endothermic reaction. Density and viscosity increased as the solute concentration increased and the temperature decreased. On the other hand, thermal properties (specific heat and thermal conductivity) decreased under these conditions. Apart from the nutritional and technological properties of isomaltulose, it was observed advantages compared to conventional sugar solutions as sucrose. At 40% of solute concentration and 45 °C, isomaltulose presents comparable characteristics to sucrose solution with adequate properties for further use in the food industry processes. Mathematical models were able to predict the experimental data with good accuracy, highlighting the polynomial model and the Arrhenius exponential-type equation for the specific case of viscosity. The data presented for isomaltulose solutions can be interestingly used to evaluate the replacement of conventional sugar solutions in processes aiming at alternative carbohydrates with healthy attributes.

Credit authorship contribution statement

Juliana Rodrigues do Carmo: Conceptualization; Formal analysis; Writing - Original draft preparation. **Jefferson Luiz Gomes Corrêa:** Conceptualization; Formal analysis; Writing - review & Editing; Supervision; Funding acquisition. **Tiago Carregari Polachini:** Formal analysis; Writing- Original draft preparation. **Javier Telis-Romero:** Conceptualization; Formal analysis; Writing - review & Editing; Supervision; Funding acquisition.

Conflict of interest

The authors have no conflict of interest.

Acknowledgments

The authors are thankful to the following Brazilian agencies for financial support: Coordination for the Improvement of Higher-Level Personnel (Code 001 and Grant 88887.468140/2019-00), National Council for Scientific and Technological Development (308567/2017-0 and 310632/2018-8) and Research Support Foundation of the State of Minas Gerais. J. R. Carmo (studentship 166378/2018-6) thanks CNPq.

References

[1] M. Fleddermann, A. Rauh-Pfeiffer, H. Demmelmair, L. Holdt, D. Teupser, B. Koletzko. Effects of a follow-on formula containing isomaltulose (Palatinose™) on metabolic response, acceptance, tolerance and safety in infants: a randomized-controlled trial. *PLoS One*, 11 (2016), 1–14. https://doi.org/10.1371/journal.pone.0151614. eCollection 2016.

[2] W. Mu, W. Li, X. Wang, T. Zhang, B. Jiang. Current studies on sucrose isomerase and biological isomaltulose production using sucrose isomerase. *Appl. Microbiol. Biotechnol.*, 98 (2014), 6569–6582. https://doi.org/10.1007/s00253-014-5816-2

[3] P. Sridonpai, S. Komindr, W. Kriengsinyos Impact of isomaltulose and sucrose based breakfasts onpostprandial substrate oxidation and glycemic/insulinemic changes in type-2 diabetes mellitus subjects. *J. Med. Assoc. Thai.*, 99 (2016), 282–289.

[4] S. Shyam, A. Ramadas, S. K. Chang. Isomaltulose: Recent evidence for health benefits. *J. Funct. Foods*, 48 (2018), 173–178. https://doi.org/10.1016/j.jff.2018.07.002

[5] A. Maeda, J. Miyagawa, M. Miuchi. Effects of the naturally-occurring disaccharides, palatinose and sucrose, on incretin secretion in healthy non-obese subjects. *J. Diabetes Investig.*, 4 (2013), 281–286. https://doi.org/10.1111/jdi.12045

[6] R. P. Aidoo, F. Depypere, E. O. Afoakwa, K. Dewettinck, K. Industrial manufacture of sugarfree chocolates – Applicability of alternative sweeteners and carbohydrate polymers as raw materials in product development. *Trends Food Sci. Technol.*, 32 (2013), 84–96. https://doi.org/10.1016/j.tifs.2013.05.008

[7] L. Dye, M. B. Gilsenan, F. Quadt, V. E. Martens, A. Bot, N. Lasikiewicz, D. Camidge, F. Croden, C. Lawton, C. Manipulation of glycemic response with isomaltulose in a milk-based drink does not affect cognitive performance in healthy adults. *Mol. Nutr. Food Res.*, 54 (2010), 506–515. https://doi.org/10.1002/mnfr.200900196

[8] M. M. L. Lopez, R, M. S. C. Morais, A. M. M. B. Morais, A. M. M. B. Flavonoid enrichment of fresh-cut apple through osmotic dehydration-assisted impregnation. *British Food Journal*, 123 (2020), 820–832. https://doi.org/ 10.1108/BFJ-03-2020-0176

[9] K. S. Mendonça, J. L. G. Corrêa, J. R. J. Junqueira, M. Angelis-Pereira, M. A. Cirillo, M. A. Mass transfer kinetics of the osmotic dehydration of yacon slices with polyols. *J. Food Proces. Preserv.*, 41 (2017), 1–8. https://doi.org/ 10.1111/jfpp.12983

[10] M. J. N. Martins, B. Guimarães, T. C. Polachini, J. Telis-Romero. Thermophysical properties of carbohydrate solutions: correlation between thermal and transport properties. *J. Food Process Eng.*, 43 (2020), 1–15. https://doi.org/10.1111/jfpe.13483

[11] G. R. Carvalho, F. Chenlo, R. Moreira, J. Telis-Romero. Physicothermal properties of aqueous sodium chloride solutions. *J. Food Process Eng.*, 38 (2015), 234–242. https://doi.org/10.1111/jfpe.12160

[12] M. Baghbanbashi, G. Pazuki. A new hydrogen bonding local composition based model in obtaining phase behavior of aqueous solutions of sugars. *J. Mol. Liq.*, 195 (2014), 47–53. https://doi.org/10.1016/j.molliq.2014.01.028

[13] L. E. Figueroa, D. B. Genovese. Fruit jellies enriched with dietary fibre: Development and characterization of a novel functional food product. *LWT – Food Sci. Technol.*, 111 (2019), 423–428. https://doi.org/10.1016/j.lwt.2019.05.031

[14] M. J. N. Martins, P. E. D. Augusto, J. Telis-Romero, T. C. Polachini. Transport properties of saturated sucrose and maltitol solutions as affected by temperature. *J. Mol. Liq.*, 336 (2021), 1162545. https://doi.org/10.1016/j.molliq.2021.116254

[15] A. Sentko, I. Willibaldettle. Isomaltulose, in: K. O'Donnell, M. W. Kearsley (Eds)., *Sweeteners and Sugar Alternatives in Food Technology*, Wiley-Blackwell, New Jersey, 2012, pp. 397−413.

[16] S. Song, J. Guo, J. Qiu, J. Liu, M. An, D. Yi, P. Wang, H. Zhang. Solid−liquid equilibrium of isomaltulose in five pure solvents and four binary solvents from (283.15 to 323.15) K. *J. Chem. Eng. Data*, 64 (2019), 963−971. https://doi.org/10.1021/acs.jced.8b00823

[17] A. M. Peres, E. A. Macedo. Measurement and modeling of solubilities of D-glucose in water/alcohol and alcohol/alcohol systems. *Ind. Eng. Chem. Res*, 36 (1997), 2816–2820. https://doi.org/10.1021/ie9604583

[18] D. G. Archer. Thermodynamic properties of synthetic sapphire (α-Al_2O_3), standard reference material 720 and the effect of temperature-scale differences on thermodynamic properties. *J. Phys. Chem. Ref. Data*, 22 (1993), 144. https://doi.org/10.1063/1.555931

[19] D. Bellet, M. Sengelin, C. Thirriot, C. Determination of thermophysical properties of non-newtonian liquids using a coaxial cylindrical cell. *Int. J. Heat Mass Transf.*, 18 (1975), 1177–1187. https://doi.org/10.1016/0017-9310(75)90139-8

[20] T. C. Polachini, L. F. L. Betiol, M. G. Bastos, M. G., Telis, V. R. N., Souza, A. C., & Telis-Romero, J. Density, thermal expansion coefficient, and rheological behaviour of meat extract under different temperaturesand solids concentrations. *Can. J. Chem. Eng.*, 94 (2016), 988–994. https://doi.org/10.1002/cjce.22468

[21] G. Peng, X. Chen, W. Wu, X. Jiang. Modeling of water sorption isotherm for corn starch. *J. Food Eng.*, 80 (2007), 562–567. https://doi.org/1016/j.jfoodeng.2006.04.063

[22] C. J. Lomauro, A. S. Bakshi, T. P. Labuza. Evaluation of food moisture sorption isotherm equations. Part I. Fruit, vegetable and meat products. *LWT – Food Sci. Technol.*, 18 (1985), 111–117.

[23] J. R. J. Junqueira, J. L. G. Corrêa, D. B. Ernesto. Microwave, convective, and intermittent microwave-convective drying of pulsed vacuum osmodehydrated pumpkin slices. *J. Food Proces. Preserv.*, 41 (2017), 1–8. https://doi.org/10.1111/jfpp.13250

[24] H. Schiweck. Palatinit® – Herstellung, technologische eigenschaften und analytik palatinithaltiger lebensmittel. *Alimenta*, 19 (1980), 5–16.

[25] J. E. Huheey, E. A. Kelter, R. L. Kelter, J. Shapley, *Inorganic chemistry: principles of structure and reactivity*, fifth ed., London, Pearson, 2010.

[26] L. Maugeri, S. Busch, S. E. McLainc, L. C. Pardod, F. Brunia, M. A. Ricc. Structure-activity relationships in carbohydrates revealed by their hydration. *Biochim. Biophys. Acta*, 1861 (2017), 1486–1493. https://doi.org/10.1016/j.bbagen.2016.12.017

[27] C. E. Crestani, A. Bernardo, C. B. B. Costa, M. Giulietti. Experimental data and estimation of sucrose solubility in impure solutions. *J. Food Eng.*, 218 (2018), 14 –23. https://doi.org/10.1016/j.jfoodeng.2017.08.023

[28] R. Darros-Barbosa, M. O. Balaban, A. A. Teixeira. Temperature and concentration dependence of density of model liquid foods. *Int. J. Food Prop.*, 6, 195–214 (2003). https://doi.org/10.1081/JFP-120017815

[30] M. T. Zafarani-Moattar, H. Shekaari, E. Mazaher. Effect of ionic liquid, 1-hexyl-3-methylimidazolium bromide on the volumetric, acoustic and viscometric behavior of aqueous sucrose solutions at different temperatures. *J. Chem. Thermodyn.*, 93 (2016), 60–69. https://doi.org/10.1016/j.jct.2015.09.021

[31] M. Werner, A. Baars, F. Werner, C. Eder, A. Delgado. Thermal conductivity of aqueous sugar solutions under high pressure. *Int. J. Thermoph.* 28 (2007), 1161–1180. https://doi.org/10.1007/s10765-007-0221-z

[32] R. Darros-Barbosa, M. O. Balaban, A. A. Teixeira. Temperature and concentration dependence of heat capacity of model aqueous solutions. *Int. J. Food Prop.*, 6, 239–258 (2003). https://doi.org/10.1081/JFP-120017845

[33] L. T. Nguyen, L. T., V. M. Balasubramaniam, S. K. Sastry. Determination of in-situ thermal conductivity, thermal diffusivity, volumetric specific heat and isobaric specific heat of selected foods under pressure. *Int. J. Food Prop.*, 15 (2012), 169–187. https://doi.org/10.1080/10942911003754726

[34] H. C. B. Costa, D. O. Silva, L. G. M. Vieira. Physical properties of açai-berry pulp and kinetics study of its anthocyanin thermal degradation. *J. Food Eng.*, 239 (2018), 104–113. https://doi.org/10.1016/j.jfoodeng.2018.07.007

[35] S. R. Boreddy, J. Subbiah, J. Physical and thermal properties of spray-dried egg white powder. *Trans. Asabe*, 58 (2015), 1409–1416. https://doi.org/10.13031/trans.58.11232

[36] F. F. Chen, T. T. Zhao, J. M. Liang, W. M. Cao, Y. R. Jiang, X. B. Xu. Specific heat capacity measurements of frying oil using modulated differential scanning calorimetry. *J. Am. Oil Chem. Soc.*, 96 (2019), 1011–1018. https://doi.org/10.1002/aocs.12254

[37] X. Y. Zhu, D. M. Phinney, S. Paluri, D. R. Heldman, D. R. Prediction of liquid specific heat capacity of food lipids. *J. Food Sci.*, 83 (2018), 992–997. https://doi.org/10.1111/1750-3841.14089

[38] Y. Muramatsu, A. Tagawa, T. Kasai. Thermal conductivity of several liquid foods. *Food Sci. Technol. Res.*, 11 (2005), 288–294. https://doi.org/10.3136/fstr.11.288

[39] M. K. Krokida, N. M. Panagiotou, Z. B. Maroulis, G. D. Saravacos. Thermal conductivity: literature data compilation for foodstuffs. *Int. J. Food Prop.*, 4 (2001), 111–137. https://doi.org/10.1081/JFP-100002191

[40] L. Riedel. Wärmeleitfähigkeitsmessungen an zuckerlösungen, fruchtsäften und milch. *Chem. Ing. Tech.*, 21 (1949), 340–341. https://doi.org/10.1002/cite.330211706

[41] P. D. Sawale, A. M. Shendurse, M. S. Mohan, G. R. Patil. Isomaltulose (Palatinose) – an emerging carbohydrate. *Food Bioscience*, 18 (2017), 46–52. https://doi.org/10.1016/j.fbio.2017.04.003

[42] A. Bozdogan. Viscosity and physicochemical properties of cornelian cherry (*Cornus mas* L.) concentrate. *J. Food Meas. Charact*., 11 (2017), 1326–1332, 2017. https://doi.org/10.1007/s11694-017-9510-9

[43] R. Kumar, S. Manjunatha, T. Kathiravan, S. Vijayalakshmi, S. Nadanasabapathi, P. S. Raju, Rheological characteristics of inulin solution at low concentrations: Effect of temperature and solid content. *J. Food Sci. Technol.*, 52 (2015), 5611–5620. https://doi.org/10.1007/s13197-014-1671-5

[44] W. P. Schellart. Rheology and density of glucose syrup and honey: Determining their suitability for usage in analogue and fluid dynamic models of geological processes. *J. Struct. Geol.*, 33 (2011), 1079–1088. https://doi.org/10.1016/j.jsg.2011.03.013

[45] V. R. N. Telis, J. Telis-Romero, H. B. Mazzotti, A. L. Gabas. Viscosity of aqueous carbohydrate solutions at different temperatures and concentrations. *Int. J. Food Prop.*, 10 (2007), 185–195. https://doi.org/10.1080/10942910600673636

[46] M. Mathlouthi, C. Luu, A. M. Meffroy-Biget, D. V. Luu. Laser-Raman study of solute-solvent interactions in aqueous solutions of D-fructose, D-glucose and sucrose. *Carbohydr.*, 81 (1980), 213–223. https://doi.org/10.1016/S0008-6215(00)85653-0

[47] T. C. Polachini, A. C. K. Sato, R. L. Cunha, J. Telis-Romero. Density and rheology of acid suspensions of peanut waste in different conditions: An engineering basis for bioethanol production. *Powder Technol.*, 294 (2016), 168–176. https://doi.org/10.1016/j.powtec.2016.02.022

[48] K. B. Belibağli, A. C. Dalgic. Rheological properties of sour-cherry juice and concentrate. *Int. J. Food Sci. Technol.*, 42 (2007), 773–776. https://doi.org/10.1111/j.1365-2621.2007.01578.x

[49] M. B. M. Castilhos, L. F. L. Betiol, G. R. Carvalho, J. Telis-Romero. Experimental study of physical and rheological properties of grape juice using different temperatures and concentrations. Part II: Merlot. *Food Res. Int.*, 105 (2018), 905–912. https://doi.org/10.1016/j.foodres.2017.12.026

[50] S. Bodbodak, M. Kashaninejad, J. Hesari, S. M. A. Razavi. Modeling of rheological characteristics of “malasyazdi” (*Punicia granatum* L.) pomegranate juice. *J. Agric. Sci. Technol.*, 15 (2013), 961–97. http: sid.ir/en/journal/ViewPaper.aspx?id=357416

[51] J. W. Mullin. *Crystallisation*, third ed., London, Butterworth–Heinemann, 1993.

[52] R. S. Norrish. *Selected tables of physical properties of sugar solutions*. Leatherhead, British Food Manufacturing Industries Research Association, 1967.

ARTICLE 2 – **Modeling mass transfer during osmotic dehydration of mangos with sucrose and isomaltulose (Palatinose®) solutions: effect of solute concentration and temperature**

Juliana Rodrigues do CARMO [a*], Jefferson Luiz Gomes CORRÊA [a], Rosinelson da Silva PENA [b]

[a] Department of Food Science (DCA), Federal University of Lavras, 37200-900, Lavras, Brazil. E-mail: juliana_docarmo@yahoo.com.br; jefferson@ufla.br

[b] Graduate Program in Food Science and Technology, Federal University of Pará, 66075-110, Belém, Brazil. E-mail: rspena@ufpa.br

Running head: Mass transfer models in osmodehydrated fruit

Novelty impact statement

For the first time, osmotic dehydration (OD) kinetics was evaluated with isomaltulose carbohydrate – an emerging substitute of conventional sugars in the OD of fruits, due to healthy aspects. The empirical and diffusive models predicted with good accuracy the water loss and solid gain of mangos slices at different temperatures, solute concentration and solute type. The physicochemical characteristics of final product showed that isomaltulose can be promising in the replacement of sucrose in OD of mango slices.

[*]**Corresponding author:** Juliana Rodrigues do CARMO (E-mail: juliana_docarmo@yahoo.com.br)

(Elaborated in accordance to the Journal of Food Processing and Preservation)

***Abstract*:** Mango slices were osmotically dehydrated at 25, 35 and 45 °C, using sucrose and isomaltulose solutions at 25, 30 and 35%. The empirical models of Azuara and Peleg were used to predict the kinetics of water loss (WL) and solid gain (SG) of the samples. In turn, the diffusive model of Fick was used for the determination of effective diffusivity (D_{eff}) of WL and SG. At the end of osmotic dehydration (OD) time (300 min), the volumetric shrinkage, water activity (a_w) and total soluble solids (TSS) were evaluated. The results showed that the samples subjected to a sucrose and isomaltulose solutions had WL and SG values of the same order of magnitude. All models evaluated had a good fit to the OD data, but the Azuara equation was the model chosen for describe the WL and SG for OD of mango with sucrose and isomaltulose solutions. The Fick diffusive model showed that D_{eff} increasing as temperature and solute concentration increases. Moreover, according Tukey's test, volumetric shrinkage, a_w and TSS evidenced that for the same type of solute, most treatments showed no statistically significant difference ($p > 0.05$). In this way, isomaltulose can be potential sucrose substitute in osmotic processes, with advantage of presenting healthy attributes (low glycemic and insulinemic indexes).

Keywords: *Tommy Atkins*, carbohydrate, empirical models, effective diffusivity, physicochemical characteristics

1 Introduction

Mango (*Mangifera indica* L.) is the tropical fruit most consumed in the world. It is a source of fiber, phenolic compounds, vitamin C and pro-vitamin A (β-carotene), calcium, phosphorus, and iron. However, it is an extremely perishable fruit, which needs specific care for its conservation (Lebaka et al., 2021).

Osmotic dehydration (OD) consists of immersing the food in a hypertonic solution, with consequent water loss (WL) and solid gain (SG) in simultaneous isothermal flows without any phase change. This process offers the possibility of modifying food properties, especially in relation to taste and structural characteristics and it could be a useful strategy for conservation of mango, since this technique can partially remove the water of the fruit (Abrahão & Corrêa, 2021).

The mass transfer in OD process occurs through a semipermeable membrane of the food, in order to balance the concentration of the medium. This process is benefited by the increase in the concentration of the osmotic solution, mainly close to saturation, stimulating the WL in the product, reducing the losses of water-soluble solutes, such as vitamins and minerals due to the formation of a layer of solute around the fruit, which prevent the exit of these substances. Saturated osmotic solutions are also more viscous, making it even more difficult to transfer sugars into the fruit (Carmo et al., 2022; Martins et al., 2020). However, depending on the process conditions (e.g, high temperatures), a high solid gain can affect the nutritional and sensory profile of the food (Kushwaha et al., 2018).

Mathematical models are useful to describe mass transfer during OD, but diffusion equations have analytical solutions only for classical geometries. For unusual geometries, numerical methods are required for their solution (Schmidt et al., 2009). Simple empirical models that has no geometric restrictions for their application have been reported for describing mass transfer in food subjected to OD, as the ones proposed by Azuara et al. (1992) and Peleg (1988).

Diffusive and empirical models have been largely employed to represent OD rates of several fruits using sucrose as osmotic agent (Assis et al., 2017; Mehta et al., 2021; Mello Júnior et al., 2019; Zielinska & Markowski, 2018). However, there no found works in the literature about the application of empirical models for describing WL and SG on mangos with isomaltulose. Although sucrose be a lower cost and more available carbohydrate than isomaltulose, it is considered a highly cariogenic carbohydrate, besides being rapidly digested, and consequently, inducing high glycemic response. Therefore, the replace it by healthier carbohydrate is required.

In this sense, isomaltulose is an isomer carbohydrate of sucrose, naturally present in honey and sugarcane juice, non-cariogenic and it has low glycemic and insulinemic indexes (Sawale et al., 2017).

The knowledge of the mass transfer kinetics during OD is important for a successful design of a drying system or other industrial processes. Moreover, it has a great technological importance, as it allows estimating the immersion time of fruits in an osmotic solution to obtain products with determined carbohydrate and moisture contents (Abrahão & Corrêa, 2021). Thus, the aim of the present work was to study the effect of temperature (25, 35 and 45 °C), solute concentration (25, 30 and 35 %) and osmotic agent (sucrose and isomaltulose) on mass transfer kinetics of mango slices during the OD process. Additionally, the Fick diffusive model was fitted to the experimental data for estimate the WL and SG effective diffusivity; and the empirical models of Azuara and Peleg were fitted to the WL and the SG data of the product from 10 to 300 min OD process. Finally, the water activity (a_w), volumetric shrinkage and total soluble solids (TSS) of mangos fruit at the end of the OD process were determinate in order to evaluate the influence of the treatment on physicochemical characteristics of the obtained product.

2 Material and methods

2.1 Material and sample preparation

Half-ripe mango fruits (*Tommy Atkins*) were acquired in the local market of Lavras (Minas Gerais State, Brazil) (21° 14'43 S e 44° 59'59 W). The fruits had reddish-green skin peel color; 84.53% (± 1.83) moisture; 12.33 °B (± 0.60) total soluble solids (TSS); 2.86% citric acid (± 0.21) titratable total acidity; 4.72 (± 0.16) ratio; 3.60 (± 0.04) pH, 0.990 (± 0.003) water activity (a_w) and 31.13 N (±3.27) firmness. Mangos were sanitized with chlorinated water at 200 mg/L for 5 min. Then, the seed and peel were removed and slices were obtained with the aid of a stainless steel molder (4.00 ± 0.01 cm length, 2.00 ± 0.01 cm width, and 0.40 ± 0.01 cm thickness).

2.2 Osmotic solution obtaining

The osmotic solutions were prepared with distilled water and commercial sucrose (União, São Paulo, Brazil) or isomaltulose, commercially known as Palatinose® (Beneo, Mannheim, Germany).

2.3 Osmotic dehydration (OD) experiments

The OD experiments occurred without recirculation and were performed at temperatures of 25, 35, and 45 °C in a thermostatic chamber (Eletrolab EL111/4, São Paulo, Brazil) at atmospheric pressure. The samples were immersed in glass containers with the osmotic solutions at a ratio of solution/sample of 10: 1 (v /w) to avoid dilution of the solution (Tiroutchelvame, et al., 2019). The solute concentration (25, 30 and 35 w/w) and temperature ranges were chosen according to osmotic solutions properties (solubility, density, heat specific, thermal conductivity and viscosity) investigated recently by Martins et al. (2020) and Carmo et al. (2022).

2.4 OD kinetics

The effect of the contact time (10, 20, 30, 45, 60, 90, 120, 240, and 300 min) on WL and SG were determined to assess OD process kinetics. The samples were removed from the solution after each predetermined time and immediately immersed in a water and ice bath for 10 s to stop dehydration and to remove the remaining osmotic solution on the surface. Then, the samples had their surface dried with absorbent paper. All analyses were performed in triplicate and the results were presented as the replicates mean.

The moisture content of fresh and osmotically treated samples was determined according to AOAC (2010). Then, the mass transfer parameters, WL and SG, of each sample subjected to the different OD conditions were evaluated according to Eq. 1 and Eq. 2 (Viana et al., 2014), respectively.

$$WL(\%) = \frac{x_0 m_0 - x_t m_t}{m_0} \times 100 \quad (1)$$

$$SG(\%) = \frac{m_t S_t - m_0 S_0}{m_0} \times 100 \quad (2)$$

where: WL is the water loss (%), SG is the solid gain (%), x is the moisture content on a wet basis (kg of water/kg wb), m is the sample weight (kg) and S is solid content on a wet basis (kg

solid/kg wb). The subindices “0” and “t” refer to fresh samples and samples after osmotic treatment, respectively.

2.5 Osmotic dehydration process modeling

Azuara, Peleg and Fick diffusive models were used to predict the kinetics of WL and SG during OD of mangos slices.

2.5.1 Azuara model

Azuara et al. (1992) proposed a model to predict the mass transfer parameters WL (Eq. 3) and SG (Eq. 4) and to evaluate of the equilibrium values of WL (WL_∞) and SG (SG_∞) during the OD, based on the mass balances.

$$WL = \frac{S_1 t WL_\infty}{1 + S_1 t} \tag{3}$$

$$SG = \frac{S_2 t SG_\infty}{1 + S_2 t} \tag{4}$$

where: S_1 is the parameter related to the rate of water diffusion from the product and S_2 is the parameter associated with the rate of solute diffusion into the product.
The linearization of Eq. 3 and Eq. 4 for WL and SG leads to Eq. 5 and Eq. 6, respectively.

$$\frac{t}{WL} = \frac{1}{S_1(WL_\infty)} + \frac{t}{WL_\infty} \tag{5}$$

$$\frac{t}{SG} = \frac{1}{S_2(SG_\infty)} + \frac{t}{SG_\infty} \tag{6}$$

where: the equilibrium WL (WL_∞) (%) and SG (SG_∞) (%) may be estimated from the slope of the linear regression of (t/WL) or (t/SG) versus time (t).

2.5.2 Peleg model

Peleg (1988) proposed a two-parameter model to describe the kinetics of moisture sorption that approaches equilibrium asymptotically. The adapted form of this model for the osmotic dehydration is given by Eq. 7.

$$WL(\text{or } SG) = \pm \frac{t}{k_1 + k_2 t} \tag{7}$$

In the Eq. 7 "±" becomes "+" for SG and "–" for WL. According to this model, the reciprocal value of k_1 is the initial rate (t = 0) of WL or SG (Eq. 8).

$$\left.\frac{d(WL \text{ or } SG)}{d(t)}\right|_{t=0} = \pm\frac{1}{k_1} \tag{8}$$

For a condition of long immersion time ($t \rightarrow \infty$), the values WL_∞ and SG_∞ at equilibrium were estimated from the $1/k_2$ ratio for the respective processes (Eq. 9).

$$WL_\infty (\text{or } SG_\infty) = \pm\frac{1}{k_2} \tag{9}$$

where: k_1 is Peleg rate constant (h/(g/g wet basis)) and k_2 is Peleg capacity constant ((g/g wet basis)$^{-1}$).

2.5.3 Fick model

Crank (1975) proposed an equation for unidirectional diffusion, based on Fick's second law, for an infinite plane sheet with uniform initial concentration and constant concentration at the surface (Dirichlet boundary condition) (Eq. 10). The simplified form of this model for short contact time (t) can be applied to the initial phase of the process, when diffusion is assumed to occur in a semi-infinite medium. The effective diffusivity coefficient (D_{eff}) value, calculated from Eq. 10, is the mean value of D_{eff} for the solute concentration range during the diffusion process. The values of D_{eff} for WL and SG were calculated from the slope of the linear region of the curves WLt/WL_∞ and SGt/SG_∞ versus $t^{1/2}$, respectively.

$$\frac{WL_t}{WL_\infty}\left(\text{or } \frac{SG_t}{SG_\infty}\right) = 2\left(\frac{D_{eff}\, t}{\pi L^2}\right)^{0.5} \tag{10}$$

where: WL_t or SG_t is the value of WL or SG for the product at a given time (t), WL_∞ and SG_∞ is the value of WL or SG for the product at the equilibrium (infinite time), D_{eff} is effective diffusivity (m^2/s) and L is half-thickness of the sample (m).

The WL_∞ and SG_∞ values can be estimated from experimental data by an empirical equation, as Peleg or Azuara model. In this work, the latter model was used for estimate these parameters.

2.6 Osmodehydrated product assessment

After the OD treatments time (300 min), the samples were submitted to analyzes of water activity (a_w), volumetric shrinkage and TSS. a_w was determined at 25 °C with a digital

thermohygrometer (AquaLab 3TE, Decagon, USA). Volumetric shrinkage was determined by measuring the area and thickness of the samples. The area was obtained by free software Image J®1.45 s, which provides the sample area by converting the pixels in the image into real dimensions, from a known scale (Nahimana et al., 2011). The thickness was determined through five different points of the samples with the aid of a digital caliper (Western, DC-6 model, China). The dimensionless volume (β) was determined according to Eq. 11. (Junqueira et al., 2017). TSS were determined by direct reading at 20 °C in a portable digital refractometer (Hanna Instruments, model HI96801, Woonsocket, USA) according to AOAC (2010). The samples were macerated and diluted in distilled water at a 1:10 ratio (w/v).

$$\beta = \frac{V_f}{V_0} \tag{11}$$

where: V_f is the apparent volume of the sample after OD (m^3) and V_0 is the initial volume of the sample (m^3).

2.7 Statistical analysis

The statistical analyses were carried out using Statistica Software (version 10). Factorial ANOVA and Tuckey's test at 95% confidence interval were performed to analyze the data of a_w, shrinkage and TSS. The Azuara model was fitted by linear regression using Microsoft Excel® (2013). The Peleg and Fick models were fitted by non-linear regression using Statistica Software. Goodness of fit was assessed using coefficient of determination (R^2) and root mean square error (RMSE) (Eq. 12).

$$RMSE = \left[\frac{1}{N} \Sigma_{i=1}^{N} (V_{exp,i} - V_{pre,i})^2 \right]^{0.5} \tag{12}$$

where: $V_{exp,i}$ and $V_{pre,i}$ are the WL or SG determined from the experimental data and predicted by the fitted model, respectively, N is number of experimental measurements and n is number of parameters in the model.

3 Results and discussion

3.1 OD kinetic of the WL

The kinetic data of WL at different temperature and solute concentration for sucrose and isomaltulose is presented in Table 1 and Table 2, respectively. For both the solute, the mass

transfer of water from the fruit to the osmotic solution was little in the initial phase (from 10 to 30 min), followed by progressive increasing in the second stage (from 30 to 180 min). On the last phase (from 180 to 300 min) had stabilization on WL, indicating the attainment of pseudo equilibrium. This behavior was more noticed for solute concentration than temperature.

For sucrose, during the initial phase, the WL variation was 0.3% at 25 ºC and 25% solute concentration (minimum experimental condition – MIC), and, 6.4% at 45°C and 35% solute concentration (maximum experimental condition – MAC). However, the second phase resulted in 9.8% and 14.8% of WL variation for MIC and MAC, respectively. For isomaltulose, the WL variation was 1.4% for MIC and 13.4% for MAC during initial phase, and 8.1% for MIC and 16.2% for MAC on second stage, for the same experimental conditions. Prithani and Dash (2020) reported that the dehydration of apples with sucrose was most effective for the first 30 min of the OD process. The different findings in current study could be due apples are much more porous than mangos (Fernandes et al., 2019).

According to Table 1, the highest WL value for sucrose was 42.48% and lowest value was 15.84%, which correspond to MAC and MIC, respectively. For isomaltulose, the highest and lowest WL values were 37.15% (MAC) and 13.43% (MIC) (Table 2). This phenomenon of increase in WL rates is due to increasing in the rate of diffusion of water present in the product as temperature increases. Moreover, the high temperature releases the air retained from the tissue, resulting in a more efficient removal of water by osmotic pressure, in addition to plasticizing the cell membrane of the product and decreasing the viscosity of the osmotic solution (Ruskova et al., 2016). Devic et al. (2010) observed that the use of temperature at 45 °C has nutritional benefits, such as a decrease in the loss of vitamin C. Above this temperature, damage to the cell wall can occur, reducing mass transfer.

Table 1. OD kinetics of mangos cv. Tommy Atkins in sucrose solutions at different solute concentrations and temperatures.

Time (min)	Water loss (WL) (%)								
	Solute concentration / Temperature								
	25% / 25°C	**30% / 25°C**	**35% / 25°C**	**25% / 35°C**	**30% / 35°C**	**35% / 35°C**	**25% / 45°C**	**30% / 45°C**	**35% / 45°C**
10	4.59±0.17	6.09±0.88	11.08±0.15	6.63±0.53	8.89±0.50	9.83±0.34	5.09±0.68	8.04±1.00	10.45±0.22
20	4.68±1.14	6.16±0.51	14.28±0.32	6.38±1.00	12.37±0.42	12.00±1.01	4.17±0.04	10.36±0.75	13.16±0.12
30	4.87±0.80	6.80±0.96	14.27±0.33	7.28±1.17	13.88±0.71	14.02±0.81	9.49±0.72	11.51±0.35	16.89±0.62
45	5.04±0.76	13.15±0.87	15.60±1.14	11.76±0.14	17.48±0.79	19.00±0.85	9.56±1.31	11.64±0.18	17.40±2.37
60	10.38±0.46	13.65±0.43	25.87±0.57	12.90±0.75	18.33±0.94	23.82±0.15	10.12±2.30	16.07±0.71	23.36±1.21
90	11.34±1.29	14.29±0.74	25.70±1.16	19.06±1.26	23.58±1.57	29.08±0.08	10.07±1.13	21.83±0.40	26.12±0.98
120	14.81±0.12	22.99±1.56	29.05±0.96	20.64±0.67	25.81±0.88	30.67±1.26	10.16±0.18	26.75±1.82	30.16±1.33
180	14.66±2.74	24.43±1.40	30.66±0.28	25.02±0.62	31.79±1.03	36.81±0.65	12.72±0.48	27.47±0.73	31.69±0.69
240	15.09±0.90	23.32±1.37	31.34±1.29	25.11±0.16	30.63±0.76	37.60±0.42	12.79±0.41	28.02±0.45	35.79±0.51
300	15.84±1.52	23.68±0.25	31.04±2.42	25.22±1.36	28.62±0.41	37.87±0.88	14.81±0.62	33.80±0.19	42.48±1.67
Time (min)	**Solid gain (SG) (%)**								
	Solute concentration / Temperature								
	25% / 25°C	**30% / 25°C**	**35% / 25°C**	**25% / 35°C**	**30% / 35°C**	**35% / 35°C**	**25% / 45°C**	**30% / 45°C**	**35% / 45°C**
10	0.95±0.10	1.47±0.51	1.66±0.14	1.25±0.14	1.25±0.22	1.45±0.21	1.28±0.48	0.80±0.21	1.63±0.34
20	0.99±0.32	1.26±0.75	2.35±0.39	1.33±0.26	1.31±0.27	1.43±0.56	1.00±0.05	1.48±0.67	1.78±0.14
30	1.01±0.25	1.57±0.15	2.61±0.13	1.55±0.21	1.65±0.28	1.86±0.91	1.08±0.32	1.98±0.15	1.88±0.19
45	1.17±0.16	2.18±0.46	3.44±0.36	2.25±0.29	2.73±0.15	2.57±0.42	1.02±0.11	2.40±0.17	3.16±0.05
60	2.56±0.12	2.31±0.33	4.90±0.26	3.04±0.14	3.45±0.05	3.83±0.08	1.73±0.42	2.85±0.25	3.04±0.48
90	4.56±0.51	2.98±0.32	5.10±0.11	3.07±0.01	3.77±0.14	3.93±0.44	1.15±0.20	2.93±0.47	3.77±0.66
120	4.14±0.26	2.64±1.20	5.23±0.17	4.12±0.26	4.40±0.56	4.16±0.64	1.86±0.46	3.74±0.47	4.04±0.36
180	5.23±1.00	2.81±0.44	6.50±0.51	4.13±0.12	4.52±0.46	4.50±0.59	2.17±0.47	4.21±0.94	4.49±0.22
240	5.24±0.22	3.94±0.29	6.91±0.16	5.86±0.82	6.45±0.16	7.17±0.57	5.48±0.72	5.50±0.29	6.75±0.99
300	5.00±0.20	5.44±0.46	7.15±0.18	6.17±0.13	6.49±0.43	7.64±0.08	6.06±.1.00	6.09±1.30	8.02±1.16

Means ± standard deviation (n=5).

Table 2. OD kinetics of mangos cv. Tommy Atkins in isomaltulose solutions at different solute concentrations and temperatures.

Time (min)	Water loss (WL) (%)								
	Solute concentration / Temperature								
	25% / 25°C	**30% / 25°C**	**35% / 25°C**	**25% / 35°C**	**30% / 35°C**	**35% / 35°C**	**25% / 45°C**	**30% / 45°C**	**35% / 45°C**
10	3.19±0.32	9.10±0.91	6.69±0.28	6.27±0.26	7.15±0.11	10.89±0.37	2.21±0.08	5.84±0.19	5.67±0.41
20	4.29±0.30	8.27±0.24	6.91±0.27	7.02±0.13	7.24±0.34	11.50±0.76	4.94±0.45	8.09±0.26	8.88±0.70
30	4.63±0.54	9.56±0.06	9.81±0.52	8.23±0.86	7.73±1.42	12.02±1.58	6.78±0.20	10.15±0.44	19.08±0.58
45	5.40±0.88	11.56±1.45	14.26±0.72	8.39±0.25	7.85±0.51	12.13±0.51	9.38±0.33	11.68±0.39	23.30±0.76
60	5.30±0.49	11.27±1.00	15.84±0.92	9.01±0.27	8.46±0.93	11.86±0.20	9.37±0.97	13.90±0.36	22.92±0.73
90	5.50±0.65	12.91±0.52	17.46±1.60	11.96±1.00	10.87±0.36	13.96±1.21	12.07±0.30	13.15±0.16	29.41±1.36
120	6.85±0.95	14.44±0.47	17.20±0.70	14.41±0.37	12.85±1.64	23.85±0.99	12.19±0.28	13.92±1.24	32.41±0.67
180	11.31±0.16	17.02±0.64	17.09±0.34	14.30±0.06	14.63±1.51	25.70±0.95	12.67±0.90	16.27±0.47	35.23±0.91
240	13.43±0.32	24.32±0.16	24.27±2.23	14.59±1.06	14.90±0.23	28.07±0.87	13.44±0.58	17.84±0.08	37.30±0.71
300	14.61±0.77	25.88±0.53	26.88±1.38	15.96±0.60	14.49±0.14	31.85±0.03	13.73±0.40	18.05±0.97	37.15±1.16
Time (min)	**Solid gain (SG) (%)**								
	Solute concentration / Temperature								
	25% / 25°C	**30% / 25°C**	**35% / 25°C**	**25% / 35°C**	**30% / 35°C**	**35% / 35°C**	**25% / 45°C**	**30% / 45°C**	**35% / 45°C**
10	1.12±0.57	2.10±0.07	1.98±0.16	0.79±0.10	1.01±0.20	1.21±0.27	0.85±0.19	1.66±0.05	1.67±0.18
20	1.39±0.01	2.44±0.56	3.01±0.10	0.97±0.25	1.40±0.08	2.42±0.28	1.13±0.09	1.73±0.18	1.90±0.11
30	1.54±0.27	2.30±0.18	3.37±0.57	0.98±0.23	1.60±0.22	2.52±0.38	1.17±0.37	2.88±0.07	3.17±0.15
45	3.43±0.84	3.19±0.49	3.50±0.75	1.21±0.18	1.67±0.38	3.03±0.30	1.16±0.15	2.95±0.63	3.48±0.42
60	3.65±0.70	3.47±0.82	4.23±0.11	1.32±0.05	1.82±0.24	3.45±0.54	1.31±0.10	3.29±0.34	3.62±0.18
90	3.44±0.15	3.41±0.97	4.81±0.22	1.39±0.04	2.67±0.40	4.56±0.55	0.99±0.03	3.64±0.59	3.58±0.02
120	3.08±0.30	3.69±1.00	4.92±1.02	1.46±0.04	2.79±0.35	4.95±0.09	2.82±0.29	4.48±0.63	4.31±0.78
180	3.63±0.56	4.40±0.20	5.75±0.23	1.46±0.12	4.35±0.28	5.28±0.46	2.73±0.31	5.95±0.91	5.77±0.24
240	3.68±0.77	5.26±0.27	7.58±0.33	2.21±0.23	4.95±1.55	5.74±1.37	2.75±0.43	7.14±0.35	8.43±0.79
300	3.25±0.43	5.54±0.17	8.23±0.42	3.47±0.54	5.30±0.27	8.30±0.65	4.56±0.24	9.18±0.70	10.02±0.39

Means ± standard deviation (n=5).

In which concerns the solute concentration, the mass transfer in OD occurs through a semipermeable membrane of the product to balance the concentration of the medium. This is benefited by the increase in the concentration of the osmotic solution, mainly close to saturation, stimulating the WL in the product, reducing the losses of water-soluble solutes, such as vitamins and minerals due to the formation of a layer of solute around the fruit, preventing the exit of these substances.

3.2 OD kinetic of the SG

OD of mangos slices showed a linear increase of t/SG with immersion time at all the temperatures during the dehydration process (Fig. 1), as well as for WL. The slow increasing in SG rates during the initial phase (until 30 min) of OD reached 2-3 times values in the last stage (from 30 to 180 min) (Tables 1 and 2). The behavior was also more evident with solute concentration than temperature increases.

For sucrose, during the initial phase, the SG variation was 0.1% at 25 ºC and 25% solute concentration (MIC), and 0.3% at 45°C and 35% solute concentration (MAC). However, the second phase resulted in a WL variation of 4.2% for MIC and 6.1% for MAC (Table 1). For isomaltulose, the WL variation was 0.4% for MIC and 1.5% for MAC during initial phase, and 2.1% for MIC and 6.8% for MAC on second stage (Table 2).

According to Table 1, the highest SG for sucrose was 8.02% (MAC) and the lowest was 5.0% (MIC). For isomaltulose, the highest and lowest SG values were 10.02% (MAC) and 3.25% (MC) (Table 2). Studies about SG of sucrose solution in mango, pineapple, apple and pequi showed values of 6.3–13.4% for solutions with 44-65% soluble solids in range temperature 30-60 °C (Assis et al., 2017; Mendonça et al., 2017).

The increase in SG with increasing temperature can be attributed to the effect of temperature on the membrane permeability namely higher temperature made the membrane more permeable to solute exchanges. In which concerns to solute concentration, the higher gradients of soluble solids between osmotic solution and intercellular (native) solution of product leads to higher incorporation. Although the concentrated osmotic solutions are also more viscous, hindering to transfer sugars into the fruit, depending on the process conditions (i.e, at higher temperatures) a high solid gain can be reached (Oladejo et al., 2013). Kushwaha et al. (2018) observed in their study on the influence of the osmotic agent on guava, that higher concentrations of sucrose resulted in higher flows of WL and SG.

In a general way, the results showed that the samples subjected to a sucrose solution obtained a slight greater WL than those that were osmotically dehydrated with isomaltulose. On the other hand, the samples pretreated with isomaltulose had a slight greater SG for all studied conditions. Despite the solubility of aqueous sucrose solution is greater than isomaltulose solution (Carmo et al., 2022*)*, the a_w of both solutions are close (0.970 for sucrose solution and 0.972 for isomaltulose solution). This causes similar osmotic pressure gradients and, consequently, WL and SG values are of the same order of magnitude for both the solutes. Although there are no studies about OD of mango in isomaltulose solutions in literature, for sucrose solutions, the results for WL and SG were similar to those reported in other studies (Galdino et al., 2021; Zongo et al., 2021). The isomaltulose incorporation in mangos is promising, since the final product should be a partially dried and enriched product with low glycemic and insulinemic indexes agent, as mentioned previously.

3.3 Modeling of WL for the osmotic dehydration of mangos

The parameters of mathematical modeling of Azuara, Peleg and Fick models to the WL and SG data are shown in Table 3 for sucrose and in Table 4 for isomaltulose. In general, all the models were able to satisfactorily represent the kinetics of the WL and SG due to high R^2 and low RMSE, under different temperatures and solute concentration.

Azuara model presented a very good fit for sucrose ($R^2 \geq 0.928$ and RMSE ≤ 4.05) (Table 3) and isomaltulose ($R^2 \geq 0.765$ and RMSE ≤ 3.55) (Table 4) solutions. In general, the values of Azuara model parameters for WL (S_1, WL_∞) increased with temperature and solute concentration, irrespective of the solute type. The Peleg model had also a very good fit for sucrose ($R^2 \geq 0.841$ and RMSE ≤ 2.33) (Table 3) and isomaltulose ($R^2 \geq 0.754$ and RMSE $\leq$ 3.53) (Table 4) solutions. In general, the reciprocal of the parameter k_1 that indicates the initial water transfer rate and the parameter k_2 that indicates the water transfer rate of the samples after long immersion periods increased with the increase of temperature and solute concentration. Predict values of WL_∞ obtained by Azuara model better corroborated for both, order of magnitude and behavior with the OD observed values (Table 1 and 2). Therefore, it was chosen to describe the WL kinetics of mangos (Fig. 1 and Fig. 2). Similar results were found by Assis et al. (2017) for OD of apple cubes in sucrose solution.

The diffusive model of Fick predicted with very good accuracy D_{eff} of samples in sucrose (R^2 ≥ 0.729 and RMSE ≤ 0.77) and isomaltulose ($R^2 \geq 0.868$ and RMSE ≤ 0.91) solutions. The D_{eff}

values for the mangos immersed in sucrose solutions varied from $2.28 \cdot 10^{-12}$ to $8.58 \cdot 10^{-10}$ m^2/s, while for isomaltulose solutions the D_{eff} values varied from $1.23 \cdot 10^{-11}$ to $4.60 \cdot 10^{-8}$.

In general, the D_{eff} values increased with temperature and solute concentration for both sucrose and isomaltulose solutions. However, for sucrose at 35 °C and 45 °C the effect of solute concentration was less evident. It could be due to solubilities of sucrose in these temperatures are closest (Carmo et al., 2022).

Table 3. Parameters of mathematical modeling of osmotic dehydration kinetics of mangos in sucrose solutions at different temperatures.

Model	Parameter	Solute concentration / Temperature								
		25% / 25°C	**30% / 25°C**	**35% / 25°C**	**25% / 35°C**	**30% / 35°C**	**35% / 35°C**	**25% / 45°C**	**30% / 45°C**	**35% / 45°C**
Azuara (WL)	**WL_∞**	19.80	30.21	35.21	32.57	34.01	45.45	15.50	38.91	46.51
	S_1	0.014	0.015	0.030	0.013	0.027	0.019	0.027	0.022	0.017
	R^2	0.928	0.946	0.988	0.965	0.984	0.991	0.972	0.956	0.969
	RMSE	1.42	2.06	2.26	1.48	1.74	1.42	1.34	4.05	2.37
Azuara (SG)	**SG_∞**	8.22	5.39	8.42	7.82	7.71	9.53	2.46	7.52	9.28
	S_2	0.007	0.013	0.018	0.010	0.014	0.009	0.030	0.010	0.009
	R^2	0.715	0.822	0.989	0.911	0.933	0.845	0.931	0.934	0.825
	RMSE	0.59	0.59	0.31	0.40	0.40	0.63	0.70	0.36	0.73
Peleg (WL)	**k_1**	0.059	0.039	0.016	0.040	0.020	0.021	0.031	0.032	0.021
	k_2	0.049	0.032	0.028	0.030	0.028	0.021	0.069	0.025	0.022
	R^2	0.908	0.921	0.914	0.963	0.951	0.982	0.841	0.942	0.944
	RMSE	1.41	2.04	2.26	1.45	1.69	1.38	1.24	2.08	2.33
Peleg (SG)	**k_1**	0.248	0.246	0.112	0.252	0.208	0.232	1.075	0.246	0.243
	k_2	0.128	0.183	0.119	0.119	0.117	0.094	-0.054	0.127	0.092
	R^2	0.895	0.758	0.973	0.945	0.952	0.907	0.848	0.954	0.880
	RMSE	0.59	0.59	0.31	0.40	0.40	0.63	0.70	0.35	0.70
Fick (WL)	**D_{eff}**	$2.28 \cdot 10^{-12}$	$5.01 \cdot 10^{-10}$	$1.87 \cdot 10^{-10}$	$3.27 \cdot 10^{-10}$	$7.39 \cdot 10^{-10}$	$8.58 \cdot 10^{-10}$	$2.38 \cdot 10^{-10}$	$3.06 \cdot 10^{-10}$	$5.87 \cdot 10^{-10}$
	R^2	0.968	0.812	0.859	0.832	0.979	0.947	0.729	0.987	0.924
	RMSE	0.07	0.32	0.55	0.36	0.48	0.77	0.16	0.47	0.77
Fick (SG)	**D_{eff}**	$2.64 \cdot 10^{-12}$	$5.50 \cdot 10^{-11}$	$1.81 \cdot 10^{-10}$	$9.19 \cdot 10^{-11}$	$3.56 \cdot 10^{-10}$	$2.03 \cdot 10^{-10}$	$9.68 \cdot 10^{-12}$	$9.55 \cdot 10^{-11}$	$1.06 \cdot 10^{-10}$
	R^2	0.832	0.890	0.978	0.898	0.881	0.838	0.760	0.983	0.825
	RMSE	0.08	0.20	0.04	0.06	0.07	0.11	0.35	0.06	0.10

WL is water loss; SG is solid gain; WL_∞ is the equilibrium values of water loss (%); S_1 is the parameter related to the rate of water diffusion from the product; SG_∞ is the equilibrium values of solid gain (%); S_2 is the parameter associated with the rate of solute diffusion into the product; k_1 is Peleg rate constant (h/(g/g wet basis)) and k_2 is Peleg capacity constant ((g/g wet basis)$^{-1}$); D_{eff} is the effective diffusivity (m^2/s); R^2 is coefficient of determination; RMSE is root mean square error.

Table 4. Parameters of mathematical modeling of osmotic dehydration kinetics of mangos in isomaltulose solutions at different temperatures.

Model	Parameter	Solute concentration / Temperature								
		25% / 25°C	**30% / 25°C**	**35% / 25°C**	**25% / 35°C**	**30% / 35°C**	**35% / 35°C**	**25% / 45°C**	**30% / 45°C**	**35% / 45°C**
Azuara (WL)	**WL_∞**	18.35	28.90	28.99	17.54	16.50	37.45	15.82	19.61	45.66
	S_1	0.009	0.014	0.017	0.028	0.029	0.013	0.024	0.032	0.017
	R^2	0.765	0.878	0.925	0.986	0.982	0.872	0.991	0.992	0.983
	RMSE	1.52	2.94	2.15	1.19	1.47	3.55	0.63	0.89	1.96
Azuara (SG)	**SG_∞**	3.72	5.99	9.11	3.12	6.68	8.71	3.50	10.94	11.99
	S_2	0.054	0.023	0.016	0.012	0.010	0.013	0.017	0.008	0.008
	R^2	0.972	0.964	0.934	0.712	0.903	0.901	0.911	0.838	0.740
	RMSE	0.50	0.50	0.67	0.46	0.45	0.63	0.62	0.75	1.02
Peleg (WL)	**k_1**	0.139	0.044	0.031	0.032	0.031	0.038	0.041	0.023	0.019
	k_2	0.043	0.035	0.036	0.059	0.063	0.026	0.063	0.053	0.022
	R^2	0.866	0.754	0.886	0.886	0.787	0.793	0.975	0.954	0.954
	RMSE	1.42	2.92	2.13	1.16	1.45	3.53	0.59	0.82	1.81
Peleg (SG)	**k_1**	0.098	0.100	0.115	0.521	0.367	0.157	0.610	0.242	0.255
	k_2	0.248	0.183	0.114	0.283	0.117	0.114	0.135	0.073	0.058
	R^2	0.761	0.821	0.876	0.628	0.901	0.883	0.775	0.911	0.869
	RMSE	0.48	0.48	0.66	0.45	0.45	0.67	0.55	0.69	0.93
Fick (WL)	**D_{eff}**	$5.67\cdot10^{-11}$	$6.34\cdot10^{-11}$	$7.78\cdot10^{-10}$	$5.56\cdot10^{-11}$	$1.23\cdot10^{-11}$	$2.05\cdot10^{-11}$	$6.27\cdot10^{-10}$	$4.64\cdot10^{-10}$	$4.60\cdot10^{-8}$
	R^2	0.977	0.868	0.935	0.945	0.916	0.929	0.994	0.995	0.927
	RMSE	0.08	0.33	0.35	0.08	0.11	0.57	0.08	0.07	0.91
Fick (SG)	**D_{eff}**	$1.26\cdot10^{-10}$	$3.57\cdot10^{-10}$	$1.41\cdot10^{-9}$	$4.97\cdot10^{-11}$	$2.04\cdot10^{-10}$	$7.69\cdot10^{-10}$	$3.70\cdot10^{-11}$	$5.93\cdot10^{-10}$	$1.21\cdot10^{-9}$
	R^2	0.992	0.865	0.962	0.963	0.966	0.928	0.913	0.868	0.890
	RMSE	0.14	0.39	0.81	1.21	0.39	0.71	0.15	0.87	0.99

WL is water loss; SG is solid gain; WL_∞ is the equilibrium values of water loss (%); S_1 is the parameter related to the rate of water diffusion from the product; SG_∞ is the equilibrium values of solid gain (%); S_2 is the parameter associated with the rate of solute diffusion into the product; k_1 is Peleg rate constant (h/(g/g wet basis)) and k_2 is Peleg capacity constant ((g/g wet basis)$^{-1}$); D_{eff} is the effective diffusivity(m^2/s); R^2 is coefficient of determination; and RMSE is root mean square error.

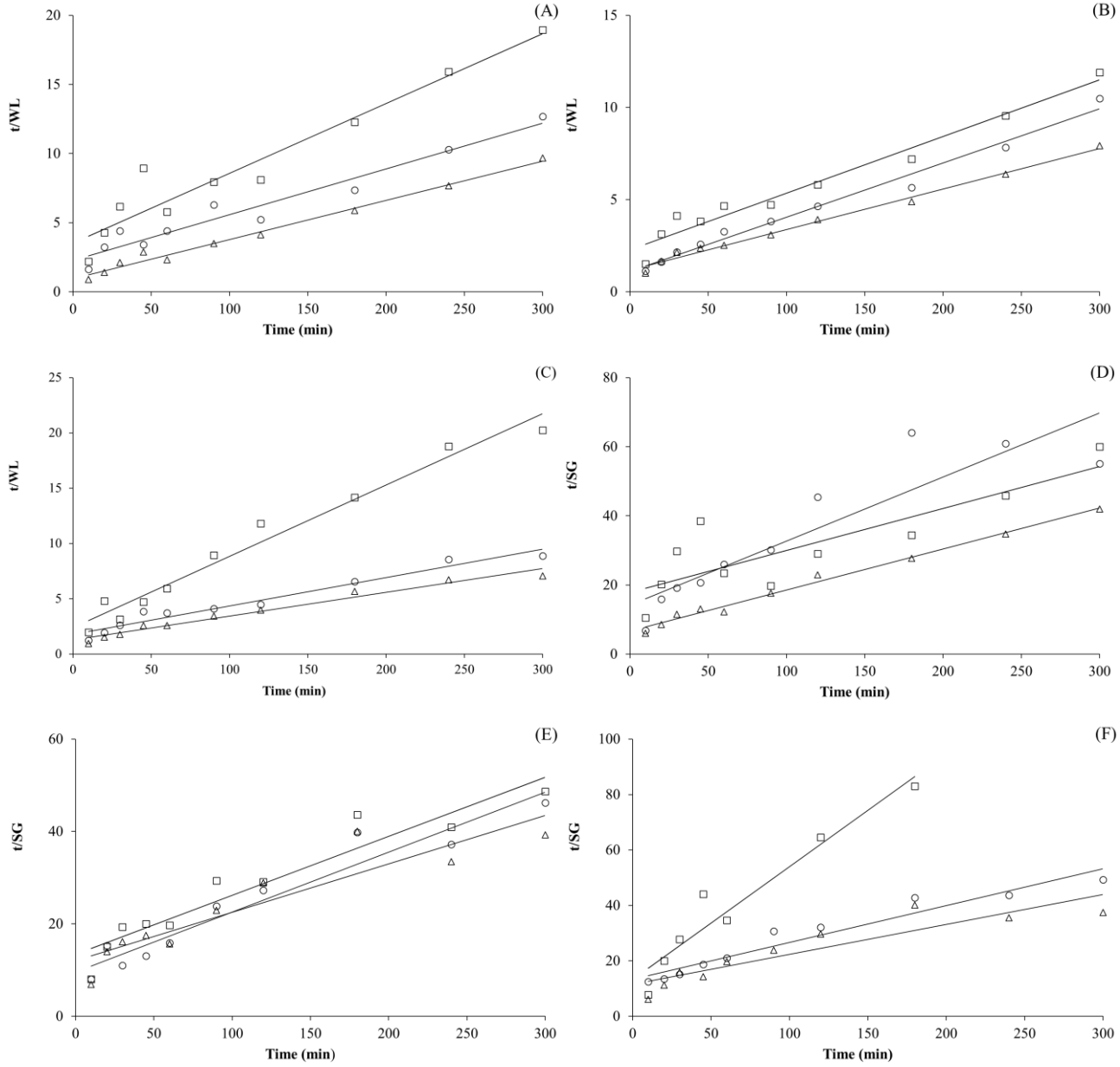

Fig 1. Evolution of water loss at 25 °C (A), 35 °C (B) and 45 °C (C) and solid gain at 25 °C (D), 35 °C (E) and 45 °C (F) as function of time for sucrose solutions. (□) 25%, (○) 30% and (△) 35% solute concentration. Lines represent the fit by linearized Azuara model.

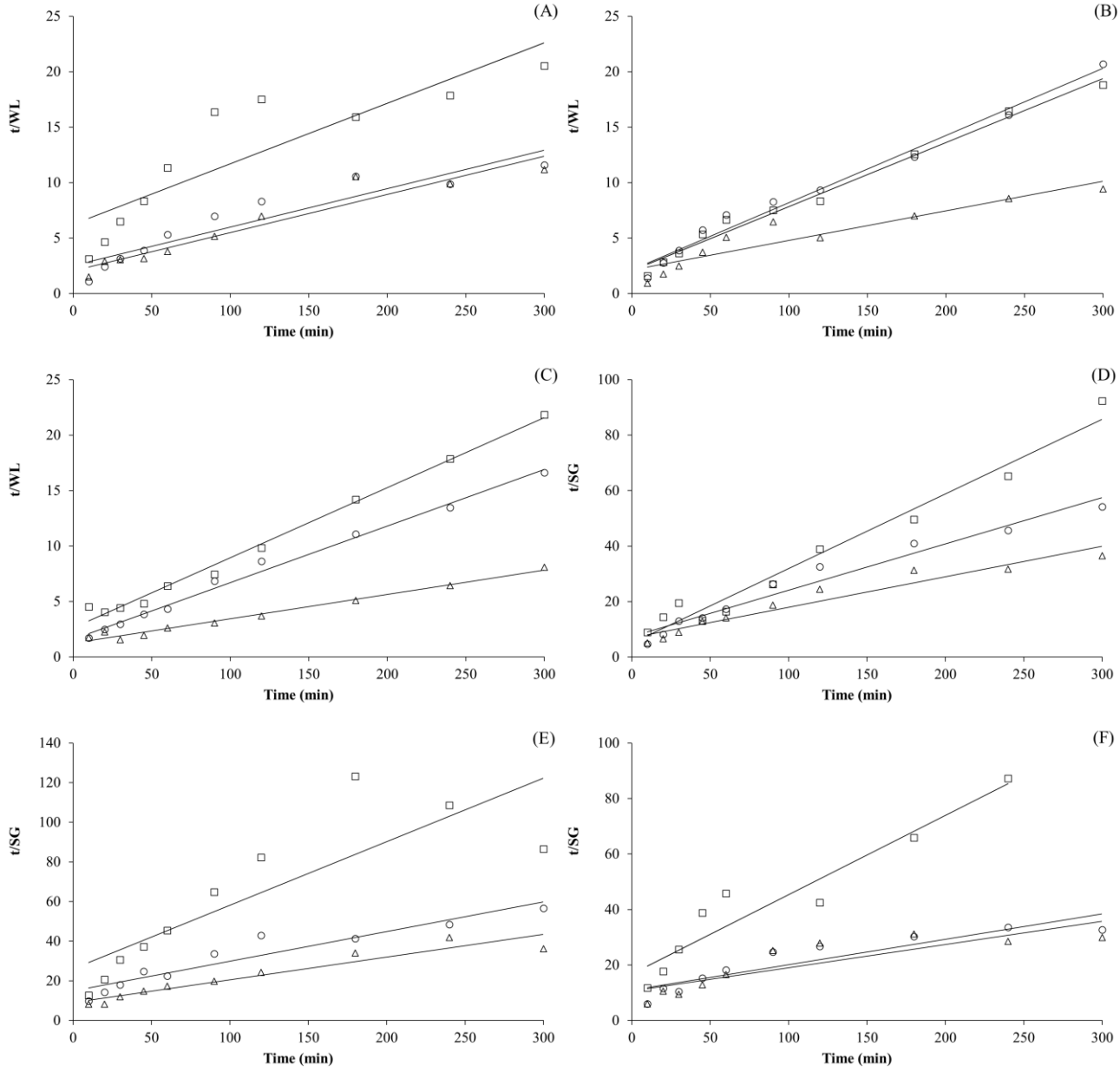

Fig 2. Evolution of water loss at 25 °C (A), 35 °C (B) and 45 °C (C) and solid gain at 25 °C (D), 35 °C (E) and 45 °C (F) as function of time for isomaltulose solutions. (□) 25%, (○) 30% and (△) 35% solute concentration. Lines represent the fit by linearized Azuara model.

3.4 Modeling of SG for the osmotic dehydration of mangos

Azuara model presented a good fit for sucrose ($R^2 \geq 0.715$ and RMSE ≤ 0.73) and isomaltulose ($R^2 \geq 0.712$ and RMSE ≤ 1.02) solutions. In general, the values of Azuara model parameters for SG (SG_∞ and S_2) increased with temperature and solute solution increases, irrespective of the solute type. The Peleg model had also a good fit for sucrose ($R^2 \geq 0.758$ and RMSE ≤ 0.70) and isomaltulose ($R^2 \geq 0.761$ and RMSE ≤ 0.93) solutions.

In general, the reciprocal of the parameters k_1 and k_2 increased also with the temperature and solute concentration. As for WL, predict values obtained by Azuara model were closest than Peleg model for SG and SG_∞ observed values (Table 1 and Table 2). Therefore, the Azuara was the model chosen to describe the SG kinetics for OD of mangos in sucrose and isomaltulose solutions (Fig. 1 and Fig. 2). Similar findings were found by Mello Júnior et al. (2019) and Mehta et al. (2021) for OD of green figs and aonla in sucrose solutions.

Fick model presented best fits for isomaltulose ($R^2 \geq 0.865$ and RMSE ≤ 1.21) than for sucrose ($R^2 \geq 0.760$ and RMSE ≤ 0.35) solutions. The D_{eff} values for the mangos immersed in sucrose solutions varied from $2.64 \cdot 10^{-12}$ to $3.56 \cdot 10^{-10}$ m^2/s, while for isomaltulose solutions the D_{eff} values varied from $3.70 \cdot 10^{-11}$ to $1.41 \cdot 10^{-9}$ m^2/s. In general, for both the solutes, the D_{eff} values increased with temperature and solute concentration. This behavior was more evident for isomaltulose than for sucrose.

3.5 a_w, shrinkage and TSS of osmodehydrated products

In general, the highest shrinkage values were observed for the osmodehydrated mangos with 35% of solute concentration, and the lowest shrinkage values were observed for the mangos OD with 25% of solute concentration, regardless of the solute and temperature (Table 5). For the same type of solute, most treatments showed no statistically difference ($p > 0.05$). This can be due to higher and lower solute incorporation in the samples in these treatments (Table 1 and Table 2).

Table 5. Volumetric shrinkage, total soluble solids (TSS) and water activity (a_w) of osmodehydrated mangos in sucrose and isomaltulose solutions.

Solute	Temperature (°C)	Solute concentration (%)	Volumetric shrinkage	a_w	TSS (°B)
Sucrose	25	25	0.29±0.03^{def}	0.974±0.002^{a}	31.2±3.3^{cde}
		30	0.34±0.08^{abcdef}	0.961±0.002^{ab}	31.3±1.6^{cde}
		35	0.423±0.07^{abcd}	0.947±0.003^{bc}	47.3±1.9^{a}
	35	25	0.26±0.04^{ef}	0.967±0.011^{ab}	30.5±5.1^{cde}
		30	0.39±0.05^{abcde}	0.957±0.005^{ab}	38.8±7.4^{abc}
		35	0.44±0.01^{abc}	0.929±0.010^{c}	44.6±5.4^{ab}
	45	25	0.24±0.02^{f}	0.972±0.002^{a}	28.2±3.0^{cde}
		30	0.31±0.03^{cdef}	0.963±0.001^{ab}	37.7±0.8^{abc}
		35	0.35±0.02^{abcdef}	0.964±0.002^{ab}	47.0±1.6^{a}
Isomaltulose	25	25	0.34±0.04^{bcdef}	0.973±0.002^{a}	19.1±0.2^{e}
		30	0.40±0.01^{abcde}	0.970±0.002^{a}	27.5±6.2^{cde}
		35	0.46±0.01^{ab}	0.963±0.002^{ab}	32.6±0.9^{bcd}
	35	25	0.22±0.02^{f}	0.974±0.004^{a}	21.5±0.2^{de}
		30	0.29±0.03^{def}	0.962±0.001^{ab}	31.4±0.4^{cde}
		35	0.32±0.04^{cdef}	0.960±0.005^{ab}	33.3±0.4^{bcd}
	45	25	0.28±0.05^{def}	0.973±0.002^{a}	21.9±0.6^{de}
		30	0.32±0.03^{cdef}	0.967±0.001^{ab}	22.7±1.4^{de}
		35	0.48±0.04^{a}	0.960±0.002^{ab}	28.3±1.2^{cde}

Means ± standard deviation (n=5). Values with different letters in same column differ significantly ($p \leq 0.05$) according to Tukey's test.

Fresh mango sample has a high a_w value (0.990 ± 0.003), which is specific to fruit and vegetables. According to the Tukey's test, the samples with the highest a_w were those treated with 25% solute, regardless of temperature and type of solute (Table 5). The treatments with the lowest a_w were those obtained with 35% sucrose at 35 °C and 25 °C, which were the ones that presented high WL contents (Table 1). For all treatments, the osmodehydrated mangos had a_w > 0.6 (0.933-0.974), which cannot guarantee the microbiological stability of the products (Jay, 2005). However, Kroehnke et al. (2021) affirm that the increases carbohydrate content, resulting from the OD, may also have a beneficial influence for products. The use of concentrated solutions creates a barrier limiting the growth and adhesion of microorganisms on the sample surface, even in a material with an a_w value of 0.85. This may result from the reduced mobility of microorganisms due to higher surface viscosity.

The samples pretreated with sucrose solutions with 35% of solutes at 25 °C presented higher TSS, and the sample pretreated with isomaltulose at 25% and 25 °C showed lower TSS (Table 5). The former is characterized by having around twice times more WL and SG than latter. In general, there was no significant difference between treatments ($p > 0.05$) for this parameter in relation to the type of solute.

The results of these properties showed that the isomaltulose could be promising in the replacement of conventional sugar solutions, as sucrose, in osmotic processes aiming at alternative carbohydrates with healthy attributes.

4 Conclusions

The use of healthy carbohydrate, such as isomaltulose, on less porous fruit presented a satisfactory incorporation, opening the way for other studies in this area. The Azuara and Peleg model were able to predict with good accuracy the WL and SG data of mangos slices at different temperatures (25-45 °C), solute concentration (25-35%) and solute type (sucrose and isomaltulose). The diffusive model of Fick predicted with good accuracy the D_{eff} for WL and SG for all conditions of OD studied, which increased with temperature and solute concentration. Moreover, the results of volumetric shrinkage, a_w and total soluble solids evidenced that isomaltulose can be promising in the replacement of sucrose in OD of mango slices.

Conflicts of interest

There are no conflicts of interest to declare.

Acknowledgments

The authors would like to thank the following Brazilian agencies for funding: National Council for Scientific and Technological Development (Conselho Nacional de Desenvolvimento Científico e Tecnológico-CNPq) (314191/2021-6) and Minas Gerais Research Support Foundation (FAPEMIG). J. R. Carmo would also like to thank CNPq for scholarship 166378/2018-6.

Data availability statement

Research data are not shared.

Ethical statement

Ethical approval was not necessary for this study.

Credit authorship contribution

Juliana Rodrigues do Carmo: Conceptualization; Formal analysis; Writing - Original draft preparation. **Jefferson Luiz Gomes Corrêa:** Conceptualization; Formal analysis; Writing - review & Editing; Supervision; Funding acquisition. **Rosinelson da Silva Pena:** Conceptualization; Formal analysis; Writing - review & Editing; Supervision.

References

Abrahão, F. R., & Corrêa, J. L. G. (2021). Osmotic dehydration: More than water loss and solid gain. *Critical Reviews in Food Science and Nutrition,* 29, 1–20. http://doi.org/ 10.1080/10408398.2021.198376

AOAC. (2010). *Association of Official Analytical* Chemists – *Official methods of analysis of Association of Official Analytical Chemists International* (18th ed.). Arlington: AOAC.

Assis, F. R., Morais, R. M. S. C., Morais, A. M. M. B. (2017). Mathematical modelling of osmotic dehydration kinetics of apple cubes. Journal of Food Processing and Preservation, 41, e12895. http://doi.org/10.1111/jfpp.12895

Azuara, E., Cortés, R., Garcia, H. S., & Beristain, C. I. (1992). Kinetic model for osmotic dehydration and its relationship with Fick's second law. *International Journal of Food*

Science and Technology, 27, 409–418. http://doi.org/10.1111/j.1365-2621.1992.tb01206.x

Carmo, J. R., Corrêa, J. L. G., Polachini, T. C., & Telis-romero, J. (2022). Properties of Isomaltulose (Palatinose®) – an emerging healthy carbohydrate: effect of temperature and solute concentration. *Journal of Molecular Liquids*, 347, 118304. http://doi.org/10.1016/j.molliq.2021.118304

Crank, J. (1975). *The Mathematics of diffusion*. 2 ed. Oxford: Carendon press ed.

Devic, E., Guyot, S., Daudin, J., & Bonazzi, C. (2010). Effect of temperature and cultivar on polyphenol retention and mass transfer during osmotic dehydration of apples. *Journal Agricultural and Food Chemistry*, 58, 606–614. https://doi.org/10.1021/ jf903006g

Fernandes, F. A. N., Braga, T. R., Silva, E. O., & Rodrigues, S. (2019). Use of ultrasound for dehydration of mangoes (*Mangifera indica* L.): kinetic modeling of ultrasound-assisted osmotic dehydration and convective air-drying. *Journal of Food Sience and Technology*, 56, 1793–1800. https://doi.org/10.1007/s13197-019-03622-y

Galdino, P. O., Queiroz, A. J. D., Figueiredo, R. M. F., Santiago, A. M., & Galdino, P. O. (2021). Production and sensory evaluation of dried mango. *Revista Brasileira de Engenharia Agrícola e Ambiental*, 25, 44–50. http://doi.org/10.1590/1807-1929/agriambi.v25n1p44-50

Kroehnke, J., Szadzinska, J., Radziejewska-Kubzdela, E., Bieganska-Marecik, R., Musielak, G., & Dominik Mierzwa. (2021). Osmotic dehydration and convective drying of kiwifruit (*Actinidia deliciosa*) – The influence of ultrasound on process kinetics and product quality. *Ultrasonics – Sonochemistry*, 71, 105377. https://doi.org/10.1016/j.ultsonch.2020.105377

Kushwaha, R., Singh, V., Singh, M., & Kaur, D. (2018). Influence of osmotic agents on drying behavior and product quality of guava fruit. *Plant Archives*, 18, 205–209.

Lebaka V.R., Wee Y.-J., Ye W., & Korivi M. (2021). Nutritional composition and bioactive compounds in three different parts of mango fruit. *International Journal of Environmental Research and Public Health*, 18, 741. http://doi.org/10.3390/ijerph18020741

Martins, M. J. N., Guimarães, B., Polachini, T. C., & J. Telis-Romero. (2020). Thermophysical properties of carbohydrate solutions: correlation between thermal and transport

properties. *Journal of Food Process and Engineering*, 43, 1–15. http://doi.org/10.1111/jfpe.13483

Mehta, A., Singh, A., Singh, A. P., Prabhakar, P. K., & Kumar, N. (2021). Ultrasonic induced effect on mass transfer characteristics during osmotic dehydration of aonla (*Phyllanthus emblica* L.) slices: A mathematical modeling approach. Journal of Food Process Engineering, 44, e13887. http://doi.org/10.1111/jfpe.13887

Mello Júnior R. E., Correa, J. L. G., Lopes, F. J., Souza, A. U., & Silva, K. C. R. (2019). Kinetics of the pulsed vacuum osmotic dehydration of green fig (*Ficus carica* L.) *Heat and Mass Transfer*, 55, 1685–1691. http://doi.org/10.1007/s00231-018-02559-w

Mendonça, K. S., Corrêa, J. L. G., Junqueira, J. R. J., Cirillo, M. A., Figueira, F. V., & Carvalho, E. E. N. (2017). Influences of convective and vacuum drying on the quality attributes of osmo-dried pequi (*Caryocar brasiliense* Camb.) slices. *Food Chemistry*, 224, 212–218. http://doi.org/ 10.1016/j.foodchem.2016.12.051.

Oladejo, D., Ade-Omowaye, B. I. O., & Dekanmi, A. O. (2013). Experimental study on kinetics, modeling and optimisation of osmotic dehydration of mango (*Mangifera indica* L.). *International Journal of Engineering Science*, 2, 1–8.

Peleg, M. (1988). An empirical model for the description of moisture sorption curves. *Journal of Food Science*, 53, 1216–1219

Prithani, R., & Dasha, K. K. (2020). Mass transfer modelling in ultrasound assisted osmotic dehydration of kiwi fruit. *Innovative Food Science & Emerging Technologies*. 64, 102407. https://doi.org/10.1016/j.ifset.2020.102407

Ruskova, M., Aleksandrov, S., Petrova, T., Bakalov, I., Gotcheva, V., & Penov, N. (2016). Effect of osmotic dehydration variables on the water loss of blackcurrants. *Journal of Food and Packaging Science, Technique and Technologies*, 10, 10–13.

Schmidt, F. C., Carciofi, B. A. M., & Laurindo, J. B. (2009). Application of diffusive and empirical models to hydration, dehydration and salt gain during osmotic treatment of chicken breast cuts. *Journal of Food Engineering*, 91, 553–559. http://doi.org/10.1016/j.jfoodeng.2008.10.003

Tiroutchelvame, D., Maran, J. P., & Pragalyaashree, M. M. (2019). Response surface analysis and optimization of osmotic dehydration of *Musa acuminata* slices. *Journal of Microbiology, Biotechnology and Food Sciences*, 8, 1016–1020. http://doi.org/10.15414/jmbfs.2019.8.4.1016-1020

Viana, A. D., Corrêa, J. L. G., & Justus, A. (2014). Optimisation of the pulsed vacuum osmotic dehydration of cladodes of fodder palm. *International Journal of Food Science and Technology*, 49, 726–732. http://doi.org/10.1111/ijfs.12357

Zielinska, M., & Markowski, M. (2018). Effect of microwave-vacuum, ultrasonication, and freezing on mass transfer kinetics and diffusivity during osmotic dehydration of cranberries. Drying Technology, 36, 1158–1169 http://doi.org/10.1080/07373937.2017.1390476

Zongo, A. P., Khalloufi, S., & Ratti, C. (2021). Effect of viscosity and rheological behavior on selective mass transfer during osmotic dehydration of mango slices in natural syrups. *Journal of Food Process Engineering*, 44, e13745. http://doi.org/10.1111/jfpe.13745

ARTICLE 3 – **Mango enriched with sucrose and isomaltulose (Palatinose®) by osmotic dehydration: effect of temperature and solute concentration through the application of a multilevel statistical models**

Juliana Rodrigues do CARMO [a*], Jefferson Luiz Gomes CORRÊA [a], Mariana RESENDE [b], Marcelo Ângelo CIRILLO [b], Edith CORONA-JIMÉNEZ [c], Javier TELIS-ROMERO [d]

[a] Department of Food Science (DCA), Federal University of Lavras, 37200-900, Lavras, Brazil. E-mail: juliana_docarmo@yahoo.com.br (Orcid ID: 0000-0002-9083-4863); jefferson@ufla.br (Orcid ID: 0000-0002-6818-6927)

[b] Department of Statistic (DES), Federal University of Lavras, 37200-900, Lavras, Brazil. E-mail: mresende31@gmail.com (Orcid ID: 0000-0001-8814-4997); macufla@gmail.com (Orcid ID: 0000-0003-2026-6802)

[c] Facultad de Ingeniería Química, Benemérita Universidad Autónoma de Puebla, 72570, Puebla, México. E-mail: edith.coronaji@correo.buap.mx (Orcid ID: 0000-0001-8553-4447)

[d] Department of Food Engineering and Technology, São Paulo State University, São José do Rio Preto 15054-000, Brazil. E-mail: javier.romero@unesp.br (Orcid ID: 0000-0003-2555-2410)

Running head: Multilevel models of osmotic process on fruits

Novelty impact statement

Through the osmotic dehydration it is possible to enrich mango samples with isomaltulose due to its healthy attributes. Instead a traditional statistical analysis, the multilevel statistical modelling was applied, which was suitable for evidence that highest solute concentration and temperature conditions promoted the greatest water loss and solid gain, favoring the enrichment process.

[*]**Corresponding author:** Juliana Rodrigues do CARMO (E-mail: juliana_docarmo@yahoo.com.br)

(Accept in the Journal of Food Processing and Preservation)

Abstract: Osmotic dehydration (OD) is a useful for enrichment of mangos with interest solutes. Isomaltulose has healthier properties than sucrose and its use is still scarce in OD processes. The OD of mangos with isomaltulose and sucrose was evaluated and the effect of solute concentrations (25, 30, 35%) and temperatures (25, 35, 45 °C) were estimated by multilevel statistical analysis in order to find the best conditions for a greater water loss (WL) and solid gain (SG). In sucrose OD, the highest concentration (35%) had the greatest effect than temperature for WL and SG. For isomaltulose OD, the concentration provided greater WL and SG, but the effect of temperature was slightly more expressive for SG than WL. The maximum working conditions (35% of isomaltulose or sucrose and 45 °C) promoted greater WL and SG for both carbohydrates, and with the OD it was possible to enrich mango with isomaltulose by taking advantage of the osmotic gradient, getting an osmodehydrated product with low glycemic and isulinemic indexes.
Keywords: osmotic dehydration, sucrose, Palatinose®, multilevel regression models.

1 Introduction

Mango (*Mangifera indica* L.) is one of the most popular tropical fruits. It is a source of fiber, phenolic compounds and vitamins, such as C and pro-vitamin A (betacarotene), and minerals such as calcium, phosphorus, and iron (Lebaka *et al.*, 2021). Despite its considerable nutritional value, mango is an extremely perishable fruit, which needs specific care for its conservation Kumar & Sagar, 2014). One of the main strategies is the use of appropriate dehydration techniques to obtain a microbiologically stable product with decreasing physicochemical and sensory qualities reduction (Mello *et al.*, 2020).

Osmotic dehydration (OD) consists of immersing the food in a hypertonic solution, with consequent water loss (WL) and solid gain (SG) in simultaneous isothermal flows without any phase change. In OD, three types of counter-current mass transfer occur: (i) water flows from the product to the solution, (ii) a solute transfer from solution to the product and (iii) a leaching out of the native solutes (sugars, organic acids, minerals, vitamins, etc.). The OD process offers the possibility of modifying food properties, especially in relation to taste and structural characteristics (Abrahão & Corrêa, 2021).

Sucrose is the most common solute used in osmotic solution (Fernandes *et al.*, 2019). Its advantages are its low-cost and availability. However, it is considered a highly cariogenic sugar. This carbohydrate is rapidly digested, inducing high glycemic and insulinemic response. One way around these disadvantages is to replace sucrose with other carbohydrates that do not induce glycemic and insulinemic peaks and are slowly digested by the body (Mendonça *et al.*, 2016).

Isomaltulose, commercially known as Palatinose®, is naturally present in honey and sugarcane juice. Although isomaltulose has a half of the sweet taste and similar caloric value of sucrose (~4 kcal/g), it can be considered a healthy, since it is a non-cariogenic carbohydrate and presents low glycemic and insulinemic indexes (Sawale *et al*, 2017). Due to it, this disaccharide is becoming increasingly used by sportsmen and disease people, such as diabetic, obese and heart diseases (Maeda *et al.*, 2013). In this regard, isomaltulose could be added in fruits and vegetables by OD for enriching and obtaining a healthy product, as has been recently studied (Lopez *et al.*, 2020 Macedo *et al.*, 2021; Macedo *et al.*, 2021).

Apart from the proven influence of the type of solute and its concentration in OD processes, temperature is another relevant factor (Jiménez *et al.*, 2021). These factors can interfere with the OD efficiency (ratio WL/SG). High efficiency can favor dehydrating processes in the fruit,

whereas lower efficiency favors the process of enriching the fruit (Kvapil *et al.*, 2021). Therefore, to evaluate the best dehydration or enrichment condition, strategic statistical methods must be used, such as those that work with observations nested in groups, that is, they can evaluate the simultaneous effect of individual characteristics as a collective characteristics and their interactions on an response of the osmotic dehydration, that is, studying the role played by OD process factors (solute concentration and temperature) and their influence on dehydration or enrichment (WL or SG) of samples subjected to different osmotic solutions and tend to have a hierarchical or nested structure.

Multilevel modeling is a generalization of regression methods, and as such can be used for several purposes, as prediction, data reduction, and causal inference from experiments and observational studies. It can be essential for prediction multilevel modeling, useful for data reduction and helpful for causal inference (Gelman, 2006). An advantage of using the multilevel methodology is attributing random effects to other elements of the model, not only to the experimental error as occurs in traditional analysis. Another advantage is that it is possible to answer questions focusing on random effects, which are limited to other tests. Studies about that have been applied the multilevel statistical models on OD processes were not found in the literature. In this context, this work aimed presenting data on the enrichment of the mangos with isomaltulose through the evaluation of the WL and SG variables on mangos submitted to OD in a 25, 30 and 35% sucrose or isomaltulose solutions at 25, 35 and 45 °C with the performance of the multilevel statistical analysis. This analysis evaluated the effect of solute concentration and temperature for the studied conditions for each osmotic solute evaluated, which the best condition was sought to have a greater WL and one greater SG.

2 Material and methods

2.1 Material

Mango fruits (*Mangifera indica* L. cv. Tommy Atkins) were purchased in a local market (Lavras, Minas Gerais, Brazil) (21°14'43 S and 44°59'59 W). The fruits were selected in a similar degree of maturation (half-ripe) and with the general characteristics of reddish-green skin color, 85.14 ± 0.55% moisture; 12.3 ± 0.6 °Brix; 4.72 ± 0.16 °Brix/acidity (ratio), 3.60 ± 0.04 pH and 47.50 ± 5.55 N firmness. The mango fruits were washed with a disinfectant solution (chlorinated water at 200 ppm) during 5 min. After, the seed and peel were removed and the experimental samples were obtained from the fruit pulp. The samples were sliced into

pieces of 4.00±0.01×2.00±0.01×0.40±0.01 cm (long×wide×thickness) employing a stainless-steel mold.

2.2 Preparation of osmotic solution

The osmotic solutions were prepared with distilled water and commercial sucrose (União, São Paulo, Brazil) or isomaltulose, commercially known as Palatinose® (Beneo, Mannheim, Germany). The solution concentrations chosen were 25, 30 and 35 w/w. They were based on osmotic solutions properties (solubility, density, heat specific, thermal conductivity and viscosity) investigated recently by Carmo et al. (2022). The water activity (a_w) of the osmotic solutions was determined at 25 °C with a digital thermohygrometer (AquaLab 3TE, Decagon, USA).

2.3 Osmotic dehydration (OD)

The OD experiments were carried out with samples immersed into a glass container without recirculation and with the osmotic solutions with a ratio of solution/sample of 10:1 (v/w) to avoid dilution of the solution (Tiroutchelvame *et al.*, 2019). The experiments were performed at different temperatures (25, 35 and 45 °C) in a thermostatic chamber (Eletrolab EL111/4, São Paulo, Brazil) at atmospheric pressure, during 300 min, then, samples were removed from the solution and immediately immersed in a water and ice bath for 10 s to stop dehydration and to remove the remaining osmotic solution on the surface. Then, they had their surface dried with absorbent paper (Viana *et al.*, 2014). The OD time (300 min) was chosen based on preliminary tests that showed that the osmotic equilibrium was reached at that time period. Other authors also used similar time periods (Grzelak-Blaszczyk *et al.*, 2020; Junqueira *et al.*, 2018; Prithani & Dash, 2020).

The moisture content of fresh and osmotically treated samples was determined according to AOAC (2010).

For each condition of osmotic process, the water loss (WL) and solid gain (SG) (%) were determined according to Eq. 1 and 2, respectively (Viana *et al.*, 2014):

$$WL(\%) = \frac{x_0^w M_0^o - x_t^w M_t^o}{M_0^o} x100 \quad (1)$$

$$SG(\%) = \frac{w_t S_t - w_0 S_0}{w_0} x100 \quad (2)$$

where w is the sample weight (kg), S is the solid content (kg solid/kg fruit) and x is the moisture content based on wet basis (w. b.) (kg water/kg fruit). Sub-indexes "0" and "t" refer to the fresh samples and the samples after osmotic treatment, respectively.

All analyses were performed in triplicate and the results were presented as the replicates mean.

2.4 Statistical analysis

Multilevel statistical models are used when the data structure is hierarchical with elementary units. It is an increasingly popular approach to substitute classical regression in predictive accuracy. One feature of multilevel models is the ability to separately estimate the predictive effects of an individual predictor and its group-level mean, which are sometimes interpreted as "direct" and "contextual" effects of the predictor. It has been replaced traditional statistical methods, which ignore the correlation of outcomes within clusters and tend to underestimate standard errors. This artificially increases the significance of hypothesis tests, increasing the risk of falsely concluding that significant associations exist. The analysis type is common for data in health research and population studies (Austin, 2001).

Therefore, in the present work, multilevel models at two hierarchical levels were created for the first time for food data and these were defined as: 1st level = Temperature and 2nd level = Solute concentration for WL and SG variables. Considering the above, four models (Table 1) were taken in order to select the one that most closely matches the real conditions of the experiment and to assess where the random effect should be attributed – for WL and SG variables. Then, the selection of the appropriate model to explain the variation of WL and SG was made initially by means of the probability of significance, obtained as function of the chi-square statistic. Thus, models that were not significant were selected and subsequently evaluated using as a criterion the model that had the highest intraclass correlation coefficient, being possible to justify the hierarchy between the factors, as well as, the imposition of random parameters. Statistical software R Core Team (2021) was used to analyze the data.

Table 1. Description of the models with identification of the fixed and random effects attributed to the parameters and levels of the factors.

Model	Code	Number of the parameters	Fixed effects parameters	Random effects parameters
Random Intercepts	Mod0	3	Intercept	Intercept for each factor level (Solute concentration) and residual
Random intercepts and fixed slopes	Mod1	4	Intercept for each factor level (Temperature)	Intercept for each factor level (Solute concentration) and residual
Random intercepts and slopes	Mod2	6	Intercept for each factor level (Temperature)	Intercept for each factor level (Solute concentration) with random slopes for each factor (Temperature) and residual
Intercepts and slopes random with inclusion of variable SG at the second level.	Mod3	8	Intercept for each factor level (Temperature), SG and interaction Temperature × SG	Intercept for each factor level (Solute concentration) with random slope, for each factor level (Temperature) and residual

Mod0 – model 0; Mod1 – model 1; Mod2 – model 2; Mod3 – model 3.

3 Results and discussion

3.1 Osmotic dehydration

The results obtained for WL and SG of mango slices at different temperatures and solute concentrations of sucrose and isomaltulose are showed in Figure 1.

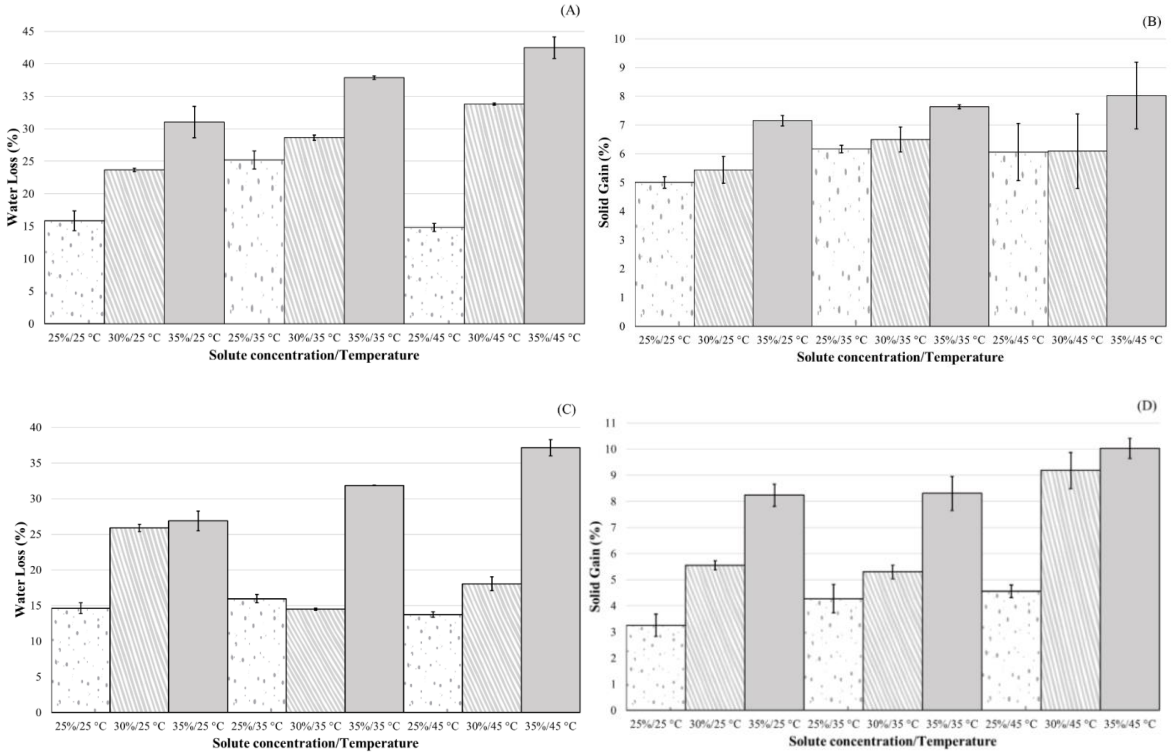

Fig. 1. Water loss (%) and solid gain (%) of osmodehydrated mangos in sucrose solutions (A and B, respectively) and isomaltulose solutions (C and D, respectively) at different solute concentrations and temperatures for 300 min. Means ± standard deviation (n=3).

The WL results showed that, this variable increases for a constant temperature, as the concentration of the sucrose solution increases (Figure 1A), therefore, an effect of the solutes is eminent during the OD, also, the highest moisture loss (42.48%) was reached at the highest processing conditions (35%, 45 °C). In the case of the samples treated with the isomaltulose solution (Figure 1C), it could only be observed that the 35% of concentration obtained an increase of WL values due to the effect of the temperature and only at 45 °C a trend of increased by the presence of the solutes was showed, obtaining the greatest loss of water (37.15%) at 35% of concentration and 45 °C of temperature, in a similar way than samples subjected with sucrose. The rest of the concentrations and temperatures did not show a clear trend.

On the other hand, the SG results showed that there was a trend in its increase due to the effect of the increase in the presence of solutes, the behavior being more evident in the samples subjected to the isomaltulose solution. However, such a clear effect of temperature was not observed, only at the highest study temperature. The highest solids gain for both cases (sucrose and isomaltulose) was at the highest process conditions (35% and 45°C), with the isomaltulose samples (10.02%) having a higher solute enrichment than the sucrose samples (8.02%).

In a general way, the results of mango slices osmodehydrated with sucrose solution presented WL values from 14.81 to 42.48% and SG from 5.00 to 8.02% in temperature range studied (25–45 °C), while for the samples with isomaltulose solution, the WL was from 13.73 to 37.15% and the SG, from 3.25 to 10.02%, under the same conditions. Therefore, the results showed that the samples subjected to a sucrose solution obtained a greater loss in the amount of water than those that were osmotically dehydrated with isomaltulose, so the latter showed partial dehydration. However, the samples treated with isomaltulose presented a greater number of solutes, so there was an enrichment of the sample with this osmotic agent. Although the solubility of aqueous sucrose solution is greater than isomaltulose solution (Galdino *et al.*, 2021), the a_w of both solutions are close (0.979, 0.974 and 0.970 for sucrose solutions and 0.978, 0.978 and 0.972 for isomaltulose solutions for 25, 30 and 35% solute concentration, respectively) and this causes similar osmotic pressure gradients and, consequently, WL and SG values are of the same order of magnitude for all conditions studied (Figure 1). In spite there are no studies about OD of mango in isomaltulose solutions in literature, for sucrose solutions, the results obtained for WL and SG were similar to those previously reported in other works of OD under similar dehydration conditions (Galdino *et al.*, 2021; Zongo *et al.*, 2021).

In this way, the present work shows that under the conditions studied, the use of isomaltulose is interesting as an osmotic agent and it may turn out even more promising, because it can be a partially dried and enriched food with low glycemic and insulinemic indexes agent, as mentioned previously (Macedo *et al.*, 2021; Macedo *et al.*, 2022).

According to Fernandes et al. (2019), fruits like apple, pineapple and strawberry have a porous tissue structure with thin cell walls. Thus, for these fruits, water and soluble solids mass transfer from the fruit to the solution and vice versa suffers little resistance at the border of the fruit samples. Mangos are denser and much less porous (porosity = 0.04 to 0.05) than most fruits (pineapple porosity = 0.16 to 0.25; apple porosity = 0.18 to 0.22; strawberry porosity = 0.47) (Ozcan & Haciseferogullan, 2007). Thus, the use of healthy carbohydrate in the process of OD

in a less porosity fruit with a satisfactory incorporation, opens the way for further studies in this area.

3.2 Multilevel statistical modelling for sucrose

3.2.1 Selection criteria for modelling of sucrose solutions

Table 2 shows the selection criteria for the tested models for sucrose solutions. The comparison was performed according to the chi-square criterion. Three replicates were used for each level that served to give more accuracy in the mean response and the models were adjusted by the mean. The selected model was one whose chi-square statistic is not significant. Therefore, for the WL variable, none of the models was discarded according to the criteria used. For the SG variable, model 2 (with intercept and slope, both random) and model 3 (with intercept and slope, both random, and inclusion of a variable at the second level) were discarded. The covariate introduced in the second level was the SG, in order to investigate the effect of the SG with the WL. For WL, model 3 was selected as it presented a higher intraclass correlation coefficient. For the SG, model 1 was selected (random intercept and fixed slope), since among the models tested, it was the only one that did not show significance in the chi-square statistic.

Table 2. Models selection criteria for mango OD in sucrose solutions.

Water Loss			
Model	**Df**	**Chisq**	**Pr(>Chisq)**
Model 0	3		
Model 1	4	0.9650	0.32594
Model 2	6	2.2805	0.31974
Model 3	8	5.1626	0.07567
Solid Gain			
Model	**Df**	**Chisq**	**Pr(>Chisq)**
Model 0	3		
Model 1	4	2.3168	0.127984
Model 2	6	6.1554	0.046066 *
Model 3	8	10.2819	0.005852 *

Df – Degrees of freedom; Pr – Probability of significance. *Indicates the chi-square statistic is significant.

To proceed with the analysis, the structure of the design was evaluated in both variables. The intraclass correlation coefficients for temperature (ρ_1) was 0.18% and 8.02% and for solute concentration (ρ_2), was 99.82% and 91.98% for WL and SG, respectively Then, it was concluded that the temperature depends on the solute concentration of the selected models.
Thus, greater intraclass correlation (ρ_2) indicated greater the dependence between individuals in the same group and it justifies the use of regression model that respects the structure and the aggregation structure of the data. In addition, for sucrose solutions, means that the variance in WL and SG can consequently be attributed to the solute concentration level. Thus, there are several temperature levels considered homogeneous for each level of solute concentration, giving rise to a hierarchy structure. The relatively high value of intraclass correlation justifies the use of a multilevel approach to analysis instead of a traditional regression.

3.2.2 Water loss (WL) modelling of sucrose solutions – effect of solute concentration

Model 3 for WL is represented in Figure 2A, in which the random intercept and random temperature with inclusion of covariate (SG) in the second level are showed. The inclusion of the covariate implied the difference between the solute concentration, because as can be seen in the plot, the intercepts are quite different indicating a significant difference between the different levels of solute concentrations. So, it is possible to observe that 35% sucrose concentration has an initial value with an intercept with a greater difference from the others (25 and 30%).

3.2.3 Solid gain (SG) modelling of sucrose solutions – effect of solute concentration

Figure 2B shows model 1 for SG, with random intercept and fixed temperature. In this sense, considering fixed intercept implies zero temperature, that is, all levels have the same mean. In this plot, the temperature was placed as a fixed effect and the effect of the solute concentration was considered random. So, it is possible to observe that 25% of sucrose concentration has an initial value with a greater difference intercept from the others. The others sucrose concentrations (30 and 35%) were statistically similar, since their intercepts started close together. Therefore, it can be said that 25% sucrose concentration is statistically different from 30 e 35% sucrose concentration.

3.2.4 Water loss (WL) modelling of sucrose solutions – effect of temperature

Figure 3 shows the behavior of the random effects of the selected models, in which the lines represent the fixed levels and the points are the mean of the replicates. The plot for WL (Figure 3A) presents different behavior for different solute concentrations, that is, the inclusion of the covariate SG had a great influence on the results. It is observed that WL increases with an increase of temperature for 25 and 35% sucrose concentration, being more expressive at 25% sucrose concentration, since the slope of the line is slightly stronger than the 35% sucrose concentration, which has a more linear effect. On other hand, at 30% sucrose concentration there was a decrease in WL with increasing temperature. Thus, for WL there is a difference between solute concentrations, being 35% sucrose concentration ones that has the greatest effect on this variable, since its estimates are highest than others.

3.2.5 Solid gain (SG) modelling of sucrose solutions – effect of temperature

In Figure 3B, the slopes of the temperature lines are the same, so it justifies keeping it fixed. In addition, the effect of the slope is extremely small, since it is a model with a fixed inclination. In practical terms, the effect of temperature on SG is considered constant for each solute concentration. So, it is possible to increase or decrease the temperature that the adjusted lines are indicating little evidence of SG. This plot can be understood and explored as an offshoot for each level of solute concentration in relation to temperature. In other words, statistically, the solute concentration had the greatest influence on this variable.

3.3 Multilevel statistical modelling for isomaltulose

3.3.1 Selection criteria for modelling of isomaltulose solutions

As for sucrose, the same four models (Table 1) were compared to select the one that most closely matches the real conditions of the experiment for the variables WL and SG for isomaltulose solutions. Table 3 describes the selection criteria for the tested models. The selection of the appropriate model was also obtained as a function of the probability of significance of the chi-square statistic. Three replicates were also used for each level that served to give more accuracy in the mean response and the models were adjusted by the mean.

As previously mentioned, the model selected was the one whose chi-square statistic was not significant. Therefore, for the WL variable the model 3 does not fit the data satisfactorily and should be discarded. For the SG variable the models 1 and 3, must be discarded.

For WL and SG, models 1 and 2 were selected, respectively, as they presented a higher intraclass correlation coefficient.

The intraclass correlation coefficients for temperature (ρ_1) was 25.77% and 23.13% and for solute concentration (ρ_2), was 74.23% and 76.86% for WL e SG, respectively. The greater intraclass correlation means that the variance in WL and SG in isomaltulose solutions can be attributed to the solute concentration level, as sucrose solutions.

Table 3. Models selection criteria for mango OD in isomaltulose solutions.

Water Loss			
Model	**Df**	**Chisq**	**Pr(>Chisq)**
Model 0	3		
Model 1	4	0.0198	0.8881
Model 2	6	3.2706	0.1949
Model 3	8	18.7299	$8.568x10^{-5}$ *
Solid Gain			
Model	**Df**	**Chisq**	**Pr(>Chisq)**
Model 0	3		
Model 1	4	5.6161	0.0177959 *
Model 2	6	0.1138	0.9447103
Model 3	8	17.8583	0.0001325 *

Df – Degrees of freedom; Pr – Probability of significance. *Indicates the chi-square statistic is significant.

3.3.2 Water loss (WL) modelling of isomaltulose solutions – effect of solute concentration

Figure 2C for WL shows that 35% isomaltulose concentration has an initial value with intercept with greater difference in relation to 25 and 30%, being statistically different from the latter, which in turn are statistically equal, as their intercepts started close.

3.3.3 Solid gain (SG) modelling of isomaltulose solutions – effect of solute concentration

Figure 2D for SG is represented by model 2, which evaluation is made only in the intercept. It is observed in the plot that there is a difference between all intercepts, when temperature is fixed, since there is a noticeable difference in the place where their intercepts start, so there is a significant difference between them. For solute concentration, the 35% isomaltulose has the greatest effect on the SG, as its estimates are the highest. Thus, this concentration provided greater WL and SG.

3.3.4 Water loss (WL) modelling of isomaltulose solutions – effect of temperature

In Figure 3C, the lines do not show evident inclination. It can be attributed due to the effect of the inclination is extremely small and the model has a fixed inclination. So, according to the adjusted lines, the increase or decrease in temperature has little effect on WL.

3.*3.5 Solid gain (SG) modelling of isomaltulose solutions – effect of temperature*

The plot for SG (Figure 3D) shows that by increasing the temperature there is a slight increase in SG. However, as compared with WL, for the SG the effect of temperature was more expressive.

In general, maximum working conditions promoted greater WL and SG. It occurs because at the increase of solute concentration, the mass transfer in OD occurs through a semipermeable membrane of the food, in order to balance the concentration of the medium. It is benefited by the increase in the concentration of the osmotic solution, mainly close to saturation, stimulating the loss of water in the product, reducing the losses of water-soluble solutes, such as vitamins and minerals due to the formation of a layer of solute around the fruit, preventing the exit of these substances. Concentrated osmotic solutions are also more viscous, making it even more difficult to transfer sugars into the fruit. However, depending on the process conditions (i.e, at higher temperatures), a high solid gain can affect the nutritional and sensory profile of the food (Oladejo *et al.*, 2013). Kushwaha et al. (2018) observed in their study on the influence of the osmotic agent on guava, that higher concentrations of sucrose, resulted in higher flows of WL and SG.

In which concerns the temperature, its increase promotes the diffusion of water inside the food (Alabi *et al.*, 2022; Dimakopoulou-Papazoglou & Katsanidis, 2020; Dimakopoulou-

Papazoglou *et al*., 2022). Moreover, the fruits have a porous structure, so that the high temperature also releases the air retained from the tissue, resulting in more efficient removal of water by osmotic pressure (Ramya & Jain, 216). The increase of temperature led to the swelling and plasticization of the cell membrane during osmotic dehydration, which increases its permeability and decrease the viscosity of the osmotic solution (Kumar & Singh, 2014; Ruskova *et al.*, 2016). According to Ahmed *et al.* (2016), the mass exchange in plant cells follows two major pathways – apoplasmic and symplasmic. The apoplasmic pathway is made possible by the connection between the cell components (cell wall and middle lamella), while the symplasmic pathway occurs via linked protoplasm of the surrounding cells, thus allowing cell to cell mass transport. The loss of the cell membrane selectivity makes it easier for solute to diffuse from the solution into the product (Campos *et al.*, 2012). This set of factors improves water removal and solids absorption. Another benefits can be observed. As example, Devic *et al.* (2010) verified greater retention of vitamin C at 45 °C and that above this temperature, damage to the cell wall could occur, reducing mass transfer.

This knowledge is very important to aid in the choice of best osmotic process conditions for a dehydrating effect (SG is much less than WL), in order to facilitate the subsequent drying process; or the incorporating effect (SG is slightly less than the WL), in order to promote the food-enrichment with a solute of interest; or the both effects.

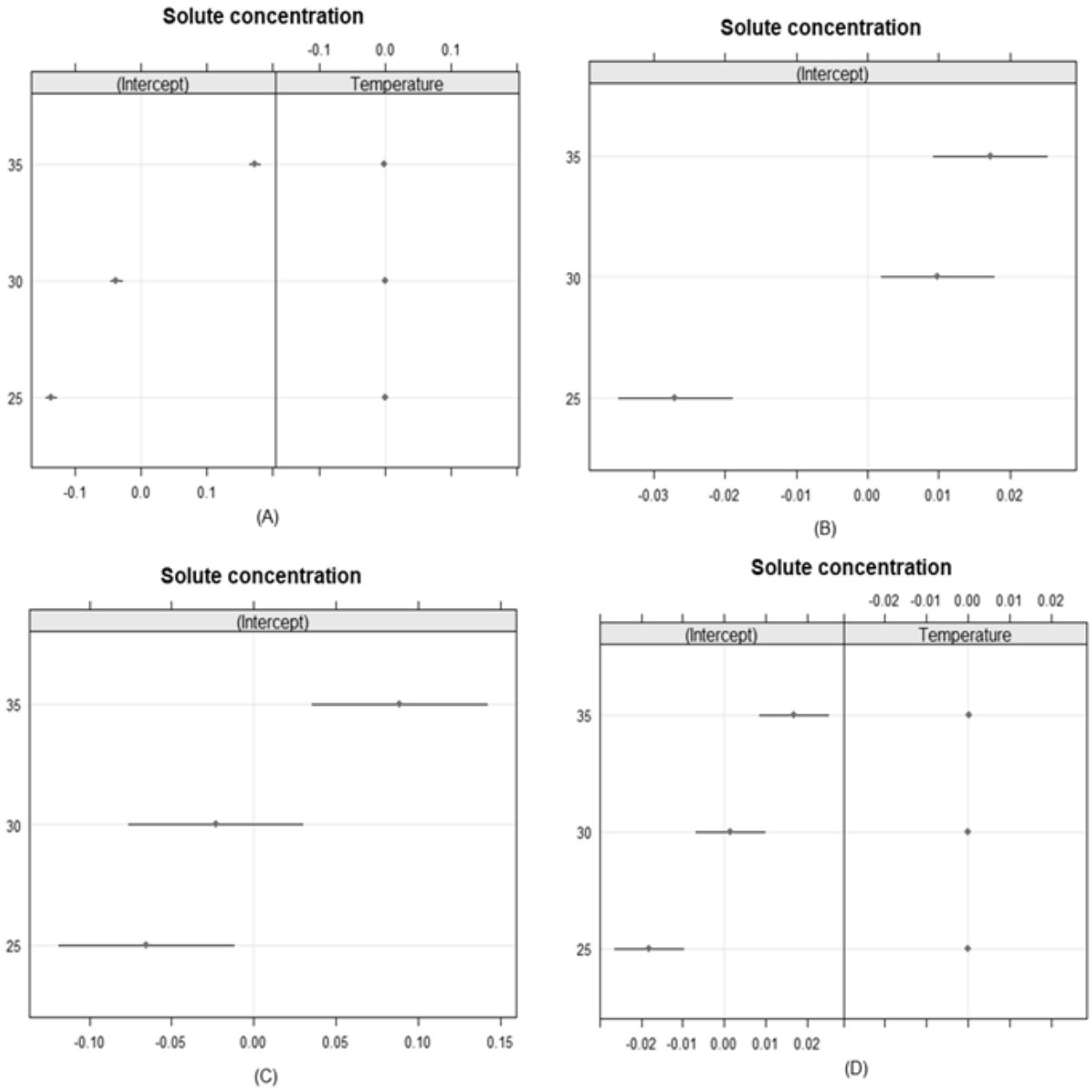

Fig. 2. Dotplot plots representing the fixed and random variables of the selected model for water loss (%) and solid gain (%) in sucrose solutions (A and B, respectively) and isomaltulose solutions (C and D, respectively).

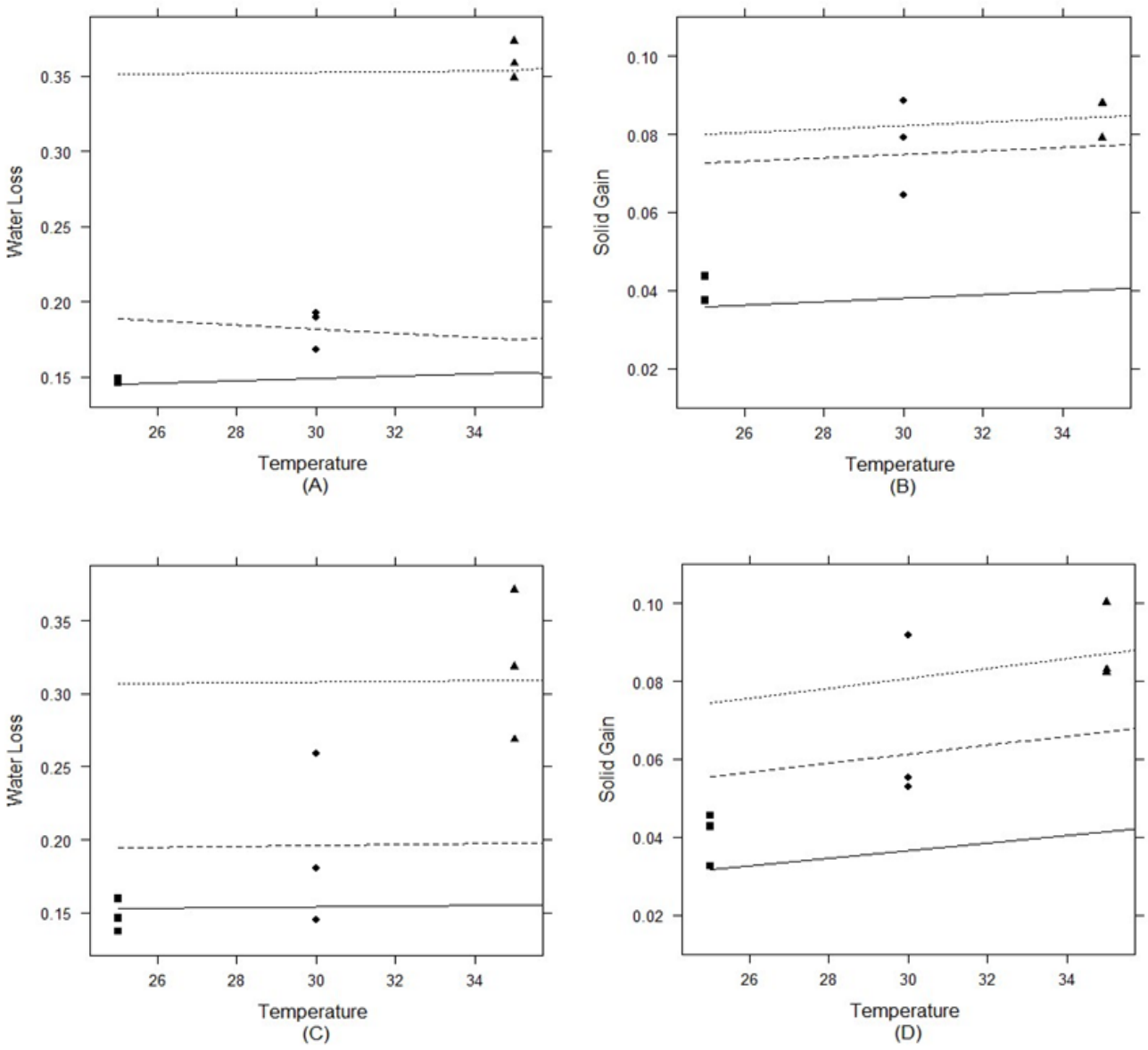

Fig. 3. Behavior of random model parameters for water loss (%) and solid gain (%) in sucrose solutions (A and B, respectively) and isomaltulose solutions (C and D, respectively). Filled, dashed and dotted lines represent the fit of model 3 (A), model 1 (B), model 1 (C) and model 2 (D) to the experimental values of (■) 25%, (◆) 30% and (▲) 35% solute concentration, respectively.

4 Conclusions

The results of osmotic dehydration (OD) with both osmotic solutions showed that the highest solute concentration (35%) and the highest temperature (45 °C) conditions, promoted the greatest water loss (WL) and solid gain (SG) in both solutions. However, the sucrose solution resulted in greater WL than isomaltulose, showing a high dehydration of samples, while a slight influence of temperature on the SG for isomaltulose solution was observed and a significant enrichment of samples was obtained with this osmotic agent with a less WL. Moreover, the multilevel analysis was applied on OD processes analysis and it was feasible to be applied since it was possible to adjust a model that was closest to the actual conditions of the experiment in order to analyses the relationship between the studied variables. Thus, the performance of the multilevel statistical analysis was suitable to evaluate the effect of solute concentration and temperature for the studied conditions for each osmotic solute evaluated.

Hence, this study not only examined the application of multilevel analysis on OD processes in food science, but it also offered the possibility of determine adequate OD processing conditions for the enrichment of mango with isomaltulose for the obtention of healthy product.

Furthermore, through this work the application of multilevel analysis can be extended to other foods, besides opening way to evaluate other parameters of the process, as well as, other types of osmotic solutions.

Conflicts of interest

The authors have no conflict of interest. The authors alone are responsible for the content and writing of the paper.

Acknowledgments

The authors would like to thank the following Brazilian agencies for funding: National Council for Scientific and Technological Development (Conselho Nacional de Desenvolvimento Científico e Tecnológico-CNPq) (314191/2021-6) and Minas Gerais Research Support Foundation (FAPEMIG). J. R. Carmo would also like to thank CNPq for scholarship 166378/2018-6.

Data availability statement

Research data are not shared.

Ethical statement

Ethical approval was not necessary for this study.

Credit authorship contribution

Juliana Rodrigues do Carmo: Conceptualization; Formal analysis; Writing - Original draft preparation. **Jefferson Luiz Gomes Corrêa:** Conceptualization; Formal analysis; Writing - review & Editing; Supervision; Funding acquisition. **Mariana Resende:** Formal analysis; Writing- Original draft preparation. **Marcelo Ângelo Cirillo:** Conceptualization; Formal analysis; Writing - review & Editing; Supervision. **Edith Corona-Jiménez:** Formal analysis; Writing - review & Editing. **Javier Telis-Romero:** Writing - review & Editing; Supervision.

References

Ahmed, I., Mabood, Q. I., & Jamal, S. (2016). Developments in osmotic dehydration technique for the preservation of fruits and vegetables. *Innovative Food Science & Emerging Technologies, 34,* 29–43. doi: 10.1016/j.ifset.2016.01.003

Alabi, K. P., Olalusi, A. P., Olaniyan, A. M., Fadeyibi, A., & Gabriel, L.O. (2022). Effects of osmotic dehydration pretreatment on freezing characteristics and quality of frozen fruits and vegetables. *Journal of Food Process Engineering, 45*, e14037. doi: 10.1111/jfpe.14037

Abrahão, F. R., & Corrêa, J. L. G. (2021). Osmotic dehydration: More than water loss and solid gain. Critical *Reviews in Food Science and Nutrition, 1*, 1–20. doi:10.1080/10408398.2021.198376

Association of Official Analytical Chemists – AOAC. (2010). *Official methods of analysis of association of Official Analytical Chemists International* (18th ed.). Arlington: AOAC.

Austin, P., Goel. V., & Walraven, C. (2001). An introduction to multilevel regression models. *Canadian Journal of Public Health, 92,* 150–154. doi:10.1007/BF03404950

Campos, C. D. M.; Sato. A. C. K.; Tonon, R. V.; Hubinger. M. D.; Cunha, R. L. (2012). Effect of process variables on the osmotic dehydration of star-fruit slices. *Food Science and Technology*, *32*, 357 – 365. doi:10.1590/S0101-20612012005000034

Carmo, J. R., Corrêa, J. L. G., Polachini, T. C., & Telis-romero, J. (2022). Properties of Isomaltulose (Palatinose®) – an emerging healthy carbohydrate: effect of temperature and solute concentration. *Journal of Molecular Liquids*, *347*, 118304. doi:10.1016/j.molliq.2021.118304

Devic, E., Guyot, S., Daudin, J-D., & Bonazzi, C. (2010). Effect of temperature and cultivar on polyphenol retention and mass transfer during osmotic dehydration of apples. *Journal of Agricultural and Food Chemistry*, *58*, 606–614. doi:10.1021/jf903006g

Dimakopoulou-Papazoglou, D., & Katsanidis, E. (2020). Osmotic processing of meat: Mathematical modeling and quality parameters. *Food Engineering Reviews*, *12*, 32–47. doi:10.1007/s12393-019-09203-1

Dimakopoulou-Papazoglou, D., Lazaridou, A., Biliaderis, C.G., Katsanidis, E. (2022). Effect of process temperature on the physical state of beef meat constituents – implications on diffusion kinetics during osmotic dehydration. *Food Bioprocess and Technology*, *15*, 706–716. doi:10.1007/s11947-022-02778-4

Fernandes, F. A. N., Braga, T. R., Silva, E. O., & Rodrigues, S. (2019). Use of ultrasound for dehydration of mangoes (*Mangifera indica* L.): kinetic modeling of ultrasound-assisted osmotic dehydration and convective air-drying. *Journal of Food Sience and Technology*, *56*, 1793–1800. doi:10.1007/s13197-019-03622y

Galdino, P. O., Queiroz, A. J. D., Figueiredo, R. M. F., Santiago, A. M., & Galdino, P. O. (2021). Production and sensory evaluation of dried mango. *Revista Brasileira de Engenharia Agrícola e Ambiental*, *25*, 44–50. doi: 10.1590/1807-1929/agriambi.v25n1p44-50

Gelman, A. Multilevel (hierarchical) modeling: what it can and cannot do? (2006). *Technometrics*, *48*, 432–435. doi:10.1198/004017005000000661

Grzelak-Blaszczyk, K., Czarnecki, A., & Kiewicki, R. (2020). The effect of osmotic dehydration on the polyphenols content in onion. *Acta Scientiarum Polonorum-Technologia Alimentaria*, *19*, 37–45. doi: 10.17306/J.AFS.2020.0766

Jiménez, N., Bassama, J., Soto, M., Dornier, M., Pérez, A. M., Vaillant, F., & Bohuon, F. (2020). Coupling osmotic dehydration with heat treatment for green papaya

impregnated with blackberry juice solution. *International Journal of Food Science and Technology*, *55*, 2551–2561. doi:10.1111/ijfs.14507.

Junqueira, J. R. J., Corrêa, J. L. G., Mendonça, K. S., Mello, R. E., & Souza, A. U. (2018). Pulsed vacuum osmotic dehydration of beetroot, carrot and eggplant slices: effect of vacuum pressure on the quality parameters. *Food and Bioprocess Technology*, *11*, 1863–1875. doi:/10.1007/s11947-018-2147-9

Kumar, P. S., & Sagar, V. R. (2014). Drying kinetics and physico-chemical characteristics of osmo-dehydrated mango, guava and aonla under different drying conditions. *Journal of Food Science Technology*, *51*, 1540–1546. doi:10.1007/s13197-012-0658-3

Kumar, P. S., & Singh, S. V. (2014). Osmotic dehydration of fruits and vegetables: A review. *Journal of Food Science and Technology*, *51*, 1 – 9. doi: 10.1007/s13197-012-0659-2

Kushwaha, R., Singh, V., Singh, M., & Kaur, D. (2018). Influence of osmotic agents on drying behavior and product quality of guava fruit. *Plant Archives*, *18*, 205–209.

Kvapil, M. F., Rodríguez, S. C., Qüesta, A. G., & Mascheroni, R. H. (2021). Evaluation of process conditions on osmotic dehydration and quality indexes of pumpkin (*Cucurbita moschata*) and further polymeric film selection for packaging and refrigerated storage. *International Journal of Food Science and Technology*, *56*, 1959–1971. doi:10.1111/ijfs.14827

Lebaka V.R., Wee Y.-J., Ye W., & Korivi M. (2021). Nutritional composition and bioactive compounds in three different parts of mango fruit. *International Journal of Environmental Research and Public Health*, 18, 741. doi:10.3390/ijerph18020741

Lopez, M. M. L., Morais, R. M. S. C., & Morais, A. M. M. B. (2020). Flavonoid enrichment of fresh-cut apple through osmotic dehydration-assisted impregnation. *British Food Journal*, *123*, 820–832. doi:10.1108/BFJ-03-2020-0176

Maeda, A., Miyagawa, J., & Miuchi, M. (2013). Effects of the naturally-occurring disaccharides, palatinose and sucrose, on incretin secretion in healthy non-obese subjects. *Journal of Diabetes Investigation*, *4*, 281–286. doi:/10.1111/jdi.12045

Macedo, L. L., Corrêa, J. L. G., Araújo, C. S., Vimercati, W. C., & Petri Junior, I. (2021). Convective drying with ethanol pre-treatment of strawberry enriched with isomaltulose. *Food and Bioprocess Technology*, *14*, 2046–2061 doi:10.1007/s11947-021-02710-2

Macedo, L. L., Corrêa, J. L. G., Petri Junior, I., Araújo, C. S., & Vimercati, W. C. (2022). Intermittent microwave drying and heated air drying of fresh and isomaltulose

(Palatinose) impregnated strawberry. *LWT – Food Science and Technology*, *155*, 112918. doi: 10.1016/j.lwt.2021.112918

Mello R. E., Fontana A., Mulet A., Corrêa, J. L. G., & Cárcel, J. A. (2020). Ultrasound-assisted drying of orange peel in atmospheric freezedryer and convective dryer operated at moderate temperature. *Drying Technology 38*, 259–267. doi:10.1080/07373937.2019.1645685

Mendonça, K. S., Corrêa, J. L. G., Junqueira, J. R. J., Pereira, M. C. A., & Vilela, M. N. (2016). Optimization of osmotic dehydration of yacon slices. *Drying Technology, 34*, 386–394. doi:10.1080/07373937.2015.1054511

Oladejo, D., Ade-Omowaye, B. I. O., & Dekanmi, A. O. (2013). Experimental study on kinetics, modeling and optimisationof osmotic dehydration of mango (*Mangifera indica* L.). *The International Journal of Engineering and Science, 2*, 1–8.

Ozcan, M. M., & Haciseferogullan, H. (2007). The strawberry (*Arbutus unedo* L.) fruits: chemical composition, physical properties and mineral contents. *Journal of Food Engineering, 78*, 1022–1028. doi: 10.1016/j.jfoodeng.2005.12.014

Prithani, R., & Dash, K. (2020). Mass transfer modelling in ultrasound assisted osmotic dehydration of kiwi fruit. *Innovative Food Science & Emerging Technologies*, *64*, (102407). doi: 10.1016/j.ifset.2020.102407

Ramya, V., & Jain, N. K. (2016). A review on osmotic dehydration of fruits and vegetables: An integrated approach. *Journal of Food Process Engineering*, *20*, 1–22. doi: 10.1111/jfpe.12440

R Core Team (2021). *R: a language and environment for statistical computing*. R Foundation for Statistical Computing, Vienna, Austria.

Ruskova, M., Aleksandrov, S., Petrova, T., Bakalov, I., Gotcheva, V., & Penov, N. (2016). Effect of osmotic dehydration variables on the water loss of blackcurrants. *Journal of Food and Packaging Science, Technique and Technologies*, *10*, 10–13.

Sawale P. D., Shendurse, A. M., Mohan, M. S., & Patil, G. R. (2017). Isomaltulose (Palatinose) – an emerging carbohydrate. *Food Bioscience*, *18*, 46–52. doi:/10.1016/j.fbio.2017.04.003

Tiroutchelvame, D., Maran, J. P., & Pragalyaashree, M. M. (2019). Response surface analysis and optimization of osmotic dehydration of *Musa acuminata* slices. *Journal of*

Microbiology, Biotechnology and Food Sciences, 8, 1016–1020. doi:10.15414/jmbfs.2019.8.4.1016-1020

Viana, A. D., Corrêa, J. L. G., & Justus, A. (2014). Optimisation of the pulsed vacuum osmotic dehydration of cladodes of fodder palm. *International Journal of Food Science and Technology, 49*, 726–732. doi:10.1111/ijfs.12357

Zongo, A. P., Khalloufi, S., & Ratti, C. (2021). Effect of viscosity and rheological behavior on selective mass transfer during osmotic dehydration of mango slices in natural syrups. *Journal of Food Process and Engendering 44*, e13745. doi:10.1111/jfpe.13745

ARTICLE 4 – **Mango enriched with Palatinose® by pulsed vacuum osmotic dehydration: evaluation of process variables on mass transfer, water activity, and color changes**

Juliana Rodrigues do CARMO [a*], Jefferson Luiz Gomes CORRÊA [a], Mariana RESENDE [b], Marcelo Ângelo CIRILLO [b]

[a] Department of Food Science (DCA), Federal University of Lavras, 37200-900, Lavras, Brazil. E-mail: juliana.carmo@estudante.ufla.br; jefferson@ufla.br

[b] Department of Statistic (DES), Federal University of Lavras, 37200-900, Lavras, Brazil. E-mail: mariana.resende2@estudante.ufla.br; macufla@ufla.br

Running title: Fruit enrichment by vacuum treatment

Practical application

This study presents a relevant contribution to the industrial processes due to the current use of Palatinose®, besides showing the application of a statistical analysis that generates plots of the relationships between a set of variables. Palatinose® is a promising substitute of sucrose in the osmotic dehydration (OD) of mangos slices. It is due to Palatinose® having similar properties than sucrose, with advantage of presenting low glycemic and insulinemic indexes. During the OD, the use of vacuum on intermediary process conditions (time and vacuum) can provide a satisfactory enrichment of this carbohydrate on mangos slices, besides promote good results on quality of the product. The performance of Multidimensional Scaling (MDS) technique to evaluate the influence of the combination of different time and vacuum can reduce the complexity of a dataset, allowing visualization of the underlying relational structures. This plots reduce the complexity inherent to a large table of proximities.

[*]**Corresponding author:** Juliana Rodrigues do CARMO (E-mail: juliana_docarmo@yahoo.com.br)

(Submitted to the Journal of Food Process Engineering)

Abstract: Pulsed vacuum osmotic dehydration (PVOD) has been used for the incorporation of solutes of interest into fruits. In this study, the vacuum time at the beginning of the process varied from 5 to 20 min at different absolute pressures (24 and 48 kPa) in PVOD of mangos slices with the healthy carbohydrate Palatinose®. The impact of these variables on parameters such as water loss (*WL*), solids gain (*SG*), water activity, and color was evaluated. The multidimensional scaling (MDS) technique was effective in indicating that the PVOD treatment with 10 min of vacuum pulse at 48 kPa provided a final product with higher *SG*, *WL*, and lightness; and lower water activity and total color difference. The Tukey's test corroborated with MDS technique, since it did not show statistically significant difference for 10 and 15 min at 24 or 48 kPa ($p > 0.05$) for the most of studied parameters.

Keywords: Mango, Enrichment, Palatinose®, PVOD, Multidimensional scaling.

1 Introduction

Mango is an important source of macronutrients, such as carbohydrates, lipids, fatty acids, proteins, amino acids, and organic acids. In addition, mango contains micronutrients, such as vitamins and minerals, and non-nutrient compounds, such as phenolic compounds, flavonoids, and other polyphenols, chlorophyll, carotenoids, and volatile compounds, and is an important fruit in the human diet (Corrales-Bernal *et al.*, 2014; Lebaka *et al.*, 2021). Despite its nutritional value, mango has a short shelf life, and thus processes for its preservation to make it available off-season are necessary.

Osmotic dehydration (OD) is a mass transfer process that partially removes water and simultaneously increases the soluble solids content of the fruit in an osmotic solution (Abrahão & Corrêa, 2021). The use of vacuum in OD in a process known as pulsed vacuum osmotic dehydration (PVOD) usually increases the mass transfer between the food and the osmotic solution (Junqueira *et al*., 2021; Macedo *et al*., 2022). The application of vacuum leads to the removal of gases trapped in pores and entry of the solution, with consequent changes in the structure of the food via the hydrodynamic mechanism of PVOD (Fito, 1994; Mendonça *et al*., 2016; Oliveira *et al*., 2021). The influence of the duration and intensity of the vacuum pulse on the impregnation of the solute depends mainly on the structure of the material and its mechanical properties (Junqueira *et* al., 2021).

Because it intensifies the exchanges between the food and the solution, PVOD is indicated for the enrichment of foods with functional ingredients in the pores of the product, such as texture retaining agents, antioxidants, and antimicrobials, that increase their quality and shelf life. In this context, the enrichment of foods with sugars with healthier aspects, such as Palatinose® – a potential and promising sucrose substitute in osmotic processes – has also been investigated (Lopez *et al.*, 2020; Macedo *et al.*, 2021; Shyam *et al*., 2018).

Although Palatinose® be more expensive and has half of the sweet taste of sucrose, it is more slowly digested by α-glucosidase in the small intestine than sucrose. Clinical studies provided convincing evidence to support its applications for controlling postprandial glucose profile in humans, besides being a non-cariogenic carbohydrate (Carmo *et al.*, 2022; Shyam *et al.*, 2018). Palatinose® is commonly used in diets based on low glycemic and insulinemic indexes. Thus, this disaccharide is becoming used by athletes and diabetic, obese and heart disease people (Maeda *et al.*, 2013).

Multidimensional scaling (MDS) is a tool with which researchers can obtain quantitative estimates of similarity between groups of variables; i.e., MDS refers to a set of statistical techniques that are used to reduce the complexity of a dataset, allowing visualization of the underlying relational structures. When similarity estimates are subjected to MDS analysis, plots of the relationships between a set of variables are generated. This plot reduces the complexity inherent to a large table of proximities. The major purpose of MDS analysis is to reveal the relational structures between the variables evaluated.

The objective of this study was to evaluate the influence of the combination of different time (5, 10, 15, and 20 min) and vacuum (24 kPa and 48 kPa, absolute pressure) conditions on the enrichment of mangos with Palatinose® and the impact of these processes on parameters such as water loss (*WL*), solids gain (*SG*), water activity, and color of the final product through the use of the MDS statistical technique.

2 Materials and methods

2.1 Raw material

Mango cv. Tommy Atkins fruits were purchased from the local market of Lavras, Minas Gerais state, Brazil (21° 14'43 S and 44° 59'59 W), and selected based on a similar degree of ripeness (half-ripe) (Nordey *et al.*, 2014). These fruits had the following characteristics: reddish-green peel

color, 85.14 ± 0.55% moisture, 12.3 ± 0.6 °B, 4.72 ± 0.16 Brix/acidity ratio, 3.60 ± 0.04 pH, and 47.50 ± 5.55 N firmness.

2.2 Preparation of the raw material

The mango fruits were washed with disinfectant solution (chlorinated water at 200 ppm) for 5 min. The experimental samples were obtained from the fruit pulp, which was sliced into pieces of 4.00 ± 0.01 cm in length, 2.00 ± 0.01 cm in width, and 0.40 ± 0.01 cm in thickness employing a stainless-steel molder.

2.3 Preparation of the osmotic solution

The 35% (w/w) osmotic solution was prepared with distilled water and isomaltulose, known commercially as Palatinose® (Beneo, Mannheim, Germany). The isomaltulose solution had the following parameters: water activity (a_w) of 0.972 (± 0.001); solubility of 0.4092 (± 0.001) kg of isomaltulose·kg of solution^{-1}; density of 1105.8 (± 0.5) kg·m^{-3}; specific heat of 3.440 (± 0.048) kJ·kg^{-1}·K^{-1}; thermal conductivity of 0.483 (± 0.007) W·m^{-1}·K$^{-1;}$ and viscosity of 2.405 (± 0.024) mPa·s at the working temperature (45 °C) (Carmo *et al.*, 2022).

2.4 Pulsed vacuum osmotic dehydration (PVOD)

The PVOD of the mango slices was performed in a temperature-controlled oven (Solab SL104/40, Piracicaba, Brazil) coupled to a vacuum pump (model DV95, Dosivac, Buenos Aires, Argentina), where the mango slices were immersed in glass containers containing osmotic solution at a ratio of 1:10 (w/v) at 45 °C for 300 min. These temperature and time conditions were determined in a previous study (Carmo *et al*., 2022). PVOD was performed by applying a vacuum of 24±1 kPa (76.3% vacuum) and 48±1 kPa (52.6% vacuum) (absolute pressure) during the first 5, 10, 15, and 20 min of the process (Ito *et al*., 2007; Junqueira *et al*., 2021; Sirijariyawat *et al*., 2012), according

to Table 1. Then, the atmospheric pressure was resumed (101.3 kPa). Five samples were subjected to each PVOD process condition and analysed.

Table 1. Pulsed vacuum osmotic dehydration (PVOD) treatments employing different time and absolute pressure conditions.

Code	***Time (min)***	***Absolute pressure (kPa)***
t5P24	5	24
t10P24	10	24
t15P24	15	24
t20P24	20	24
t5P48	5	48
t10P48	10	48
t15P48	15	48
t20P48	20	48

The mass transfer parameters (*WL* and *SG*) of each sample subjected to the different PVOD conditions were evaluated according to Eq. 1 and Eq. 2 (Viana *et al*., 2014), respectively. The moisture content of the fresh and osmotically treated samples was determined according to the AOAC (2010).

$$WL(\%) = \frac{x_0^w M_0^o - x_t^w M_t^o}{M_0^o} \times 100 \quad (1)$$

$$SG(\%) = \frac{x_t^{ST} M_t^o - x_0^{ST} M_0^o}{M_0^o} \times 100 \quad (2)$$

where *WL* is the water loss, *SG* is the soluble solids gain (%), x_0^w is the initial moisture content on a wet basis (wb) (kg of water kg of fruit^{-1}) and x_t^w is the final moisture content on a wet basis (wb)

(kg of water kg of fruit^{-1}), M_0^o is initial sample weight (kg), M_t^o is final sample weight (kg), x_t^{ST} is final solids content (kg solids kg fruit^{-1}) and x_0^{ST} is initial solids content (kg solids kg fruit^{-1}), The subindices "*0*" and "*t*" refer to fresh samples and samples after osmotic treatment, respectively.

2.5 Analysis of the osmodehydrated samples

2.5.1 Water activity (a_w)

The a_w of the samples was determined at 25 °C with a digital thermohygrometer (AquaLab 3TE, Decagon, USA).

2.5.2 Color evaluation

The color was evaluated by tristimulus colorimetry in a digital colorimeter (Konica-Minolta, CR 400, Tokyo, Japan). The operating conditions of the equipment were diffuse light/viewing angle of 0° (specular component included), and a D65 light source. The lightness (L^* = 0 black and L^* = 100 white) and the chromaticity coordinates (-a^* = green and +a^* = red, -b^* = blue and +b^* = yellow) were used to define the chroma value (C^*), which indicates color saturation (0 = neutral color and 60 = intense color) (Eq. 3), and the hue angle (h°), which indicates the basic color unit (0° and 360° = red, 90° = yellow, 180° = green and 270° = blue) (Eq. 4) (Carmo & Pena, 2019). Eq. 5 was used to calculate the total color difference (ΔE) of the osmodehydrated samples relative to the fresh fruit.

$$C^* = \sqrt{\left(a^*\right)^2 + \left(b^*\right)^2} \tag{3}$$

$$h° = cos^{-1} \frac{a^*}{\sqrt{\left(a^*\right)^2 + \left(b^*\right)^2}} \tag{4}$$

$$\Delta E = \sqrt{\left(L_0^* - L_t^*\right)^2 + \left(a_0^* - a_t^*\right)^2 + \left(b_0^* - b_t^*\right)^2} \quad (5)$$

where subindices "*0*" and "*t*" refer to the fresh samples and samples after osmotic treatment, respectively.

2.5.3 Statistical analysis

First, the data were transformed (Eq. 6) so that the responses were limited to a continuous scale from 0 to 1, making it possible to interpret them as indices, represented by $x_{ij,}$ since the variables under study had different scales.

$$x_{ij} = \frac{x_i - minimum(x._j)}{maximum(x._j) - minimum(x._j)} \quad (6)$$

The similarity between the PVOD treatments was determined by the MDS technique, which obtained the coordinate vectors represented by $x_{ij} = (x_{i1}, \ldots, x_{iq})$, thus considering the Euclidean distance matrix $D = [d_{ij}]$ of order *n x n* formed from the dataset for all variables. Each element of this matrix was calculated using the Euclidean distance defined by $d_{ij}^2 = \|x_i - x_{i'}\|^2$r for $i \neq i'$, with $i = 1,\ldots, n$, where *n* is the number of treatments. The variables represented in each axis are independent, therefore, it is a favorable case to determine the similarity between the treatments defined by the combination of vacuum pulse pressure and time, that is, they are variables considered as if it were a factor and not as a response variable. Subsequently, the correlated variables were excluded, and a new dissimilarity matrix, defined as $\Delta = [\delta_{ii'}]$, was adjusted to consider a smaller number of variables. Thus, considering the proximity of each element, i.e., $d_{ii'} \approx \delta_{ii'}$, the stress function configuration was used as a validation criterion (De Leeuw, 1988). The nonmetric MDS defined by Jaworska and Anastasova (2009) and based on this algorithm considers the choice of a monotonic function to represent the relationship between distances d_{ij} and δ_{ij}, which was applied. The algorithm used to minimize the stress function was

previously described (Kruskal, 1964), and further details on this algorithm are found in Cirillo and Barroso (2014).

It must be emphasized, that in this work MDS technique has been treated in the absence of any model, with reference to Cox & Cox (2001). These authors suggest that the transformation of dissimilarity based on spline regression make the model very complicated, computationally and in terms of inference. Therefore, it has been assumed the transformation on 0-1 scale and performed the MDS, in its essence, that is, treating it as a method of dimension reduction, considering the dissimilarity matrix of the response variables. Here it should be noted that the objective is to determine the combination of the response variables, eliminating redundant information (highly correlated variables).

Borg & Groenen (2005), highlight the use of MDS as a technique that tests in what way, certain criteria, an individual can differentiate objects of interest considering a certain metric. Contextualizing this statement for this work, and as a result of each response variable present different magnitudes and magnitudes, the use of the technique is adequate.

To validate the results, the biplot technique was used to study the similarity between the treatment groups, considering a multivariate approach, using the BiplotGUI package of the software R (R Core Team, 2021).

One-way analysis of variance (ANOVA) also was employed by Statistica v.10.0 (StatSoft, Inc., Tulsa, USA) in order to find out whether the differences in the means were significant. The Tukey's test at 95% confidence interval has been chosen. The test of means to treatments, ± 1 standard error, was used precisely to complement the results obtained in the MDS. At this point, this inference considered only the variables selected in the MDS.

3 Results and discussion

3.1 PVOD

Table 2 shows the results for the mass transfer (*WL* and *SG*) and quality parameters (a_w and color – L^* a^*, b^*, C^*, $h°$ and ΔE) of the osmodehydrated mango slices. The results for *WL* ranged from 41.97% (t20P24) to 50.28% (t15P48), where, in general, the treatments with higher vacuum pulse pressure (24 kPa) are lower ($p \leq 0.05$). Regarding *SG*, the achieved enrichment ranged from 7.06% (t5P48) to 9.54% (t20P24), which no differed statistically ($p > 0.05$). Studies do not recommend the use of prolonged time and high vacuum levels because these factors could lead to cell collapse, causing irreversible deformation of the fruit tissue and leading to a reduction in porosity and decrease in the free volume available for impregnation (Oliveira *et al*., 2021). In addition, the application of long vacuum time (> 15 min) leads to softening of the samples (Ito *et al*., 2007; Corrêa *et al*., 2010). According to Lin *et al*. (2016), cell wall softening occurs when water exits the fruit. Thus, the tissue structure can collapse, physically hindering the penetration of solids into the fruit. This behavior is clearly observed in Table 2, where the treatments with the highest *WL* show the lowest *SG*.

Table 2. Water loss (*WL*), solids gain (*SG*), water activity (a_w), lightness (L^*), chromaticity coordinates (a^* and b^*), chroma (C^*), hue angle ($h°$), and total color difference (ΔE) of the pulsed vacuum osmotic dehydration (PVOD) treatments employing different time and absolute pressure conditions.

Code	*WL (%)*	*SG (%)*	a_w	L^*	a^*	b^*	C^*	$h°$	ΔE
t5P24	47.59±3.44^{ab}	8.51±1.26^{a}	0.954±0.001^{a}	66.99±1.48^{ab}	-2.04±0.18^{ab}	50.28±3.25^{b}	50.16±3.03^{ab}	92.30±0.28^{ab}	11.58±2
t10P24	43.52±1.67^{ab}	9.26±0.33^{a}	0.954±0.004^{a}	64.20±3.70^{ab}	-1.97±0.01^{ab}	47.58±3.13^{b}	47.61±3.12^{b}	92.35±0.21^{ab}	15.13±4
t15P24	46.86±2.50^{ab}	7.68±1.07^{a}	0.959±0.001^{a}	67.58±0.97^{ab}	-0.93±0.40^{a}	54.44±1.67^{ab}	54.44±1.67^{ab}	90.85±0.35^{b}	10.20±0
t20P24	41.97±1.80^{b}	9.54±0.97^{a}	0.960±0.001^{a}	67.81±1.65^{b}	-2.28±0.04^{ab}	52.23±3.89^{ab}	52.16±3.00^{ab}	92.60±0.42^{ab}	10.47±0
t5P48	49.31±0.52^{ab}	7.06±0.70^{a}	0.952±0.008^{a}	74.79±1.29^{a}	-3.68±1.16^{b}	55.23±0.14^{ab}	55.35±0.06^{ab}	93.75±1.20^{a}	3.33±1.
t10P48	48.30±1.32^{ab}	9.35±0.48^{a}	0.948±0.001^{a}	74.02±2.01^{a}	-2.13±0.50^{ab}	59.52±0.35^{a}	59.56±0.33^{a}	92.00±0.42^{ab}	5.82±1.
t15P48	50.28±0.31^{a}	7.35±0.65^{a}	0.947±0.001^{a}	74.06±3.86^{a}	-1.61±0.42^{a}	55.62±0.23^{ab}	55.64±0.24^{ab}	91.60±0.42^{b}	5.37±2.
t20P48	48.38±0.04^{ab}	7.35±1.46^{a}	0.945±0.004^{a}	76.01±1.52^{a}	-3.88±0.04^{b}	54.49±0.29^{ab}	54.62±0.29^{ab}	94.00±0.14^{a}	2.77±0.

Mean values of five replicates ± standard deviation. The vacuum pulse time are 5, 10, 15 and 20 (min), and the vacuum pulse pressures are 24 kPa and 48 kPa. Values with different letters in same column differ significantly ($p \leq 0.05$) according to Tukey's test.

Table 2 shows that the a_w values for the samples at 48 kPa also no differed statistically than those at 24 kPa ($p > 0.05$). Low a_w values could restrict biochemical and microbial changes, thus preserving quality of fruits and vegetables (Khubber et al., 2020). Even lower values can be achieved with complementary processes such as convective drying.

The color parameters indicate that the osmodehydrated mangos show a strong tendency to yellow (positive b^*), a slight tendency to green (negative a^*), and good lightness. The C^* values show that the product has an intense color, and the $h°$ values confirm the yellow color of the fruit since the hue angle value is close to 90°. In general, according to L^* values, the samples treated at 24 kPa are darker than the samples treated at 48 kPa ($p \leq 0.05$). This may be associated with the rupture of the cell structure at high vacuum levels, enabling the formation of the enzyme-substrate complex and thus favoring enzymatic browning (Tonolli *et al.*, 2021).

Regarding the ΔE values, the samples with higher quality are those whose colors are closer to the original color of the fresh sample; therefore, low total color difference values are desired. In the treatments at 48 kPa vacuum, the ΔE value was lower than that at 24 kPa ($p \leq 0.05$); the former treatment condition leads to a smaller difference from the color of the fresh sample. This behavior is directly related to the values of the L^*, a^* and b^* color parameters, as shown in Eq. 5.

3.2 Multidimensional scaling (MDS)

The results were evaluated by MDS of the interpretations of the generated biplots.

Figure 1 contains the following variables: *WL*, *SG*, water activity (a_w), and the color parameters that indicate lightness (L^*), chromaticity coordinates for green–red (a^*) and blue–yellow (b^*), chroma (C^*), hue angle ($h°$) and total color difference (ΔE). In this figure, the treatments are grouped in regions delimited by the variables under study. The t15P24 kPa treatment is clearly distinct from the others. It represents the initial time of 15 min of PVOD with a vacuum pulse pressure of 24 kPa and was the most differentiated treatment in relation to the following variables:

the a^* chromaticity coordinate (-0.4 and -0.5) and *SG* (0.08). This indicates that the higher the *SG* is, the lower the a^*chromaticity coordinate.

The t5P48, t10P48 and t15P48 treatments are basically indistinguishable in terms of *h*° (0.0 and 0.006) and a^* chromaticity coordinate (-0.2 and -0.3). The similar values for these samples indicate that a vacuum pulse pressure of 48 kPa is well accepted, regardless of the time used. This, in turn, suggests that the vacuum pulse pressure more significantly reduces the a^* chromaticity coordinate.

The t20P24, t5P24, t20P48 and t10P24 treatments produce data points grouped based on the values of the variables *SG* (0.06 and 0.08), *h*° (0 and 0.004) and a^* chromaticity coordinate (0 and -0.1). This indicates that although the vacuum pulse pressure of 24 kPa improves the *SG* and *h*°, it decreases the a^* chromaticity coordinate.

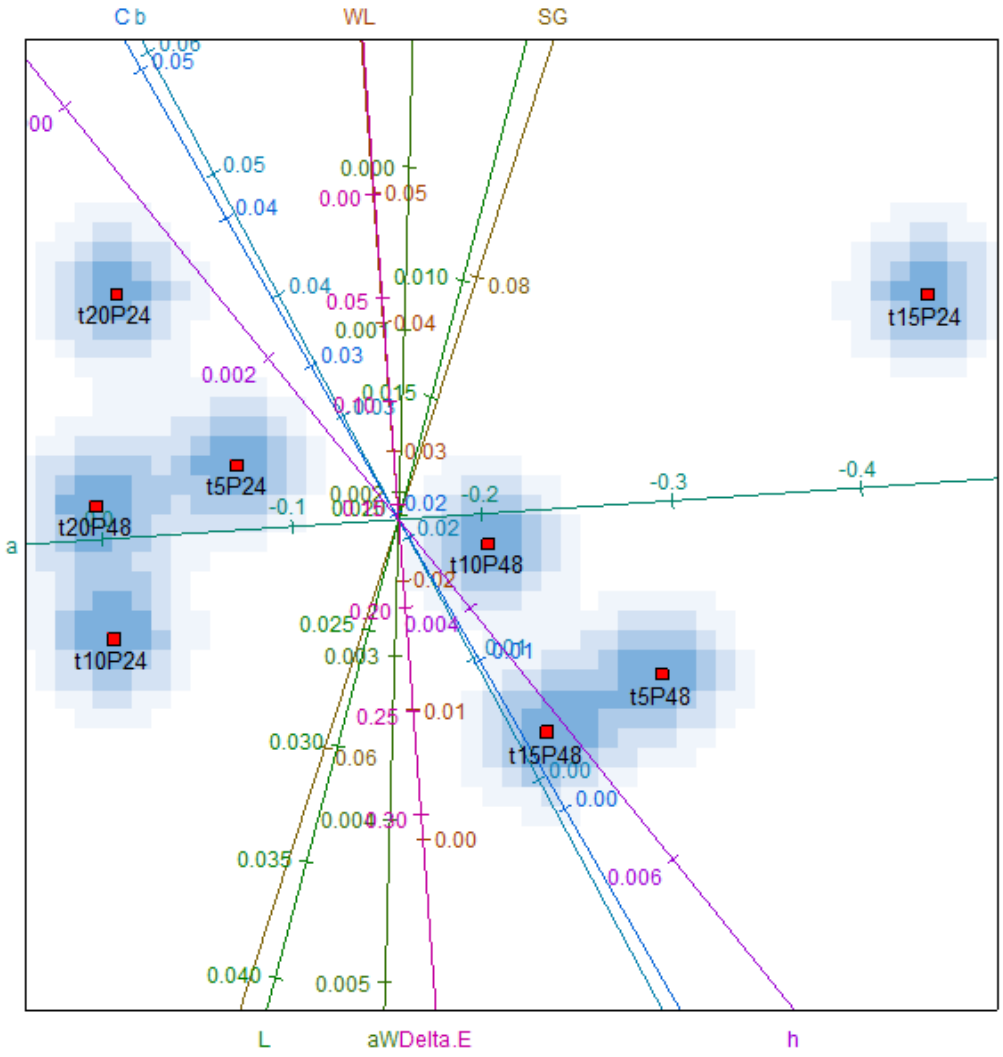

Fig. 1. Biplots considering all variables in the pulsed vacuum osmotic dehydration (PVOD) treatments: water loss (*WL*), solids gain (*SG*), water activity (a_w), and the color parameters that indicate lightness (L^*), chromaticity coordinates for green–red (a^*) and blue–yellow (b^*), chroma (C^*), hue angle ($h°$) and total color difference (ΔE). The vacuum pulse time are 5, 10, 15 and 20 (min), and the vacuum pulse pressures are 24 kPa and 48 kPa.

The degree to which all treatments are similar is determined considering all experimental variables. Figure 1 shows that the variables C^* and b^*; *SG* and L^*; and *WL*, a_w and ΔE strongly correlate. This suggests that the homogeneity of these treatments should also be evaluated in a way that considers only the independent variables. The results of this evaluation are shown in Figure 2.

Regarding the validity of ordering the treatments in different sets, a loss of information occurs when evaluating data based on all variables versus excluding correlated variables. The variable reduction is appropriate here because the graph of the stress function (Figure 3) shows values close to zero. Thus, there is evidence that the statistical grouping determined by the independent variables is validated, without loss of information, for all variables illustrated in Figure 2.

As a confirmation of the interpretations made previously, it is possible to observe that Figure 2 shows a trend toward clustering of the data points for t5P48 and t15P48 with respect to ΔE and L^* and for t15P24 and t20P24 with respect to ΔE, a_w and L^*, considering that the variables a^*, $h°$, C^* and b^* are excluded because they are implicitly represented by ΔE (Eqs. 3, 4, and 5). This result shows the tendency of the variables to be grouped by the vacuum pulse pressure value. The t10P48 and t10P24 treatments show great similarity in relation mainly to the variable ΔE, with values close to zero, and similarity in relation to the variable L^* (0.020 and 0.035).

According to Figure 2, the t20P24 treatment presented the lowest values for the variables ΔE and a_w; the t20P48 treatment, for L^* and *WL*; and the t10P24 treatment, for *SG*. Thus, in general, when longer time (20 minutes) and higher vacuum pulse pressure (24 kPa) are employed, the responses of the variables tend to present lower values. On the other hand, higher values of ΔE and a_w were obtained for the t15P48 treatment; *SG*, for t20P48 treatment; L^*, for t10P24 treatment and *WL*, for t20P24 treatment. So, in this study, to obtain best values and in relation to the studied variables, intermediate values of time (10 and 15 minutes) and lower vacuum pulse pressure (48 kPa) are required.

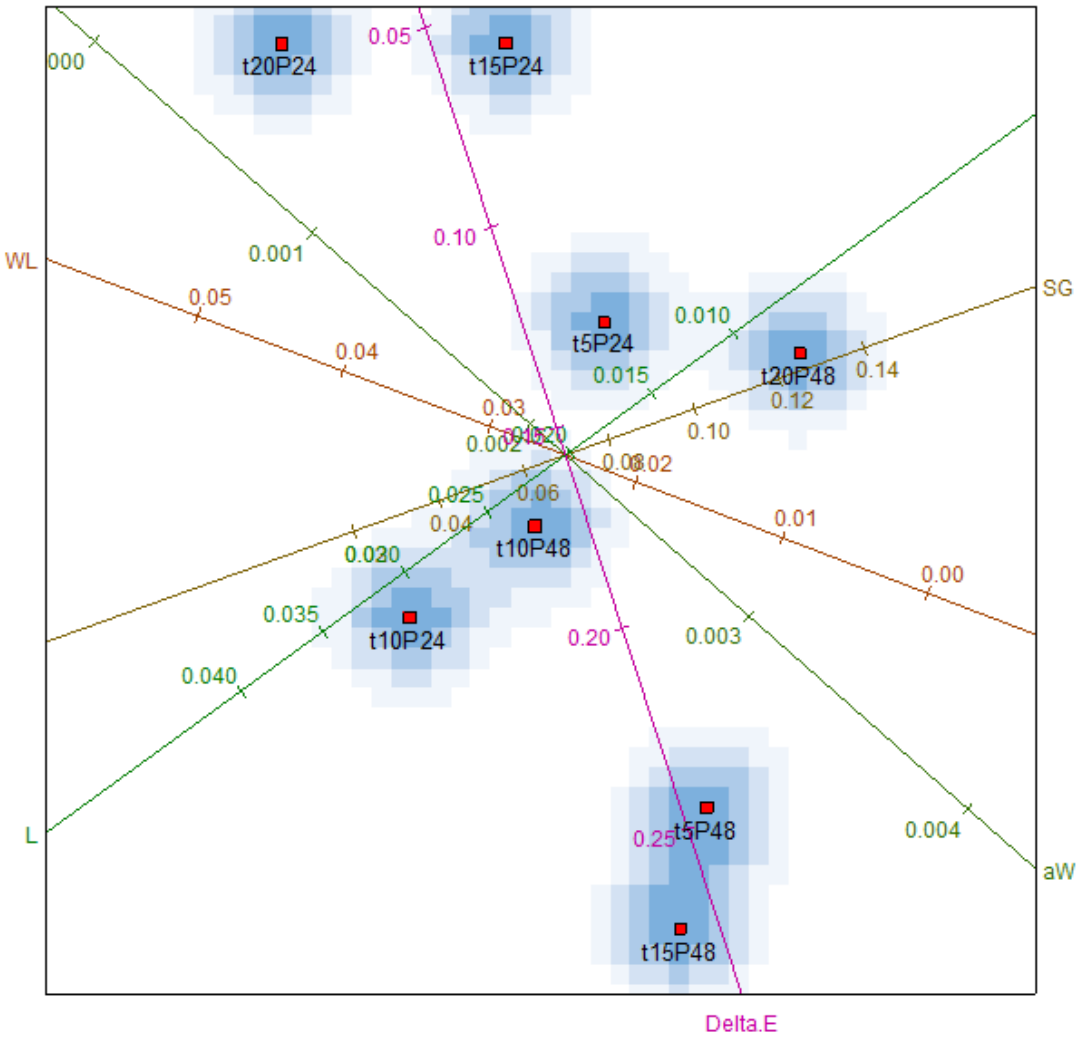

Fig. 2. Biplots considering the independent variables: water loss (*WL*), solids gain (*SG*), water activity (a_w), color parameter indicating lightness (L^*), and total color difference (ΔE). The vacuum pulse time are 5, 10, 15 and 20 (min), and the vacuum pulse pressures are 24 kPa and 48 kPa.

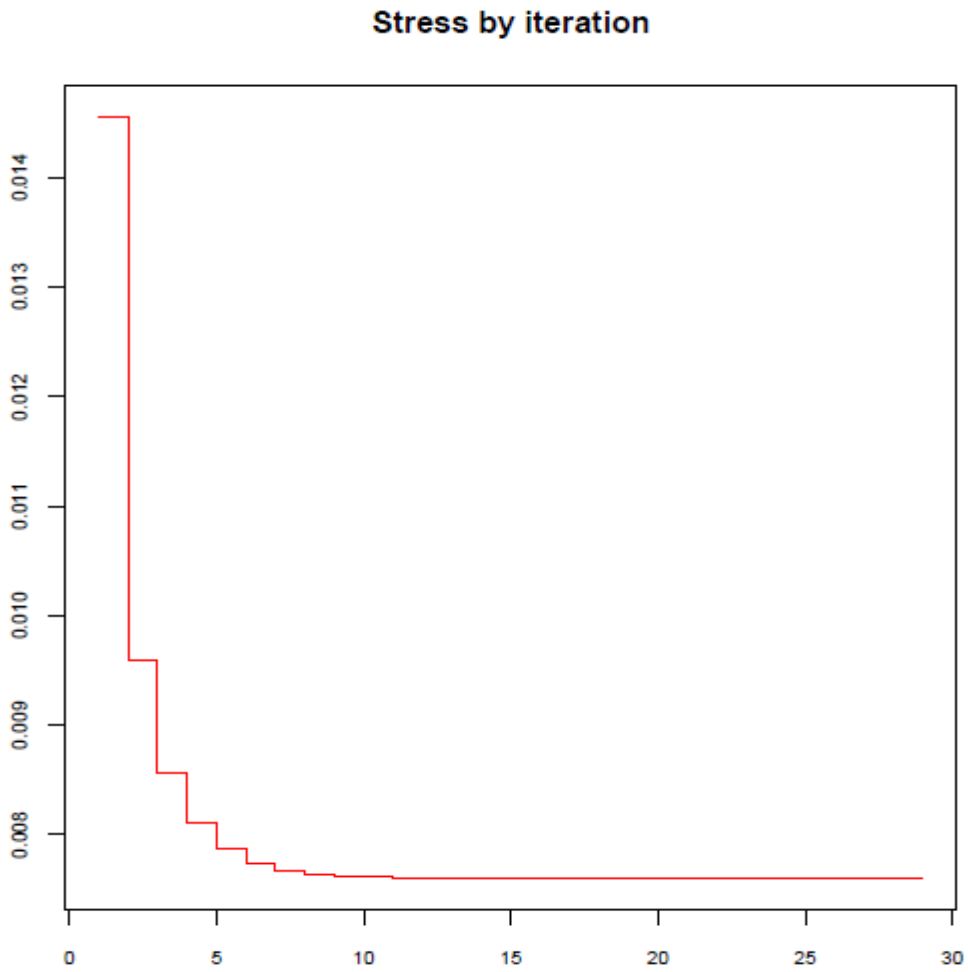

Fig. 3. Plot of the stress function calculated with only independent variables from the pulsed vacuum osmotic dehydration (PVOD) data.

The most appropriate treatment selected for future experiments is the t10P48 treatment, which represents a vacuum pulse time of 10 min and a vacuum pulse pressure of 48 kPa. Its ranking in terms of the studied variables is considered in the selection; that is, this treatment presented the best values in relation to the set of variables as a whole.

The variables in question show intermediate values in treatment t10P48 since they are closer to the centre of the graph, while other treatments show very high or very low values for some variables. Selecting the treatment with intermediate values is more interesting because this treatment would not show losses in any of the variables under study. This is because the purpose of this evaluation in the present study was to determine a PVOD treatment that would provide a final product with higher incorporation of solids (higher *SG*), higher *WL*, lower a_w, higher L^* and lower ΔE, as discussed in Section 3.1. Thus, through the MDS analysis, it was possible to choose the treatment that spatially (centre of the graph) satisfied this condition.

4 Conclusions

Although the use of prolonged vacuum time and higher vacuum pressure in osmotic processes seems to result in higher solutes incorporation, an intermediate situation could even offer this scenario. The evaluation of the results by the MDS statistical technique was able to indicate that the treatment with 10 min and 48 kPa of vacuum pulse pressure promoted greater fruit enrichment (higher *SG*) in addition to higher *WL* and lightness and lower water activity and total color difference. Moreover, according to the Tukey's test, there was not statistically significant difference for the most of the studied parameters for 10 or 15 min and at 24 or 48 kPa ($p > 0.05$).

Conflicts of interest

There are no conflicts of interest to declare.

Acknowledgments

The authors would like to thank the following Brazilian agencies for funding: National Council for Scientific and Technological Development (Conselho Nacional de Desenvolvimento Científico e Tecnológico-CNPq) (314191/2021-6) and Minas Gerais Research Support Foundation (FAPEMIG). J. R. Carmo would also like to thank CNPq for scholarship 166378/2018-6.

Data availability statement

Research data are not shared.

Ethical statement

Ethical approval was not necessary for this study.

Credit authorship contribution

Juliana Rodrigues do Carmo: Conceptualization; Formal analysis; Writing - Original draft preparation. **Jefferson Luiz Gomes Corrêa:** Conceptualization; Formal analysis; Writing - review & Editing; Supervision; Funding acquisition. **Mariana Resende:** Formal analysis; Writing- Original draft preparation. **Marcelo Ângelo Cirillo:** Conceptualization; Formal analysis; Writing - review & Editing; Supervision.

References

Abrahão, F. R., & Corrêa, J. L. G. (2021). Osmotic dehydration: More than water loss and solid gain. *Critical Reviews in Food Science and Nutrition*. https://doi.org/ 10.1080/10408398.2021.198376

Association of Official Analytical Chemists – AOAC. (2010). *Official methods of analysis of association of Official Analytical Chemists International* (18th ed.). Arlington: AOAC.

Borg, I. & Groenen, P. J. (2005). *Modern multidimensional scaling: theory and applications*. New York: Springer.

Carmo, J. R., & Pena, R. S. (2019). Influence of the temperature and granulometry on the hygroscopic behavior of tapioca flour. *CyTA - Journal of Food*, 17, 900–906. https://doi.org/10.1080/19476337.2019.1668860

Carmo, J. R., Corrêa, J. L. G., Polachini, T. C., & Telis-Romero, J. (2022). Properties of Isomaltulose (Palatinose®) – an emerging healthy carbohydrate: effect of temperature and solute concentration. *Journal of Molecular Liquids*, 347, 118304. https://doi.org/10.1016/j.molliq.2021.118304

Carmo, J. R., Corrêa, J. L. G., Resende, M., Cirillo, M. A., Corona-Jiménez, E., & Telis-Romero, J. (2022). Mango enriched with sucrose and isomaltulose (Palatinose®) by osmotic dehydration: effect of temperature and solute concentration through the application of a multilevel statistical models. *Journal of Processing and Preservation, In press*. https://doi.org/10.1111/jfpp.17147

Cirillo, M. A., & Barroso, L. P. (2014). Aspectos socioeconômicos e ecológicos por escalonamento multidimensional e modelos de equações estruturais: Um estudo de caso do ZEE-MG. Revista Brasileira de Estatística, 75, 89e112.

Corrales-Bernal A., Maldonado M. E., Urango L. A., Franco M. C., & Rojano B. A. (2014). Mango de azúcar (*Mangifera indica* L.) variedad de Colombia: características antioxidantes, nutricionales y sensoriales. Revista chilena de nutrición. 41, 312–318. https://doi.org/10.4067/S0717-75182014000300013

Corrêa, J. L. G., Pereira, L. M., Vieira, G. S., Hubinger, M. D. (2010). Mass transfer kinetics of pulsed vacuum osmotic dehydration of guavas. Journal of Food Engineering, 96, 498–504. https://doi.org/10.1016/j.jfoodeng.2009.08.032

Cox, T. F. & Cox, M. A. A. (2001). *Multidimensional scaling* (2nd Ed.). London: Chapman & Hall/CRC.

De Leeuw, J. (1988). Convergence of the majorization method for multidimensional scaling. *Journal of Classification*, 5, 163e180.

Fito, P. Modeling of vacuum osmotic dehydration of food. *Journal of Food Engineering*, 22, 313–328, 1994.

Ito, A. P., Tonon, R. V., Park, K. J., & Hubinger, M. D. (2007). Influence of process conditions on the mass transfer kinetics of pulsed vacuum osmotically dehydrated mango slices. *Drying Technology*, 25, 1769–1777. https://doi.org/10.1080/07373930701593263

Jaworska, N., & Anastasova, A. C. (2009). A review of multidimensional scaling (MDS) and its utility in various psychological domains. *Tutorials in Quantitative Methods for Psychology*, 5, 1e10. https://doi.org/10.20982/tqmp.05.1.p001

Junqueira, J. R. J., Corrêa, J. L. G., Mendonça, K. M., Mello Junior, R. E., & Souza, A. U. (2021). Modeling mass transfer during osmotic dehydration of different vegetable structures under vacuum conditions. *Food Science and Technology*, 41, 439–448. https://doi.org/10.1590/fst.02420

Khubber, S., Chaturvedi, K., Gharibzahedi, S. M. T., Cruz, R. M. S., Lorenzo, J. M., Gehlot, R., & Barba, F. J. (2020). Non-conventional osmotic solutes (honey and glycerol) improve mass transfer and extend shelf life of hot-air dried red carrots: Kinetics, quality, bioactivity, microstructure, and storage stability, 131, 109764. https://doi.org/10.1016/j.lwt.2020.109764

Kruskal, J. B. (1964). Nonmetric multidimensional scaling: A numerical method. *Psychometrika*, 29, 115e129.

Lebaka V.R., Wee Y.-J., Ye W., & Korivi M. (2021). Nutritional composition and bioactive compounds in three different parts of mango fruit. *International Journal of Environmental Research and Public Health,* 18, 741. https://doi.org/10.3390/ijerph18020741

Lin, X., Luo, C., & Chen, Y. (2016). Effects of vacuum impregnation with sucrose solution on mango tissue. *Journal of Food Science*, 81, 1412–1418. https://doi.org/10.1111/1750-3841.13309

Lopez, M. M. L., Morais, R. M. S. C., & Morais, A. M. M. B. (2020). Flavonoid enrichment of fresh-cut apple through osmotic dehydration-assisted impregnation. *British Food Journal*, 123, 820–832. https://doi.org/10.1108/BFJ-03-2020-0176

Maeda, A., Miyagawa, J., Miuchi, M. (2013). Effects of the naturally-occurring disaccharides, palatinose and sucrose, on incretin secretion in healthy non-obese subjects. Journal of Diabetes Investigation, 4, 281–286. https://doi.org/10.1111/jdi.12045

Macedo, L. L., Corrêa, J. L. G., Araújo, C. S., Vimercati, W. C., & Petri Junior, I. (2021) Convective drying with ethanol pre-treatment of strawberry enriched with isomaltulose. *Food and Bioprocess Technology*. https://doi.org/10.1007/s11947-021-02710-2

Macedo, L. L., Corrêa, J. L. G., Araújo, C. S., & Vimercati, W. C. (2022). Effect of osmotic agent and vacuum application on mass exchange and qualitative parameters of osmotically dehydrated strawberry. *Journal of Food Processing and Preservation*, In press. https://doi.org/10.1111/jfpp.16621

Mendonça, K. S., Corrêa, J. L. G., Junqueira, J. R. J., Pereira, M. C. A., & Vilela, M. N. (2016). Optimization of osmotic dehydration of yacon slices. *Drying Technology*, 34, 386–394. https://doi.org/10.1080/07373937.2015.1054511

Nordey, T., Joas, J., Davrieux, F., Génard, M., & Léchaudel, M. (2014). Non-destructive prediction of color and pigment contents in mango peel. *Scientia Horticulturae*, 171, 37–44. https://doi.org/10.1016/j.scienta.2014.01.025

Oliveira, L. F., Corrêa, J. L. G., Silveira, P. G., Vilela, M. B., & Junqueira, J. R. J. (2021). Drying of ‘yacon’ pretreated by pulsed vacuum osmotic dehydration. *Revista Brasileira de*

Engenharia Agrícola e Ambiental, 25, 560–565. https://doi.org/10.1590/1807-1929/agriambi.v25n8p560-565

R Core Team (2021). *R: a language and environment for statistical computing*. R Foundation for Statistical Computing, Vienna, Austria.

Shyam, S., Ramadas, A., & Chang, S. K. (2018). Isomaltulose: Recent evidence for health benefits. *Journal of Functional Foods*, 48, 173–178. https://doi.org/10.1016/j.jff.2018.07.002

Sirijariyawat, A., Charoenrein, S., & Barrett, D. M. (2012). Texture improvement of fresh and frozen mangoes with pectin methylesterase and calcium infusion. *Journal of the Science of Food and Agriculture*, 92, 2581–2586. https://doi.org/10.1002/jsfa.5791

Tonolli, P. N., Franco, F. F., & Silva, A. F. G. (2021). Historical construction of the concept of the enzyme and approaches in biology textbooks. *História, Ciências, Saúde – Manguinhos*, 28, 727–744. https://doi.org/10.1590/S0104-59702021000300006

Viana, A. D., Corrêa, J. L. G., & Justus, A. (2014). Optimisation of the pulsed vacuum osmotic dehydration of cladodes of fodder palm. *International Journal of Food Science and Technology*, 49, 726–732. https://doi.org/10.1111/ijfs.12357

ARTICLE 5 – **Moisture sorption isotherms and thermodynamic properties of mangos: influence of osmotic treatment with sucrose and a healthy carbohydrate – Palatinose®**

Juliana Rodrigues do CARMO [a*], Jefferson Luiz Gomes CORRÊA [a], Maria Júlia Neves MARTINS [b], Marcio Augusto Ribeiro SANCHES [b], Javier TELIS-ROMERO [b]

[a] Department of Food Science (DCA), Federal University of Lavras, 37200-900, Lavras, Brazil. E-mail: juliana_docarmo@yahoo.com.br (Orcid ID: 0000-0002-9083-4863); jefferson@ufla.br (Orcid ID: 0000-0002-6818-6927)

[b] Department of Food Engineering and Technology, São Paulo State University, São José do Rio Preto 15054-000, Brazil. E-mail: nevesmartins.mj@gmail.com (Orcid ID: 0000-0001-5936-734X); mar.sanches@unesp.br (Orcid ID: 0000-00031898-9091); javier.romero@unesp.br (Orcid ID: 0000-0003-2555-2410).

[*]**Corresponding author:** Juliana Rodrigues do CARMO (E-mail: juliana_docarmo@yahoo.com.br)

(Elaborated in accordance to the Food and Bioproducts and Processing)

Abstract: Moisture sorption isotherms and thermodynamic properties of fresh and osmodehydrated mangos were determined. For the osmotic processes, two carbohydrates (sucrose and isomaltulose – Palatinose®) were used as osmotic agent. Moisture adsorption isotherms of products were determined from 313.15 K to 353.15 K range temperature by the gravimetric-static method. The net isosteric heat of sorption was determined by using Clausius-Clapeyron Equation. The differential enthalpy and entropy and the free Gibbs energy were calculated using the sorption data. The sorption isotherms exhibited type II and type III shape. The microbiological stability in operating temperatures was assured below 0.20, 0.15 and 0.20 g water/g dry matter for fresh mangos and pretreated mangos with sucrose and isomaltulose, respectively. The GAB model was selected to describe the sorption isotherms, since it presented good accuracy ($R^2 > 0.994$, $\chi^2 \leq 6.9 \cdot 10^{-4}$ and $RMSE \leq 2.6 \cdot 10^{-2}$). The isosteric heat and sorption entropy behaviors indicated that the magnitude of the interaction between water and the product components shows physical properties of pure water starting at 0.35 g water/g dry matter. The positive Gibbs Free Energy value indicated that moisture adsorption of fresh mangos was non-spontaneous process, but it was spontaneous for treated samples. The enthalpy-entropy compensation theory indicated the sorption processes of products are enthalpy-controlled. The differential thermodynamic properties of sorption showed that samples immersed in isomaltulose solutions had greater affinity with water, and therefore presented the highest values in order of magnitude for the studied properties.

Keywords: *Tommy Atkins*, osmotic dehydration, carbohydrate, isosteric heat, differential entropy.

1 Introduction

Mango (*Mangifera indica* L.) is one of the most consumed tropical fruits and whose composition is rich on vitamins (A, C, E, K, B1, B2, B3, B5, B6, B12), minerals (calcium, iron, phosphorus, potassium, magnesium, zinc, manganese), dietary fibers (cellulose, hemicellulose, lignin) and antioxidants (vitamin C, ß-carotene, dehydroascorbic acid) (Yao et al. 2020). Despite its considerable nutritional value, mango is an extremely perishable fruit, which needs specific care for its conservation (Kumar & Sagar, 2014). Therefore, the use of appropriate dehydration techniques to obtain a product with greater physicochemical and sensory stability.

Osmotic dehydration (OD) is a technique that consists of immersing the food in a hypertonic solution, with consequent water loss (WL) and solid gain (SG) in simultaneous isothermal flows without any phase change. In OD, three types of counter-current mass transfer occur: (1) water flows from the product to the solution, (2) a solute transfer from solution to the product and (3) a leaching out of the native solutes (sugars, organic acids, minerals, vitamins, etc.) (Abrahão & Corrêa, 2021).

Sucrose is the most common solute used in osmotic solution. Its advantages are its low-cost and availability. However, it is considered a highly cariogenic sugar. This carbohydrate is rapidly digested, inducing high glycemic and insulinemic response (Fernandes et al., 2019). Isomaltulose, commercially known as Palatinose®, is a naturally-occurring disaccharide in honey, sugarcane, and molasses. It can also be obtained from sucrose using microbial enzymatic conversion (Shyam et al., 2018). Although isomaltulose has half of the sweet taste and similar caloric value of sucrose (~4 $kcal \cdot g^{-1}$), it is more slowly digested by α-glucosidase in the small intestine than sucrose, besides being a non-cariogenic carbohydrate (Sridonpai et al., 2016).

The hygroscopicity of a fresh or partially dehydrated food is linked to its physical, chemical, and microbiological stability, which makes it essential to know its hygroscopic behavior from moisture sorption isotherms (Cavalcante et al., 2018). The different solutes used in OD can affect the

compositional and structural characteristics of the food, modifying its water sorption isotherms, which describe the relationship between equilibrium moisture content and water activity (a_w) of this product at a constant temperature (Martins et al., 2015). This information is essential for modeling, and optimizing drying processes, predicting shelf-life stability, predicting moisture changes that may occur during storage and selecting the appropriate packaging material (Carmo & Pena, 2019).

Several mathematical empirical, semi-empirical, or theoretical models have been proposed to describe the behavior of moisture sorption in foods. Among the models available in the literature, GAB was the model chosen to predict the hygroscopic behavior of the different osmodehydrated products (Fan et al., 2019; Mrad et al., 2013; Wangcharoen, 2013) and dried products (Bouba et al., 2014; Engin, 2020; Kar & Sutar, 2022) in the temperature range 313.15 – 353.15 K.

Sorption thermodynamic properties of foods such as sorption net isosteric heat (q_{st}) or differential enthalpy (ΔH), differential entropy (ΔS), isokinetic temperature (T_β), Gibbs free energy (ΔG) and enthalpy-entropy compensation theorycan be estimated from moisture sorption isotherms obtained at different temperatures (Iglesias & Chirife, 1976). In general, these properties are used to estimate the amount of energy involved in the moisture sorption process, besides providing information about the state of water in a food product. So, the present research aimed obaitining the moisture sorption isotherms at drying temperatures, as well as the thermodynamic properties of fresh and osmodehydrated mangos were determined, in order to evaluate the influence of incorporation the sucrose and isomaltulose on hygroscopic behavior of mangos.

2 Material and Methods

2.1 Raw Material

Mango fruits (*Mangifera indica* L. cv. Tommy Atkins) were purchased in a local market (São José do Rio Preto, São Paulo, Brazil) (20°49'11" S 49°22.766' W). The fruits were selected in a similar

degree of maturation, that is, 50% ripening (50% yellow skin surface color) and approximately 16 °Brix. The mango fruits were washed with a disinfectant solution (chlorinated water at 200 ppm) during 5 min, then, seed and peel were removed and the experimental samples were obtained from the fruit pulp, which was sliced into pieces of 4.20±0.01×4.20±0.01×0.50±0.01 cm (long×wide×thickness) employing a stainless-steel molder. The proximate composition of the raw material was obtained according to AOAC (2010).

2.2 Preparation of osmotic solution

The saturated osmotic solutions were prepared with distilled water and analytical grade sucrose and isomaltulose (Palatinose®) (Sigma Aldrich, Steinheim, German). The solutes were weighed in an analytical balance model AUX220 with an accuracy of 0.1 mg (Shimadzu, Kyoto, Japan). The saturation of the solution at 313.15 K was in accordance with data from Martins et al. (2020) and Carmo et al. (2022). In order to ensure saturation, the solution was kept under stirring in a magnetic stirrer (C-MAG HS 7, IKA, USA) with temperature monitoring through a thermocouple (AK05, AKASO, Brazil). After complete dissolution of the solute, the soluble solids content was determined with a portable digital refractometer (HI 86801, Hanna Instruments, Romania) to check saturation.

2.2 Osmotic treatment

The samples were immersed in glass containers with the osmotic solutions at a ratio of solution/sample of 20:1 (v/w) to avoid dilution of the solution. The OD experiments occurred without recirculation and were performed at temperatures of 313.15 ± 1.10 K at atmospheric pressure. The processing temperature was controlled by an ultrathermostat bath (Marconi, model MA-184) and a thermocouple (AUX220, Shimadzu, Japan), during 24 h. The effect of the contact time (1, 2 3, 4, 5, 6, 7, 8, 10, 12, 15, 18, 22 and 24 h) on water loss (WL) and solid gain (SG) were

determined to assess OD process kinetics. Thus, the samples were removed from the solution after each predetermined time and immediately immersed in a distilled water at 276.15 ± 1.00 K for 30 s to stop dehydration and to remove the remaining osmotic solution on the surface. Then, they had their surface dried with absorbent paper.

The samples were weighed and dried at 333.15 K and 25 mmHg in a vacuum oven model TE-395 (TECNAL), and the moisture content of fresh and osmotically treated samples was determined according to AOAC (2010). All analyses were performed in triplicate and the results were presented on graphs of WL and SG as function of time (h).

The mass transfer parameters (WL and SG) of each sample subjected to the different OD time were evaluated according to Eq. 1 and Eq. 2, respectively (Viana et al., 2014).

$$WL(\%) = \frac{x_0^w M_0^o - x_t^w M_t^o}{M_0^o} \times 100 \quad (1)$$

$$SG(\%) = \frac{x_t^{ST} M_t^o - x_0^{ST} M_0^o}{M_0^o} \times 100 \quad (2)$$

where WL is the water loss, SG is the solid gain (%), x_0^w is the initial moisture content on a wet basis (wb) (kg of water·kg of fruit^{-1}) and x_t^w is the final moisture content on a wet basis (wb) (kg of water·kg of fruit^{-1}), M_0^o is initial sample weight (kg), M_t^o is final sample weight (kg), x_t^{ST} is final solids content (kg solids·kg fruit^{-1}) and x_0^{ST} is initial solids content (kg solids·kg fruit^{-1}), The subindices “0” and “t” refer to fresh sample and samples after osmotic treatment, respectively.

2.3 Sorption isotherms obtaining

The fresh and osmodehydrated mangos in saturated solutions of sucrose and isomaltulose after 24 h were used to obtain the sorption isotherms. The moisture sorption isotherms at five different

temperatures (313.15, 323.15, 333.15, 343.15 and 353.15 K) were determined by using the gravimetric-static method. Theses temperatures simulate the drying process and they were controlled in a thermostatic chamber (MA415, Marconi, Piracicaba, Brazil) for 313.15 K and an oven (MA030, Marconi, Piracicaba, Brazil) for 323.15 – 353.15 K. Glass desiccators with saturated salt solutions were used aiming to reach different relative humidity (RH = a_w x 100). The values of water activity (a_w) for each salt solution at different temperatures are presented in Table 1.

Table 1. Water activity of saturated salt solutions at different temperatures.

Salt	Water activity				
	Temperature (K)				
	313.15	323.15	333.15	343.15	353.15
LiBr	0.0580	0.0553	0.0533	0.0523	0.0520
LiCl	0.1121	0.1110	0.1095	0.1075	0.1051
LiI	0.1455	0.1238	0.0998	0.0723	-
$MgCl_2$	0.3160	0.3054	0.2926	0.2777	0.2605
NaI	0.3288	0.2921	0.2595	0.2357	0.2252
K_2CO_3	-	-	-	-	-
$Mg(NO_3)_2$	0.4842	0.4544	-	-	-
NaBr	0.5317	0.5093	0.4966	0.4970	0.5143
KI	0.6609	0.6449	0.6311	0.6193	0.6097
NaCl	0.7468	0.7443	0.7450	0.7506	0.7629
$(NH_4)_2SO_4$	0.7991	0.7920	-	-	-
KCl	0.8232	0.8120	0.8025	0.7949	0.7890
KNO_3	0.8903	0.8478	-	-	-
K_2SO_4	0.9641	0.9582	-	-	-

Adapted from Greenspan (1977). Lithium Bromide (LiBr), Lithium Chloride (LiCl), Lithium Iodide (LiI), Magnesium Chloride ($MgCl_2$), Sodium Iodide (NaI), Potassium Carbonate (K_2CO_3), Magnesium Nitrate ($Mg(NO_3)_2$), Sodium Bromide (NaBr), Potassium iodide (KI), Sodium Chloride (NaCl), Ammonium Sulfate ($(NH_4)_2SO_4$), Potassium Chloride (KCl), Potassium Nitrate (KNO_3), Potassium Sulfate (K_2SO_4).

2.0 g ± 0.1 mg of samples were weighted in small containers, in triplicate, and put in the desiccators. The samples are suspended from a support so as not to contact with the salt solutions. All experiments were performed at atmospheric pressure. The samples were previously weighed on an analytical balance (AUW220D, Shimadzu, Japan) to determine the initial moisture content. After reaching equilibrium, the samples were weighed again. The equilibrium moisture content (x_{eq}) of each condition was calculated using the initial and final mass. a_w and equilibrium moisture data were used for built the moisture sorption isotherms.

2.4 Sorption isotherms modelling

The mathematical models (theoretical, empirical, and semi-empirical) presented in Table 2 were adjusted to the experimental moisture sorption data of the mangos. Goodness of fit was assessed using coefficient of determination (R^2) (Eq. 3), reduced chi-square (χ^2) (Eq. 4) and root mean squared error (RMSE) (Eq. 5).

$$R^2 = 1 - \frac{\sum_{i=1}^{n}\left(Y_i^* - Y_i\right)^2}{\sum_{i=1}^{n}\left(Y_i^* - \bar{Y}_i\right)^2} \quad (3)$$

$$\chi^2 = \sum_{i=1}^{n}\left(Y_i^* - Y_i\right)^2 \Big/ Y_i \quad (4)$$

$$RMSE = \sqrt{\frac{\sum_{i=1}^{n}\left(Y_i - Y_i^*\right)^2}{n}}$$

where Y_i, Y_i^* and $\bar{Y}_i$ are the predicted, experimental and mean values, respectively, and n is the number of experimental measurements.

Table 2. Models used to fit sorption isotherm data from fresh and osmodehydrated mangos.

Model	Equation	Reference
GAB	$x_{eq} = \frac{X_m \cdot C \cdot k \cdot a_w}{(1-k \cdot a_w)\cdot(1+(c-1)\cdot k \cdot a_w)}$	(Vand den Berg, 1984)
Peleg	$x_{eq} = k_1 \cdot a_w^{n_1} + k_2 \cdot a_w^{n_2}$	(Peleg, 1993)
Oswin	$x_{eq} = M \cdot \left(\frac{a_w}{1-a_w}\right)^N$	(Oswin,1946)
Henderson	$x_{eq} = \left(-\frac{1}{H_1}\cdot \ln(1-a_w)\right)^{\frac{1}{H_2}}$	(Boquet et al., 1978)
Halsey	$x_{eq} = \left(-h_1 \cdot \ln(a_w)\right)^{-\frac{1}{h_2}}$	(Halsey, 1948)

where x_{eq} is the equilibrium moisture content, a_w is the water activity and X_m (monolayer moisture content – dry basis), C, k, k_1, k_2, n_1, n_2, M, N, H_1, H_2, h_1 and h_2 are constants of the model.

2.5 Thermodynamic Properties

2.5.1 Net isosteric heat of sorption

The value of net isosteric heat of sorption (q_{st}) (J/mol) was calculated by the integrated form of the Clausius-Clapeyron equation (Eq. 6) based on slope of the line obtained by the ratio ln(a_w) *versus* 1/T (isostere) for a constant equilibrium moisture (Rizvi, 1986).

$$\left[\frac{d(\ln a_w)}{d(T)}\right]_{x_{eq}} = \frac{-q_{st}}{R} \qquad (6)$$

where a_w is water activity (dimensionless), T is temperature (K), R is universal gas constant (8.314 J/K.mol), x_{eq} is equilibrium moisture content (g water/g dry matter).

2.5.2 Differential entropy and gibbs free energy

Sorption differential entropy (ΔS, J/mol) was determined based on the Gibbs-Helmholtz equation (Eq. 7) (Telis et al, 2000), whereas Gibbs free energy (ΔG, J/mol) was calculated by the van't Hoff equation (Eq. 8). For a desorption process, the enthalpy change (ΔH) is positive and equal to the q_{st}, since heat is absorbed by the system. If heat is released by the system, as in an adsorption process, q_{st} should be negative. The combination of these equations yielded Eq. 9, used to calculate the value of ΔS from the linear coefficient (ΔS/R) of the line obtained from the correlation $\ln(a_w)$ *versus* 1/T for a constant equilibrium moisture content (x_{eq}).

$$\Delta G = q_{st} - \Delta S T \tag{7}$$

$$\Delta G = -RT \ln a_w \tag{8}$$

$$\ln a_w = -\frac{q_{st}}{RT} + \frac{\Delta S}{R} \tag{9}$$

2.5.3 Evaluation of the enthalpy-entropy compensation theory

Enthalpy-entropy compensation theory was assessed using Eq. 10. This theory can be applied when the isokinetic temperature (T_B, K) is different from the harmonic mean temperature (T_{hm}, K), defined by Eq. 11. If $T_B > T_{hm}$, the sorption process is enthalpy-controlled, otherwise, it is entropy-controlled (Krug et al., 1976a).

$$\Delta H = T_B \Delta S + \Delta G_B \tag{10}$$

$$T_{hm} = \frac{n}{\sum_{1}^{n} 1/T} \tag{11}$$

where ΔG_B is Gibbs free energy (J/mol) at T_B, n is number of temperatures at which the isotherms were obtained.

The T_B can be determined by Eq. (12) for a confidence interval of (1-0.05) 100%.

$$T_B = T_B \pm t_{m-2,\alpha/2\sqrt{Var(T_B)}} \quad (12)$$

where

$$T_B = \frac{\sum\left(\Delta H - \overline{\Delta H}\right)\left(\Delta S - \overline{\Delta S}\right)}{\sum\left(\Delta S - \overline{\Delta S}\right)^2} \quad (13)$$

$$Var(T_B) = \frac{\sum\left(\Delta H - \overline{\Delta G_B} - T_B \Delta S\right)^2}{\sum(m-2)\sum\left(\Delta S - \overline{\Delta S}\right)^2} \quad (14)$$

where m is the number of data pairs (ΔH, ΔS), $\overline{\Delta S}$ is mean entropy and $\overline{\Delta H}$ is mean enthalpy.

2.6 Satistical analysis

The results of chemical composition were presented as mean values ± standard deviation of three replicates. The sorption models were fitted by non-linear regression using the mathematical software OriginPro 8.0 (OriginLab Corporation, Northampton, MA). The models whose fits had R^2 values close to one and reduced χ^2 and RMSE close to zero were considered effective (Vegá-Galvez et al., 2010).

3 Results and Discussion

3.1 Osmotic treatment

Fresh mango had 85.27% (±0.24) moisture, 0.34% (±0.01) ashes, 0.22% (±0.01) lipids, 0.90% (±0.01) proteins, 11.17% (±0.23) total carbohydrates and 2.10% (±0.02) fibers (wet basis). Similar values of composition were observed by Maldonado-Celis et al. (2019) and Lebaka et al. (2021) for this product. Low contents of ashes, lipids, and proteins on mangos fruits were noticed. However, the moisture content of mango fruit showed high value, which evidence the necessity of

drying techniques, as OD, in order to partially removing water and consequently assisting in subsequent drying processes (Polachini et al., 2016).

In this study, after 24 h of osmotic process, the final moisture content of mango was 58.60% (±0.01) and 62.24% (±0.49) for sucrose and isomaltulose solutions at 313.15 K, respectively. The kinetics obtained for WL and SG of mango slices in the different osmotic solutes are showed in Fig. 1.

In a general way, the results of mango slices osmodehydrated with sucrose solution presented WL values from 15.04 to 31.05% while for the samples with isomaltulose solution, the WL was from 12.94 to 26.96% (Fig. 1a). The SG varied from 5.50 to 9.32%, and from 6.05 to 9.98%, for sucrose and isomaltulose solutions (Fig. 1b), respectively, under the same conditions. Therefore, the results showed that the samples subjected to a sucrose solution obtained a slight greater WL than those that were osmotically dehydrated with isomaltulose. However, the samples treated with isomaltulose presented a slight greater amount of solutes. This behavior also was observed recently by Carmo et al. (2022).

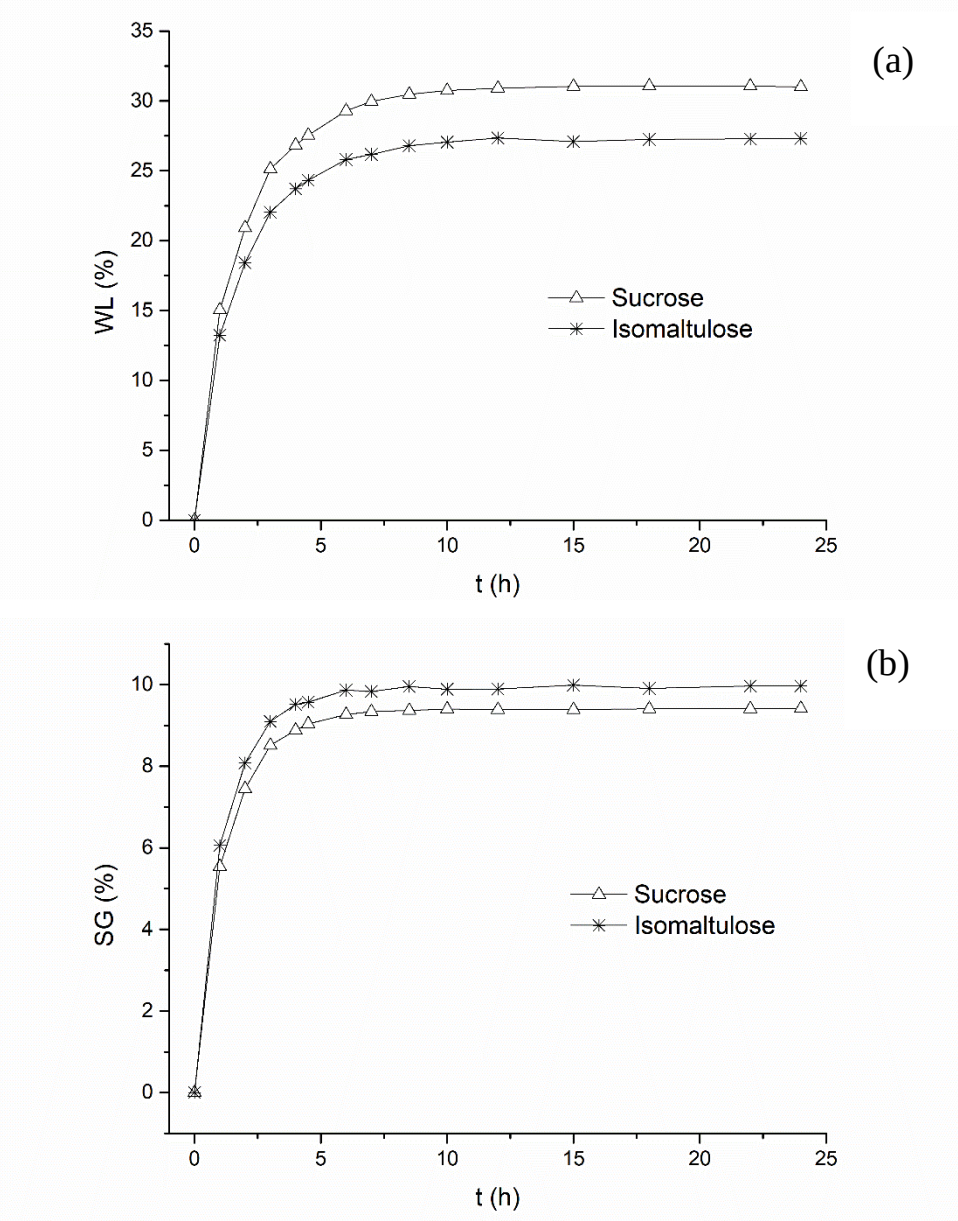

Fig. 1. Kinetics of water loss (a) and Solid gain (b) of mangos subjected to osmotic dehydration from 1 to 24 h with errors bars.

Although the solubility of aqueous sucrose solution is greater than isomaltulose solution (Carmo et al., 2022), the a_w of both solutions are close (0.970 for sucrose solution and 0.972 for isomaltulose solution) and this causes similar osmotic pressure gradients and, consequently, WL and SG values are of the same order of magnitude for both the solutes.

Despite there are no studies about OD of mango in isomaltulose solutions in literature, for sucrose solutions, the results obtained for WL and SG were similar to those reported in other works (Galdino et al., 2021; Zongo et al., 2021). The isomaltulose incorporation is interesting and promising, because the final product can be a partially dried and enriched food with low glycemic and insulinemic indexes agent, as mentioned previously. In addition, mangos are much less porous and denser than others fruits, such as apple and pineapple (Fernandes et al., 2019) and the use of healthy carbohydrate in OD process with a satisfactory incorporation, opens the way for further studies in this area.

3.2 Moisture sorption isotherms of mangos

Fig. 2 shows that the osmodehydrated mango with sucrose had lower moisture content than the mango *in natura* and osmodehydrated mango with isomaltulose for a constant a_w in all range temperature studied. As observed, the osmotic pretreatment of mangos in the isomaltulose solution made the product more hygroscopic than in sucrose solution. Although, they are isomers, as a result of the stronger bond between the two monosaccharides, isomaltulose distinctly differs in its nutritional and physiological properties from those of sucrose (Sentko & Willibald-Ettle, 2007). According to Udomkun et al. (2015), the types of the carbohydrates present in the fruit affect the isotherm behavior, since their solubilization properties are different due to the differences in the binding site availability and bound energy of different structures. Falade and Awoyele (2005) also observed greater hygroscopicity in bananas submitted to osmotic treatment in sucrose solutions than untreated samples after 12 h of treatment.

The sorption isotherms indicate that fresh mangos and pretreated mangos with sucrose and isomaltulose samples microbiologically stable (a_w < 0.6) (Jay, 2005) at 313.15 K if their moisture levels are up to, approximately, 0.20, 0.15 and 0.20 g water/g dry matter, respectively. These results indicate the mango *in natura* and pretreated with isomaltulose required greater care during storage. According to the quantitative criteria proposed by Yanniotis & Blahovec (2009) for the classification of moisture sorption isotherms, in general, the fresh samples adsorption isotherm behaved as more solution-like type-II isotherms. For the osmodehydrated products similar behavior was evident up to 323.15 K. However, from 333.15 K, the isotherms showed type-III shape. Both, type-II and type-III moisture sorption isotherms have been also observed for another osmodehydrated products (Bejar et al., 2012; Engin, 2020; Fan et al., 2019; Zhao et al., 2018).

The sorption isotherms behavior showed that at a_w > 0.60 the product moisture increased exponentially (Fig. 2). It is in agreement with the reported shape for high sugar food stuffs and may be due to the dissolution of crystalline sugar at low water activity and the conversion of crystalline sugar into amorphous sugar at high a_w (Saltmarch & Labuza, 1980). This behavior indicated that these products requires greater care when stored or handled in an environment with RH above 60%. Under such conditions, the product should be stored in packaging with low water vapor permeability (Carmo et al., 2019). Additionally, due to presence of bioactive compounds such as ascorbic acid, carotenoids and total phenolics, which are very susceptible to oxidative processes, the packages also must be impermeability to air and does not allow light to pass through (Pombo et al., 2019).

(a)

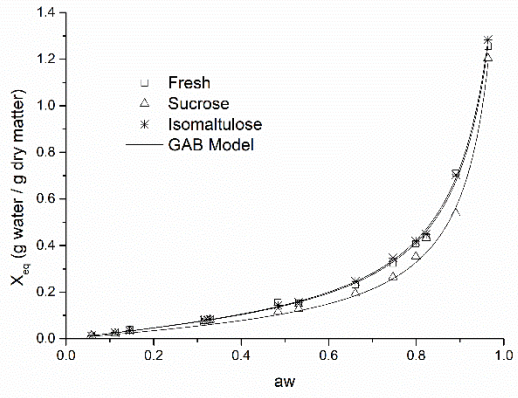
Fresh
Sucrose
Isomaltulose
GAB Model
X_{eq} (g water / g dry matter)
aw

(b)

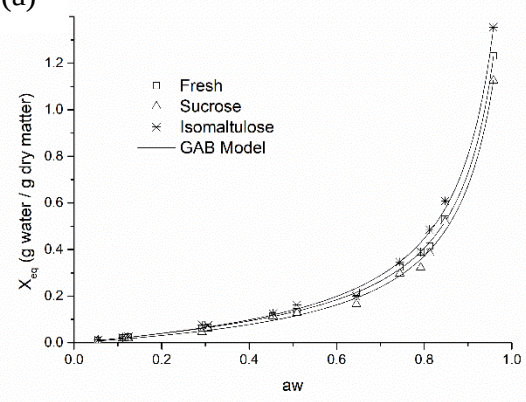
Fresh
Sucrose
Isomaltulose
GAB Model
X_{eq} (g water / g dry matter)
aw

(c)

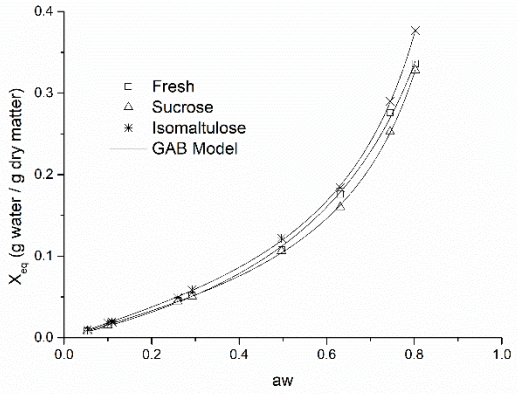
Fresh
Sucrose
Isomaltulose
GAB Model
X_{eq} (g water / g dry matter)
aw

(d)

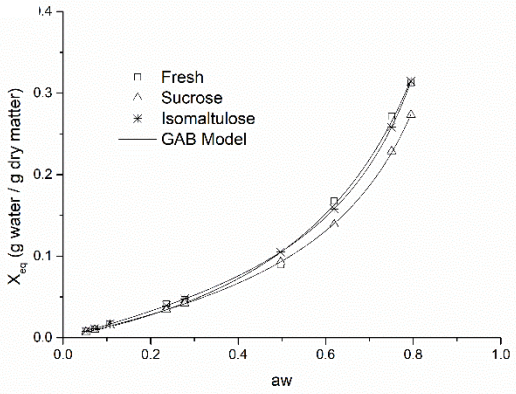
Fresh
Sucrose
Isomaltulose
GAB Model
X_{eq} (g water / g dry matter)
aw

(e)

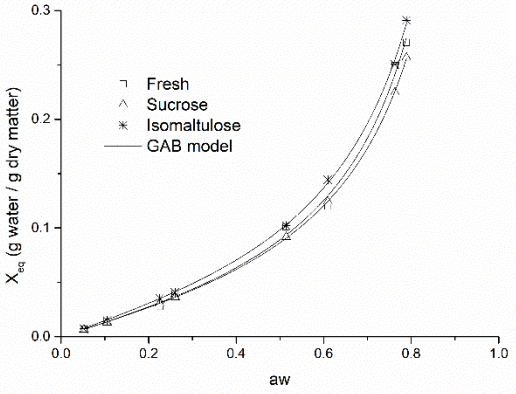
Fresh
Sucrose
Isomaltulose
GAB model
X_{eq} (g water / g dry matter)
aw

Fig. 2. Sorption isotherms fitted to the GAB model of fresh and osmodehydrated mangos with sucrose and isomaltulose at drying temperatures of (a) 313.15; (b) 323.15; (c) 333.15; (d) 343.15 and (e) 353.15 K.

For constant a_w, the moisture of all samples decreased as temperature increased, an effect that was more representative of the sample osmodehydrated with sucrose. The behavior observed is explained by the excitation state of water molecules, which increases with temperature, leading to lower sorption and, consequently, lower product moisture (McLaughlin & Magee, 1998). At increased temperatures, the attractive forces between molecules decrease due to an increase in kinetic energy of water molecules. This leads to the increase of their mobility. Therefore, water molecules with slow motion at low temperatures are bound more easily to suitable binding sites on surface. Studies on other osmodehydrated products showed a similar behavior (Fan et al., 2019; Sangeeta & Hathan, 2017).

3.3 Mathematical modelling of sorption isotherms

According to the values of the statistics used to assess goodness of fit (R^2, RMSE and χ^2) (Tables 3–5), among the models evaluated, the Peleg and GAB models showed good performance on predicting to describe the moisture adsorption of the untreated and pretreated mangos in the experimental domain. The chosen of the GAB model is based on physical means of its constants and lesser number of constants than Peleg model. The isotherms generated by the GAB model are presented in Fig 2. Overall, the literature indicates the GAB model as having the best fits to the moisture sorption data of another partially dried and dried products (Prothon & Ahrne, 2004; Falade & Aworh, 2004; Engin, 2020; Fan et al., 2019).

According to GAB model (Table 2), the monolayer moisture (X_m) of the samples varied from 0.07 to 0.12 g water/g dry matter; from 0.07 to 0.12 g water/g dry matter (Table 3) and 0.07 from 0.13 to g water/g dry matter for the untreated mango and pretreated with sucrose (Table 4) and

isomaltulose (Table 5), respectively. As observed, the monolayer moisture content decreased with increasing temperature The temperature dependence of the monolayer value has been linked (Iglesias et al., 1975) to a reduction in sorption active sites as a result of physicochemical changes induced by temperature. Iglesias and Chirifie (1976) reported this behavior for almost 100 different foods and food systems. Similar behavior was also observed with sucrose solution in mangos (Falade & Aworh, 2004; Zhao et al., 2018).

According to Labuza (1984), foods with $X_m \leq 0.10$ g water/g dry matter are considered stable. Thus, the products were considered with good stability from 333.15 K. The monolayer concept is useful because of its relationship with several aspects of physical and chemical deterioration in dehydrated foods, since corresponds to the optimal moisture content, which should be achieved and maintained in order to minimize deteriorative reactions during storage (Zhao et al., 2018).

3.4 Thermodynamic properties

For thermodynamic properties determination, equilibrium moisture ranging from 0.15 to 0.60 g water/g of dry matter were fixed and the a_w values were determined from the parameters of the GAB model. This procedure was applied at all temperatures.

3.4.1 Isosteric sorption heat and differential entropy

The q_{st} behavior for the moisture sorption processes of mango samples as a function of moisture content is presented in Fig. 3. For moisture levels below 0.35 g water/g dry matter, q_{st} values increased exponentially as moisture decreases, particularly in higher order of magnitude for isomaltulose. The product obtained with this carbohydrate showed greater water retention capacity, which reflected a greater adsorption of water when compared to the fresh product, the same behavior was presented by Paes et al. (2021) for cambuci samples osmodehydrated with sorbitol.

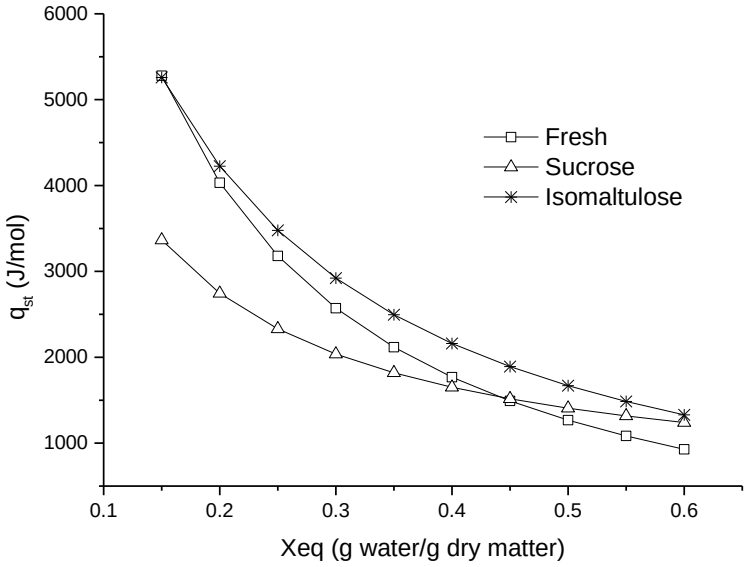

Fig. 3. Isosteric net sorption heat for fresh mango and osmodehydrated with sucrose and isomaltulose as a function of equilibrium moisture content.

Fig. 3 shows q_{st} ranging between 928.09–5279.47; 1240.20–3365.76 and 1328.83–5258.44 J/mol for the treatment with fresh mango and osmodehydrated with sucrose and isomatulose, respectively. This behavior was similar for green bananas (Zabalaga et al., 2016), papaya seeds (Rosa et al., 2021), cambuci (Paes et al., 2021), quince (Noshad et al., 2012) and papaya (Udomkun et al., 2015). At 0.45 g water/g of dry matter the curves of the in natura and sucrose treatment intersected, resulting in an inversion of behavior. In general, a greater amount of isosteric heat of sorption is required for drying, at lower moisture contents of the mango. This is due to at lower moisture levels, water molecules are strongly linked to the structure of the food, mainly the macromolecules, such as carbohydrates, fibers and proteins of the fruit. The magnitude of the interactions between water molecules and product components continuously decreases until a

moisture level is reached at which the water contained in the product begins exhibiting the physical properties of pure water (Tsami et al., 1990).

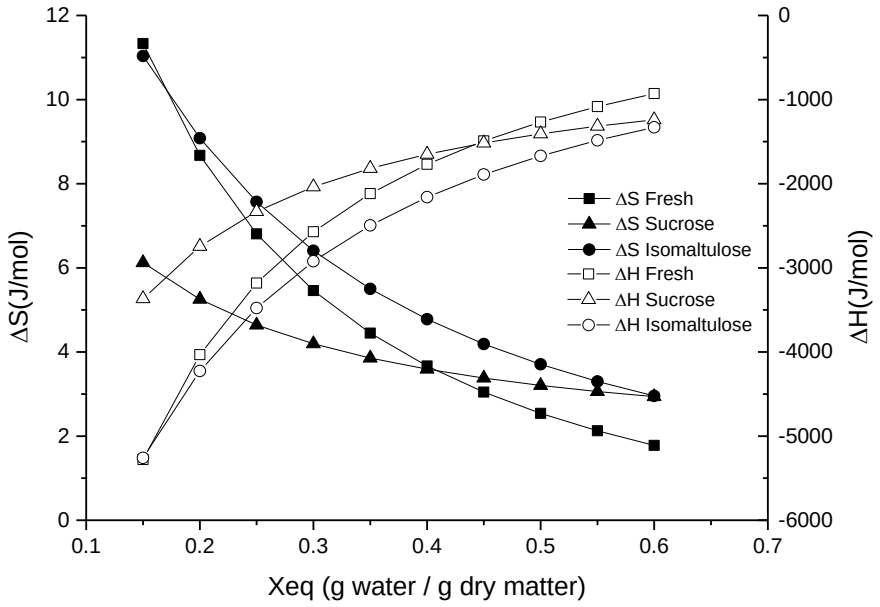

Fig. 4. Change in enthalpy and entropy as a function of equilibrium moisture contents.

In Fig. 4, the behavior of ΔH showed negative values in a range from -928.09 to -5279.47 J/mol. Negative enthalpy values represent an exothermic process and the presence of forces that act as binding forces during the sorption process (McMinn et al., 2005).

ΔS represents the degree of order or disorder present in the sorption system, in which it is associated with the spatial arrangements of the molecules and the binding or repulsion forces between the water and the matrix (McMinn et al., 2005). In the present study, ΔS ranged from 1.78 to 11.33, 2.94 to 6.12 and 2.96 to 11.04 J/mol for fresh mango and osmodehydrated with sucrose and isomaltulose, respectively (Fig. 4). The gradual decreasing behavior with increasing equilibrium

moisture was expected, as this property is related to the availability of sorption sites (Madamba et al., 1996; McMinn & Magee, 2003). The decrease in entropy causes a reduction in energy for the mobility of molecules as the sorption of available sites with higher energy occurs and, consequently, saturation. Conversely, with increasing entropy, water molecules have greater mobility and they are free to form multilayers. Fig. 4 shows that higher entropies are determined at lower equilibrium moisture, that is, there is a greater the difficulty and energy expenditure for a water molecule to carry out the sorption process (Rizvi, 1995).

3.4.2 Gibbs free energy and entalphy-entropy theory

ΔG represents the energy available to perform useful work (Rizvi, 1995). According to McMinn et al. (2005) it may indicate a spontaneous ($\Delta G < 0$) or non-spontaneous ($\Delta G > 0$) sorption process. From the linear regression of Eq. 10 was determined the ΔG and the isokinetic temperature (T_B). For the process with fresh mango, ΔG = 106.96 J/mol, indicated a non-spontaneous process of moisture sorption, while for the osmodehydrated processes, it indicated the spontaneity of these processes (ΔG = -727.69 and -131.59 J/mol for sucrose and isomaltulose, respectively).

Compensation theory was determined by the linear relationship between the enthalpy and entropy modules and in Fig. 5 it is confirmed for untreated and pretreated mangos processes ($R^2 \geq 0.995$) on studied moisture range. This means that ΔH change simultaneously affects ΔS and ΔG (Polachini et al., 2016). The linear chemical compensation pattern was determined in all processes due to the inexistence of equality between the T_B and harmonic mean temperature (T_{hm}) (Krug et al., 1976 a,b), which was T_{hm} = 332.55 K and T_B = 454.14±3.73, 663.57±20.41 and 482.36±34.61 K for fresh and osmodehydrated mangos with sucrose and isoamltulose, respectively. Therefore, T_B was higher than T_{hm}, indicated that the moisture adsorption of the studied samples are enthalpy-controlled processes (Leffler, 1955). Noshad et al. (2012) also showed the enthalpy-controlled

adsorption process during osmotic dehydration of quince in of 40 – 60% sucrose solution at 303.15 – 333.15 K.

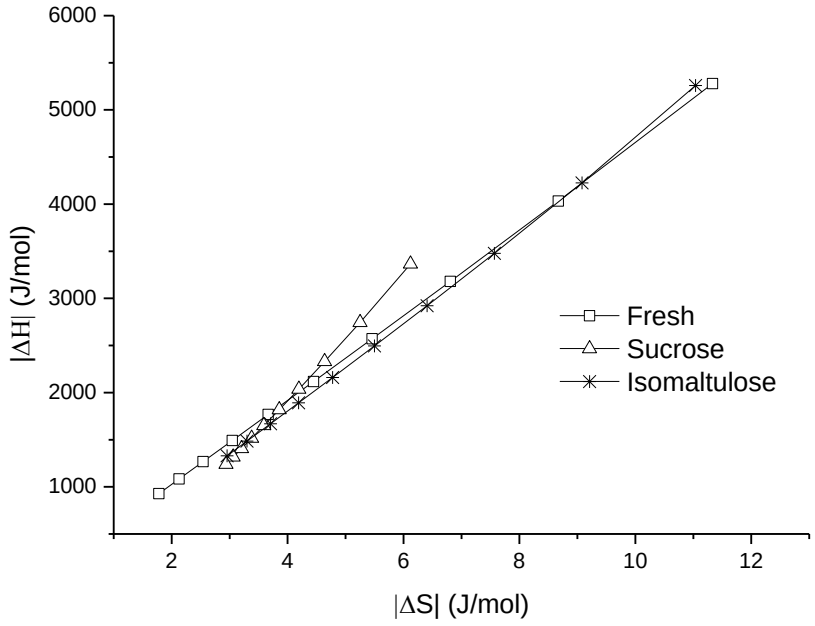

Fig. 5. Linear regression of differential enthalpy versus differential entropy values.

Table 3. Predicted parameters of fitted models for sorption isotherms of fresh mango at different temperatures.

T(K)	GAB						
	X_m	C	K	R^2	χ^2	RMSE	
313.15	0.1169	2.0000	0.9453	0.998	$2.7\cdot10^{-4}$	$1.6\cdot10^{-2}$	
323.15	0.1158	1.6214	0.9510	0.999	$4.2\cdot10^{-5}$	$6.5\cdot10^{-3}$	
333.15	0.0897	1.6990	0.9802	0.999	$2.1\cdot10^{-5}$	$4.6\cdot10^{-3}$	
343.15	0.0960	1.4598	0.9488	0.997	$3.8\cdot10^{-5}$	$6.2\cdot10^{-3}$	
353.15	0.0694	1.8862	0.9893	0.995	$5.1\cdot10^{-5}$	$7.1\cdot10^{-3}$	
	Peleg						
	k_1	n_1	k_2	n_2	R^2	χ^2	RMSE
313.15	0.3533	1.2211	1.3431	10.4226	0.999	$1.1\cdot10^{-4}$	$8.9\cdot10^{-3}$
323.15	1.3661	11.4232	0.4195	1.5951	0.999	$8.3\cdot10^{-5}$	$7.6\cdot10^{-3}$
333.15	0.1655	1.0023	0.5258	4.2777	0.999	$4.2\cdot10^{-6}$	$1.5\cdot10^{-3}$
343.15	0.1114	0.8197	0.5366	3.8097	0.999	$4.5\cdot10^{-5}$	$5.0\cdot10^{-3}$
353.15	0.1971	1.2165	0.6969	7.1636	0.997	$5.5\cdot10^{-5}$	$5.2\cdot10^{-3}$
	Oswin						
	M	N	R^2	χ^2	RMSE		
313.15	0.1698	0.6152	0.990	$1.3\cdot10^{-3}$	$3.6\cdot10^{-2}$		
323.15	0.1532	0.6693	0.995	$5.3\cdot10^{-4}$	$2.3\cdot10^{-2}$		
333.15	0.1115	0.8055	0.997	$3.9\cdot10^{-5}$	$6.2\cdot10^{-2}$		
343.15	0.1047	0.8288	0.995	$7.5\cdot10^{-5}$	$8.6\cdot10^{-2}$		
353.15	0.0889	0.8566	0.996	$4.3\cdot10^{-5}$	$6.6\cdot10^{-2}$		
	Henderson						
	H_1	H_2	R^2	χ^2	RMSE		
313.15	2.8603	0.6791	0.994	$7.3\cdot10^{-4}$	$2.7\cdot10^{-2}$		
323.15	2.7979	0.6348	0.997	$3.5\cdot10^{-4}$	$1.9\cdot10^{-2}$		
333.15	3.8688	0.7969	0.998	$3.1\cdot10^{-5}$	$5.5\cdot10^{-3}$		
343.15	3.8767	0.7740	0.994	$7.9\cdot10^{-5}$	$8.9\cdot10^{-3}$		
353.15	4.1343	0.7466	0.992	$8.8\cdot10^{-5}$	$9.4\cdot10^{-4}$		
	Halsey						
	h_1	h_2	R^2	χ^2	RMSE		
313.15	0.0537	1.4688	0.978	$2.8\cdot10^{-3}$	$5.3\cdot10^{-2}$		
323.15	0.0581	1.3465	0.984	$1.8\cdot10^{-3}$	$4.2\cdot10^{-2}$		
333.15	0.0824	0.9412	0.986	$2.0\cdot10^{-4}$	$1.4\cdot10^{-2}$		
343.15	0.0832	0.9107	0.986	$1.9\cdot10^{-4}$	$1.4\cdot10^{-2}$		
353.15	0.0763	0.8889	0.992	$9.2\cdot10^{-5}$	$9.6\cdot10^{-3}$		

Table 4. Predicted parameters of fitted models for sorption isotherms of osmodehydrated mango with sucrose at different temperatures.

T(K)	GAB						
	X_m	C	K	R^2	χ^2	RMSE	
313.15	0.0861	2.0000	0.9646	0.994	$6.9\cdot10^{-4}$	$2.6\cdot10^{-2}$	
323.15	0.1150	1.1990	0.9457	0.996	$4.2\cdot10^{-4}$	$2.1\cdot10^{-2}$	
333.15	0.1064	1.4789	0.9130	0.999	$7.2\cdot10^{-6}$	$2.7\cdot10^{-3}$	
343.15	0.0858	1.5974	0.9344	0.999	$9.4\cdot10^{-7}$	$9.7\cdot10^{-4}$	
353.15	0.0690	1.9085	0.9724	0.999	$8.8\cdot10^{-7}$	$9.4\cdot10^{-4}$	
	Peleg						
	k_1	n_1	k_2	n_2	R^2	χ^2	RMSE
313.15	0.4739	1.8421	1.4502	17.7766	0.994	$8.0\cdot10^{-4}$	$2.4\cdot10^{-2}$
323.15	1.2924	9.3678	0.2755	1.2599	0.998	$2.8\cdot10^{-4}$	$1.4\cdot10^{-2}$
333.15	0.2266	1.1919	0.6837	6.7801	0.998	$2.3\cdot10^{-6}$	$1.1\cdot10^{-3}$
343.15	0.1766	1.1226	0.4641	5.3283	0.998	$5.4\cdot10^{-7}$	$5.0\cdot10^{-4}$
353.15	0.2030	1.2607	0.6416	7.6267	0.998	$2.1\cdot10^{-6}$	$1.0\cdot10^{-3}$
	Oswin						
	M	N	R^2	χ^2	RMSE		
313.15	0.1355	0.6653	0.996	$4{,}2\cdot10^{-4}$	$2{,}1\cdot10^{-2}$		
323.15	0.1384	0.6743	0.990	$1{,}0\cdot10^{-3}$	$3{,}2\cdot10^{-2}$		
333.15	0.1045	0.8182	0.999	$3{,}5\cdot10^{-6}$	$1{,}9\cdot10^{-3}$		
343.15	0.0926	0.8071	0.999	$5{,}7\cdot10^{-6}$	$2{,}4\cdot10^{-3}$		
353.15	0.0859	0.8276	0.999	$1{,}5\cdot10^{-6}$	$1{,}2\cdot10^{-3}$		
	Henderson						
	H_1	H_2	R^2	χ^2	RMSE		
313.15	3.0071	0.6153	0.990	$1.1\cdot10^{-3}$	$3.4\cdot10^{-2}$		
323.15	2.9537	0.6280	0.994	$6.1\cdot10^{-4}$	$2.5\cdot10^{-2}$		
333.15	3.9650	0.7844	0.996	$5.7\cdot10^{-5}$	$7.6\cdot10^{-3}$		
343.15	4.5475	0.8045	0.998	$2.2\cdot10^{-5}$	$4.6\cdot10^{-3}$		
353.15	4.5667	0.7793	0.997	$3.2\cdot10^{-5}$	$5.6\cdot10^{-3}$		
	Halsey						
	h_1	h_2	R^2	χ^2	RMSE		
313.15	0.0481	1.3684	0.989	$1{,}2\cdot10^{-3}$	$3{,}4\cdot10^{-2}$		
323.15	0.0517	1.3379	0.978	$2{,}1\cdot10^{-3}$	$4{,}6\cdot10^{-2}$		
333.15	0.0801	0.9274	0.993	$9{,}9\cdot10^{-5}$	$9{,}9\cdot10^{-3}$		
343.15	0.0710	0.9283	0.991	$9{,}5\cdot10^{-5}$	$9{,}7\cdot10^{-3}$		
353.15	0.0691	0.9148	0.994	$5{,}7\cdot10^{-5}$	$7{,}6\cdot10^{-3}$		

Table 5. Predicted parameters of fitted models for sorption isotherms of osmodehydrated mango with isomaltulose at different temperatures.

T(K)	GAB					
	X_m	C	K	R^2	χ^2	RMSE
313.15	0.1220	1.9393	0.9433	0.999	$1.2\cdot10^{-4}$	$1.1\cdot10^{-2}$
323.15	0.1325	1.3900	0.9486	0.997	$4.6\cdot10^{-4}$	$2.2\cdot10^{-2}$
333.15	0.0973	1.8924	0.9671	0.999	$3.5\cdot10^{-6}$	$1.9\cdot10^{-3}$
343.15	0.0904	1.7551	0.9523	0.999	$5.2\cdot10^{-9}$	$7.2\cdot10^{-5}$
353.15	0.0790	1.9083	0.9684	0.999	$7.6\cdot10^{-6}$	$2.8\cdot10^{-3}$
	Peleg					
	k_1	n_1	k_2	n_2	R^2	χ^2	RMSE
313.15	0.4555	1.5478	1.3268	12.1160	0.999	$1.4\cdot10^{-4}$	$9.8\cdot10^{-3}$
323.15	0.3145	1.1647	1.5655	9.2297	0.999	$2.4\cdot10^{-4}$	$1.3\cdot10^{-2}$
333.15	0.2615	1.2030	0.7813	6.7768	0.999	$4.7\cdot10^{-6}$	$1.6\cdot10^{-3}$
343.15	0.2174	1.1701	0.5880	6.0248	0.999	$2.0\cdot10^{-6}$	$1.1\cdot10^{-3}$
35315	0.2413	1.2940	0.8020	8.3366	0.999	$1.3\cdot10^{-5}$	$2.6\cdot10^{-3}$
	Oswin					
	M	N	R^2	χ^2	RMSE	
313.15	0.1723	0.6169	0.992	$1.1\cdot10^{-3}$	$3.3\cdot10^{-2}$	
323.15	0.1675	0.6718	0.991	$1.2\cdot10^{-3}$	$3.5\cdot10^{-2}$	
333.15	0.1196	0.8206	0.999	$5.0\cdot10^{-6}$	$2.2\cdot10^{-3}$	
343.15	0.1050	0.8140	0.999	$3.1\cdot10^{-6}$	$1.8\cdot10^{-3}$	
353.15	0.0976	0.8215	0.999	$7.3\cdot10^{-6}$	$2.7\cdot10^{-3}$	
	Henderson					
	H_1	H_2	R^2	χ^2	RMSE	
313.15	2.8236	0.6795	0.997	$4.5\cdot10^{-4}$	$2.1\cdot10^{-2}$	
323.15	2.6311	0.6298	0.994	$8.1\cdot10^{-4}$	$2.9\cdot10^{-2}$	
333.15	3.5467	0.7815	0.996	$7.3\cdot10^{-5}$	$8.5\cdot10^{-3}$	
343.15	4.0439	0.7966	0.997	$3.5\cdot10^{-5}$	$5.9\cdot10^{-3}$	
353.15	4.1979	0.7864	0.996	$4.3\cdot10^{-5}$	$6.6\cdot10^{-3}$	
	Halsey					
	h_1	h_2	R^2	χ^2	RMSE	
313.15	0.0552	1.4639	0.979	$2.7\cdot10^{-3}$	$5.2\cdot10^{-2}$	
323.15	0.0662	1.3427	0.981	$2.7\cdot10^{-3}$	$5.2\cdot10^{-2}$	
333.15	0.0913	0.9251	0.993	$1.3\cdot10^{-4}$	$1.2\cdot10^{-2}$	
343.15	0.0810	0.9214	0.992	$1.1\cdot10^{-4}$	$1.0\cdot10^{-2}$	
353.15	0.0766	0.9204	0.993	$8.2\cdot10^{-5}$	$9.0\cdot10^{-3}$	

where T is temperature, X_m (monolayer moisture content – dry basis), C, k, k_1, k_2, n_1, n_2, M, N, H_1, H_2, h_1 and h_2 are constants of the model, R^2 is coefficient of determination, RMSE is root mean square error and χ^2 is reduced chi-square.

4 Conclusions

The hygroscopic assessment of fresh and osmodehydrated mangos showed that moisture sorption isotherms of the products were type II and type III. The microbiological stability for fresh mangos and pretreated mangos with sucrose and isomaltulose at 313.15 K was assured below 0.20, 0.15 and 0.20 g water/g dry matter, respectively. These results indicated the fresh mango and pretreated with isomaltulose requires greater care during storage. The GAB model was used with good precision to describe the sorption isotherms of the products. The thermodynamic properties showed that the enthalpy and entropy behaviors presented interaction between water and the product components, which was similar to physical properties of pure water from 0.35 g water/g dry matter. Gibbs free energy value indicated that sorption of fresh mango was a non-spontaneous process, while for pretreated samples it was spontaneous process. The enthalpy-entropy compensation theory indicated the sorption processes of all products are enthalpy-controlled.

Acknowledgements

The authors acknowledge the following Brazilian agencies for financial support: Coordination for the Improvement of Higher-Level Personnel (Code 001 and Grant 88887.468140/2019-00), National Council for Scientific and Technological Development (308567/2017-0 and 314191/2021-6) and Research Support Foundation of the State of Minas Gerais. J. R. Carmo (studentship 166378/2018-6) thanks CNPq.

References

Abrahão, F. R., & Corrêa, J. L. G. (2021). Osmotic dehydration: More than water loss and solid gain. *Crit. Rev. Food Sci. Nut.*, 29, 1–20. http://doi.org/10.1080/10408398.2021.198376

AOAC. (2010). *Association of Official Analytical* Chemists – *Official methods of analysis of Association of Official Analytical Chemists International* (18th ed.). Arlington: AOAC.

Bejar, A. K., Mihoubi, N. B., & Kechaou, N. (2012). Moisture sorption isotherms – experimental and mathematical investigations of orange (*Citrus sinensis*) peel and leaves. *Food Chem.*, 132, 1728–1735. http://doi.org/10.1016/j.foodchem.2011.06.059

Boquet, R., Chirife, J., & Iglesias, H. A. (1978). Equations for fitting water sorption isotherms of foods: Part 2 – Evaluation of various two-parameter models. *Int. J. Food Sci. Technol.*, 13, 159–174. http://doi.org/10.1111/j.1365-2621.1978.tb00792.x

Bouba, A. A., Njintang, N. Y., Nkouam, G. B., Mang, Y. D., Mehanni, A. E., Scher, J., Montet, D., & Mbofung, C. M. (2014). Desorption isotherms, net isosteric heat and the effect of temperature and water activity on the antioxidant activity of two varieties of onion (*Allium cepa* L.). *Int. J. Food Sci. Technol.*, 49, 444–452. http://doi.org/10.1111/ijfs.12321

Carmo, J. R., & Pena, R. S. (2019). Influence of the temperature and granulometry on the hygroscopic behavior of tapioca flour. *CyTA – J. Food*, 17, 900–906, http://dx.doi.org/10.1080/19476337.2019.1668860

Carmo, J. R., Corrêa, J. L. G., Polachini, T. C., & Telis-romero, J. (2022). Properties of Isomaltulose (Palatinose®) – an emerging healthy carbohydrate: effect of temperature and solute concentration. *J. Mol. Liq.*, 347, 118304. http://doi.org/10.1016/j.molliq.2021.118304

Carmo, J. R., Corrêa, J. L. G., Resende, M., Cirillo, M. A., Corona-Jiménez, E., & Telis-Romero, J. (2022). Mango enriched with sucrose and isomaltulose (Palatinose®) by osmotic dehydration: effect of temperature and solute concentration through the application of a

multilevel statistical models. *Journal of Processing and Preservation*, *In press*. https://doi.org/10.1111/jfpp.17147

Cavalcante, C. E. B., Rodrigues, S., Afonso, M. R. A., & Costa, J. M. C. (2018). Hygroscopic behaviour of spray dried soursop pulp powder. *Braz. J. Food Techol.*, 21, 1–8. http://dx.doi.org/10.1590/1981-6723.12117.

Crank, J. (1975). *The Mathematics of diffusion*. 2 ed. Oxford: Carendon press ed.

Engin, D. (2020). Effect of drying temperature on color and desorption characteristics of oyster mushroom. *Food Sci. Technol.*, 40, 187–193. http://doi.org/10.1590/fst.37118

Engin, D. (2020). Effect of drying temperature on color and desorption characteristics of oyster mushroom. *Food Sci. Technol.*, 40, 187–193. http://doi.org/10.1590/fst.37118

Falade, K. O., & Aworh, O. C. (2004). Adsorption isotherms of osmo-oven dried african star apple (*Chrysophyllum albidum*) and african mango (*Irvingia gabonensis*) slices. *Eur. Food Res. Technol.*, 218, 278–283. http://dx.doi.org/10.1007/s00217-003-0843-8

Falade, K. O., &, Awoyel O. O. (2005). Adsorption isotherms and heat of sorption of fresh and preosmosed oven-dried bananas. *J. Food, Agri. Environ.*, 3 97–102.

Fan, K., Zhang, M., & Bhandarid, B. (2019). Osmotic-ultrasound dehydration pretreatment improves moisture adsorption isotherms and water state of microwave-assisted vacuum fried purple-fleshed sweet potato slices. *Food Bioprod. Process.*, 115, 154–164. http://doi.org/10.1016/j.fbp.2019.03.011

Fernandes, F. A. N., Braga, T. R., Silva, E. O., & Rodrigues, S. (2019). Use of ultrasound for dehydration of mangoes (*Mangifera indica* L.): kinetic modeling of ultrasound-assisted osmotic dehydration and convective air-drying. *J. Food Sci. Technol.*, 56, 1793–1800. http://doi.org/10.1007/s13197-019-03622y

Galdino, P. O., Queiroz, A. J. D., Figueiredo, R. M. F., Santiago, A. M., & Galdino, P. O. (2021). Production and sensory evaluation of dried mango. *Rev. Bras. Eng. Agríc. Ambient.*, 25, 44–50. http://doi.org/10.1590/1807-1929/agriambi.v25n1p44-50

Greenspan L. (1977). Humidity Fixed Points of Binary Saturated Aqueous Solutions. *Journal of Research of the National Bureau of Standards. Section A, Physics and Chemistry*, 81, 89–96. https://doi.org/10.6028/jres.081A.011

Halsey, G. (1948). Physical adsorption on non-uniform surfaces. *J. Chem. Phys.*, 16, 931–937. http://doi.org/10.1063/1.1746689

Iglesias, H. A., & Chirife, J. (1976). Prediction of the effect of temperature on water sorption isotherms of food material. *J. Food Technol*, 11, 109–116. https://doi.org/10.1111/j.1365-2621.1976.tb00707.x22.

Iglesias, H. A., Chirife, J., & Lombardi, J. L. (1975). Water sorption isotherms in sugar beet root. *Int. J. Food Sci. Technol.*, 11, 299–308. http://doi.org/10.1111/j.1365-2621.1975.tb00033.x

Jay, M. J. (2005). *Microbiologia de alimentos* (6th ed.). Porto Alegre, Brasil: Artmed.

Kar, S., & Sutar, P. P. (2022). Shelf life prediction of dried garlic powder under accelerated storage conditions. *J. Food Sci. Technol. (Mysore)*, In press. http://doi.org/10.1007/s13197-022-05431-2

Krug, R. R., Hunter, W. G., & Grieger, R. A. (1976). Enthalpy-entropy compensation. 1. Some fundamental statistical problems associated with the analysis of van't Hoff and Arrhenius data. *J. Chem. Phys.*, 80, 2335–2341. http://doi.org/10.1021/j100562a006

Krug, R. R., Hunter, W. G., & Grieger, R. A. (1976b). Enthalpy-entropy compensation. 2. Separation of the chemical from the statistical effect. *J. Chem. Phys.*, 80, 21, 2341–2351. http://doi.org/10.1021/j100562a007

Kumar, P. S., & Sagar, V. R. (2014). Drying kinetics and physico-chemical characteristics of osmo-dehydrated mango, guava and aonla under different drying conditions. *J. Food Sci. Technol.*, 2014, 51, 1540–1546. http://doi.org/10.1007/s13197-012-0658-3

Labuza, T. P. (1984). Application of chemical kinetics to deterioration of foods. *J. Chem. Educ.*, 61, 348–358. http://dx.doi.org/10.1021/ed061p348

Lebaka, V. R., Wee, Y.-J., Ye, W., & Korivi, M. (2021). Nutritional composition and bioactive compounds in three different parts of mango fruit. *Int. J. Environ. Res. Public Health*, 18, 741. http://doi.org/10.3390/ijerph18020741

Leffler, J. E. (1955). The enthalpy-entropy relationshipg and its implications for organic chemistry. *J. Org. Chem.*, 20, 1202–1231.

Madamba, P. S., Driscoll, R. H., & Buckle, K. A. (1996). Enthalpy-entropy compensation models for sorption and browning of garlic. *J. Food Eng.*, 28, 2, 109–111. http://doi.org/10.1016/0260-8774(94)00072-7

Maldonado-Celis, M. E., Yahia, E. M., Bedoya, R., Landázuri, P., Loango, N., Aguillón, J., Restrepo, B., & Ospina J. C. G. (2019). Chemical composition of mango (*Mangifera indica* L.) fruit: nutritional and phytochemical compounds. *Front. Plant Sci.*, 10, 1073. http://doi.org/10.3389/fpls.2019.01073.

Martins, M. G., Martins, D. E. G., & Pena, R. S. (2015). Drying kinetics and hygroscopic behavior of pirarucu (*Arapaima gigas*) fillet with different salt contents. *LWT – Food Sci. Technol.*, 62, 144 –151. http://dx.doi.org/10.1016/j.lwt.2015.01.010.

Martins, M. J. N., Guimarães, B., Polachini, T. C., & J. Telis-Romero. (2020). Thermophysical properties of carbohydrate solutions: correlation between thermal and transport properties. *J. Food Process Eng.*, 43, 1–15. http://doi.org/10.1111/jfpe.13483

McLaughlin, C. P., & Magee, T. R. A. (1998). The determination of sorption isotherm and the isosteric heats of sorption for potatoes. *J. Food Eng.*, 35, 267–280. http://doi.org/10.1016/S0260-8774(98) 00025-9

McMinn, W. A. M., & Magee, T. R. A. (2003). Thermodynamic properties of moisture sorption of potato. *J. Food Eng.*, 60, 2, 157–165. https://doi.org/10.1016/S0260-8774(03)00036-0

McMinn, W. A. M., Al-Muhtaseb, A. H., & Magee, T. R. A. (2005). Enthalpy-entropy compensation in sorption phenomena of starch materials. *Food Res. Int.*, 38, 5, 505–510. http://doi.org/10.1016/j.foodres.2004.11.004

Mrad, N. D., Bonazzi, C., Courtois, F., Kechaou, N., & Mihoubi, N. B. (2013). Moisture desorption isotherms and glass transition temperatures of osmo-dehydrated apple and pear. *Food Bioprod. Process.*, 91, 121–128. http://doi.org/10.1016/j.fbp.2012.09.006

Mulet, A., Garcia-Reverter, J., Sanjuán, R., & Bon, J. (1999). Sorption isosteric heat determination by thermal analysis and sorption isotherms. *J. Food Sci.*, 64, 64–68. http://doi.org/10.1111/j.1365-2621.1999.tb09862.x

Noshad, M., Mohebbi, M., Shahidi, F., & Mortazavi, S. A. (2012). Effect of osmosis and ultrasound pretreatment on the moisture adsorption isotherms of quince. *Food Bioprod. Process.*, 90, 2, 266–274. http://doi.org/10.1016/j.fbp.2011.06.002

Oswin, C. R. (1946). The kinetics of package life. III. The isotherm. *J. Soc. Chem. Ind.*, 65, 419–421. https://doi.org/10.1002/jctb.5000651216

Paes, M. S., Alcântara Pessoa Filho, P., & Tadini, C. C. (2021). Sorption properties of cambuci (*Campomanesia phaea O. Berg*) untreated and pre-treated with sorbitol as osmotic solute. *Food Sci. Technol. – LWT*, 139, 110569. http://doi.org/10.1016/j.lwt.2020.110569

Peleg, M. (1993). Assessment of a semi-empirical four parameter general model for sigmoid moisture sorption isotherms. *J. Food Process Eng.*, 16, 21–37. http://doi.org/10.1111/j.1745-4530.1993.tb00160.x

Polachini, T. C., Betiol, L. F. L., Lopes-Filho, J. F., & Telis-Romero, J. (2016). Water adsorption isotherms and thermodynamic properties of cassava bagasse. *Thermoch. Acta*, 632, 79–85. http://doi.org/10.1016/j.tca.2016.03.032

Pombo, J. C. P., Carmo, J. R., Araújo, A. L., Medeiros, H. H. B. R., & Pena, R. S. (2019). Moisture sorption behavior of cupuassu powder. *Open Food Sci. J.*, 11, 66–73. http://doi.org/10.2174/1874256401911010066

Prothon, F., & Ahrne, L. M. (2004). Application of the Guggenheim, Anderson and De Boer model to correlate water activity and moisture content during osmotic dehydration of apples. *J. Food Eng.*, 61, 467–470. https//dx.doi.org/10.1016/S0260-8774(03)00119-5

Rizvi, S. S. (2014). Thermodynamic properties of foods in dehydration. In *Engineering properties of foods*, 261–348. CRC Press.

Rizvi, S. S. H. (1986). Thermodynamic properties of foods in dehydration. In: Rao, M. A., Rizvi, S. S., Dutta, A. K. (Eds.). *Engineering properties of foods*. Marcel Dekker, New York, pp.133-214.

Rosa, D. P., Evangelista, R. R., Machado, A. L. B., Sanches, M. A. R., & Telis-Romero, J. (2021). Water sorption properties of papaya seeds (*Carica papaya L.*) formosa variety: An assessment under storage and drying conditions. *Food Sci. Technol. – LWT*, 138, 110458. http://doi.org/10.1016/j.lwt.2020.110458

Saltmarch, M., & Labuza, T. P. (1980). Influence of relative humidity on the physico-chemical state of lactose in spray-dried sweet whey powders. *J. Food Sci.*, 45, 1231–1236.

Sangeeta, & Hathan, B.S. (2017). Sorption behavior, thermodynamic properties and storage stability of ready-to-eat Elephant Foot Yam (*Amorphophallus spp.*) product: physic-chemical properties, minerals, total dietary fiber and phenolic content of stored product. *J. Food Meas. Charac.*, 11, 401–416. http://doi.org/10.1007/s11694-016-9408-y

Sentko, A., & Willibald-Ettle, I. (2007). Isomaltulose™ (isomaltulose). Leatherhead ingredients handbook sweeteners (3rd ed.). Oxford: Blackwell Publishing.

Shyam, S., Ramadas, A., & Chang, S. K. (2018). Isomaltulose: Recent evidence for health benefits. *J. Funct. Foods*, 48, 173–178. http://doi.org/10.1016/j.jff.2018.07.002

Sridonpai, P., Komindr, S., & Kriengsinyos, W. (2016). Impact of isomaltulose and sucrose based breakfasts onpostprandial substrate oxidation and glycemic/insulinemic changes in type-2 diabetes mellitus subjects. *J. Medic. Assoc. Thai.*, 99, 282–289.

Telis, V. R. N., Gabas, A. L., Menegalli, F. C., & Telis-Romero, J. (2000). Water sorption thermodynamic properties applied to persimmon skin and pulp. *Thermoch. Acta*. 343, 49–56. http://doi.org/10.1016/S0040-6031(99)00379-2

Tsami, E., Maroulis, Z. B., Marinos-Kouris, D., & Saravacos, G. D. (1990). Heat of sorption of water in dried fruits. *Int. J. Food Sci. Technol., 25*, 350-359. https://doi.org/10.1111/j.1365-2621.1990.tb01092.x

Udomkun, P., Argyropoulos, D., Nagle, M., Mahayothee, B. & Muller, J. (2015). Sorption behaviour of papayas as affected by compositional and structural alterations from osmotic pretreatment and drying. *J. Food Process Eng.*, 157, 14–23. http://doi.org/10.1016/j.jfoodeng.2015.01.022

Udomkun, P., Argyropoulos, D., Nagle, M., Mahayothee, B., & Müller, J. (2015). Sorption behaviour of papayas as affected by compositional and structural alterations from osmotic pretreatment and drying. *J. Food Eng.*, 157, 14–23. http://doi.org/10.1016/j.jfoodeng.2015.01.022

Van den Berg, C. (1984). Description of water activity of foods for engineering purposes by means of the GAB model of sorption. In: Mckenna B. M. (Ed.), *Engineering and Food*s. Elsevier, New York, pp. 311-321.

Vegá-Galvez, A., Miranda, M., Díaz, L. P., Lopez, L., Rodriguez, K., & Scala, K. D. (2010). Effective moisture diffusivity determination and mathematical modelling of the drying curves of the olive-waste cake. *Bioresour Technol.*, 101, 7265–7270. http://doi.org/10.1016/j.biortech.2010.04.040

Viana, A. D., Corrêa, J. L. G., & Justus, A. (2014). Optimisation of the pulsed vacuum osmotic dehydration of cladodes of fodder palm. *Int. J. Food Sci. Technol.*, 49, 726–732. http://doi.org/10.1111/ijfs.12357

Wangcharoen, W. (2013). Development of dried chewy longan arils. *Maejo Int. J. Food Sci. Technol*, 7, 467–477. http://doi.org/10.14456/mijst.2013.38

Yanniotis, S., & Blahovec, J. (2009). Model analysis of sorption isotherms. *LWT – Food Sci.Technol.*, 42, 1688-1695. http://dx.doi.org/10.1016/j.lwt.2009.05.010.

Yao, L., Fan, L., & Duan, Z. (2020). Effect of different pretreatmentsfollowed by hot-air and far-infrared drying on the bioactive com-pounds, physicochemical property and microstructure of mango slices. *Food Chem.*, 305, 125477. http://doi.org/10.1016/j.foodchem.2019.125477

Zabalaga, Rosa F., La Fuente, C. I. A., Tadini, C. C. (2016). Experimental determination of thermophysical properties of unripe banana slices (*Musa cavendishii*) during convective drying. *J. Food Eng.*, 187, 62–69. http://doi.org/10.1016/j.jfoodeng.2016.04.020

Zhao, J-H., Ding, Y., Yuan, Y-J., Xiao, H-W., Zhou, C-L., Tan2, M-L., & Tang, X-M. (2018). Effect of osmotic dehydration on desorption isotherms and glass transition temperatures of mango. *Int. J. Food Sci. Technol.*, 53, 2602–2609. http://doi.org/10.1111/ijfs.13855

Zongo, A. P., Khalloufi, S., & Ratti, C. (2021). Effect of viscosity and rheological behavior on selective mass transfer during osmotic dehydration of mango slices in natural syrups. *J. Food Process Eng.*, 44, e13745. http://doi.org/10.1111/jfpe.13745

ARTICLE 6 – **Influence of ultrasound-assisted osmotic dehydration (UAOD) and hot air drying on quality and hygroscopicity of mangos incorporated with Palatinose®**

Juliana Rodrigues do CARMO [a*], Jefferson Luiz Gomes CORRÊA [a], Cristiane Nunes da SILVA [b], Cassiano OLIVEIRA [c], Adriano Lucena de ARAÚJO [d], Rosinelson da Silva PENA [d]

[a] Department of Food Science (DCA), Federal University of Lavras, 37200-900, Lavras, Brazil. E-mail: juliana_docarmo@yahoo.com.br; jefferson@ufla.br

[b] Department of Nutrition and Health (DNU), Federal University of Lavras, 37200-900, Lavras, Brazil. E-mail: kristtiane2015@gmail.com

[c] Institute of Exact and Thecnological Sicences, Federal University of Viçosa, 38810-000, Rio Paranaíba, Brazil. E-mail: croliveira1979@yahoo.com.br

[d] Graduate Program in Food Science and Technology, Federal University of Pará, 66075-110, Belém, Brazil. E-mail: rspena@ufpa.br; adriano.lucena4@gmail.com

[*]**Corresponding author:** Juliana Rodrigues do CARMO (E-mail: juliana_docarmo@yahoo.com.br)

(Elaborated in accordance to the Food and Bioproducts and Processing)

***Abstract*:** In this study, ultrasound assisted osmotic dehydration (UAOD) of mangos with Palatinose® solutions before and after the convective drying was assessed via their quality properties (water activity, color, texture, volumetric shrinkage, ascorbic acid content, total carotenoids, total phenolic compounds and antioxidant activity) and hygroscopic behavior. In order to determinate the best processing time, UAOD (28 °C, 35 °B) was performed at 25 kHz for 10, 20, 25, 30, 35 and 40 min. The samples were dried in a tunnel dryer at a temperature of 60 °C and an air velocity of 1.5 m/s. At 20 min the incorporation was maximum (approx. 5% solids gain) and did not differ of the longer times ($p > 0.05$). Ascorbic acid, carotenoids, total phenolics, as well as their antioxidant activity, were preserved on mangos subjected UAOD. After drying, the samples ultrasound pretreated had lower water activity and similar bioactive compounds content in relation to untreated dried samples ($p \leq 0.05$,) except for the ascorbic acid content. Thin-layer drying kinetics models showed excellent fits to the experimental data ($R^2 \geq 0.984$, RMSE ≤ 0.0399 and $\chi^2 \leq 1.7 \cdot 10^{-3}$) and the incorporation of isomaltulose by ultrasound resulted in a less hygroscopic product compared to the fresh one, as shown by the studies using sorption isotherms.

Keywords: *Mangifera indica*, isomaltulose, cavitation, bioactive compounds, sorption isotherms.

1 Introduction

Mango (*Mangifera indica* L.) is one of the most consumed tropical fruits and whose production increases yearly (Yao et al. 2020). It has a rich profile of vitamins (A, C, E, K, B1, B2, B3, B5, B6, B12), minerals (calcium, iron, phosphorus, potassium, magnesium, zinc, manganese), dietary fibers (cellulose, hemicellulose, lignin) and antioxidants (vitamin C, ß-carotene, dehydroascorbic acid) (Jiménez-Hernández et al., 2017). Despite this, its high water content makes it a highly perishable fruit with up to 50% wasted during post-harvest period, storage, transport, and ripening (Maldonado-Celis et al., 2019).

Processed mango enjoys a substantial worldwide trade, in particular dried mango (Akoyo, 2014; Dereje & Abera, 2020). The osmotic dehydration (OD) process, with subsequent drying, should enrich this fruit with a solute of interest, besides improving its nutritive and sensorial values (Abrahão & Corrêa, 2021). In this context, the isomaltulose, commercially known as Palatinose®, appears as an excellent alternative of osmotic solute as it is a non-cariogenic carbohydrate with a low glycemic and insulinemic indexes. This product has been recently studied to obtain healthier dry products (Lopez et al., 2020; Macedo et al., 2021).

In solid materials, alternative compressions and expansions generated by the ultrasonic waves produce an effect similar to that observed when a sponge is repeatedly compressed and released (Sakooei-Vayghan et al., 2020). This "sponge effect" produces the release of liquid from the inside of the particle to the solid surface and the entry of fluid from the outside. The forces involved in this mechanism can be greater than the surface tension that keeps the water molecules inside the capillaries of the material, creating microscopic channels and facilitating the transfers of matter (Muralidhara et al., 1985).

The use of ultrasound, when applied efficiently, becomes interesting in applications involving heat or mass transport, reducing the external and internal resistance to transport. For these reasons, ultrasound has been widely used to intensify transport phenomena in solid-liquid systems, such as

osmotic dehydration processes (Amami et al., 2017; Corrêa et al., 2017; Delgado et al., 2017; Fernandes et al., 2016; Soquetta et al., 2018).

Ultrasound assisted osmotic dehydration (UAOD) becomes the appropriate technology for enrichment of less porous fruits, such as mango, since it increases tissue structure deformation due to ultrasonic waves and pressure-generating osmotic channels (Prithani & Dasha, 2020). In a recent study, Fernandes et al. (2019) observed that, although mangos pretreated with UAOD reduced the apparent water diffusivity during convective drying, there was a reduction in the initial moisture content after the osmotic process, culminating in a shorter drying time. These authors also assessed the of treatment time on mass transfer parameters (water loss (WL), solid gain (SG) and weight reduction (WR)) in UAOD of mangos with sucrose. Additionally, the combination of an UAOD pretreatment and subsequent convective drying is a compromise solution that could combine the advantages of both processes (Sagar & Kumar, 2010), since these processes that reduces the negative effects of convective drying (Kroehnke et al., 2021).

The hygroscopicity of a dried food is linked to its physicochemical, and microbiological stability, which makes it essential to know its hygroscopic behavior from moisture adsorption and desorption isotherms (Cavalcante et al., 2018). They are essential for modeling, and optimizing drying processes, predicting shelf-life stability and moisture changes that may occur during storage and selecting the appropriate packaging material (Carmo & Pena, 2019)

Studies about UAOD with use of Palatinose® in mangos were not found on literature. As a more effective contribution for the study of the UAOD of mangos, the present research aimed to study the effect of treatment time on mass transfer in mango slices in order to verify the time for maximum incorporation of Palatinose®. Additionally, an osmodehydrated and dried product was obtained, their quality was evaluated – in particular, color, ascorbic acid, carotenoids, total phenolics and antioxidant activity – and a hygroscopic study was carried out.

2 Material and methods

2.1 Raw material

Mango fruit cv. *Tommy Atkins* in degree of maturation half-ripe were acquired in the local market of Lavras (Minas Gerais, State, Brazil) (21° 14'43 S and 44° 59'59 W). The characteristics of the fruits were reddish-green skin peel color; 84.53% (± 1.83) moisture; 12.33 °B (± 0.60) total soluble solids; 2.86% citric acid (± 0.21) titratable total acidity; 4.72 (± 0.16) ratio; 3.60 (± 0.04) pH and 31.13 N (±3.27) firmness. The fruits were washed with disinfectant solution (chlorinated water at 200 ppm) for 5 min, and then the seed and peel were removed. Slices of the fruit fresh were obtained with the aid of a stainless steel mold in following dimensions: 4.00 ± 0.01 cm in length, 2.00 ± 0.01 cm in width, and 0.40 ± 0.01 cm in thickness.

2.2 Osmotic solution characterization

The 35% (w/w) osmotic solution was prepared with distilled water and Palatinose® (Beneo, Mannheim, Germany). This solute concentration was determined in preliminary tests. The solution had the following parameters: water activity (a_w) of 0.972 (± 0.001); solubility of 0.3255 kg of isomaltulose/kg of solution; density of 1126.1 kg/m^3; specific heat of 3.426 kJ/kg·K; thermal conductivity of 0.485 W/m·K and viscosity of 3.154 mPa·s at the working temperature (28 °C) (Carmo et al., 2022).

2.3 Ultrasound assisted osmotic dehydration (UAOD)

For the UAOD tests, the mango slices were immersed in the aqueous solution of Palatinose® osmotic solution at a ratio of 1:10 (w/v) to avoid dilution of the solution and at 28±1 °C and submitted to ultrasonic waves for 10, 20, 25, 30, 35 and 40 min in an ultrasonic bath (Unique, USC-2850, Indaiatuba, Brazil, volume = 0.0095 m^3, frequency = 25 kHz, effective ultrasonic power density = 23.2 kW/m^3) (Fernandes et al., 2019).

After the UAOD treatments, the mass transfer parameters (WL, SG, WR) were determined in the samples. The WL, SG and WR of each sample subjected to the different UAOD conditions were evaluated according to Eq. 1, Eq. 2 and Eq. 3 (Viana et al., 2014), respectively. The moisture content of the fresh and osmotically treated samples was determined according to the AOAC (2010). The tests were carried out in quintuplicate.

$$WL(\%) = \frac{x_0 m_0 - x_t m_t}{m_0} \times 100 \quad (1)$$

$$SG(\%) = \frac{m_t S_t - m_0 S_0}{m_0} \times 100 \quad (2)$$

$$WR(\%) = \frac{m_0 - m_t}{m_0} \times 100 \quad (3)$$

where: WL is the water loss (%), SG is the solid gain (%) and WR is weight reduction (%), x is the moisture content on a wet basis (wb) (kg of water/kg of fruit), m is the sample weight (kg) and S is solid content (wb) (kg solid/kg fruit). The subindices "0" and "t" refer to fresh samples and samples after osmotic treatment, respectively.

2.4 Properties of fresh and osmodehydrated mangos

Fresh and treated samples were characterized for water activity, texture, color, ascorbic acid content, total carotenoids, total phenolic compounds and antioxidant activity. Besides, the treated samples were characterized by volumetric shrinkage.

2.4.1 Water activity (a_w)

The a_w of the samples was determined at 25 °C with a digital thermohygrometer (AquaLab 3TE, Decagon, USA).

2.4.2 Texture

The texture of the fresh mango and treated samples impregnated was measured as firmness (N) of the product surface using a texturometer (TA-X2T; Stable Micro Systems, Surrey, England) at room temperature according to the methodology of Medeiros et al. (2019), with minor modifications. The penetration tests were conducted with a cylindrical probe (TA10) of 20 mm in diameter. The parameters used were the following: pretest and posttest speeds of 1 and 1.5 mm/s, respectively. The penetration distance was set to 2 mm, the trigger force was 5 g, and deformation rate of 50%. All tests were carried out in quintuplicate for each sample.

2.4.3 Volumetric shrinkage

It was determined by measuring the area and thickness of the samples. The free software Image J®1.45 s was used to measure the area by image analysis. It provides the sample area by converting the pixels in the image into real dimensions, from a known scale (Nahimana et al., 2011). For each sample, the thickness was observed at five different points with the aid of a digital caliper (Western, DC-6 model, China). The dimensionless volume (β) was determined according to Eq. 4. (Junqueira et al., 2017).

$$\beta = \frac{V_f}{V_0} \quad (4)$$

where: V_f is the apparent volume after osmotic dehydration and drying processing (m^3), and V_0 is the initial volume (m^3).

2.4.4 Color evaluation

The color was evaluated by tristimulus colorimetry in a digital colorimeter (Konica-Minolta, CR 400, Tokyo, Japan). The operating conditions of the equipment were diffuse light/viewing angle of

0° (specular component included), and a D65 light source. The lightness (L^* = 0 black and L^* = 100 white) and the chromaticity coordinates ($-a^*$ = green and $+a^*$ = red, $-b^*$ = blue and $+b^*$ = yellow) were used to define the chroma value (C^*) (Eq. 5), and the hue angle (h°) (Eq. 6) (Carmo et al., 2019). Eq. 7 was used to calculate the total color difference (ΔE) of the treated samples relative to the fresh fruit.

$$C^* = \sqrt{\left(a^*\right)^2 + \left(b^*\right)^2} \tag{5}$$

$$h° = \cos^{-1} \frac{a^*}{\sqrt{\left(a^*\right)^2 + \left(b^*\right)^2}} \tag{6}$$

$$\Delta E = \sqrt{\left(L_0^* - L_t^*\right)^2 + \left(a_0^* - a_t^*\right)^2 + \left(b_0^* - b_t^*\right)^2} \tag{7}$$

where: the subindices “0” and “t” refer to fresh samples and treated samples, respectively.

2.4.5 Ascorbic acid

The ascorbic acid analysis was performed according to Barcia et al. (2010). For extract preparation, 10 g (±0.0001) sample were added to 30 mL of aqueous metaphosphoric acid solution (4.5%). The solution was left to stand for 1 h in amber glass and then it was transferred to a 50 mL flask and made up to volume with ultrapure water. Afterwards, the sample was filtered through filter paper, and the supernatant was centrifuged at 4163 × g for 10 min. (Sigma 3K30). For quantification, high-performance liquid chromatography (HPLC, Shimadzu, LC-20AT) equipped with a UV detector (Shimadzu, SPD-20A) was used. A Phenomenex 5 μm C18 column (250 × 4.6 mm) was used for separation at 30 °C. An aqueous solution of acetic acid 0.15% (v/v) with a flow rate of 1.0 mL/min was used as the mobile phase. Detection was performed at 254 nm.

The identification of the ascorbic acid peak was performed according to retention time compared to standard solutions. The analytical curve was obtained from the standard chromatograms that

measure the ascorbic acid peak areas under the same separation conditions applied to the samples. Standard ascorbic acid concentrations ranged from 1 to 100 mg/L and the results were expressed as µg/g of sample (dry basis). All the analyses were carried out in quintuplicate.

2.4.6 Total carotenoids content

Carotenoids from 1 g of sample were extracted with acetone by maceration with Celite® followed by vacuum-filtration. The extraction was repeated until the extract became colorless. All the filtered extracts were combined and directed to liquid-liquid partition in a separation funnel with petroleum ether/diethyl ether (1:1, v/v) and washed with distilled water. After partition, the carotenoid extract was evaporated under vacuum (T < 38 °C) and resuspended in petroleum ether for spectrophotometric quantification at 450 nm (Matos et al., 2019). The total carotenoids content of the samples were calculated by using the specific extinction coefficient of β-carotene in petroleum ether ($E_{1cm}^{1\%} = 2592$) (Rodriguez-Amaya & Kimura, 2004) and expressed as µg/g of sample (dry basis). All the analyses were carried out in triplicate.

2.4.7 Total phenolic compounds and antioxidant activity

The extracts for phenolic compound and analysis of antioxidant activity were prepared according to the method described by Larrauri et al. (1997)**,** with minor modifications. Firstly, the extracts were prepared by dissolving 5 g of sample in 20 mL of methanol 50%. The solution was homogenized for 60 min. Then, the samples were filtered in filter paper and the obtained residue was homogenized for 60 min with acetone 70%. The supernatant from two steps of extraction was mixed and made up to 50 mL with deionized water.

Phenolic compounds were estimated following the method of Folin-Ciocalteu, as described by Waterhouse (2002), the absorbance was read at a wavelength of 750 nm, and results were expressed as mg of gallic acid equivalent per 100 g dry basis – db (mg GAEs/100 g db).

The antioxidant activity of fresh and treated samples was determined by the 2,2-diphenyl-1-picrylhydrazyl radical-scavenging activity (DPPH), 2,2'-azino-bis(3-ethylbenzothiazoline-6-sulfonic acid (ABTS) and β-carotene/linoleic acid methods. DPPH free radical scavenging ability was carried out according to Brand-Williams et al. (1995)**.** The absorbance readings in a spectrophotometer at 515 nm, and the results were expressed in g db/g DPPH. The ABTS method, followed the procedure developed by Re et al. (1999)**,** where the absorbance was read at a wavelength of 734 nm and the results were expressed as micromoles of Trolox-equivalent per gram db (µmol of TEs/g db).

The β-carotene method was performed as previously described by Marco (Marco, 1968) and modified by Miller (Miller, 1971), with minor modifications. Absorbance measurements were performed at 2 min and 120 min at 470 nm. Results were expressed as % inhibition of β-carotene oxidation. All readings of antioxidant activity analyzes (DPPH, ABTS and β-carotene) were performed in the spectrophotometer (SP-22, VIS 325-1000 nm, Biospectro, Taboão da Serra, SP, Brazil).

2.5 Drying experiment

Fresh and treated samples were inserted into a tunnel dryer (Eco Engenharia Educacional, MD018 model, Brazil) with forced air circulation (1.5 m/s) and subjected to drying at 60 °C until the samples reached moisture 11.0 ± 1.0 % (db) A digital scale (Marte Científica, AD33000 model, São Paulo, Brazil), ± 0.01 g precision, coupled to the dryer sample holder mass was used to measure the mass of the samples during the experiments. The drying tests were carried out in three repetitions.

2.5.1 Drying kinetic modelling

The models present in Table 1, classically used to describe the kinetics of thin-layer drying processes (Martins et al., 2017), were fitted by nonlinear regression to the experimental drying data. Goodness of fit was assessed using coefficient of determination (R^2), root mean square error (RMSE) (Eq. 8), and reduced Chi squared (χ^2) (Eq. 9).

Table 1. Mathematical models used to adjust the drying kinetics of osmotically dehydrated mango.

Model	**Equation**
Diffusion Approximation	$MR = a \cdot e^{-k.t} + (1-a) \cdot e^{-k.b.t}$
Logarithmic	$MR = a \cdot e^{-k.t} + c$
Page	$MR = e^{-k.t^n}$
Modified Page	$MR = e^{-(k.t)^n}$
Henderson and Pabis	$MR = a \cdot e^{-k.t}$
Newton	$MR = e^{-k.t}$
Wang and Singh	$MR = 1 + a \cdot t + b \cdot t^2$

MR is moisture ratio (dimensionless), t is process time (s), and a, b, c, k, and n are constant of the models.

$$RMSE = \left[\frac{1}{N} \Sigma_{i=1}^{N} (V_{exp,i} - V_{pre,i})^2 \right]^{1/2} \quad (8)$$

$$\chi^2 = \frac{\Sigma_{i=1}^{N} (V_{exp,i} - V_{pre,i})^2}{N - n} \quad (9)$$

where: $V_{exp,i}$ and $V_{pre,i}$ are the MR determined from the experimental data and predicted by the fitted models, respectively, N is number of experimental measurements and n is number of parameters in the model.

2.5.2 Prediction of effective diffusivity

For drying curves modelling, it was assumed that the main mechanism during the downward rate period was moisture diffusion. When moisture diffusion controls the drying rate during a downward rate period, the diffusion equation, represented by Fick's second law of diffusion at non-steady state, can be used with Cartesian coordinates and in the dimensionless form (Eq. 10).

$$\frac{\partial m(t)}{\partial t} = \frac{\partial}{\partial z}\left(D_{eff} \frac{\partial m(t)}{\partial z} \right) \qquad (10)$$

where: $\partial m(t)$ is the amount of water at the time, D_{eff} is the effective diffusivity and z is a generic directional coordinate. The solid sample is considered a 2 L-thick plate; initial conditions include uniform moisture, $m_{(z,0)} = m_0$; boundary conditions include concentration symmetry, $\left.\frac{\partial m(t)}{\partial t}\right|_{z=0}$ and the equilibrium content on the surface of the material, $m_{(L,t)} = m_{eq}$.

Taking into account the initial and boundary conditions, Fick's unidirectional diffusion equation (Crank, 1975) becomes (Eq. 11):

$$MR = \frac{8}{\pi^2} \sum_{i=1}^{\infty} \frac{1}{(2i+1)^2} \exp\left(-(2i+1)^2 \pi^2 D_{eff} \frac{t}{4L^2} \right) = \frac{m(t) - m_{eq}}{m_0 - m_{eq}} \qquad (11)$$

where: i is the number of terms in the series, D_{eff} is the effective diffusivity, L is the characteristic length (half the thickness of the sample), t is the time and MR is the quotient of the difference between moisture at a time t (m(t)) and moisture at equilibrium (m_{eq}) and the difference between

initial moisture (m_0) and moisture at equilibrium (m_{eq}). The m_{eq} is the point until the sample's mass variation was below 1% (equilibrium condition).

2.5.3 Hygroscopicity study

Dried samples also were characterized according to "section 2.4". Additionally, the hygroscopicity study was carried out. For the hygroscopicity, moisture adsorption and desorption isotherms were built at 25°C (Carmo & Pena, 2019). The isotherms were obtained in a vapor sorption analyzer (Aqualab VSA, Decagon, Puma, WA, USA) using the DVS (dynamic vapor sorption) method, which consists of monitoring the moisture and a_w values of a sample exposed to environments with different relative humidity (RH) levels. Approximately 1 g sample was weighed in a stainless-steel capsule in the microanalytical balance of the VSA. To obtain equilibrium data, the sample was submitted to different levels of RH induced by changes in the injection of dry and saturated vapor. The data were obtained for an a_w range between 0.1 and 0.9, and the condition of equilibrium was programmed for a change in mass per change in time (trigger % dm/dt value) below 0.1 for three consecutive measures.

The moisture of the monolayer (M_0) for the adsorption and desorption processes was determined from the linear and angular coefficients of the straight obtained through the linear regression of the $a_w/(1 - a_w)M$ versus a_w correlation, using the linearized form of the BET (Eq. 12) (Brunauer et al., 1938). This model has been chosed, as according to findings of Timmermann (2003), GAB model overstime the monolayer values.

$$\frac{a_w}{(1-a_w)M} = \frac{1}{M_0 C} + \frac{(C-1)}{M_0 C} a_w \qquad (12)$$

where: M is equilibrium moisture content (g H_2O/100 g db), a_w is water activity (dimensionless), M_0 is monolayer moisture content (g H_2O/100 g db) and C is constant related to the heat of sorption of the first layer on primary sites.

The GAB mathematical model (Maroulis et al., 1988) (Eq. 13) was adjusted to the experimental moisture sorption data of dried mango, since GAB model has been reported to give a good fit for sorption isotherms of several materials (Fan et al., 2019). Goodness of fit was assessed using R^2, RMSE (Eq. 8), and mean relative deviation (P) (Eq. 14).

$$M = \frac{M_0 C K a_w}{(1 - K a_w)(1 - K a_w + C K a_w)} \tag{13}$$

$$P = \frac{100}{N} \sum_{i=1}^{N} \frac{\left| V_{exp,i} - V_{pre,i} \right|}{V_{exp,i}} \tag{14}$$

where: M is equilibrium moisture content (g H_2O/100 g db), M_0 is monolayer moisture content (g H_2O/100 g db), a_w is water activity (dimensionless), K and C are model's parameters, $V_{exp,i}$ and $V_{pre,i}$ are the equilibrium moisture contents determined from the experimental data and predicted by the fitted models, respectively and N is number of experimental measurements.

2.6 Statistical Analysis

One-way analysis of variance (ANOVA) was performed by Statistica v.10.0 (StatSoft, Inc., Tulsa, USA) in order to find out whether the differences in the averages were significant. The differences were reported trough of the Tukey's test at 95% confidence interval. To evaluate the results of time of drying and apparent diffusivity, a Student's t-test was used at 95% confidence interval. The drying and sorption models were fitted by non-linear regression using the same software and the Levenberg-Marquardt algorithm with a convergence criterion of 10^{-6}.

3 Results and discussion

Fig. 1 showed the kinetics of WL, SG and WR of mangos slices from 10 to 40 min. The samples presented from 9.23 to 15.75% WL, from 3.18 to 5.02% SG and from 4.36 to 11.67% WR. The highest WL values were at 20 and 25 min, SG at 20 to 40 min and WR up to 25 min, and under

these conditions there was no statistically significant difference ($p > 0.05$) for each variable studied. Thus, it is recommended to use a time of 20 min for the enrichment of mangos with Palatinose®, since the incorporation (SG) already begins to not be evident with the increase of the UAOD time. In addition, for this time, a decrease in the WL and WR of the mango slices was observed, this may be related to changes in the cell wall of the fruit at high times in the ultrasound (Prithani & Dasha, 2020).

Therefore, in this study the osmotic process was performed up to 20 min. (UAOD) and then submitted to convective drying (UAOD + D). To assess the impact of osmotic dehydration and drying, the fresh fruit was also analyzed and subjected to drying (fresh + D).

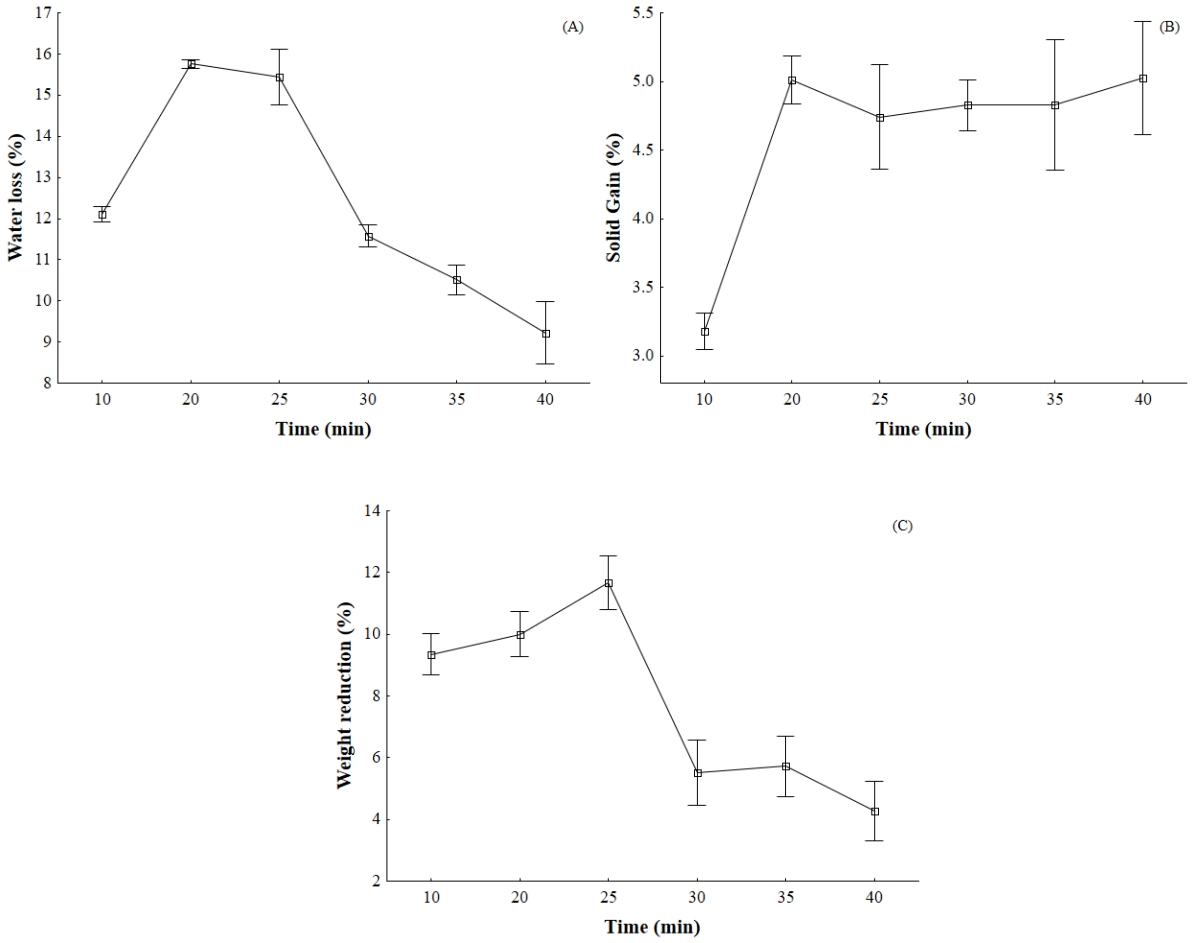

Fig. 1. Kinetics of water loss (A), solid gain (B) and weight reduction (C) of mangos slices subjected to ultrasound assisted osmotic dehydration from 10 to 40 min.

3.1 Influence of UAOD treatment and drying on a_w, texture and shrinkage of mangos

Fig. 2A shows that although the osmotic treatment with ultrasound did not decrease the a_w of the sample (a_w = 0.973 ± 0.004), after drying there was a significantly different reduction in fresh fruit (a_w = 0.990 ± 0.003) in relation to untreated dried (a_w = 0.561 ± 0.030) and pretreated (a_w = 0.491

± 0.023) fruits ($p \leq 0.05$). The UAOD + D had lower a_w probably because during sonication, cavitation bubbles may form in the water, which may collapse, causing cell damage. This may promote leaching and ultimately diffusion of water and dry matter from the tissue into the environment (Wiktor et al., 2018). Moreover, in both dried mangos slices, a_w was below 0.6, which can guarantee the microbiological stability of the tested samples (Jay, 2005).

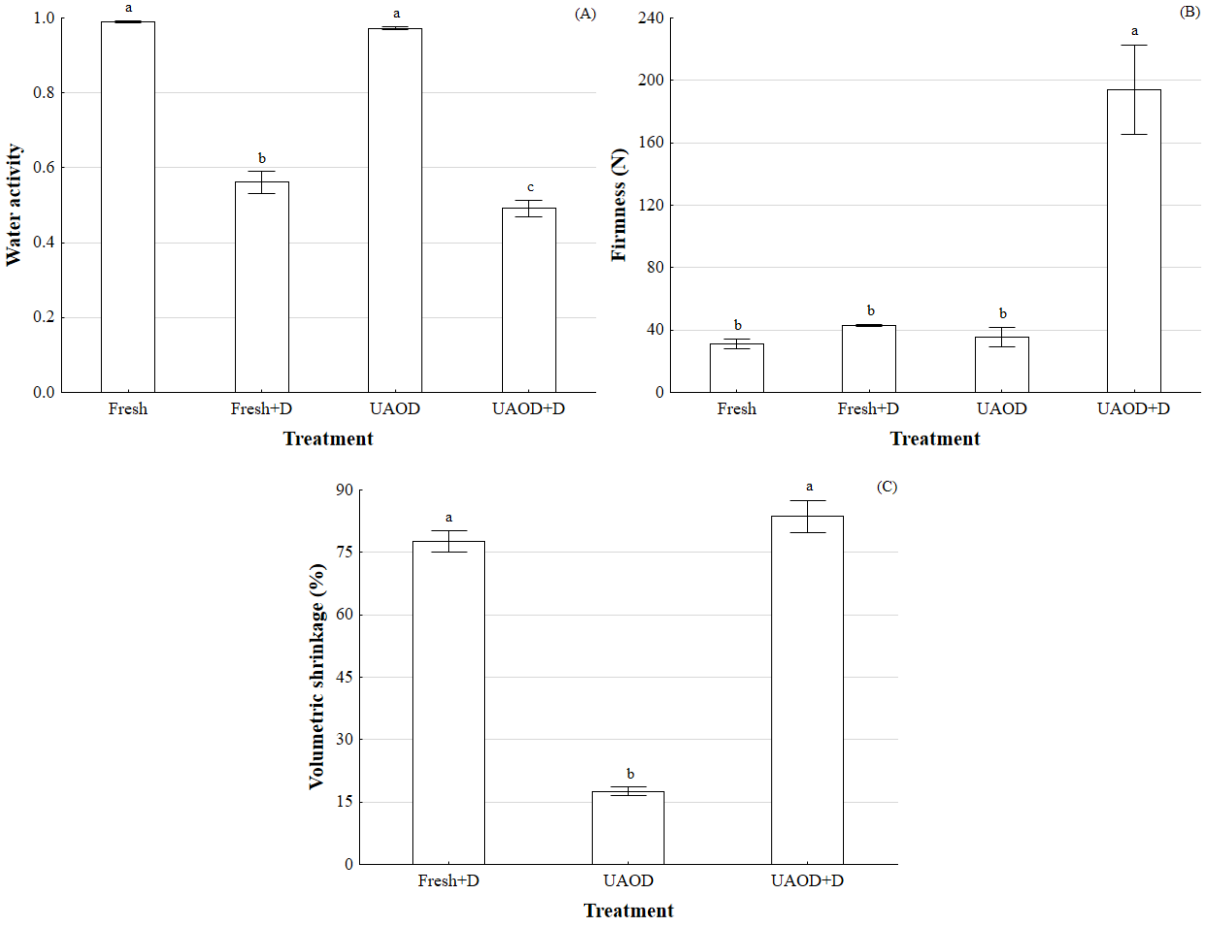

Fig. 2. Water activity (A), firmness (B) and volumetric shrinkage (C) of mangos subjected to the different treatment conditions; groups with different letters differ significantly ($p \leq 0.05$).

The results of firmness of samples are showed in Fg. 2B. The UAOD + D sample presented higher firmness (167.95 ± 10.91 N) than fresh, fresh + D and UAOD samples (31.13 ± 3.27, 43.65 ± 1.00 and 35.62 ± 6.16 N) ($p \leq 0.05$). This might be related to the osmotic solutes that were absorbed by the mangos slices, which formed a dense solid layer on the surface of this fruit and thus increased the firmness of them (Medeiros et al., 2019). According to Moreno et al. (2013), when the vegetable tissue is subjected processing to moisture removal, textural changes occurs due to the degradation of the middle lamella, which causes loss of turgor and movement of ions from the cell wall to the media. These changes create internal stress, leading to cellular disruption and plasmolysis, such as volumetric shrinkage presented in Fig. 2C.

All treatments exhibited volume reduction (Fig. 2C) and was not differed statistically ($p > 0.05$) for dried samples (shrinkage > 77%). The UAOD treatment represented approximately 17.5% shrinkage compared to the fresh sample and this may be due to water loss (9.94%) during the osmotic dehydration and structural changes as mentioned previously.

3.2 Influence of UAOD treatment and drying on the color of mangos

L^*, $a^*$and b^* values and color properties such as chroma and hue angle are used extensively for the illustration of optical attributes of fruits and vegetables (Sakooei-Vayghan et al., 2020). According to Fig. 3A isomaltulose impregnation by UAOD seemed to maintain lightness ($L^* = 77.07 \pm 1.59$), slight trend to green ($a^* = -4.72 \pm 0.50$) and yellowness ($b^* = 45.15 \pm 6.16$) resulting in a final product close to that of the fresh fruit ($L^* = 78.88 \pm 1.77$, $a^* = -3.42 \pm 1.43$ and $b^* = 49.75 \pm 4.64$) ($p > 0.05$). However, the dried products were statistically different of the fresh and osmodehydrated samples ($p \leq 0.05$). Generally, as is well known, the color parameters L^* and a^* are well correlated to color changes in fruit tissues (darkening) due to enzymatic and non-enzymatic browning reactions (Fratianni et al., 2013). As browning increases, L^*values decreases. The increase in

yellowness was clear and seemed to be a result of solids uptake during osmosis pre-treatment (Fig 3C).

Based on the chroma value (Fig. 3D), the fresh + D (C^*= 59.41 ± 4.18) and UAOD + D (C^*= 59.77 ± 5.14) samples presented more vivid color than fresh sample (C^* = 50.01 ± 4.61) ($p \leq 0.05$). The h° value close to 90° confirm the prevalence of the yellow color in the all samples – typical of mangos fruits. For both untreated and pretreated dried samples this value was lower (h° = 91.84 ± 1.88 and 93.12 ± 1.55) than fresh (h° = 93.89 ± 1.28) and UAOD (h° = 96.10 ± 1.37) samples ($p \leq 0.05$) (Fig. 3E). These last ones had a lighter yellowish color, corroborating the trend presented by the chroma values (Carmo et al., 2019)

The UAOD in isomaltulose solutions presented lower influence the color changes in terms of ΔE in comparison to UAOD + D and fresh + D samples (Fig. 3F). This can be explained by the effect of sugar on reducing enzymatic browning by preventing oxygen entry (Feng et al., 2019). Futher, the dried samples are more susceptible to oxidation of ascorbic acid and loss of pigments, as carotenoids due to drying temperature (Fratianni et al., 2013).

3.3 Influence of UAOD treatment and drying on the ascorbic acid and carotenoids content of mangos

Fig. 4A showed that ascorbic content of the fresh samples (385.8 ± 116.1 µg/g) no differed statistically of fresh + D (404.6 ± 91.8 µg/g) and UAOD (225.5 ± 21.2 µg/g) samples ($p > 0.05$). However, the UAOD + D exhibited a significant decrease of in of ascorbic acid (21.8 ± 16.2 µg/g) ($p \leq 0.05$). This reduction was of 94% in relation to fresh sample. This effect could be ascribed to formation of free radicals by ultrasound waves which initiate numerous reaction that influence the ascorbic content (Nowacka et al., 2018). Additionally, the drying temperature (60 °C), may reduce this component (Devic et al., 2010).

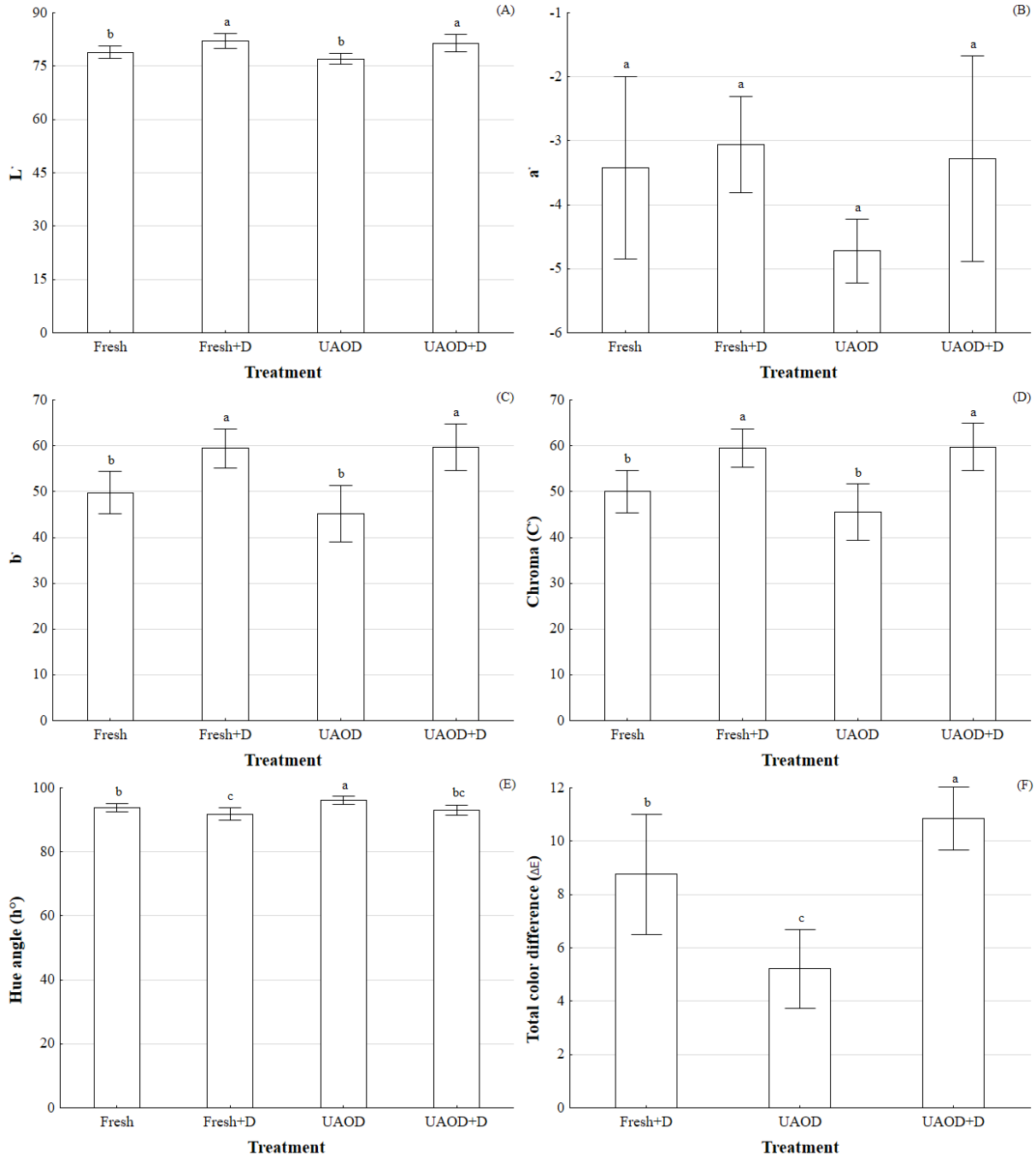
(A)
L`
90
75
60
45
30
15
0
b
a
b
a
Fresh
Fresh+D
UAOD
UAOD+D
Treatment
(B)
a`
-1
-2
-3
-4
-5
-6
a
a
a
a
Fresh
Fresh+D
UAOD
UAOD+D
Treatment
(C)
b`
70
60
50
40
30
20
10
0
b
a
b
a
Fresh
Fresh+D
UAOD
UAOD+D
Treatment
(D)
Chroma (C`)
70
60
50
40
30
20
10
0
b
a
b
a
Fresh
Fresh+D
UAOD
UAOD+D
Treatment
(E)
Hue angle (h°)
100
80
60
40
20
0
b
c
a
bc
Fresh
Fresh+D
UAOD
UAOD+D
Treatment
(F)
Total color difference (ΔE)
12
10
8
6
4
2
0
b
c
a
Fresh+D
UAOD
UAOD+D
Treatment

Fig. 3. L^* (A), a^* (B), b^* (C), C^*(D), h° (E) and ΔE (F) of mangos subjected to the different treatment conditions; groups with different letters differ significantly ($p \leq 0.05$).

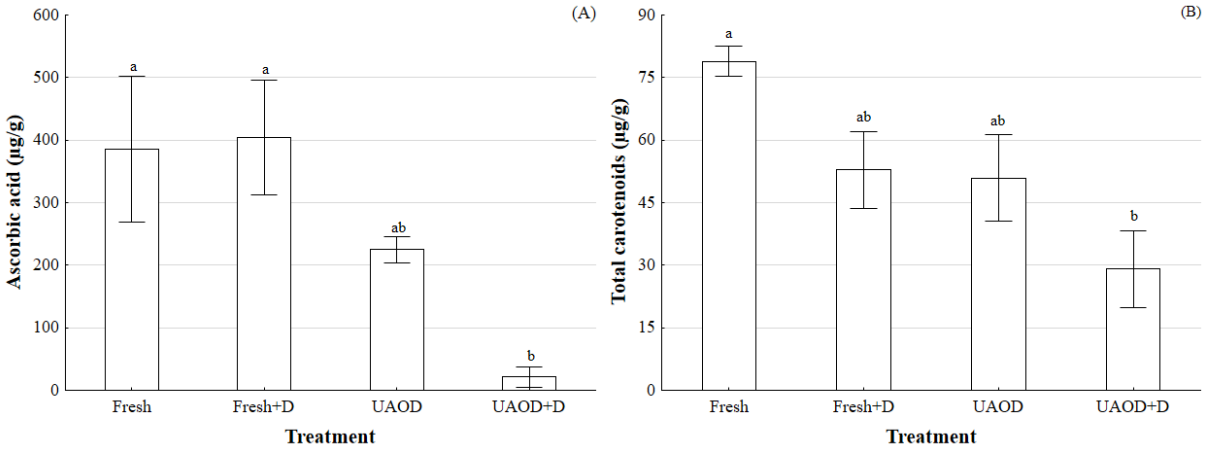

Fig. 4. Ascorbic acid (A) and total carotenoids content (B) in mangos subjected to the different treatment conditions; groups with different letters differ significantly ($p \leq 0.05$).

A significant decrease in carotenoids content of UAOD + D (29.05 ± 9.28 µg/g) also was observed ($p \leq 0.05$) in relation to fresh sample (78.94 ± 3.67 µg/g) (reduction of 39%) (Fig. 4B). This reduction can be linked to the effect of ultrasound energy to increase activity of heat stable lipoxygenase. This enzyme is detrimental because it could destroy carotenoids during drying through formation of reactive radicals (Cui et al., 2004). Oladejo et al. (2017) also noted a higher decrease in the content of carotenoids in sweet potato subjected to UAOD compared to samples dehydrated without the assistance of ultrasound. Azoubel et al. (2015) observed a similar effect in osmotically dehydrated dried papaya.

Although changes in tissue structure or the leakage of these compounds occurs to the osmotic solution, in our study, no significant decrease was observed when the samples were submitted to pretreatment with ultrasound (50.95 ± 10.30 µg/g) ($p > 0.05$).

3.4 *Influence of UAOD treatment and drying on total phenolic compounds and antioxidant activity of mango*s

The phenolics are the secondary metabolites and have played a significant role in the food nutrition. It is a nonessential compounds i.e. present in the dietary food (Rahaman et al., 2019). Total phenolics content of fresh mango was 240.14 (± 73.09) mg GAEs/100 g, and not was significantly different of UAOD (246.99 ± 33.54 mg GAEs/100 g) and UAOD + D samples ($p > 0.05$). Reduction in total phenolics content was significantly higher in fresh dried sample ($p \leq 0.05$) (Fig. 5A). The total phenolics contents of the untreated and pretreated samples after drying by hot air were 138.81 (± 14.04) and 169.44 (± 23.10) mg GAEs/100 g indicating a 42% and 29% reduction in total phenolics content, respectively. This fact can be attributed to leakage to the osmotic solution, or it can be attributed to the phenomenon of acoustic cavitation induced by ultrasound and degradation during treatment at 60 °C, or both. The scientific literature presents studies that reported that ultrasound assisted osmotic dehydration can either cause nutrient loss (Kek et al., 2013; Mothibe et al., 2014) or increase these compounds (Amami et al., 2017).

Figs. 5B, 5C and 5D shows antioxidant activity of untreated and pretreated mango samples. The fresh fruit had 22,232.45 (± 3,105.11) g/g DPPH, 29.68 (± 6.50) µmol of TEs/g and 55.89 (±12.97) % inhibition of β-carotene oxidation. The UAOD sample presented 14,752.73 (± 2399.72) g/g DPPH, 28.86 (± 8.03) µmol of TEs/g and 55.51 (± 4.51) % inhibition of β-carotene oxidation. On other hand, the fresh + D and UAOD + D had 3,451.10 (± 112.34) g/g DPPH, 9.13 (± 2.13) µmol of TEs/g and 27.48 (± 7.70) % inhibition of β-carotene oxidation, and 3,462.80 (± 252.64) g/g DPPH, 10.00 (± 1.56) µmol of TEs/g and 5.17 (± 1.17) % inhibition of β-carotene oxidation, respectively.

Antioxidant activity of fresh mangos fruit comes from the presence of ascorbic acid, carotenoids and total phenolic compounds. So, the analyzes of DPPH, ABTS and β-carotene/linoleic acid method showed the same tendency of these compounds: decreased for the dried products ($p \leq 0.05$)

and did not differ for the samples pretreated with ultrasound ($p > 0.05$) in relation to fresh sample. Amami et al. (2017) affirm that these findings suggested that the retention of bioactive compounds depends upon osmotic solution and treatment time. Overall, in the UAOD pretreatment of mangos at 20 min on isomaltulose solution, ascorbic acid, carotenoids, total phenolics, as well as their antioxidant activity, were preserved.

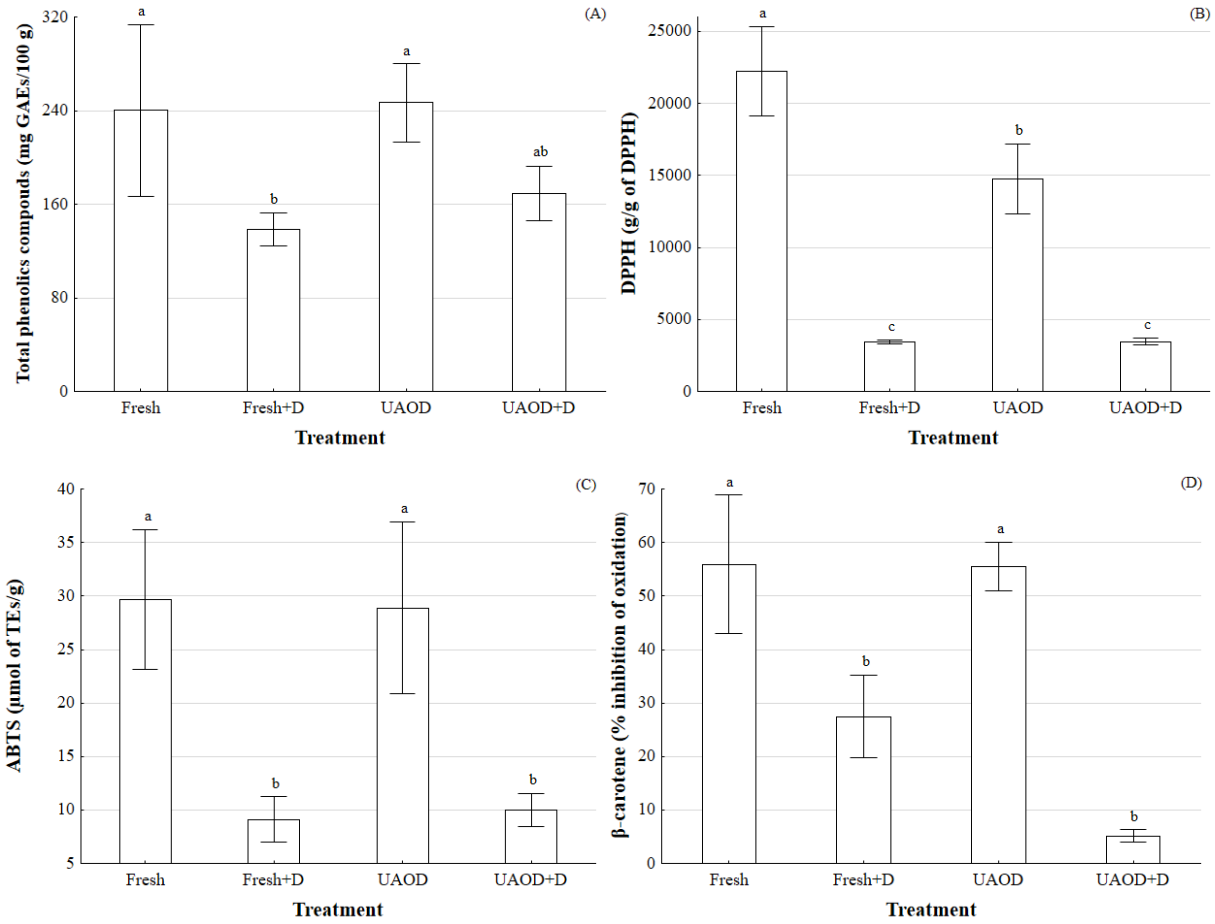

Fig. 5. Total phenolics compounds (A), DPPH (B), ABTS (C) and β-carotene (D) in mangos subjected to the different treatment conditions; groups with different letters differ significantly ($p \leq 0.05$).

3.5 Drying experiment and hygroscopicity study

Table 2 showed that all models were able to accurately predict the drying kinetic of product studied, since had $R^2 \geq 0.984$ and low RMSE (≤ 0.0399) and χ^2 ($\leq 1.7 \cdot 10^{-3}$) values. Thus, the curves were built by the Page model, which is relatively simple and has been successfully used for thin-layer drying kinetics of several fruits and vegetables (Onwude et al., 2016) (Fig. 6).

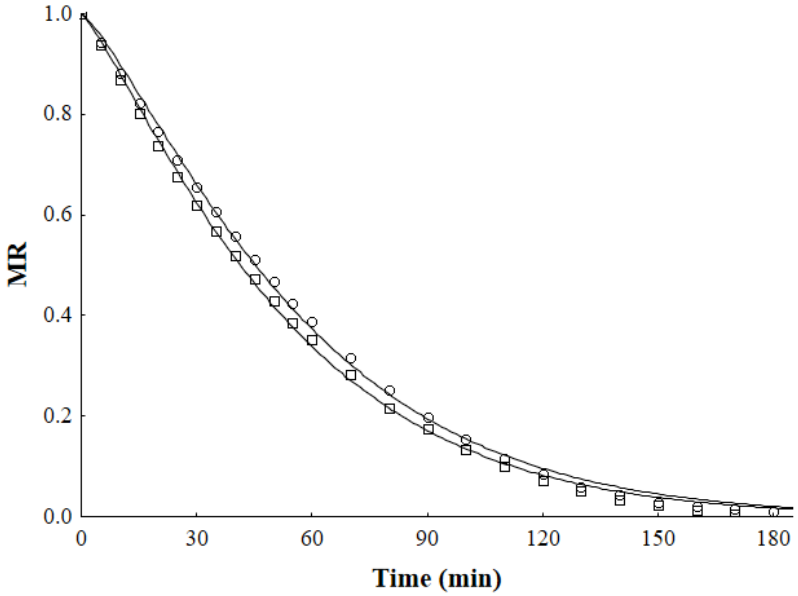

Fig. 6. Experimental values of evolution of the moisture ratio (MR) of fresh + D (○) and UAOD + D (□) samples over time at 60 °C. Predicted values using the Page model (line).

The processing time required to eliminate 87% of the initial moisture content of the mangos without pretreatment was 170 ± 10 min and 167 ± 6 min, for the samples pretreated in isomaltulose solution.

These time results not statistically differed ($p > 0.05$). However, with pretreatment by ultrasound (20 min), the total processing time was 187 min. The UAOD reduced the initial moisture content in the mango samples (78.15 ± 2.32 %) and the apparent water diffusivity of without and with pretreatment were $3.90 \cdot 10^{-10}$ m^2/s and $3.58 \cdot 10^{-10}$ m^2/s, respectively, and not statistically differed ($p > 0.05$). According to Fernandes et al. (2019), the kind of tissue structure of mangos differ from the other fruits and is less susceptible to the effects induced by ultrasound application. The similar water diffusivity values for treated sample might have been caused by saturation of soluble solids on the boundary between the fruit and the osmotic solution creating an even denser structure that raised the mass transfer resistance and reduced the mobility of water during air-drying.

Although, the UAOD is not advantageous from the point of view of economy of industrial process, due to a longer processing time in relation to the product without pre-treatment, this product obtained presented an incorporation of 4.58% (± 0.55) of isomaltulose in only 20 min of ultrasound use. Thus, this technology proves to be interesting for the incorporation of a carbohydrate with nutritional advantages in relation to common sugar. It is worth mentioning that the mango is a fruit much less porous (porosity = 0.04 to 0.05) than most fruits (pineapple porosity = 0.16 to 0.25; apple porosity = 0.18 to 0.22; strawberry porosity = 0.47) (Singh et al. 2015) and thus, even more promising results can be obtained for other fruits. Furthermore, the incorporation of isomaltulose resulted in a less hygroscopic product compared to the fresh one, as can be seen through the sorption isotherms (Fig 7).

The UAOD + D sample had lower moisture content than the fresh + D for a constant a_w at 25 °C, with the maximum moisture content ($a_w = 0.9$) de 51.59 g/100 g H_2O db (Fig. 7B) and 62.97 g/100 g H_2O db (Fig. 7A), respectively. The lower affinity for the water molecules of the first one could be due to Palatinose® incorporation in the mango fruit. Additionally, the ultrasound produced micro-channel leading to isomaltulose entry easily on mangos slices (Amami et al., 2017). Noshad

et al. (2012) presented that the osmosis and ultrasound pretreatment can also decrease equilibrium moisture content of dried quince slices.

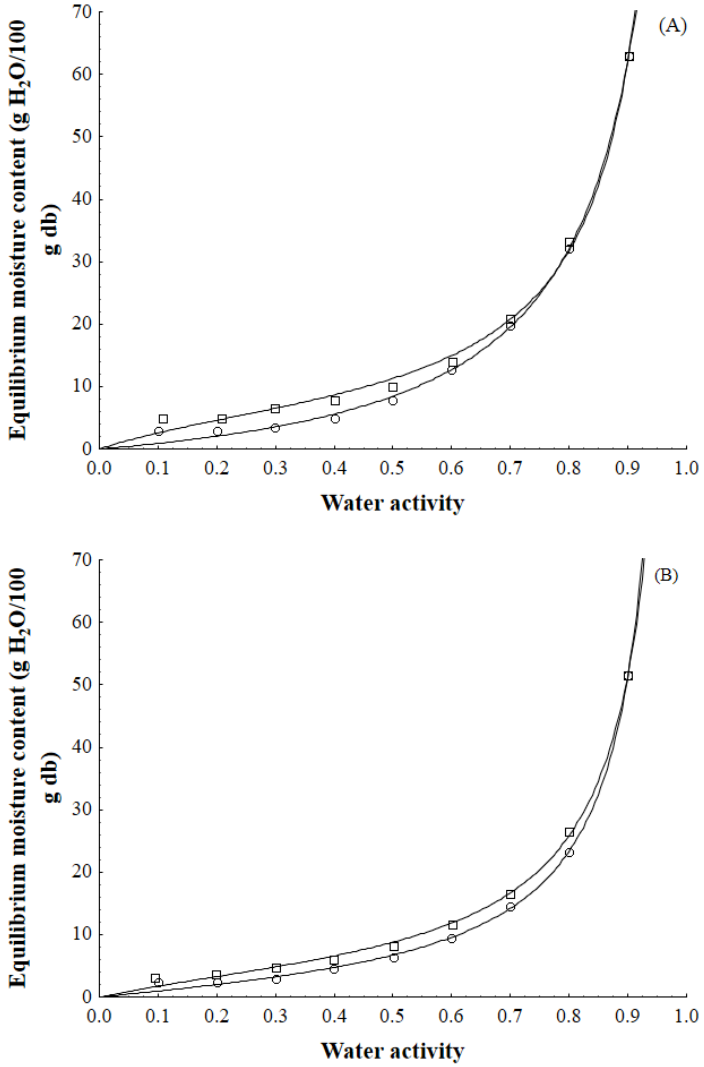

Fig. 7. Moisture sorption isotherms of fresh + D (A) and UAOD + D (B) mango. Experimental adsorption (○) and desorption (□) values and predicted values at 25 °C using the GAB model (line).

Table 2. Parameters of mathematical modeling of kinetics of drying processes to the experimental drying data.

Model	Parameters	Samples	
		Fresh +D	**UAOD +D**
Diffusion Approximation	***a***	-84.16	-67.12
	k	0.030	0.031
	b	0.992	0.991
	$\mathbf{R^2}$	0.999	0.999
	χ^2	$1.4 \cdot 10^{-4}$	$1.0 \cdot 10^{-4}$
	RMSE	0.011	0.009
Logarithmic	***a***	1.15	1.12
	k	0.014	0.015
	c	-0.117	-0.098
	$\mathbf{R^2}$	0.998	0.999
	χ^2	$2.5 \cdot 10^{-4}$	$1.2 \cdot 10^{-4}$
	RMSE	0.015	0.010
Page	***k***	0.006	0.008
	n	1.25	1.20
	$\mathbf{R^2}$	0.999	0.999
	χ^2	$1.4 \cdot 10^{-4}$	$1.2 \cdot 10^{-4}$
	RMSE	0.011	0.010
Modified Page	***k***	0.016	0.018
	n	1.25	1.20
	$\mathbf{R^2}$	0.999	0.999
	χ^2	$1.4 \cdot 10^{-4}$	$1.2 \cdot 10^{-4}$

	RMSE	0.011	0.010
Henderson and Pabis	***a***	1.06	1.05
	k	0.018	0.019
	$\mathbf{R^2}$	0.990	0.992
	$\boldsymbol{\chi^2}$	$1.2 \cdot 10^{-3}$	$8.2 \cdot 10^{-4}$
	RMSE	0.033	0.027
Newton	***k***	0.016	0.018
	$\mathbf{R^2}$	0.984	0.989
	$\boldsymbol{\chi^2}$	$1.7 \cdot 10^{-3}$	$1.2 \cdot 10^{-3}$
	RMSE	0.040	0.033
Wang and Singh	***a***	-0.012	-0.013
	b	$3.9 \cdot 10^{-5}$	$4.6 \cdot 10^{-5}$
	$\mathbf{R^2}$	0.999	0.997
	$\boldsymbol{\chi^2}$	$8.1 \cdot 10^{-5}$	$2.7 \cdot 10^{-4}$
	RMSE	0.009	0.016

Fresh + D is fresh fruit subjected to drying, UAOD + D is osmodehydrated fruit subjected to drying; a, b, c, k, and n are constant of the models, R^2 is coefficient of determination, χ^2 is reduced Chi squared, and RMSE is root mean square error.

The adsorption isotherms indicate fresh + D and UAOD + D are microbiologically stable ($a_w < 0.6$) (Jay, 2005) when stored at 25 °C if their moisture levels are 12.8% db (11.3% wb) and 9.5% db (8.7% wb), respectively. These results indicate fresh + D required greater care during storage.

According to the quantitative criteria proposed by Yanniotis & Blahovec (2009) for the classification of moisture sorption isotherms, the fresh + D adsorption isotherm behaved as type III, however, the behavior of the desorption isotherm changed and it behaved as more solution-like type-II isotherm. Similar behavior has been found by Bejar et al. (2012). On other hand, for UAOD + D product, both adsorption and desorption isotherms were classified as more solution-like type-

II isotherms. This type of isotherm has been also observed for other dried fruits (Noshad et al. 2012; Sormoli & Langrish 2015).

The hysteresis loop observed between the moisture adsorption and desorption isotherms comprehended the monolayer region until approximately 0.8 and 0.9 a_w for fresh + D and UAOD + D, respectively. Hysteresis can be used as an index of the food quality. A decrease in the hysteresis loop or its complete absence has been related to greater product stability during storage (Caurie, 2007). Thus, the pretreated mango with ultrasound can be considered a product more stable than ones untreated.

The adsorption isotherms had linear behavior up to a_w of 0.5 for fresh + D and up to a_w of 0.6 for UAOD + D. After these levels of a_w the moisture content the products increased exponentially (Fig. 7). This behavior may be attributed to the dissolution of crystalline sugar at low a_w levels and the conversion of crystalline sugar into amorphous sugar at high a_w levels (Saltmarch & Labuza, 1980). This results indicate that the fresh + D and UAOD + D requires greater care when stored or handled in an environment with RH above 50% and above 60%, respectively. Under such conditions, the products should be stored in packaging with low water vapor permeability (Carmo et al., 2019). Another particular feature of the products is the presence of bioactive compounds such as ascorbic acid, carotenoids and total phenolics (Figs. 3 and 4), which are very susceptible to oxidative processes. Therefore, in order to minimize such processes, it is strongly indicated that the packages also have impermeability to air and does not allow light to pass through (Pombo et al., 2019).

According to BET equation, the monolayer moisture content (M_0) was 2.4 and 2.1 g H_2O/100 g db for adsorption and 4.9 and 3.4 g H_2O/100 g db for desorption, for the mango without and with pretreatment, respectively ($R^2 > 0.974$). M_0 decreased for pretreated product. Similar behavior was observed with sucrose solution in mangos (Falade & Aworh, 2004; Zhao et al., 2018). According to Labuza (1984), foods with $M_0 \leq 10\%$ db are considered stable. Thus, the both dried mangos were considered products with good stability. The monolayer concept is useful because of its

relationship with several aspects of physical and chemical deterioration in dehydrated foods since corresponds to the optimal moisture content, which should be achieved and maintained in order to minimize deteriorative reactions during storage (Zhao et al., 2018).

According to the values of the statistics used to assess goodness of fit (R^2, P and RMSE) (Table 3), the GAB model was suitable to describe the moisture adsorption and desorption processes of the dried mangos. The isotherms generated by the GAB model are presented in Fig 7. Overall, the literature indicates the GAB model as having the best fits to the moisture sorption data of another dried products, such as apple, mango, mushroom, fried purple-fleshed sweet and potato slices (Prothon & Ahrne, 2004; Falade & Aworh, 2004; Engin, 2020; Fan et al., 2019).

Table 3. Parameters of GAB mathematical model of moisture sorption data of dried mango.

Parameters	**Samples**			
	Fresh + D		**UAOD + D**	
	Adsorption	**Desorption**	**Adsorption**	**Desorption**
M_0	10.57	7.00	5.21	5.77
C	0.79	4.53	1.78	3.38
K	0.95	0.99	1.00	0.99
R^2	0.998	0.998	0.999	0.998
P (%)	13.78	9.54	10.69	9.29
RMSE	0.79	1.06	0.51	0.63

Fresh + D is fresh fruit subjected to drying, UAOD + D is osmodehydrated fruit subjected to drying, M_0 is monolayer moisture content (g H_2O/100 g db), K and C are model's parameters, R^2 is coefficient of determination, P is mean relative deviation and RMSE is root mean square error.

4 Conclusions

The use of ultrasound technology proves to be interesting for the incorporation of a carbohydrate with nutritional advantages in relation to sucrose, since promoted an incorporation of 4.58% (± 0.55) of isomaltulose in only 20 min. Ascorbic acid, carotenoids, total phenolics, as well as their antioxidant activity, were preserved on mangos subjected to UAOD treatment. The ultrasound pretreated dried samples had lower water activity and similar bioactive compounds content in relation to untreated dried samples ($p \leq 0.05$,) except for the ascorbic acid content. Additionally, the incorporation of isomaltulose by ultrasound resulted in more stable product, from a hygroscopic point of view, compared to the fresh one, as shown by sorption isotherms study.

Conflict of interest

There are no conflicts of interest.

Acknowledgments

The authors thank the following Brazilian agencies for financial support: National Council for Scientific and Technological Development (CNPq) (314191/2021-6) and Fundação de Amparo à Pesquisa do Estado de Minas Gerais. (FAPEMIG) J. R. Carmo (grant 166378/2018-6) thanks CNPq.

References

Abrahão, F. R., & Corrêa, J. L. G. (2021). Osmotic dehydration: More than water loss and solid gain. *Crit. Rev. Food Sci. Nut.,* 29, 1–20. https://doi.org/ 10.1080/10408398.2021.198376

Akoy, E. O. M. (2014). Effect of drying temperature on some quality attributes of mango slices. *Int. J. Innov. Scient. Res.*, 4, 91–99.

Amami, E., Khezami, W., Mezrigui, S., Badwaik, L. S., Bejar, A. K., Perez, C. T., & Kechaou, N. (2017). Effect of ultrasound assisted osmotic dehydration pretreatment on the convective drying of strawberry. *Ultrason. – Sonochem.*, 36, 286–300, 2017. https://doi.org/10.1016/j.ultsonch.2016.12.007

Association of Official Analytical Chemists – AOAC. (2010). *Official methods of analysis of association of Official Analytical Chemists International* (18th ed.). Arlington: AOAC.

Azoubel, P. M., Amorim, M. R., Oliveira, S. S. B., Maciel, M. I. S., & Rodrigues. J. D. (2015). Improvement of water transport and carotenoid retention during drying of papaya by applying ultrasonic osmotic pretreatment. *Food Eng. Reviews*, 7, 185–192, https://doi.org/10.1007/s12393-015-9120-4.

Barcia, M. T., Jacques, A. C., *Becker, Pertuzatti, P. B., & Zambiazi, R. C. (2010).* Determination by HPLC of ascorbic acid and tocopherols in fruits. *Semina: Ciênc. Agr.*, 31, 381–390. https://dx.doi.org/10.5433/1679-0359.2010v31n2p381

Bejar, A. K., Mihoubi, N. B., & Kechaou, N. (2012). Moisture sorption isotherms – experimental and mathematical investigations of orange (*Citrus sinensis*) peel and leaves. *Food Chem.*, 132, 1728–1735. https://doi.org/10.1016/j.foodchem.2011.06.059

Brunauer, S., Emmet, T. H., & Teller, F. (1938). Adsorption of gases in multimolecular layers. *J. Am. Oil Chem. Soc.*, 60, 309–319. doi:10.1021/ja01269a023

Carmo, J. R., & Pena, R. S. (2019). Influence of the temperature and granulometry on the hygroscopic behavior of tapioca flour. *CyTA – J. Food*, 17, 900–906. https://doi.org/10.1080/19476337.2019.1668860

Carmo, J. R., Corrêa, J. L. G., Polachini, T. C., & Telis-romero, J. (2022). Properties of Isomaltulose (Palatinose®) – an emerging healthy carbohydrate: effect of temperature and solute concentration. *J. Mol. Liq.*, 347, 118304. https://doi.org/10.1016/j.molliq.2021.118304

Carmo, J. R., Costa, T. S., & Pena, R. S. (2019) Tucupi-added mayonnaise: Characterization, sensorial evaluation, and rheological behavior. *CyTA – J. Food*, 17, 479–487, https://10.1080/19476337.2019.1607561

Caurie, M. (2007). Hysteresis phenomenon in foods. *Int. J. Food Sci. Technol.*, 42, 45–49. https://doi.org/10.1111/j.1365-2621.2006.01203.x

Corrêa, J. L. G., Rasia, M. C., Mulet, A., & Cárcel, J. A. (2017). Influence of ultrasound application on both the osmotic pretreatment and subsequent convective drying of pineapple (*Ananas comosus*). *Innov. Food Sci. Emerg. Technol.*, 41, 284–291. https://doi.org/10.1016/j.ifset.2017.04.002

Crank, J. *The Mathematics of diffusion*. 2 ed. Oxford: Carendon press ed., 1975.

Cui, Z. W., Xu, S. Y., & Sun, D. W. (2004). Effect of microwave-vacuum drying on the carotenoids retention of carrot slices and chlorophyll retention of Chinese Chire leaves. *Dry. Technol.*, 22, 563–575. https://doi.org/10.1081/DRT120030001.

Delgado, T., Pereira, J. A., Ramalhosa, E., & Casal, S. (2017). Osmotic dehydration effects on major and minor components of chestnut (*Castanea sativa* Mill.) slices. *J. Food Sci. Technol.*, 54, 2694–2703. https://doi.org/10.1007/s13197-017-2706-5

Dereje, B., & Abera, S. (2020). Effect of pretreatments and drying methods on the quality of dried mango (*Mangifera indica* L.) slices. *Cog. Food Agri.*, 6, 1747961. https://doi.org/10.1080/23311932.2020.1747961

Devic, E., Guyot, S., Daudin, J., & Bonazzi, C. (2010). Effect of temperature and cultivar on polyphenol retention and mass transfer during osmotic dehydration of apples. *J. Agri. Food Chem.*, 58, 606–614. https://doi.org/10.1021/ jf903006g

Engin, D. (2020). Effect of drying temperature on color and desorption characteristics of oyster mushroom. *Food Sci. Technol.*, 40, 187–193. https://doi.org/10.1590/fst.37118

Falade, K. O., & Aworh, O. C. (2004). Adsorption isotherms of osmo-oven dried african star apple (*Chrysophyllum albidum*) and african mango (*Irvingia gabonensis*) slices. *Eur. Food Res. Technol.*, 218, 278–283. https://dx.doi.org/10.1007/s00217-003-0843-8

Fan, K., Zhang, M., & Bhandari. (2019). Osmotic-ultrasound dehydration pretreatment improves moisture adsorption isotherms and water state of microwave-assisted vacuum fried purple-fleshed sweet potato slices. *Food Bioprod. Process.*, 115, 154–164. https://doi.org/10.1016/j.fbp.2019.03.011

Feng, Y., Yu, X., ElGasim, A., Yagou, A., Xu, B., Wu, B., Zhanga, L., & Zhou, C. (2019). Vacuum pretreatment coupled to ultrasound assisted osmotic dehydration as a novel method for garlic slices dehydration, *Ultrason. – Sonochem.*, 50, 363–372. https://doi.org/10.1016/j.ultsonch.2018.09.038

Fernandes, F. A. N, Rodrigues S., García-Pérez, J. V., & Cárcel, J. A. (2016). Effects of ultrasound-assisted air-drying on vitamins and carotenoids of cherry tomatoes. *Dry. Technol.*, 34, 986–996. https://doi.org/ 10.1080/07373937.2015.1090445

Fernandes, F. A. N., Braga, T. R., Silva, E. O., & Rodrigues, S. (2019). Use of ultrasound for dehydration of mangoes (*Mangifera indica* L.): kinetic modeling of ultrasound-assisted osmotic dehydration and convective air-drying. *J. Food Sci. Technol.*, 56, 1793–1800. https://doi.org/10.1007/s13197-019-03622-y

Fratianni, A., Albanese, D., Mignogna, R., Cinquanta, L., Panfili, G., & Di Matteo, M. (2013). Degradation of carotenoids in apricot (*Prunus armeniaca L.)* during drying process. *Plant Foods Hum. Nutr.*, 68, 241–246. https://doi.org/10.1007/ s11130-013-0369-6.

Jay, M. J. (2005). *Microbiologia de alimentos* (6th ed.). Porto Alegre, Brasil: Artmed.

Jiménez-Hernandez, J., Estrada-Bahena, E. B., Maldonado-Astudillo, Y. I., Talavera-Mendoza, Ó., Arambula-Villa, G., Azuara, E., Álvarez-Fitz, P., Ramírez, M., & Salazar, R. (2017).

Osmotic dehydration of mango with impregnation of inulinand piquin-pepper oleoresin. *LWT – Food Sci. Technol.*, 79, 609–615. https://doi.org/10.1016/j.lwt.2016.11.016

Junqueira, J. R. J., Corrêa, J. L. G., & Mendonça, K. S. (2017). Evaluation of the shrinkage effect on the modeling kinetics of osmotic dehydration of sweet potato (*Ipomoea batatas* (L.)). *J. Food Process. Preserv.*, 41, e12881. https://doi.org/10.1111/jfpp.1288

Kek, S. P., Chin, N. L., & Yusof, Y. A. (2013). Direct and indirect power ultrasound assisted pre-osmotic treatments in convective drying of guava slices. *Food Bioprod. Process.*, 91, 495–506. https://doi.org/10.1016/j.fbp.2013.05.003

Kroehnke, J., Szadzinska, J., Radziejewska-Kubzdela, E., Bieganska-Marecik, R., Musielak, G., & Dominik Mierzwa. (2021). Osmotic dehydration and convective drying of kiwifruit (*Actinidia deliciosa*) – The influence of ultrasound on process kinetics and product quality. *Ultrason. – Sonochem.*, 71, 105377. https://doi.org/10.1016/j.ultsonch.2020.105377

Labuza, T. P. (1984). Application of chemical kinetics to deterioration of foods. *J. Chem. Educ.*, 61, 348–358. https://dx.doi.org/10.1021/ed061p348

Larrauri, J. A., Rupérez, P., & Saura-Calixto, F. (1997). Effect of drying temperature on the stability of polyphenols and antioxidant activity of red grape pomace peels. *J. Agri. Food Chem.*, 45, 1390–1393. http://dx.doi.org/10.1021/jf960282f.

Lopez, M. M. L., Morais, R. M. S. C., & Morais, A. M. M. B. (2020). Flavonoid enrichment of fresh-cut apple through osmotic dehydration-assisted impregnation. *Brit. Food J.*, 123, 820–832. https://doi.org/10.1108/BFJ-03-2020-0176

Macedo, L. L., Corrêa, J. L. G., Araújo, C. S., Vimercati, W. C., & Petri Junior, I. (2021). Convective drying with ethanol pre-treatment of strawberry enriched with isomaltulose. *Food Bioprocess Technol.*, 14, 2046–2061. https://doi.org/10.1007/s11947-021-02710-2

Maldonado-Celis, M. E., Yahia, E. M., Bedoya, R., Landázuri, P., Loango, N., Aguillón, J., Restrepo, B., & Ospina J. C. G. (2019). Chemical composition of mango (*Mangifera*

indica L.) fruit: nutritional and phytochemical compounds. *Front. Plant Sci.*, 10, 1073. https://doi.org/10.3389/fpls.2019.01073.

Marco, G. J. (1968). A rapid method for evaluation of antioxidants. *J. Am. Oil Chem. Soc.*, 45, 594–598. http://dx.doi.org/10.1007/BF02668958

Maroulis Z. B., Tsami, E., Arinos-Kouris, D., & Saravacos, G. D. (1988). Application of the GAB model to the sorption isotherms for dried fruits. *J. Food Eng.*, 7, 63–78. https://doi.org/10.1016/0260-8774(88)90069-6

Martins, M. G., Pena, R. S. (2017). Combined osmotic dehydration and drying process of pirarucu (*Arapaima gigas*) fillets. *J. Food Sci. Technol*., 54, 3170–3179.doi: 10.1007/s13197-017-2755-9

Matos, K. A. N., Lima, D. P., Barbosa, A. P. P., Mercadante, A. Z., & Renan Campos Chisté. (2019). Peels of tucumã (*Astrocaryum vulgare*) and peach palm (*Bactris gasipaes*) are by-products classified as very high carotenoid sources. *Food Chem.,* 272, 216–221. https://doi.org/10.1016/j.foodchem.2018.08.053

Medeiros, R. A. B., Silva Júnior, E. V., Silva, J. H. F., Ferreira Neto, O. C., Brandão, S. C. R., Barros, Z. M. P. Rocha, O. R. S., & Azoubel, P. M. Effect of different grape residues polyphenols impregnation techniques in mango. *J. Food Eng.*, 262, 1–8. https://doi.org/10.1016/j.jfoodeng.2019.05.011

Miller, H. E. (1971). A simplified method for the evaluation of antioxidant. *J. Am. Oil Chem. Soc.*, 48, 91–97. http://dx.doi.org/10.1007/BF02635693.

Moreno, J., Simpson, R., Pizarro, N., Pavez, C., Dorvil, F., Petzold, G., & Bugueño, G. (2013). Influence of ohmic heating/osmotic dehydration treatments on polyphenoloxidase inactivation, physical properties and microbial stability of apples (cv. *Granny Smith*). *Innov. Food Sci. Emerg. Technol.*, 20, 198–207. https://doi.org/10.1016/j.ifset.2013.06.006

Mothibe, K. J., Zhang, M., Mujumdar, A. S., Wang, Y. C., & Cheng, X. (2014). Effects of ultrasound and microwave pretreatments of apple before spouted bed drying on rate of dehydration and physical properties. *Dry. Technol.*, 32, 1848–1856. https://doi.org/10.1080/07373937.2014.952381

Muralidhara, H. S., Ensminger, D., & Putnam, A. (1985). Acoustic dewatering and drying (low and high frequency): state of the art review. *Dry. Technol.*, 3, 529– 566, 1985. https://doi.org/10.1080/07373938508916296

Nahimana, H., Zhang, M., Mujumdar, A. S., & Zhansheng, D. (2011). Mass transfer modeling and shrinkage consideration during osmotic dehydration of fruits and vegetables. *Food Reviews Int.*, 10, 15327–15345. https://doi.org/10.1080/87559129.2010.518298

Noshad, M., Mohebbi, M., Shahidi, F., & Mortazavi, S.A. (2012). Effect of osmosis and ultrasound pretreatment on the moisture adsorption isotherms of quince. *Food Bioprod. Process.*, 90, 266–274. https://doi.org/10.1016/j.fbp.2011.06.002

Nowacka, M., Fijalkowska, A., Dadan, M., Rybak, K., Wiktor, A., & Witrowa-Rajchert, D. (2018). Effect of ultrasound treatment during osmotic dehydration on bioactive compounds of cranberries. *Ultrason.*, 83, 18–25. https://dx.doi.org/10.1016/j.ultras.2017.06.022

Oladejo, A. O., Ma, H., Qu, W., Zhou, C., & Wu, B. (2017). Effects of ultrasound on mass transfer kinetics, structure, carotenoid and vitamin C Content of osmodehydrated sweet potato (*Ipomea batatas*). *Food Bioprocess Technol.*, 10, 1162–1172, https:// doi.org/10.1007/s11947-017-1890-7.

Onwude D. I., Hashim N., Janius R. B., Nawi N. M., & Abdan K. (2016). Modeling the thin-layer drying of fruits and vegetables: A review. *Compr. Rev. Food Sci. Food Saf.*, 15, 599–618. https://doi.org/10.1111/1541-4337.12196.

Pombo, J. C. P., Carmo, J. R., Araújo, A. L., Medeiros, H. H. B. R., & Pena, R. S. (2019). Moisture sorption behavior of cupuassu powder. *Open Food Sci. J.*, 11, 66–73. https://doi.org/10.2174/1874256401911010066

Prithani, R., & Dasha, K. K. (2020). Mass transfer modelling in ultrasound assisted osmotic dehydration of kiwi fruit. *Innov. Food Sci. Emerg. Technol.*, 64, 102407. https://doi.org/10.1016/j.ifset.2020.102407

Prothon, F., & Ahrne, L. M. (2004). Application of the Guggenheim, Anderson and De Boer model to correlate water activity and moisture content during osmotic dehydration of apples. *J. Food Eng.*, 61, 467–470. https://dx.doi.org/10.1016/ S0260-8774(03)00119-5

Rahaman, A., Zenga, X-A., Kumari, A., Rafiq, M., Siddeeg, A., Manzoor, M. F., Baloch, Z., & Ahmeda, Z. (2019). Influence of ultrasound-assisted osmotic dehydration on texture, bioactive compounds and metabolites analysis of plum. *Ultrason. – Sonochem.*, 58, 104643. https://doi.org/10.1016/j.ultsonch.2019.104643

Re, R., Pellegrini, N., Proteggente, A., Pannala, A., Yang, M., & RiceEvans, C. (1999). Antioxidant activity applying an improved ABTS radical cation decolorization assay. *Free Rad. Biol. Med.*, 26, 1231–1237. http://dx.doi.org/10.1016/S0891-5849(98)00315- 3.

Rodriguez-Amaya, D. B., & Kimura, M. (2004). HarvestPlus handbook for carotenoid analysis. HarvestPlus ed. Washington, DC and Cali: International Food Policy Research Institute (IFPRI) and International Center for Tropical Agriculture (CIAT).

Sagar, V. R., & Kumar, P. S. (2010). Recent advances in drying and dehydration of fruits and vegetables: A review. *J. Food Sci. Technol.*, 47, 15–26. https://doi.org/10.1007/s13197-010-0010-8

Sakooei-Vayghan, R., Peighambardoust, S. H., Hesaria, J., & Peressini, D. (2020). Effects of osmotic dehydration (with and without sonication) and pectin-based coating pretreatments

on functional properties and color of hot-air dried apricot cubes. *Food Chem.*, 311, 125978. https://doi.org/10.1016/j.foodchem.2019.125978

Saltmarch, M., & Labuza, T.P. (1980). Influence of relative humidity on the physico-chemical state of lactose in spray-dried sweet whey powders. *J. Food Sci. Technol.*, 45, 1231–1236. https://doi.org/10.1111/j.1365-2621.1980.tb06528.x

Singh F., Katiyar, V. K., & Singh, B. P. (2015). Mathematical modeling to study influence of porosity on apple and potato during dehydration. *J. Food Sci. Technol.*, 52, 5442–5455. https://doi.org/10.1007/s13197-014-1647-5

Soquetta, M. B., Schmaltz, S., Righes, F. W., Salvalaggio, R., & Terra, L. M. (2018). Effects of pretreatment ultrasound bath and ultrasonic probe, in osmotic dehydration, in the kinetics of oven drying and the physicochemical properties of beet snacks. *J. Food Process. Preserv.*, 42, e13393. https://doi.org/ 10.1111/jfpp.13393

Sormoli, M. E., & Langrish, T. A. (2015). Moisture sorption isotherms and net isosteric heat of sorption for spray-dried pure orange juice powder. *LWT – Food Sci. Technol.*, 62, 875–882. https://doi.org/10.1016/j.lwt.2014.09.064

Timmermann, E. O. (2003). Multilayer sorption parameters: BET or GAB values? *Colloids Surf. A Physicochem. Eng. Asp.* 220, 235-260. https://doi.org/10.1016/S0927-7757(03)00059-1

Viana, A. D., Corrêa, J. L. G., & Justus, A. (2014). Optimisation of the pulsed vacuum osmotic dehydration of cladodes of fodder palm. *Int. J. Food Sci. Technol.*, 49, 726–732. https://doi.org/10.1111/ijfs.12357

Waterhouse, A. L. (2002). *Polyphenolics: determination of total phenolics in current protocols in food analytical chemistry*. New York: John Wiley & Sons.

Wiktor, A., Gondek, E., Jakubczyk, E., Dadan, M., Nowacka, M., Rybak, K., & Witrowa-Rajchert, D. (2018). Acoustic and mechanical properties of carrot tissue treated by pulsed electric field,

ultrasound and combination of both. *J. Food Eng.*, 238, 12–21. https://doi.org/10.1016/j.jfoodeng.2018.06.001

Yanniotis, S., & Blahovec, J. (2009). Model analysis of sorption isotherms. *LWT – Food Sci. Technol.* 42, 1688-1695. http:// dx.doi.org/10.1016/j.lwt.2009.05.010.

Yao, L., Fan, L., & Duan, Z. (2020). Effect of different pretreatmentsfollowed by hot-air and far-infrared drying on the bioactive com-pounds, physicochemical property and microstructure of mango slices. *Food Chem.*, 305, 125477. https://doi.org/10.1016/j.foodchem.2019.125477

Zhao, J-H., Ding, Y., Yuan, Y-J., Xiao, H-W., Zhou, C-L., Tan2, M-L., & Tang, X-M. (2018). Effect of osmotic dehydration on desorption isotherms and glass transition temperatures of mango. *Int. J. Food Sci. Technol.*, 53, 2602–2609. https://doi.org/10.1111/ijfs.13855

ARTICLE 7 – **Influence of osmotic dehydration with and without pulsed vacuum and hot air drying on quality and hygroscopicity of mangos incorporated with Palatinose®**

Juliana Rodrigues do CARMO [a*], Jefferson Luiz Gomes CORRÊA [a], Cristiane Nunes da SILVA [b], Cassiano OLIVEIRA [c], Adriano Lucena de ARAÚJO [d], Rosinelson da Silva PENA [d]

[a] Department of Food Science (DCA), Federal University of Lavras, 37200-900, Lavras, Brazil. E-mail: juliana_docarmo@yahoo.com.br; jefferson@ufla.br

[b] Department of Nutrition and Health (DNU), Federal University of Lavras, 37200-900, Lavras, Brazil. E-mail: kristtiane2015@gmail.com

[c] Institute of Exact and Thecnological Sicences, Federal University of Viçosa, 38810-000, Rio Paranaíba, Brazil. E-mail: croliveira1979@yahoo.com.br

[d] Graduate Program in Food Science and Technology, Federal University of Pará, 66075-110, Belém, Brazil. E-mail: rspena@ufpa.br; adriano.lucena4@gmail.com

[*]**Corresponding author:** Juliana Rodrigues do CARMO (E-mail: juliana_docarmo@yahoo.com.br)

(Elaborated in accordance to the Food and Bioproducts and Processing)

***Abstract*:** The influence of osmotic dehydration (OD) and pulsed vacuum osmotic dehydration (PVOD) on mangos, subjected also to hot air drying, was investigated via quality properties (water activity, color, texture, volumetric shrinkage, ascorbic acid content, total carotenoids, phenolic total compounds and antioxidant activity) and hygroscopic behavior of the product. OD (45 °C, 35 °B at 101.3 kPa) and PVOD (45 °C, 35 °B and pulsed vacuum – 48 kPa during the first 10 min a) assays were performed for 15 h. After these pretreatments, the samples were dried in a tunnel dryer at a temperature of 60 °C and an air velocity of 1.5 m/s. The results revealed that PVOD led to the loss ascorbic acid content compared to OD. Among the pretreated dried samples, pulsed vacuum promoted smaller changes color than OD. Antioxidant activity of fresh mangos fruit comes from the presence of ascorbic acid, carotenoids and total phenolic compounds. Therefore, the different methods showed the same tendency of these compounds: decreased for pretreated osmotically or dried samples ($p \leq 0.05$) or had a weak impact for the dried products ($p > 0.05$) in relation to fresh sample. The pretreated samples showed lower water diffusivity and higher time drying than fresh samples. The incorporation of Palatinose® carbohydrate in the mangos with PVOD (14%) was higher than OD (11%). The hygroscopic study via sorption isotherms showed type II and type III shape. The microbiological stability indicated that untreated dried sample requires greater care during storage and handling. From hysteresis loop observation, the pretreated mangos were more stables than untreated samples, highlighting the mangos subjected to PVOD, which were considered more stable among the pretreated samples.

Keywords: *Mangifera indica*, isomaltulose, bioactive compounds, sorption isotherms.

1 Introduction

Mango (*Mangifera indica* L.) is one of the most popular tropical fruits. It is a source of fiber, phenolic compounds and vitamins, such as C and pro-vitamin A (β-carotene). It is a climatic and perishable fruit, due to its high water content (> 80%), which needs specific care for its conservation (Zhao et al., 2018). This fruit can be directly dried without pretreatment or with osmotic dehydration (OD) pretreatment using sugar solution before hot air drying (Khuwijitjaru et al., 2022). OD could be applied before drying or to creating new, less perishable food products or ingredients with high nutritional and sensory properties (Ciurzyńska et al., 2016).

OD is a mass transfer process that partially removes water and simultaneously increases the soluble solids content of the fruit using an osmotic solution. In OD, flux of osmotic solution into cellular tissue is induced by initial capillary pressure (Seguí et al., 2012). Meanwhile, three other mechanisms concurrently occur throughout the process: (i) cell dehydration caused by water activity gradients leading to water loss; both (ii) soluble solid diffusion and (iii) cell impregnation caused by cellular volume changes that generate pressure gradients related to mechanical deformation (Abrahão & Corrêa, 2021).

The use of vacuum in OD in a process known as pulsed vacuum osmotic dehydration (PVOD) usually increases the mass transfer between the food and the osmotic solution (Corrêa et al., 2010; Corrêa et al., 2014; Junqueira et al., 2021). In PVOD, the capillary impregnation is combined with vacuum induced impregnation, which expands internal gas and liquid in pores (when vacuum is applied) and followed by compression (when atmospheric pressure is restored). The gas partially flows out causing additional internal volume changes.

Because it intensifies the exchanges between the food and the solution, OD and PVOD could be indicated for the enrichment of foods with functional ingredients in the pores of the product, such as texture retaining agents, antioxidants, and antimicrobials, that increase their quality and shelf-life. In this context, the isomaltulose, commercially known as Palatinose®, appears as an excellent

alternative of osmotic solute as it is a non-cariogenic carbohydrate with a low glycemic and insulinemic indexes. This product has been recently studied to obtain healthier dry products (Lopez et al., 2020; Macedo et al., 2021).

The combination of an OD or PVOD pretreatment and subsequent convective drying is a compromise solution that could combine the advantages of both processes (Sagar & Kumar, 2010), since these processes that reduces the negative effects of convective drying. According to the literature, the quality of the final products is visibly better if osmotic treatments are used before the convective drying process (Kroehnke et al., 2021).

The hygroscopicity of dried food is associated to its physical, chemical, and microbiological stability and can be represented by moisture sorption isotherms, which describe the relationship between equilibrium moisture content and water activity (a_w) of this product at a constant temperature (Martins et al., 2015). The different pretreatments used in OD can affect the compositional and structural characteristics of the food, modifying its water sorption isotherms (Carmo & Pena, 2019). As a more effective contribution for the study of the dehydration of mangos, the present research aimed to evaluate the effect of pretreatments (OD and PVOD) on color, ascorbic acid, carotenoids, total phenolics compounds and antioxidant activity of osmodehydrated and dried mangos and carried out the hygroscopic study of dried products by moisture sorption isotherms.

2 Material and methods

2.1 Material and sample preparation

Half-ripe mango fruits (*Tommy Atkins*) were acquired in the local market of Lavras (Minas Gerais State, Brazil), and sanitized with chlorinated water at 200 mg/L for 5 min. Then, the seed and peel were removed and slices were obtained with the aid of a stainless steel mold (4.00 ± 0.01 cm length, 2.00 ± 0.01 cm width, and 0.40 ± 0.01 cm thickness). The fruits had reddish-green skin peel color;

84.53% (± 1.83) moisture; 12.33 °B (± 0.60) total soluble solids; 2.86% citric acid (± 0.21) titratable total acidity; 4.72 (± 0.16) ratio; 3.60 (± 0.04) pH and 31.13 N (±3.27) firmness.

2.2 Osmotic solution characterization

Osmotic solution was prepared with Palatinose® (Beneo, Mannheim, Germany) and distilled water (35:65, w/w) and had water activity (a_w) of 0.972 (± 0.001); solubility of 0.4470 (±0.004) kg of isomaltulose/kg of solution; density of 1103.7 (±0.3) kg/m^3; specific heat of 3.444 (±0.004) kJ/kg·K; thermal conductivity of 0.484 (±0.002) W/m·K and viscosity of 2.127 (±0.033) mPa·s at the working temperature (45 °C) (Carmo et al., 2022).

2.3 Osmotic dehydration (OD) and pulsed vacuum osmotic dehydration (PVOD)

Mangos slices were immersed in glass containers containing osmotic solution at a ratio of 1:10 (w/v) to avoid to avoid dilution of the solution and at 45 °C for 15 h. The choose of temperature, time and vacuum conditions were based in preliminary tests due to promote greater enrichment of solutes on mangos. The OD experiments of mangos slices were performed at atmospheric pressure (101.3 kPa) in a thermostatic chamber (Eletrolab EL111/4, São Paulo, Brazil). The PVOD was performed in a temperature-controlled oven (Solab SL104/40, Piracicaba, Brazil) coupled to a vacuum pump (model DV95, Dosivac, Buenos Aires, Argentina). PVOD was performed by applying an absolute pressure of 48.0±1 kPa (52.6% vacuum) during the first 10 min of the process (Sirijariyawat et al., 2012), Then, the atmospheric pressure was resumed and the osmotic process continued in a thermostatic chamber (Eletrolab EL111/4, São Paulo, Brazil).

After the osmotic processes, the samples were immersed in an ice bath for 10 s to interrupt the mass flow. The surfaces of the samples were blotted dried with absorbent paper (Viana et al., 2014). Five samples were subjected to each OD and PVOD process condition and analysed.

The mass transfer parameters (WL, SG and WR) of each sample subjected to the different OD and PVOD conditions were evaluated according to Eq. 1, and Eq. 2 (Viana et al., 2014), respectively. The moisture content of the fresh and osmotically treated samples was determined according to the AOAC (2010).

$$WL(\%) = \frac{x_0 m_0 - x_t m_t}{m_0} \times 100 \quad (1)$$

$$SG(\%) = \frac{m_t S_t - m_0 S_0}{m_0} \times 100 \quad (2)$$

where: WL is the water loss (%), SG is the solid gain (%), x is the moisture content on a wet basis (wet basis – wb) (kg of water/kg of fruit), m is the sample weight (kg) and S is solid content (kg solid/kg fruit wb). The subindices "0" and "t" refer to fresh samples and samples after osmotic treatment, respectively.

2.4 Product quality assessment

The quality of fresh and treated samples was analyzed through measurement of color, a_w, texture, ascorbic acid content, total carotenoids, total phenolic compounds and antioxidant activity. Besides, the treated samples were characterized by volumetric shrinkage and sorption isotherms – for hygroscopic study.

Color was evaluated by tristimulus colorimetry in a digital colorimeter (Konica-Minolta, CR 400, Tokyo, Japan). The lightness (L^* = 0 black and L^* = 100 white) and the chromaticity coordinates ($-a^*$ = green and $+a^*$ = red, $-b^*$ = blue and $+b^*$ = yellow) were used to define the chroma value (C^*) (Eq. 3), and the hue angle (h°) (Eq. 4) (Carmo et al., 2019). Eq. 5 was used to calculate the total color difference (ΔE) of the treated samples relative to the fresh fruit.

$$C^* = \sqrt{(a^*)^2 + (b^*)^2} \quad (3)$$

$$h° = \cos^{-1} \frac{a^*}{\sqrt{(a^*)^2 + (b^*)^2}} \quad (4)$$

$$\Delta E = \sqrt{(L_0^* - L_t^*)^2 + (a_0^* - a_t^*)^2 + (b_0^* - b_t^*)^2} \quad (5)$$

where: the subindices "0" and "t" refer to fresh samples and treated samples, respectively.

a_w of the samples was determined at 25 °C with a digital thermohygrometer (AquaLab 3TE, Decagon, USA). Texture was measured as firmness (N) of the product surface using a texturometer (TA-X2T; Stable Micro Systems, Surrey, England) at room temperature according to the methodology of Medeiros et al. (2019), with minor modifications. The parameters used were: a cylindrical probe (TA10) of 20 mm in diameter; pretest and posttest speeds of 1 and 1.5 mm/s, respectively; penetration distance of 2 mm; trigger force of 5 g; and deformation rate of 50%. All tests were carried out in quintuplicate for each sample.

Volumetric shrinkage was determined by measuring the area and thickness of the samples. The area was obtained by free software Image J®1.45 s, which provides the sample area by converting the pixels in the image into real dimensions, from a known scale (Nahimana et al., 2011). The thickness was determined through five different points of the samples with the aid of a digital caliper (Western, DC-6 model, China). The dimensionless volume (β) was determined according to Eq. 6. (Junqueira et al., 2017).

$$\beta = \frac{V_f}{V_0} \quad (6)$$

where: V_f is the apparent volume after osmotic dehydration and drying processing (m^3), and V_0 is the initial volume (m^3).

Ascorbic acid analysis and obtaining of extracts was carried out according to Barcia et al. (2010). For quantification, high-performance liquid chromatography (HPLC, Shimadzu, LC-20AT) equipped with a UV detector (Shimadzu, SPD-20A) was used. A Phenomenex 5 μm C18 column

(250 × 4.6 mm) was used for separation at 30 °C. An aqueous solution of acetic acid 0.15% (v/v) with a flow rate of 1.0 mL/min was used as the mobile phase. Detection was performed at 254 nm. For identification, ascorbic acid peak retention time was compared to standard solutions. The analytical curve was obtained from the standard chromatograms. Standard ascorbic acid concentrations ranged from 1 to 100 mg/L and the results were expressed as µg/g of sample (dry basis – db). The analyses were carried out in quintuplicate.

Carotenoids were extracted with acetone by maceration with Celite® followed by vacuum-filtration. Extraction and quantification was performed according to Matos et al. (2019). The total carotenoids content of the samples were calculated by using the specific extinction coefficient of β-carotene in petroleum ether ($E_{1cm}^{1\%} = 2592$) (Rodriguez-Amaya & Kimura, 2004) and expressed as µg/g of sample (db). The analyses were carried out in triplicate.

Phenolic compounds were estimated following the method of Folin-Ciocalteu, as described by Waterhouse (2002), the absorbance was read at a wavelength of 750 nm, and results were expressed as mg of gallic acid equivalent per 100 g (mg GAEs/100 g db).

The antioxidant activity of fresh and treated samples was determined by the 2,2-diphenyl-1-picrylhydrazyl radical-scavenging activity (DPPH), 2,2'-azino-bis(3-ethylbenzothiazoline-6-sulfonic acid) (ABTS) and β-carotene/linoleic acid methods.

DPPH free radical scavenging ability was carried out according to Brand-Williams et al. (1995). The absorbance readings in a spectrophotometer at 515 nm, and the results were expressed in g/g DPPH db. The ABTS method, followed the procedure developed by Re et al. (1999), where the absorbance was read at a wavelength of 734 nm and the results were expressed as micromoles of Trolox-equivalent per gram (µmol of TEs/g db). The β-carotene method was performed as previously described by Marco (Marco, 1968) and modified by Miller (Miller, 1971), with minor modifications. Absorbance measurements were performed at 2 min and 120 min at 470 nm. Results were expressed as % inhibition of β-carotene oxidation. All readings of antioxidant activity

analyzes (DPPH, ABTS and β-carotene) were performed in the spectrophotometer (SP-22, VIS 325-1000 nm, Biospectro, Taboão da Serra, SP, Brazil).

2.5 Drying operation

For each experiment, 60 g of fresh and osmodehydrated mango slices were placed in a tunnel dryer (Eco Engenharia Educacional, MD018 model, Brazil) with forced air circulation (1.5 m/s) and subjected to drying at 60 °C until the samples reached moisture 13.5 ± 1.6 % (db) (11.9 ± 1.6 % wb). A digital scale (Marte Científica, AD33000 model, São Paulo, Brazil), ± 0.01 g precision, coupled to the dryer sample holder mass was used to measure the mass of the samples during the experiments. For each drying condition, three repetitions were carried out.

To assess the impact of osmotic dehydration and drying, the fresh and pretreated (OD and PVOD) samples and ones subjected to subsequent drying (fresh + D, OD + D and PVOD + D) were analyzed.

2.5.1 Drying curves modeling

The models present below (Eqs. 7–13), classically used to describe the kinetics of thin-layer drying processes (Martins et al., 2017), were fitted by nonlinear regression to the experimental drying data. Coefficient of determination (R^2), root mean square error (RMSE) (Eq. 14), and reduced Chi-squared (χ^2) (Eq. 15) were used to evaluate goodness of fit.

Newton:

$$MR = e^{-k.t} \quad (7)$$

Page:

$$MR = e^{-k.t^n} \quad (8)$$

Modified Page:

$$MR = e^{-(k.t)^n} \quad (9)$$

Henderson and Pabis:

$$MR = a \cdot e^{-k.t} \quad (10)$$

Wang and Singh:

$$MR = 1 + a \cdot t + b \cdot t^2 \quad (11)$$

Logarithmic:

$$MR = a \cdot e^{-k.t} + b \quad (12)$$

Diffusion Approximation:

$$MR = a \cdot e^{-k.t} + (1-a) \cdot e^{-k.b.t} \quad (13)$$

$$RMSE = \left[\frac{1}{N} \Sigma_{i=1}^{N} (V_{exp,i} - V_{pre,i})^2 \right]^{1/2} \quad (14)$$

$$\chi^2 = \frac{\Sigma_{i=1}^{N} (V_{exp,i} - V_{pre,i})^2}{N - n} \quad (15)$$

where: MR is moisture ratio (dimensionless); t is process time (s); a, b, k, and n are constant of the models; $V_{exp,i}$ and $V_{pre,i}$ are the MR determined from the experimental data and predicted by the fitted models, respectively; N is number of experimental measurements and n is number of parameters in the model.

2.5.2 Prediction of effective diffusivity

Convective drying processes are governed by both the external and internal mass transfer, which are commonly modelled by means of diffusion models (García-Pérez et al., 2012). Due to the geometry of the samples used in this study, their behavior was assumed to be similar to an infinite slab; so, a unidirectional mass transport process was considered. Eq. 16 presents a unidirectional diffusion equation based on Fick's law (Crank, 1975).

$$\frac{\partial m(t)}{\partial t} = \frac{\partial}{\partial z}\left(D_{eff} \frac{\partial m(t)}{\partial z} \right) \quad (16)$$

where: $\partial m(t)$ is the amount of water at the time, D_{eff} is the effective diffusivity and z is a generic directional coordinate; the solid sample is considered a 2 L-thick plate; initial conditions include uniform moisture, $m_{(z,0)} = m_0$; boundary conditions include concentration symmetry, $\left.\frac{\partial m(t)}{\partial t}\right|_{z=0}$ and the equilibrium content on the surface of the material, $m_{(L,t)} = m_{eq}$.

Taking into account the initial and boundary conditions, Fick's unidirectional diffusion (Eq. 16) becomes (Eq. 17).

$$MR = \frac{8}{\pi^2} \sum_{i=1}^{\infty} \frac{1}{(2i+1)^2} \exp\left(-(2i+1)^2 \pi^2 D_{eff} \frac{t}{4L^2} \right) = \frac{m(t) - m_{eq}}{m_0 - m_{eq}} \quad (17)$$

where: i is the number of terms in the series, D_{eff} is the effective diffusivity, L is the characteristic length (half the thickness of the sample), t is the time and MR is the quotient of the difference between moisture at a time t (m(t)) and moisture at equilibrium (m_{eq}) and the difference between initial moisture (m_0) and moisture at equilibrium (m_{eq}). The m_{eq} is the point until the sample's mass variation was below 1% (equilibrium condition).

2.5.3 Moisture sorption isotherms

The adsorption and desorption isotherms were obtained at 25 °C in a Vapor Sorption Analyzer (VSA) (Aqualab VSA, Decagon, Puma, WA, USA) equipment, using the DVS (Dynamic Vapor Sorption) method, which is based on the readings of sample mass and a_w successively until the pre-established equilibrium condition is reached (Carmo & Pena, 2019). For the build of the isotherms, the samples of dried mangos were initially stored in desiccator with silica gel under vacuum and at 25 °C for 24 hours to ensure $a_w < 0.1$ in the sample (Souza et al., 2013). After this step,

approximately 1 g of the sample was weighed in a stainless steel capsule, in the analytical microbalance of the VSA. The data were obtained in an adsorption-desorption cycle, for a range of 0.1 to 0.9 a_w. The equilibrium condition was determined when the change in mass per change in time ($\Delta m/\Delta t$) was below 0.10 for three consecutive measures. After the analysis, the dry mass of the sample was determined by vacuum oven drying at 70 °C (AOAC, 2010).

The monolayer moisture content (M_0) for the adsorption and desorption processes was determined through the linearized form of the BET (Eq. 18) (Brunauer et al., 1938).

$$\frac{a_w}{(1-a_w)M} = \frac{1}{M_0 C} + \frac{(C-1)}{M_0 C} a_w \tag{18}$$

where: M is equilibrium moisture (g H_2O/100 g db); a_w is water activity (dimensionless), M_0 is monolayer moisture content (g H_2O/100 g db) and C is constant related to the heat of sorption of the first layer on primary sites.

The GAB mathematical model (Maroulis et al., 1988) (Eq. 19) was adjusted to the experimental moisture sorption data of dried mango, due to it give a good fit for sorption isotherms of several foods (Fan et al., 2019). Goodness of fit was assessed using R^2, RMSE (Eq. 14), and mean relative deviation (P) (Eq. 20).

$$M = \frac{M_0 C K a_w}{(1-Ka_w)(1-Ka_w+CKa_w)} \tag{19}$$

$$P = \frac{100}{N} \sum_{i=1}^{N} \frac{\left| V_{exp,i} - V_{pre,i} \right|}{V_{exp,i}} \tag{20}$$

where: M is equilibrium moisture content (g H_2O/100 g db), M_0 is monolayer moisture content (g H_2O/100 g db), a_w is water activity (dimensionless), K and C are model's parameters, $V_{exp,i}$ and $V_{pre,i}$ are the equilibrium moisture contents determined from the experimental data and predicted by the fitted models, respectively and N is number of experimental measurements.

2.6 Statistical Analysis

Analysis of one-way variance (ANOVA) and Tukey's multicomparison test was performed. Statistically significant differences were reported at $p \leq 0.05$. The drying and sorption models were fitted by non-linear regression and using the Levenberg-Marquardt algorithm with a convergence criterion of 10^{-6}. Statistica v.10.0 (StatSoft, Inc., Tulsa, USA) was used for ANOVA and mathematical modeling.

3 Results and discussion

3.1 Product quality assessment

The instrumental color parameters indicated that the dried products showed higher lightness (Fig. 1A), lower tendency to green (Fig. 1B) and higher tendency to yellow (Fig. 1C) than osmodehydrated and fresh mangos ($p \leq 0.05$). The increase in L^* values for the dried samples was clear and seemed to be a result of carbohydrate uptake (with color) during osmotic pretreatment.

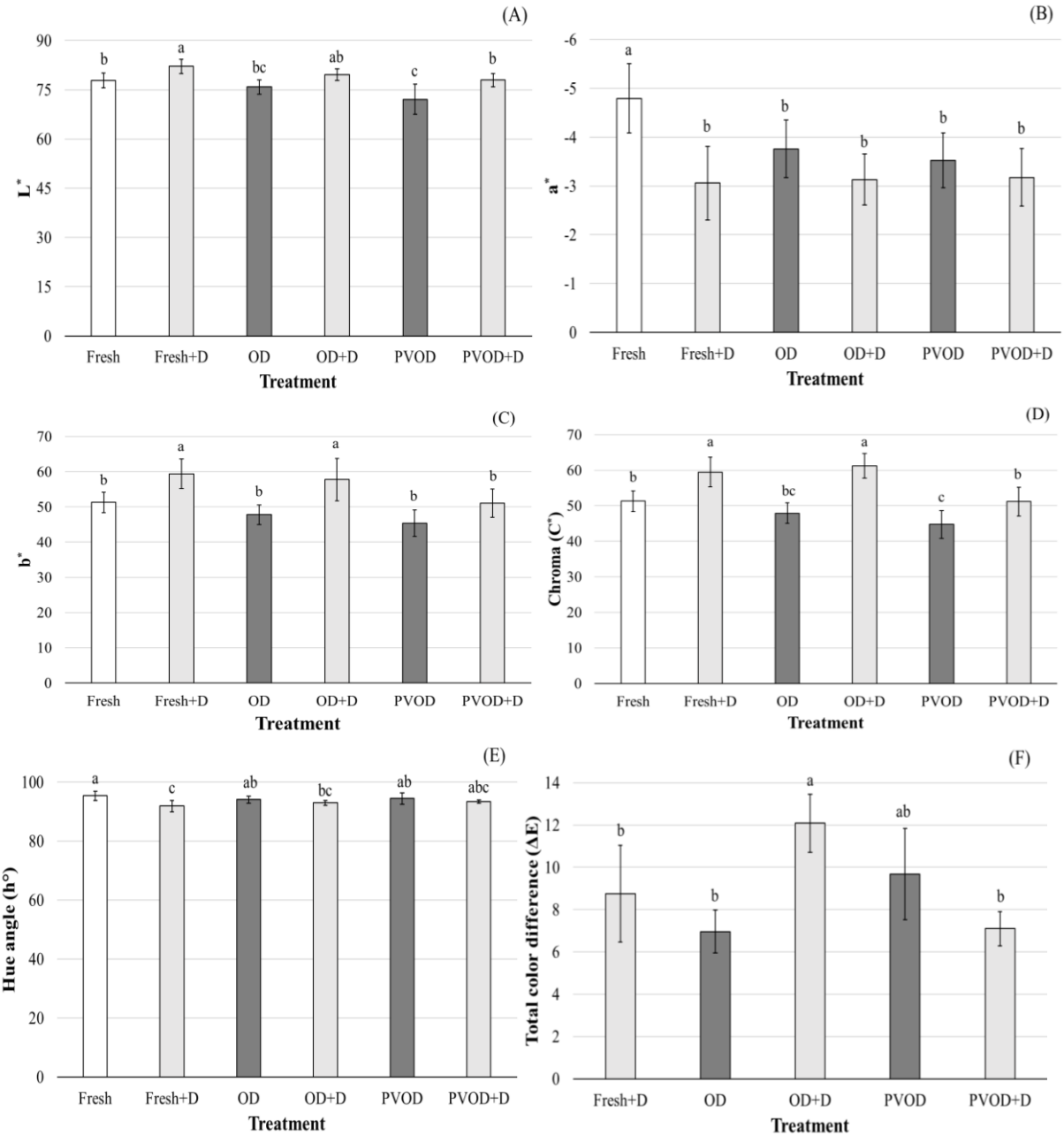
(A)
L*
Treatment
Fresh
Fresh+D
OD
OD+D
PVOD
PVOD+D
(B)
a*
(C)
b*
(D)
Chroma (C*)
(E)
Hue angle (h°)
(F)
Total color difference (ΔE)

Fig. 1. L^* (A), a^* (B), b^* (C), C^*(D), h° (E) and ΔE (F) of mangos subjected to the different treatment conditions; groups with different letters differ significantly ($p \leq 0.05$).

The C^* values show that fresh and dried products had a vivid color (close to 60) (Fig. 1D). The h° values confirm the yellow color of the fruit since the values were close to 90°, with fresh sample lighter yellowish color (Carmo et al., 2019). PVOD sample showed lower L^* (72.10 ± 4.57) and C^* (44.72 ± 3.97) values. According to Tonolli et al. (2019), PVOD treatment can significantly alter L^* and C^* parameters since the possibility of some degradation or loss of fruit pigments during the impregnation process cannot be ruled out.

Regarding the ΔE values, the samples with higher quality are those whose colors are closer to the original color of the fresh sample; therefore, low total color difference values are desired. PVOD + D (7.10 ± 0.80) in isomaltulose solutions presented lower influence the color changes in terms of ΔE in comparison to OD + D sample (12.09 ± 1.37) (Fig. 1F). This can be explained by the effect of sugar on reducing enzymatic browning by preventing oxygen entry (Feng et al., 2019). In this study the PVOD treatment incorporated 13.86 (±1.60%) and OD incorporated 11.01 (±0.07%) of Palatinose®.

Fresh mango sample had a high value of a_w (0.990 ± 0.003) that is a characteristic of fruits and vegetables. a_w values of OD and PVOD samples in isomaltulose solutions did not differ statistically from each other (0.958 – 0.967) and in relation to the untreated sample ($p > 0.05$). In turn, dried mangos slices, had lowest a_w values (0.672 – 0.677) (Fig 2A); although, the values observed for the pretreated samples were slightly higher 0.6, which are not able to ensure the microbiological stability of these samples (Jay, 2005). However, Kroehnke et al. (2021) affirmed that the increase in carbohydrate content, due to osmotic pretreatment, might have a beneficial influence on the microbial stability of the products. The use of high-concentration sugar solutions creates a barrier limiting the growth and adhesion of microorganisms on the sample surface, even in a material with

an a_w value of 0.85. This may result from the reduced mobility of microorganisms due to higher surface viscosity.

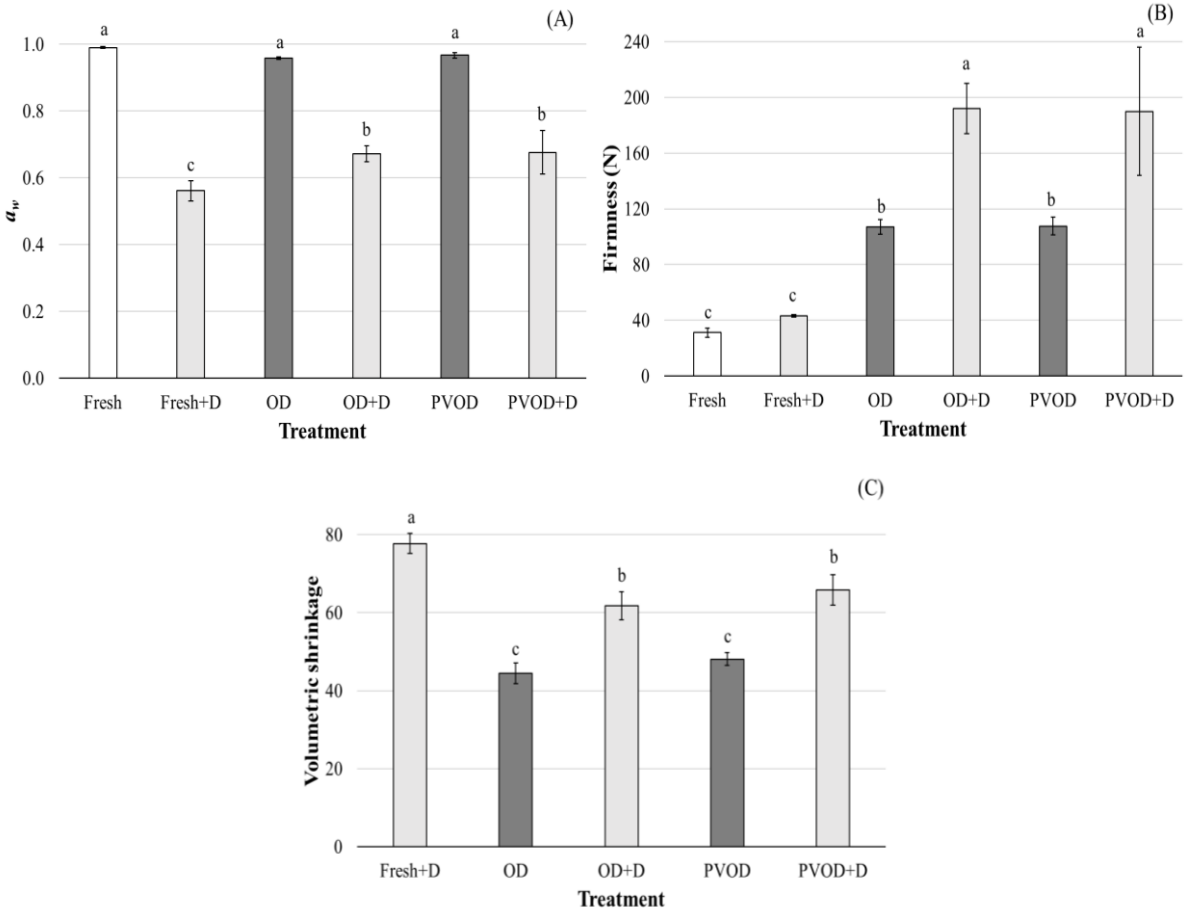

Fig. 2. Water activity (A), firmness (B) and volumetric shrinkage (C) of mangos subjected to the different treatment conditions; groups with different letters differ significantly ($p \leq 0.05$).

In this study, fresh, fresh + D, OD, OD + D, PVOD and PVOD + D presented firmness of 31.1, 43.1, 107.0, 191.9, 107.6 and 189.9 N, respectively. Osmodehydrated samples did not differ from each other, as well as the dried samples ($p > 0.05$) (Fig. 2B). According to Sucheta et al. (2019),

hot air convective drying and solute gain are associated with increase in texture of some foods. This might be related to the osmotic solutes that were incorporated in mangos slices, which formed a dense solid layer on the surface of the product and thus increased the firmness of the samples. Additionally, the water loss is osmotic processes associated with the evaporation of water during drying process could be attributable to increased texture values of dried products (Hunjek et al., 2020).

All treatments exhibited volume reduction (Fig. 2C). The fresh + D sample shrank 77.7%, however, treated dried samples had less shrank than untreated sample (61.8 – 65.6%) and the last ones were not differed statistically ($p > 0.05$). This may be related to the presence of carbohydrate incorporated in the sample, which prevents the rapid evaporation of water, maintaining the structure of the product (Sucheta et al., 2019). The OD and PVOD treatments represented approximately 44.4 and 48.1% of shrinkage, respectively. This can be due to water loss > 40% during the osmotic dehydration and structural changes as mentioned previously.

Nowadays, preserving bioactive compounds is important in osmotic dehydration and drying of fruits. However, during the OD the higher impregnation of solutes might result in lower pigments, as carotenoids (Pan et al., 2003). It occurs because the semipermeable membrane in plant cells may not assure complete isolation from the surroundings. Consequently, minerals, vitamins, and natural dyes may diffuse into the solution. In addition, drying temperature can also contribute for the decreases of these compounds (Devic et al., 2010).

Fig. 3A showed that ascorbic content of the fresh samples (532.1 ± 63.1 μg/g) differed statistically of all other samples ($p \leq 0.05$) and this reduction was of 24% for fresh + D sample; 96 and 74% for OD and OD + D samples, and 41 and 68% for PVOD and PVOD + D samples, in relation to fresh sample. These findings suggested that the PVOD treatments showed less ascorbic acid reduction compared to samples with OD, as reducing exposure to oxygen can minimize oxidization and degradation ascorbic acid (Mendonça et al., 2017).

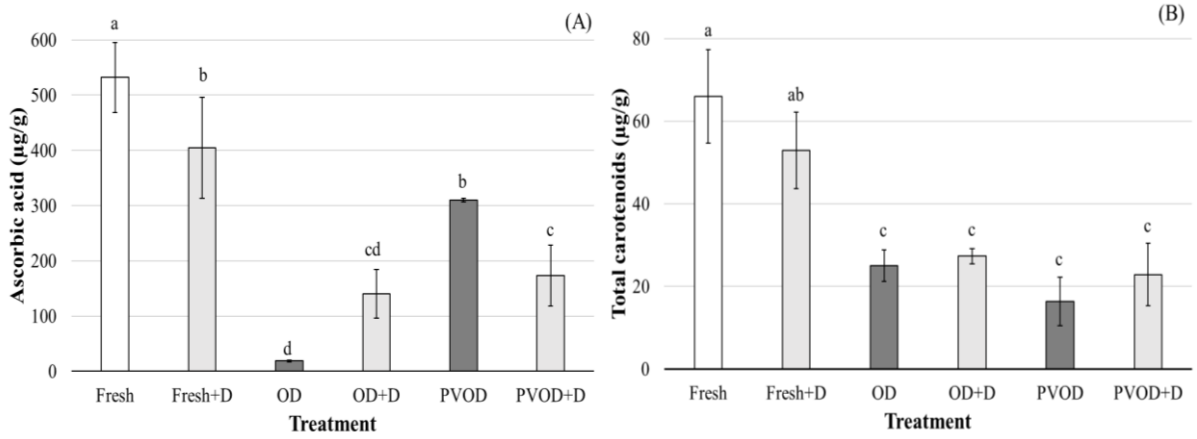

Fig. 3. Ascorbic acid (A) and total carotenoids content (B) in mangos subjected to the different treatment conditions; groups with different letters differ significantly ($p \leq 0.05$).

A significant decrease in carotenoids content was also observed for osmodehydrated (OD = 25.01 ± 3.86 µg/g and PVOD = 16.32 ± 5.90 µg/g) and for dried samples (OD + D = 27.30 ± 1.79 µg/g and PVOD + D = 22.86 ± 7.57 µg/g) in relation to fresh sample (66.00 ± 11.33 µg/g) ($p \leq 0.05$) (Fig. 3B). Mendonça et al. (2017) suggested that this reduction could not be attributed to the leaching flux, since carotenoids are hydrophobic. They are highly unsaturated molecules susceptible to degradation or isomerization followed by cleavage, in particular under the influence of heat and light during processing (Saini et al., 2015). Although changes, no significant decrease was observed when the osmodehydrated samples were submitted to drying ($p > 0.05$). It could be due to carbohydrate incorporation which could protect carotenoids from the excessive heat damage during drying (Carvalho et al., 2014).

Phenolic compounds are abundant in mango and show various activities (Tacias-Pascacio et al., 2022). The total phenolics content (TPC) of fresh mango was 275.48 (± 82.88) mg GAEs/100 g, and not was significantly different of OD + D (260.26 ± 30.49 mg GAEs/100 g) and PVOD + D (311.87 ± 50.86 mg GAEs/100 g) samples ($p > 0.05$). The last ones showed a slight increases and

the literature data suggest that technological processes may lead to the oxidation of phenolic acids as well as hydrolysis of glycosidic and ester bonds, which may result in the release of free phenolic acids and, in consequence, increase their total content (Buchner et al., 2006). On other hand, the concentration of TPC content during the drying cannot be ruled. The reduction in TPC was significantly higher in fresh +D sample (138.81 (± 14.04) mg GAEs/100 g) ($p \leq 0.05$) (Fig. 4A), evidencing that despite the shorter drying time these compounds were better preserved by osmotic treatments.

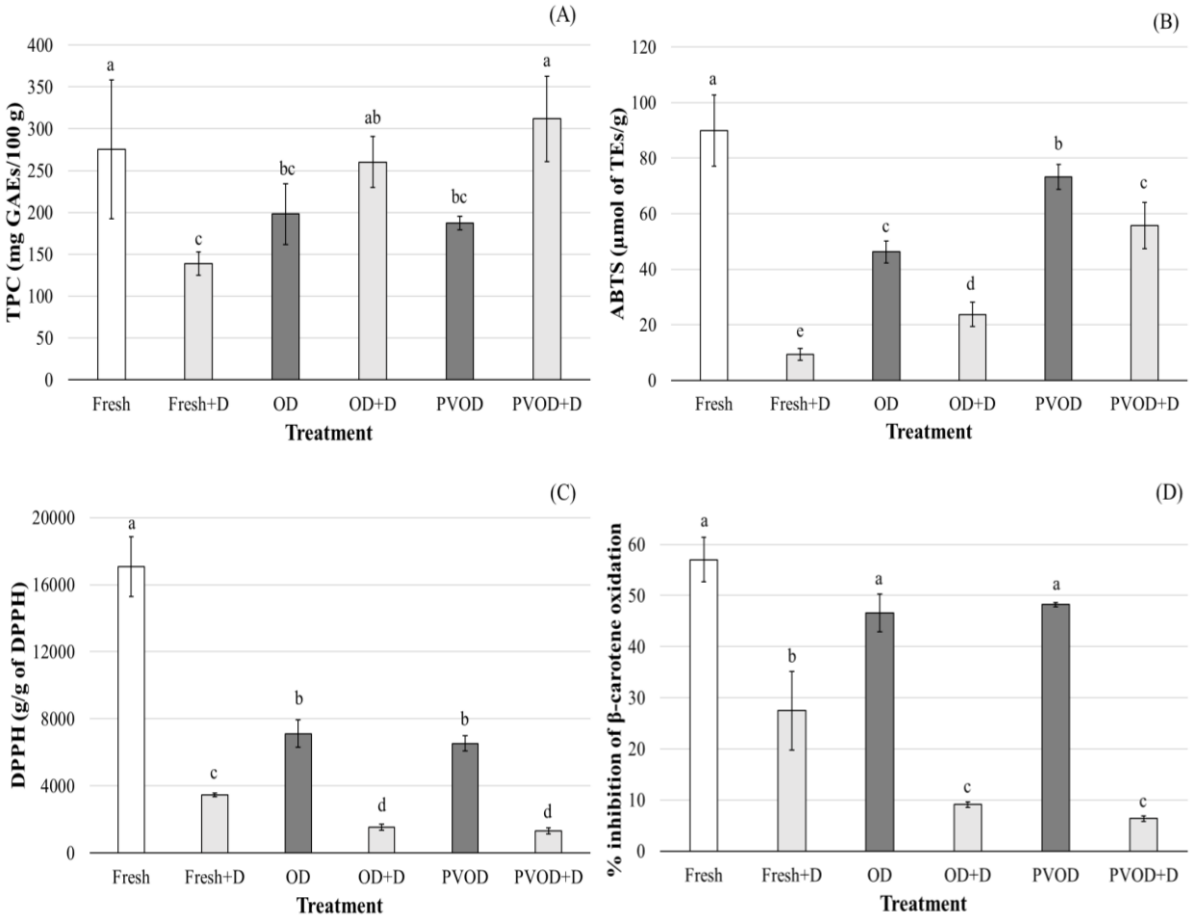

Fig. 4. Total phenolics compounds (A), ABTS (B), DPPH (C) and β-carotene (D) in mangos subjected to the different treatment conditions; groups with different letters differ significantly ($p \leq 0.05$).

Figs. 4B, 4C and 4D show antioxidant activity of untreated and pretreated mangos. The fresh fruit had 90.00 (± 12.87) μmol of TEs/g, 17,078.26 (± 1,783.80) g/g DPPH, and 57.02 (±4.35) % inhibition of β-carotene oxidation. The pretreated osmotically samples ranged narrow for ABTS (46.25 – 73.21 μmol of TEs/g), DPPH (6537.80 – 7119.50 g/g DPPH), and β-carotene/linoleic acid method (46.26 – 48.21% inhibition of β-carotene oxidation). Osmodehydrated samples did not differ from each other ($p > 0.05$), except for ABTS method. For dried samples, according to DPPH and β-carotene/linoleic acid method, OD + D and PVOD + D had at least 50% lower antioxidant activity than fresh + D sample. It could be due to leakage of these compounds to the osmotic solution, as mentioned previously.

Antioxidant activity of fresh mangos fruit comes from the presence of ascorbic acid, carotenoids and total phenolic compounds. So, the analyzes of DPPH, ABTS and β-carotene/linoleic acid methods showed the same tendency of these compounds: decreased for pretreated osmotically or dried samples ($p \leq 0.05$) or had a weak impact for the dried products ($p > 0.05$) in relation to fresh sample.

3.2 Drying experiment and moisture sorption isotherms

OD and PVOD pretreatments reduced the initial moisture content of mangos to 62.33 ± 0.98 % and 62.03 ± 1.05 %, respectively. On the other hand, lower water diffusivity values were observed to the pretreated samples ($D_{effOD} = 2.13 \cdot 10^{-10}$ m^2/s and $D_{effPVOD} = 2.45 \cdot 10^{-10}$ m^2/s, respectively) in relation to the untreated sample ($3.90 \cdot 10^{-10}$ m^2/s) ($p \leq 0.05$), which favored an increase in the drying time (Fig. 5). The drying time required to eliminate 83% of the initial moisture content of the

mangos without pretreatment was 170 ± 10 min. The air-drying time increased when the pretreatments were carried out with isomaltulose solution in OD + D (233 ± 6 min) and PVOD +D (293 ± 11 min). This behavior can be attributed to the fact that the pretreatments incorporated (solid gain) 11.01% of Palatinose® in OD and 13.86% in PVOD, as mentioned previously. Thus, the incorporation of 25% more of this carbohydrate increased around 60 min. of drying time on PVOD + D. According to Fernandes et al. (2019), soluble solids on the boundary between the fruit and the osmotic solution create an even denser structure that raised the mass transfer resistance and reduced the mobility of water during air drying.

Table 1 shows that all models were able to accurately predict the drying kinetic of product studied, since had $R^2 \geq 0.984$ and low RMSE (≤ 0.104) and χ^2 ($\leq 1.7 \cdot 10^{-3}$) values, except Wang and Singh model. Thus, the Page model has been chosen, since is relatively simple and it is widely used for thin-layer drying kinetics of several fruits and vegetables (Onwude et al., 2016) (Fig. 5).

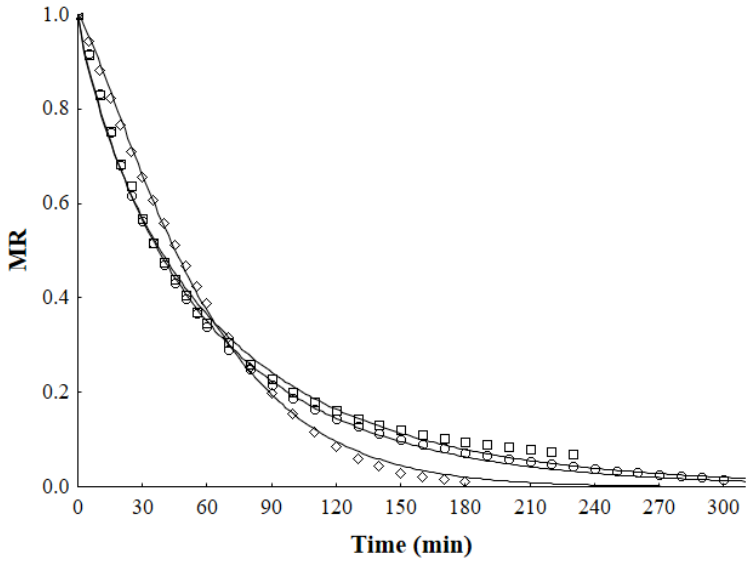

Fig. 5. Experimental values of the moisture ratio (MR) of fresh + D (◇), OD + D (□) and PVOD + D (○) samples over time at 60 °C. Predicted values using the Page model (line).

Table 1. Parameters of mathematical modeling of kinetics of drying processes to the experimental drying data.

Model	Parameters	Samples		
		Fresh + D	**OD + D**	**PVOD + D**
Newton	***k***	0.016	0.017	0.017
	$\mathbf{R^2}$	0.984	0.985	0.994
	$\boldsymbol{\chi^2}$	$1.7 \cdot 10^{-3}$	$1.1 \cdot 10^{-3}$	$5.0 \cdot 10^{-4}$
	RMSE	0.0399	0.0297	0.0196
Page	***k***	0.006	0.032	0.028
	n	1.250	0.842	0.880
	$\mathbf{R^2}$	0.999	0.997	0.999
	$\boldsymbol{\chi^2}$	$1.4 \cdot 10^{-4}$	$3.2 \cdot 10^{-4}$	$1.2 \cdot 10^{-4}$
	RMSE	0.0114	0.0172	0.104
Modified Page	***k***	0.016	0.017	0.018
	n	1.250	0.842	0.880
	$\mathbf{R^2}$	0.999	0.996	0.999
	$\boldsymbol{\chi^2}$	$1.4 \cdot 10^{-4}$	$3.2 \cdot 10^{-4}$	$1.2 \cdot 10^{-4}$
	RMSE	0.0114	0.0172	0.104
Henderson and Pabis	***a***	1.063	0.954	0.967
	k	0.018	0.016	0.017
	$\mathbf{R^2}$	0.990	0.988	0.995
	$\boldsymbol{\chi^2}$	$1.2 \cdot 10^{-3}$	$9.5 \cdot 10^{-4}$	$4.1 \cdot 10^{-4}$
	RMSE	0.0328	0.0297	0.0196
Wang and Singh	***a***	-0.012	-0.012	-0.010
	b	$3.9 \cdot 10^{-5}$	$3.7 \cdot 10^{-5}$	$2.5 \cdot 10^{-5}$

	$\mathbf{R^2}$	0.999	0.930	0.870
	$\boldsymbol{\chi^2}$	$8.1 \cdot 10^{-5}$	$5.6 \cdot 10^{-3}$	$1.1 \cdot 10^{-2}$
	RMSE	0.0087	0.0331	0.0218
Logarithmic	***a***	1.146	0.925	0.956
	k	0.014	0.020	0.019
	c	-0.117	0.073	0.033
	$\mathbf{R^2}$	0.998	0.999	0.999
	$\boldsymbol{\chi^2}$	$2.5 \cdot 10^{-4}$	$3.9 \cdot 10^{-5}$	$1.1 \cdot 10^{-4}$
	RMSE	0.0148	0.0060	0.0100
Diffusion Approximation	***a***	-84.159	0.8225	0.640
	k	0.030	0.023	0.026
	b	0.992	0.186	0.365
	$\mathbf{R^2}$	0.999	0.999	0.999
	$\boldsymbol{\chi^2}$	$1.4 \cdot 10^{-4}$	$1.4 \cdot 10^{-5}$	$1.1 \cdot 10^{-5}$
	RMSE	0.0110	0.0036	0.0031

Fresh + D is fresh fruit subjected to drying, OD + D is osmodehydrated fruit at 101.3 kPa subjected to drying, PVOD + D is osmodehydrated fruit at 48 kPa subjected to drying, D_{eff} is the effective diffusivity; a, b, c, k, and n are constant of the models; R^2 is coefficient of determination; χ^2 is reduced Chi squared and RMSE is root mean square error.

The moisture sorption isotherms of Fig. 6 show that the OD + D and PVOD + D samples had lower moisture content than the fresh + D for a constant a_w at 25 °C, with a maximum moisture content (a_w= 0.9) of 33.33, 37.16 and 62.97 g/100 g H_2O db, respectively. The lower affinity for the water molecules of the first ones can be due to Palatinose® incorporation in the mango fruit. These results indicated that the addition of Palatinose® through osmotic processes of OD and PVOD reduced the equilibrium moisture on 47% and 41%, respectively, in relation to untreated sample; showing the greater impact of this carbohydrate on improve the stability of dried fruits.

The moisture adsorption isotherms indicated that fresh + D, OD + D and PVOD + D are microbiologically stable (a_w < 0.6) (Jay, 2005) when stored at 25 °C if their moisture levels are 12.8% db (11.3 % wb), 6.7% db (6.3 % wb) and 7.2% db (6.7 % wb), respectively. These results indicate fresh + D required greater care during storage and handling.

According to the quantitative criteria proposed by Yanniotis & Blahovec (2009) for the classification of moisture sorption isotherms, the fresh + D and OD + D adsorption isotherms behaved as type III, however, the behavior of the desorption isotherm changed and it behaved as more solution-like type-II isotherm. On other hand, for PVOD + D product, both adsorption and desorption processes were classified as more solution-like type-II isotherms. These type of moisture sorption isotherms have been observed for other dried fruits (Sormoli & Langrish 2015). The hysteresis loop observed between the moisture adsorption and desorption isotherms comprehended the monolayer region until approximately 0.8 a_w for fresh + D and OD + D samples (Fig. 6). However, for OD + D, the loop is narrow, while for PVOD + D hysteresis was not observed. According to Caurie (2007), a decrease in the hysteresis loop or its complete absence has been related to greater product stability during storage. Thus, the pretreated mangos were more stables than untreated samples, highlighting the samples subjected to vacuum, which were considered more stable among the pretreateds.

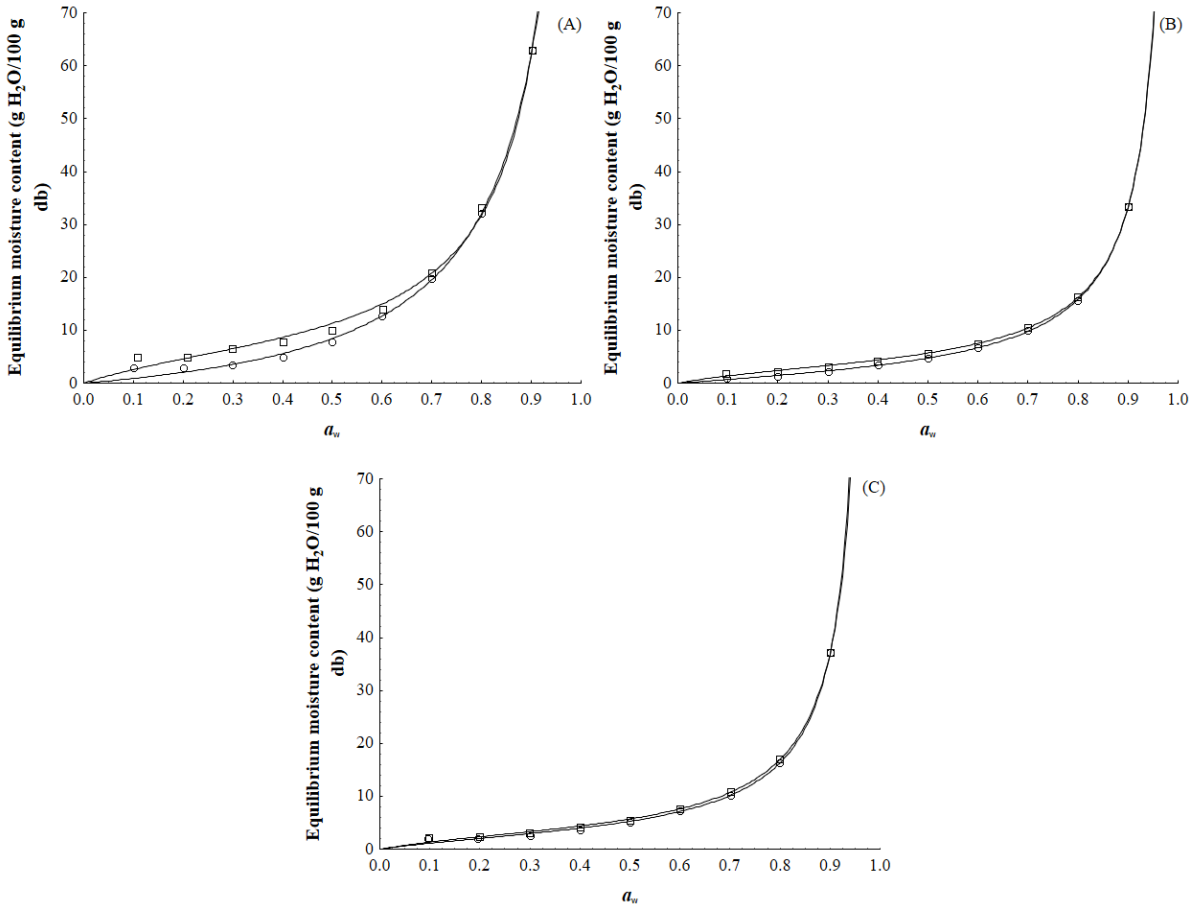

Fig. 6. Moisture sorption isotherms of fresh + D (A), OD + D (B) and PVOD + D (C) samples. Experimental adsorption (○) and desorption (□) values and predicted values at 25 °C using the GAB model (line).

BET equation showed that the monolayer moisture contents (M_0) were 2.39, 2.37 and 1.68 g H_2O/100 g db for adsorption and 4.87, 3.29 and 2.21 g H_2O/100 g db for desorption, for the mango without and with OD and PVOD pretreatment, respectively (R^2 > 0.950). M_0 decreased for pretreated product due to presence of isomaltulose. Similar behavior was also observed with

sucrose solution in mangos (Zhao et al., 2018). According to Labuza (1984), foods with $M_0 \leq 10\%$ db are considered stable. Thus, the both dried mangos were considered products with good stability. Table 2 presents the values of the statistics used to assess goodness of GAB model fit (R^2, P and RMSE), which show that the GAB model was suitable to describe the moisture adsorption and desorption isotherms of untreated and pretreated dried mangos at 25 °C. The isotherms generated by the GAB model are presented in Fig 6. GAB model showed also good fits to the moisture sorption data of another dried products, such as mango, apple, fried purple-fleshed, sweet potato slices and mushroom (Falade & Aworh, 2004; Prothon & Ahrne, 2004; Fan et al., 2019; Engin, 2020).

Table 2. Parameters of GAB mathematical model fitted of moisture sorption data of dried mango.

Parameters	**Samples**					
	Fresh + D		**OD + D**		**PVOD + D**	
	Ads	**Des**	**Ads**	**Des**	**Ads**	**Des**
M_0	10.57	7.00	3.62	3.39	3.22	3.40
C	0.79	4.53	1.94	5.22	4.01	4.86
K	0.95	0.99	1.00	1.00	1.02	1.02
R^2	0.998	0.998	0.999	0.999	0.999	0.999
P (%)	13.78	9.54	5.34	5.26	9.38	6.85
RMSE	0.79	1.06	0.13	0.21	0.38	0.31

Fresh + D is fresh fruit subjected to drying, OD + D is osmodehydrated fruit at 101.3 kPa subjected to drying, PVOD + D is osmodehydrated fruit at 48 kPa subjected to drying, Ads is adsorption, Des is desorption, M_0 is monolayer moisture content (g H_2O/100 g d.b), K and C are model's parameters, R^2 is coefficient of determination; P is mean relative deviation and RMSE is root mean square error.

The adsorption isotherms of dried products showed linear behavior up to a_w of 0.5 for fresh + D and up to a_w of 0.6 for OD + D and PVOD + D samples. After these levels of a_w the moisture

content of the products increased exponentially (Fig. 6). According to Saltmarch & Labuza (1980), this behavior can be attributed to the dissolution of crystalline sugar at low a_w and the conversion of crystalline sugar into amorphous sugar at high a_w. Thus, it is possible to state that the dried products require greater care when stored or handled in an environment with relativity humidity (RH) above 50% for the mango without pretreatment and RH above 60% for the mango with OD and PVOD pretreatments. In these RH conditions is recommended to store the dried products in packaging with low water vapor permeability (Carmo et al., 2019). Additionally, these products present bioactive compounds such as ascorbic acid, carotenoids and total phenolics (Figs. 3 and 4) in their composition, which makes them susceptible to oxidative processes. Therefore, in order to minimize such processes, it is strongly indicated that the packages have also impermeability to air and does not allow light to pass through (Costa et al., 2018).

In general, considering lower technical viability and the higher costs involved with both processes, the OD and PVOD pretreatment could be considered not satisfactory, from an industrial point of view. On other hand, the incorporation of isomaltulose resulted in a less hygroscopic products compared to the fresh one, as can be seen through the sorption isotherms (Fig 6). This fact guaranteed products with shelf-life more extended, than untreated sample. Additionally, the incorporation of isomaltulose can be a promising substitute to sucrose on osmotic processes, resulting in a final product with healthy attributes.

4 Conclusions

The study of osmotic dehydration with and without pulsed vacuum was carried out on mangos slices with the incorporation of a healthy carbohydrate (Palatinose®) for the first time. The results revealed that PVOD treatment presented advantages before and after drying convective compared to OD, such as lower loss of ascorbic acid and smaller changes color. Bioactive compounds and antioxidant activity showed the same tendency: decreased for pretreated osmotically or dried

samples or had a weak impact for the dried products in relation to fresh sample. The pretreated samples showed lower water diffusivity and higher time drying than fresh samples. It can be due to greater incorporation of Palatinose® carbohydrate in the mangos with PVOD (14%) in relation to the OD (11%). The hygroscopic study via sorption isotherms behaved type II and type III. The microbiological stability indicated that fresh + D requires greater care during storage and handling. From hysteresis loop observation, the pretreated mangos were more stables than untreated samples, highlighting the mangos subjected to vacuum, which were considered more stable among the pretreated samples.

Conflict of interest

There are no conflicts of interest.

Acknowledgments

The authors thank the following Brazilian agencies for financial support: National Council for Scientific and Technological Development (CNPq) (314191/2021-6) and Fundação de Amparo à Pesquisa do Estado de Minas Gerais (FAPEMIG) J. R. Carmo (grant 166378/2018-6).

References

Abrahão, F. R., & Corrêa, J. L. G. (2021). Osmotic dehydration: More than water loss and solid gain. *Crit. Rev. Food Sci. Nut.,* 29, 1–20. https://doi.org/ 10.1080/10408398.2021.198376

Association of Official Analytical Chemists – AOAC. (2010). *Official methods of analysis of association of Official Analytical Chemists International* (18th ed.). Arlington: AOAC.

Barcia, M. T., Jacques, A. C., *Becker, Pertuzatti, P. B., & Zambiazi, R. C. (2010).* Determination by HPLC of ascorbic acid and tocopherols in fruits. *Semina: Ciênc. Agr.*, 31, 381–390. https://dx.doi.org/10.5433/1679-0359.2010v31n2p381

Brunauer, S., Emmet, T. H., & Teller, F. (1938). Adsorption of gases in multimolecular layers. *J. Am. Oil Chem. Soc.*, 60, 309–319. ttps://doi.org/10.1021/ja01269a023

Buchner, A., Krumbein, S., Rohn, L. W., & Kroh. (2006). Effect of thermal processing on the flavonols rutin and quercetin. *Rapid Commun. Mass Spectrom.*, 20, 3229–3235. https://doi.org/10.1002/rcm.2720.

Carmo, J. R., & Pena, R. S. (2019). Influence of the temperature and granulometry on the hygroscopic behavior of tapioca flour. *CyTA – J. Food*, 17, 900–906. https://doi.org/10.1080/19476337.2019.1668860

Carmo, J. R., Corrêa, J. L. G., Polachini, T. C., & Telis-romero, J. (2022). Properties of Isomaltulose (Palatinose®) – an emerging healthy carbohydrate: effect of temperature and solute concentration. *J. Mol. Liq.*, 347, 118304. https://doi.org/10.1016/j.molliq.2021.118304

Carmo, J. R., Costa, T. S., & Pena, R. S. (2019) Tucupi-added mayonnaise: Characterization, sensorial evaluation, and rheological behavior. *CyTA – J. Food*, 17, 479–487, https://10.1080/19476337.2019.1607561

Carvalho, L. M. J. D., Smiderle, L. D. A. S. M., Carvalho, J. L. V. D., Cardoso, F. D. S. N., & Koblitz, M. G. B. (2014). Assessment of carotenoids in pumpkins after different home cooking conditions. *Food Sci. Technol.*, 34, 365–370. https://doi.org/10.1590/fst.2014.0058.

Caurie, M. (2007). Hysteresis phenomenon in foods. *Int. J. Food Sci. Technol.*, 42, 45–49. https://doi.org/10.1111/j.1365-2621.2006.01203.x

Ciurzyńska, A., Kowalska, H., Czajkowska, K., & Lenart, A. (2016). Osmotic dehydration in production of sustainable and healthy food. *Trends Food Sci. Technol.*, 50, 186–192. https://doi.org/10.1016/j.tifs.2016.01.017

Corrêa, J. L. G., Ernesto, D. B., Alves, J. G. L. F., & Andrade, R. S. (2014). Optimisation of vacuum pulse osmotic dehydration of blanched pumpkin. *Int. J. Food Sci. Technol.*, 49, 2008–2014. https://doi.org/ 10.1111/ijfs.12502

Corrêa, J. L. G., Pereira, L. M., Vieira, G., & Hubinger, M. D. (2010). Mass transfer kinetics of pulsed vacuum osmotic dehydration of guavas. *J. Food Eng.*, 96, 498–504. https://doi.org/10.1016/j.jfoodeng.2009.08.032

Costa, T. S., Carmo, J. R., & Pena, R. S. (2018). Powdered tucupi condiment: Sensory and hygroscopic. *Food Sci. Technol.*, 38, 33–40. https://doi.org/10.1590/1678-457X.36816

Crank, J. *The Mathematics of diffusion*. 2 ed. Oxford: Carendon press ed., 1975.

Devic, E., Guyot, S., Daudin, J., & Bonazzi, C. (2010). Effect of temperature and cultivar on polyphenol retention and mass transfer during osmotic dehydration of apples. *J. Agri. Food Chem.*, 58, 606–614. https://doi.org/10.1021/ jf903006g

Engin, D. (2020). Effect of drying temperature on color and desorption characteristics of oyster mushroom. *Food Sci. Technol.*, 40, 187–193. https://doi.org/10.1590/fst.37118

Falade, K. O., & Aworh, O. C. (2004). Adsorption isotherms of osmo-oven dried african star apple (*Chrysophyllum albidum*) and african mango (*Irvingia gabonensis*) slices. *Eur. Food Res.Technol.*, 218, 278–283. https://dx.doi.org/10.1007/s00217-003-0843-8

Fan, K., Zhang, M., & Bhandari. (2019). Osmotic-ultrasound dehydration pretreatment improves moisture adsorption isotherms and water state of microwave-assisted vacuum fried purple-fleshed sweet potato slices. *Food Bioprod. Process.*, 115, 154–164. https://doi.org/10.1016/j.fbp.2019.03.011

Feng, Y., Yu, X., ElGasim, A., Yagou, A., Xu, B., Wu, B., Zhang, L., & Zhou, C. (2019). Vacuum pretreatment coupled to ultrasound assisted osmotic dehydration as a novel method for garlic slices dehydration, *Ultrason. – Sonochem.*, 50, 363–372. https://doi.org/10.1016/j.ultsonch.2018.09.038

Garcia-Noguera, J., Oliveira, F. I. P., Gallão, M. I., Weller, C. L., Rodrigues, S., & Fernandes, F. A. N. (2010). Ultrasound-assisted osmotic dehydration of strawberries: Effect of pretreatment time and ultrasonic frequency. *Dry. Technol.*, 28, 294–303. https://doi.org/10.1080/07373930903530402

García-Pérez, J. V., Ortuño, C., Puig, A., Cárcel, J. A., & Pérez-Munuera, I. (2012). Enhancement of water transport and microstructural changes induced by highintensity ultrasound application on orange peel drying. *Food Bioprocess Technol.*, 5, 2256–2265. https://doi.org/10.1007/s11947-011-0645-0

Hunjek, M., Repajic, M., Scetar, S., Karlovic, N., Vahcic, D., Jezek, D., Galić, K., Levaj, B. (2020). Effect of anti-browning agents and package atmosphere on the quality and sensory fresh-cut Birgit and Lady Claire potato during storage at different temperatures. *J. Food Process. Preserv.*, 44, e14391. https://doi.org/10.1111/jfpp.14391

Jay, M. J. (2005). *Microbiologia de alimentos* (6th ed.). Porto Alegre, Brasil: Artmed.

Junqueira, J. R. J., Corrêa, J. L. G., & Mendonça, K. S. (2017). Evaluation of the shrinkage effect on the modeling kinetics of osmotic dehydration of sweet potato (*Ipomoea batatas* (L.)). *J. Food Process. Preserv.*, 41, e12881. https://doi.org/10.1111/jfpp.1288

Junqueira, J. R., Corrêa, J. L. G., Mendonça, K. M., Mello Junior, R. E., & Souza, A. U. (2021). Modeling mass transfer during osmotic dehydration of different vegetable structures under vacuum conditions. *Food Sci. Technol.*, 41, 439–448. https://doi.org/10.1590/fst.02420

Khuwijitjaru, P., Somkane, S., Nakagawa, K., & Mahayothee, B. (2022). Osmotic dehydration, drying kinetics, and quality attributes of osmotic hot air-dried mango as affected by initial frozen storage. *Foods*, 11, 489. https://doi.org/10.3390/foods11030489

Kroehnke, J., Szadzinska, J., Radziejewska-Kubzdela, E., Bieganska-Marecik, R., Musielak, G., & Dominik Mierzwa. (2021). Osmotic dehydration and convective drying of kiwifruit

(*Actinidia deliciosa*) – The influence of ultrasound on process kinetics and product quality Joanna *Ultrason. – Sonochem.*, 71, 105377. https://doi.org/10.1016/j.ultsonch.2020.105377

Labuza, T. P. (1984). Application of chemical kinetics to deterioration of foods. *J. Chem. Educ.*, 61, 348–358. https://dx.doi.org/10.1021/ed061p348

Lopez, M. M. L., Morais, R. M. S. C., & Morais, A. M. M. B. (2020). Flavonoid enrichment of fresh-cut apple through osmotic dehydration-assisted impregnation. *Brit. Food J.l*, 123, 820–832. https://doi.org/10.1108/BFJ-03-2020-0176

Macedo, L. L., Corrêa, J. L. G., Araújo, C. S., Vimercati, W. C., & Petri Junior, I. (2021). Convective drying with ethanol pre-treatment of strawberry enriched with isomaltulose. *Food Bioprocess Technol.*, 14, 2046–2061. https://doi.org/10.1007/s11947-021-02710-2

Marco, G. J. (1968). A rapid method for evaluation of antioxidants. *J. Am. Oil Chem. Soc.*, 45, 594–598. http://dx.doi.org/10.1007/BF02668958

Maroulis Z. B., Tsami, E., Arinos-Kouris, D., & Saravacos, G. D. (1988). Application of the GAB model to the sorption isotherms for dried fruits. *J. Food Eng.*, 7, 63–78. https://doi.org/10.1016/0260-8774(88)90069-6

Martins, M. G., Pena, R. S. (2017). Combined osmotic dehydration and drying process of pirarucu (*Arapaima gigas*) fillets. *J. Food Sci. Technol*., 54, 3170–3179.doi: 10.1007/s13197-017-2755-9

Matos, K. A. N., Lima, D. P., Barbosa, A. P. P., Mercadante, A. Z., & Renan Campos Chisté. (2019). Peels of tucumã (*Astrocaryum vulgare*) and peach palm (*Bactris gasipaes*) are by-products classified as very high carotenoid sources. *Food Chem.*, 272, 216–221. https://doi.org/10.1016/j.foodchem.2018.08.053

Medeiros, R. A. B., Silva Júnior, E. V., Silva, J. H. F., Ferreira Neto, O. C., Brandão, S. C. R., Barros, Z. M. P. Rocha, O. R. S., & Azoubel, P. M. Effect of different grape residues

polyphenols impregnation techniques in mango. *J. Food Eng.*, 262, 1–8. https://doi.org/10.1016/j.jfoodeng.2019.05.011

Mendonça, K. S., Corrêa, J. L. G., Junqueira, J. R., J., Cirillo, M. A., Figueira, F. V., & Carvalho, E. E. N. (2017). Influences of convective and vacuum drying on the quality attributes of osmo-dried pequi (*Caryocar brasiliense* Camb.) slices. *Food Chem.*, 224, 212–218. https://doi.org/10.1016/j.foodchem.2016.12.051

Miller, H. E. (1971). A simplified method for the evaluation of antioxidant. *J. Am. Oil Chem. Soc.*, 48, 91–97. http://dx.doi.org/10.1007/BF02635693.

Nahimana, H., Zhang, M., Mujumdar, A. S., & Zhansheng, D. (2011). Mass transfer modeling and shrinkage consideration during osmotic dehydration of fruits and vegetables. *Food Reviews Int.*, 10, 15327–15345. https://doi.org/10.1080/87559129.2010.518298

Onwude D. I., Hashim N., Janius R. B., Nawi N. M., & Abdan K. (2016). Modeling the thin-layer drying of fruits and vegetables: A review. *Compr. Rev. Food Sci. Food Saf.*, 15, 599–618. https://doi.org/10.1111/1541-4337.12196.

Pan, Y. K., Zhao, L. J., Zhang, Y., Chen, G., & Mujumdar, A. S. (2003). Osmotic dehydration pretreatment in drying of fruits and vegetables. *Dry. Technol.*, 21, 1101–1114. https://doi.org/10.1081/DRT-120021877

Prothon, F., & Ahrne, L. M. (2004). Application of the Guggenheim, Anderson and De Boer model to correlate water activity and moisture content during osmotic dehydration of apples. *J. Food Eng.*, 61, 467–470. https://dx.doi.org/10.1016/ S0260-8774(03)00119-5

Re, R., Pellegrini, N., Proteggente, A., Pannala, A., Yang, M., & RiceEvans, C. (1999). Antioxidant activity applying an improved ABTS radical cation decolorization assay. *Free Rad. Biol. Med.*, 26, 1231–1237. http://dx.doi.org/10.1016/S0891-5849(98)00315- 3.

Rodriguez-Amaya, D. B., & Kimura, M. (2004). HarvestPlus handbook for carotenoid analysis. HarvestPlus ed. Washington, DC and Cali: International Food Policy Research Institute (IFPRI) and International Center for Tropical Agriculture (CIAT).

Sagar, V. R., & Kumar, P. S. (2010). Recent advances in drying and dehydration of fruits and vegetables: A review. *J. Food Sci. Technol.*, 47, 15–26. https://doi.org/10.1007/s13197-010-0010-8

Saini, R. K., Nile, S. H., & Park, S. W. (2015). Carotenoids from fruits and vegetables: Chemistry, analysis, occurrence, bioavailability and biological activities. *Food Res. Int.*, 76(Pt 3), 735–750. https://doi.org/10.1016/j.foodres.2015.07.047

Saltmarch, M., & Labuza, T.P. (1980). Influence of relative humidity on the physico-chemical state of lactose in spray-dried sweet whey powders. *J. Food Sci.*, 45, 1231–1236. https://doi.org/10.1111/j.1365-2621.1980.tb06528.x

Seguí, L., Fito, P. J., & Fito, P. (2012). Understanding osmotic dehydration of tissue structured foods by means of a cellular approach. *J. Food Eng.*, 110, 240–247. https://doi.org/10.1016/j.jfoodeng.2011.05.012

Sirijariyawat, A., Charoenrein, S., & Barrett, D. M. (2012). Texture improvement of fresh and frozen mangoes with pectin methylesterase and calcium infusion. *J. Sci. Food Agri.*, 92, 2581–2586. https://doi.org/10.1002/jsfa.5791

Sormoli, M. E., & Langrish, T. A. (2015). Moisture sorption isotherms and net isosteric heat of sorption for spray-dried pure orange juice powder. *LWT – Food Sci. Technol.*, 62, 875–882. https://doi.org/10.1016/j.lwt.2014.09.064

Souza, T. C. L., Souza, H. A. L., & Pena, R. S. (2013). A rapid method to obtaining moisture sorption isotherms of a starchy product. *Starch*, 65, 433–436. https://doi.org/10.1002/star.201200184

Sucheta, Chaturvedi, K., & Yadav, S. K. (2019) Ultrasonication assisted salt-spices impregnation in black carrots to attain anthocyanins stability, quality retention and antimicrobial efficacy on hot-air convective drying. *Ultrason. – Sonochem.*, 58, 104661. https://doi.org/10.1016/j.ultsonch.2019.104661

Tacias-Pascacio V. G., Castañeda-Valbuena D., Fernandez-Lafuente R., Berenguer-Murcia Á., Meza-Gordillo R., Gutiérrez L.-F., Pacheco N., Cuevas-Bernardino J.C., & Ayora-Talavera T. (2022). Phenolic compounds in mango fruit: A review. *J. Food Meas. Charact.*, 16, 619–636. https://doi.org/10.1007/s11694-021-01192-2.

Tonolli, P. N., Franco, F. F., & Silva, A. F. G. (2019). A construção histórica do conceito de enzima e sua abordagem em livros didáticos de biologia. *História, Ciências, Saúde – Manguinhos*, 28, 27–744. 2019. https://doi.org/10.1590/S0104-59702021000300006

Viana, A. D., Corrêa, J. L. G., & Justus, A. (2014). Optimisation of the pulsed vacuum osmotic dehydration of cladodes of fodder palm. *Int. J. Food Sci. Technol.*, 49, 726–732. https://doi.org/10.1111/ijfs.12357

Waterhouse, A. L. (2002). *Polyphenolics: determination of total phenolics in current protocols in food analytical chemistry*. New York: John Wiley & Sons.

Yanniotis, S., & Blahovec, J. (2009). Model analysis of sorption isotherms. *LWT – Food Sci. Technol.*, 42, 1688-1695. http:// dx.doi.org/10.1016/j.lwt.2009.05.010.

Zhao, J-H., Ding, Y., Yuan, Y-J., Xiao, H-W., Zhou, C-L., Tan2, M-L., & Tang, X-M. (2018). Effect of osmotic dehydration on desorption isotherms and glass transition temperatures of mango. *Int. J. Food Sci. Technol.*, 53, 2602–2609. https://doi.org/10.1111/ijfs.13855

THIRD SECTION

GENERAL CONCLUSION

The application of different types of osmotic dehydration on mangos slices was evaluated. This technique aimed to enrich the fruit with a healthy carbohydrate. Isomaltulose (Palatinose®) was chosen due to following advantages: non-cariogenic, low glycemic and insulinemic indexes. In this study, ultrasound and pulsed vacuum technologies assisted the osmotic dehydration. Moreover, hot air convective drying was employed before some osmotic processes and the physical, chemical, nutritional and hygroscopic characteristics in the final product were assessed. Studies about the thermodynamic sorption properties were also performed in this research. The main results of this research showed that isomaltulose can be promising substitute of sucrose in osmotic processes. The mathematical modelling of osmotic dehydration kinetics was represented with good accuracy by linearized Azuara model. The best conditions for enrichment of isomaltulose in mangos, according to multilevel models, was 45 °C and 35% solute concentration. The multidimensional scaling showed that the use of 10 min and 48 kPa of absolute pressure promoted greater fruit enrichment, and best physicochemical characteristics in relation to higher vacuum and time levels. The incorporation of isomaltulose by ultrasound and pulsed vacuum technologies before drying resulted in more stable product, from a hygroscopic point of view, compared to the fresh fruit, besides higher solids content (enriched with a carbohydrate of interest) and with best quality properties. Finally, thermodynamic properties study showed that the enthalpy and entropy behaviors presented interaction between water and the product components, which was similar to physical properties of pure water from 0.35 g water/g dry matter. Gibbs free energy value indicated that sorption of fresh mango was a non-spontaneous process, while for pretreated with sucrose and isomaltulose were spontaneous processes. The enthalpy-entropy compensation theory indicated the sorption processes of all products were enthalpy-controlled.